Transcription-coupled nucleotide excision repair and its regulation by the DNA damage checkpoint

By

Michael Josef Taschner

A thesis submitted for the degree of Ph.D.

at

The University of London

August 2009

Cancer Research UK

London Research Institute

Clare Hall Laboratories

South Mimms

Herts EN6 3LD

and

Department of Biochemistry

University College London

WC1E 6BT

I, Michael J. Taschner, confirm that the work presented in this thesis is my own. Where information has been derived from other sources, I confirm that this has been indicated in the thesis.

Abstract

Elaborate DNA repair mechanisms have evolved, allowing cells to repair damages in their genomes. Nucleotide excision repair (NER) removes a variety of helix-distorting lesions, including those caused by ultraviolet (UV) irradiation. NER operates via two subpathways. Transcription-coupled repair (TC-NER) rapidly removes transcription-blocking lesions in the transcribed strand (TS) of active genes, and in the yeast *Saccharomyces cerevisiae* depends on the factors Rad26 and Rpb9. Lesions in untranscribed DNA, including the non-transcribed strand (NTS) of active genes are removed slower by global genome repair (GG-NER).

Besides activating specific DNA repair systems, DNA damage also leads to a global cellular response, known as the DNA damage checkpoint (DDC). Cell-cycle progression is temporarily stopped after DNA damage to allow sufficient time for repair and prevent replication or segregation of damaged chromosomes. The DDC is a complex signal transduction cascade involving a number of protein kinases, the central players in budding yeast being Mec1 and Tel1, the homologues of human ATR and ATM, respectively. Besides inhibiting cell-cycle progression, accumulating evidence suggests that DNA repair systems are also influenced by the checkpoint.

I have investigated the rates of repair of UV lesions in checkpoint deficient strains of *Saccharomyces cerevisiae* and found that NER is significantly inhibited on both strands of an active gene in the absence of Mec1. The effect on NTS repair seems to be caused by deficient *de novo* synthesis of repair factors, whereas TC-NER is influenced mainly by post-translational modification of one or more pre-existing proteins. I have characterised a checkpoint-dependent phosphorylation of Rad26, and have shown using point mutants that this phosphorylation increases the TC-NER capacity of cells, establishing a new link between NER and the checkpoint.

In addition to these results about the interplay between the DDC and NER pathways, preliminary data from two unrelated projects will be presented. One was an attempt to establish a system for analysis of NER factor recruitment to an artificial, highly UV-damage-prone DNA sequence. The other focussed on the regulation of UV-induced degradation of Rpb1, the largest RNA Polymerase II (RNAPII) subunit, by the DDC.

List of tables

Table of figures

Table of contents

1 Introduction

1.1 DNA damage and repair

Faithful transmission of the genetic material between generations is a prerequisite for genome integrity and cell survival in all living cells. The genome therefore needs to be replicated and segregated correctly. Failure to do so will result in the accumulation of alterations such as mutations, which could alter the functions of the proteins encoded by their respective genes. The DNA is, however, inherently unstable and is prone to chemical alterations. More than 10^4 DNA lesions are formed spontaneously per day in human cells, by spontaneous decay, cellular metabolic byproducts, and replication errors (Lindahl, 1993). This damage load is further increased by the action of various exogenous DNA damaging agents from the environment, such as the Ultraviolet (UV) components of sunlight, cigarette smoke, ionizing radiation, and many more. If left unrepaired, these lesions would interfere with essential metabolic processes occurring on the DNA (such as transcription and replication), and would also lead to an unacceptably high level of mutations, which is a strong driving force behind neoplastic transformation, and diseases in general, in multicellular organisms. It is therefore not surprising that all living cells have evolved a number of repair systems to deal with DNA lesions, many of which are conserved between prokaryotes and higher eukaryotes. The importance of these repair mechanisms is exemplified by the existence of inherited cancer-prone disorders based on the inactivation of various DNA repair pathways (Hoeijmakers, 2001). In the following sections I will give a very brief overview of the most relevant sources of DNA damage and repair by describing their respective DNA repair pathways, but the main focus will be on UV-induced lesions and Nucleotide Excision Repair (NER), as this is the pathway most relevant for the work described here.

1.1.1 Oxidative damage and Base Excision Repair (BER)

BER is the main repair pathway for lesions such as base oxidation, deamination and alkylation (Friedberg, 2006), and is the most important repair system for the removal of lesions generated by normal cellular metabolism. It also repairs single-strand DNA breaks and removes uracil from DNA, which is formed by spontaneous deamination of cytosine. The repair process is initiated by non-enzymatic base loss, or the removal of the damaged base from the sugar-phosphate backbone by a damage-specific DNA glycosylase (Krokan et al., 1997), resulting in the formation of an abasic site (AP site) (Boiteux and Guillet, 2004). This site is then

recognized by an AP endonuclease, which cleaves it to form 3' OH and 5' deoxyribose phosphate (dRP) termini (Doetsch and Cunningham, 1990). Some DNA glycosylases can carry out this cleavage themselves (bifunctional glycosylases).

After the cleavage of the phosphate backbone, two distinct pathways of BER can be distinguished, differing in the length of the newly synthesized DNA (Frosina et al., 1996). In 'Short-patch' BER (SP-BER), DNA polymerase beta (Polβ) inserts only a single base. With its intrinsic dRP-lyase activity it can cleave the dRP residue to generate a 5' phosphate, and the remaining nick can be ligated by DNA ligase III. In 'Long-patch' BER (LP-BER), the length of the newly synthesized DNA is typically 2-8 nucleotides, and involves DNA polymerases δ/ε and PCNA. Displacement of the old strand creates a 5'-flap structure, which has to be removed by a specialised flap-endonuclease, FEN-1. The remaining nick created during LP-BER is sealed by DNA ligase I.

Because of the vital importance of the BER pathway in the removal of naturally occuring DNA damage, inactivation of central BER proteins, such as DNA Polymerase β or the scaffold protein XRCC1, is lethal in higher eukaryotes (Sugo et al., 2000; Tebbs et al., 1999), but certain mutations in these proteins are also linked to cancers (Bhattacharyya and Banerjee, 2001; Divine et al., 2001).

1.1.2 Mismatch repair (MMR)

The MMR pathway is mainly responsible for the removal of incorrectly inserted nucleotides during DNA replication, but can also work on certain base modification, as well as small insertion/deletion loops caused by replication slippage (reviewed in (Li, 2008)). The prototypical MMR pathway in *E. coli* has been extensively studied. Here, the damage is recognized by the MutS protein which recruits MutL to the lesion. MutL enhances mismatch recognition by MutS and also recruits MutH to the complex. MutH binds to hemi-methylated dGATC sequences in DNA (the newly synthesized strand being transiently unmethylated after replication), and uses its endonucleoytic activity to incise the unmethylated daughter strand. The UvrD helicase removes the damaged strand, creating a single-strand gap, which is eventually filled by DNA repair synthesis and ligation.

In higher eukaryotes, MMR is more complex and less well understood. Several eukaroytic homologs of MutS and MutL exist, suggesting that the basic mechanism is conserved, but none has yet been identified for MutH (Kunkel and Erie, 2005; Modrich and Lahue, 1996). The importance of this pathway in higher eukaryotes is exemplified by the existence of an inherited

cancer-prone disorder called hereditary non-polyposis colon carcinoma (HNPCC), a heterogenous disease caused by heterozygous mutation of mainly MSH2 and MLH1 (Peltomaki and de la Chapelle, 1997).

1.1.3 Repair of DNA double strand breaks

Double strand breaks (DSBs) are particularly dangerous for a cell, because segregation of chromosomes in the presence of unrepaired DSBs can result in the loss of large amounts of genetic information. DSBs can be induced by treatment of cells with ionizing radiation, but the most physiological source is probably the replication of DNA containing single-strand breaks. Such single-strand breaks can be caused by oxidative damage to the sugar-phosphate backbone, or by the enzymatic activities of proteins such as AP-endonucleases during BER. Another endogenous source of DSBs are the actions of topoisomerases (Wang, 2002). DSB formation can also occur in a programmed way, for example in the process of mating type switching in budding yeast (Haber, 1998), during the rearrangement of immunoglobulin genes in the immune system of higher eukaryotes (Soulas-Sprauel et al., 2007), and during meiosis (Marston and Amon, 2004).

Two main pathways exist for dealing with DSBs, non-homologous end-joining (NHEJ) and homology directed recombination (HDR), and HDR can be further subdivided into gene conversion and single strand annealing (SSA). NHEJ can be seen as the simple re-ligation of free DNA ends after proper end-processing (reviewed in (Daley et al., 2005)). The Ku-complex has affinity for free DNA ends and is thought to bring the DNA ends into close proximity by the help of the MRN complex, and DNA ligase IV (together with other factors) then ligates the ends. Because of the requirement of end-processing prior to ligation, the NHEJ pathway is often accompanied by the loss of genetic information, making it error-prone.

For HDR, the ends have to be processed to form 3' ssDNA (reviewed in (West, 2003)) and this pathway requires long tracts of homology between the break point and a donor region elsewhere, which is used for repair. The 5'-3' resection is carried out by 5' specific exonucleases, and the resulting 3' single-stranded tails are recognized by a number of proteins. The Rad51 proteins forms filaments on these tails (West, 2003), a process which is facilitated by RPA and Rad52 (Sung, 1997). This filament then scans the genome for a region of homology and invades it, creating a D-loop. At this stage, other proteins such as Rad54, the Rad55-Rad57 complex and RPA play important roles (Sugawara et al., 2003; Wang and Haber, 2004; Wolner et al., 2003). Repair synthesis then takes place, extending the invading strand. Two distinct scenarios are possible after this extension step. In the classical model for

homologous recombination (HR) (Szostak et al., 1983), the D-loop is captured by the second end of the DSB, and after further repair synthesis a double holliday junction is formed. These junctions have to be resolved by specialised Holliday junction resolvases in order to disconnect the two molecules (Ip et al., 2008). In the alternative pathway, known as 'synthesis-dependent strand annealing' (SDSA) (reviewed in (Paques and Haber, 1999)), the extended strand leaves the invaded duplex and can now bind to the 3' overhang of the other end of the DSB. The resulting gaps in the two strands can be filled, and the nicks are finally ligated.

The SSA pathway can be employed for DSB repair if no homologous sequences can be found in order to carry out gene conversion (reviewed in (Paques and Haber, 1999)). Briefly, repair of the break is possible if some homology can be found further inwards between the resected ends. This leads to the formation of 3' flap structures which have to be cleaved by the endonucleases XPF/ERCC1 in humans and Rad1/Rad10 in yeast. Arising gaps can then be filled by DNA synthesis and the nicks closed by a DNA ligase.

Several much-studied proteins, such as ATM, BRCA1 and 2 and others are involved in DSB repair, and deficiencies in these proteins result in increased genomic instability and cancer predisposition (Hoeijmakers, 2001).

1.2 Nucleotide excision repair (NER)

Among all repair pathways for DNA damage, the nucleotide excision repair (NER) system is the most versatile, dealing with a wide variety of lesions, including cyclobutane pyrimidine dimers (CPDs) and 6-4 pyrimidine-pyrimidone photoproducts (6-4PPs), the two main lesions induced by UV irradiation, as well as a large number of bulky chemical adducts, such as those produced by cigarette smoke, the UV-mimetic chemical 4-nitroquinoline 1-oxide (4NQO), and cisplatin, a DNA damaging agent routinely used in cancer chemotherapy (de Laat et al., 1999; Prakash and Prakash, 2000). The basis for this versatility was believed to be the fact that instead of recognising a specific lesion, it is the damage-induced distortion of the DNA helix which is detected by the NER lesion sensors. This view has been challenged now by the finding that non-distorting lesions, such as the oxidative lesion thymine glycol (Tg), has also been shown to be a substrate for NER.

The NER pathway is conserved between *E.coli* and humans, and can be divided into 4 main steps: damage detection, formation of an open complex, dual incision leading to removal of the damaged strand, and finally repair synthesis to close the gap (de Laat et al., 1999; Prakash and Prakash, 2000). The whole reaction requires the activities of more than 30 factors in eukaryotic

cells and has been reconstituted with purified proteins from both budding yeast (Guzder et al., 1995) and humans (Aboussekhra et al., 1995; Mu et al., 1995). A speciality of the damage-detection step is that it occurs by different mechanisms depending on the transcriptional state of the damaged sequence, and so NER can be divided into two distinct subpathways. Untranscribed DNA, including the non-transcribed strand (NTS) of active genes, is repaired by Global Genome NER (GG-NER), whereas the transcribed strand (TS) of an active gene is repaired by Transcription-Coupled NER (TC-NER) (Svejstrup, 2002). In this section I will give a brief overview of the general mechanism of NER in both *E.coli* and eukaryotes, the special relationship between transcription and NER (TC-NER) will be dealt with in subsequent sections.

1.2.1 NER in *E.coli*

Prokaryotic NER is understood in detail and has been important for the elucidation of the NER mechanism in eukaryotes (reviewed in (Petit and Sancar, 1999)). In the 1960's, it was first discovered that UV-lesions were excised from bacterial DNA (Boyce and Howard-Flanders, 1964; Setlow and Carrier, 1964), followed by the formation of repair patches (Hanawalt and Haynes, 1965). The genes responsible for these observations, *uvrA, uvrB and uvrC*, were subsequently identified by complementation studies (Howard-Flanders et al., 1966).

UvrA is a protein containing two C4-type zinc fingers and two ATP Binding Cassette ATPase (ABC ATPase) domains (Doolittle et al., 1986). UvrA forms a dimer and this dimer interacts with UvrB, leading to the formation of a $UvrA_2B$ complex. This complex is recruited to the damage, and damage recognition is believed to be mediated by UvrA, as only this protein has been shown to bind damaged DNA (Mazur and Grossman, 1991).

UvrB is a member of the helicase superfamily as it contains 6 conserved helicase domains (Theis et al., 2000). It is loaded onto damaged DNA as part of the $UvrA_2B$ complex and its ATPase activity is stimulated by the presence of UvrA and damaged DNA (Caron and Grossman, 1988; Oh et al., 1989). The function of UvrB is opening of the double helix and lesion verification (Zou and Van Houten, 1999). $UvrA_2$ then dissociates from the complex, leaving behind the unwound DNA with the bound UvrB, which is subsequently recognised by the UvrC endonuclease. This endonuclease has two distinct catalytic sites and is responsible for both the 3' and the 5' incision on the damaged strand (Verhoeven et al., 2000). The UvrD helicase is responsible for unwinding and displacing the damaged strand, and the single-strand gap is finally filled by DNA polymerase I, and sealed by DNA ligase (Caron et al., 1985).

1.2.2 NER in eukaryotes

Even though the basic steps in the eukaryotic NER pathway are essentially the same as in its prokaryotic counterpart, the reaction has become more complex during evolution (de Laat et al., 1999; Prakash and Prakash, 2000). In humans, the importance of NER is exemplified by a number of rare autosomal recessive disorders caused by defects in this pathway, including Xeroderma pigmentosum (XP), Cockayne's syndrome (CS), and Trichothiodystrophy (TTD) (reviewed in (de Boer and Hoeijmakers, 2000)). XP patients display severe sensitivity to sunlight, which results in a >1000 fold increased risk of developing skin cancer in sun-exposed areas of the body, which clearly shows how important removal of UV-induced lesions is in order to avoid an accumulation of UV-induced mutations. XP was the first cancer-prone disorder to be directly linked to a defect in DNA repair (Cleaver, 1968). Seven distinct complementation groups with defects in NER components have now been identified (XP-A to G), and another group of XP-patients (XP variant; XPV) have defects in translesion DNA synthesis across unrepaired UV lesions (reviewed in (Kannouche and Stary, 2003)). Cockayne's syndrome results from a defect in TC-NER, and will be discussed later.

The individual steps in eukaryotic GG-NER, together with the responsible factors, will be presented individually below, and important mechanistic differences between the reaction in budding yeast (the model system used in this work) and human cells will be pointed out. Simplified schemes showing the NER subpathways and Rpb1 ubiquitylation pathways (discussed later) in human cells and budding yeast can be found in Figures 1.1 and 1.2, respectively.

1.2.2.1 Damage-detection

1.2.2.1.1 Yeast Rad4/Rad23 and human XPC/hRad23B

The first proteins to arrive at a DNA lesion are the Rad4/Rad23 complex in yeast (Guzder et al., 1998a; Jansen et al., 1998), or the XPC/HR23B complex in humans (Reardon et al., 1996; Sugasawa et al., 1998). Even though other factors, such as yeast Rad14 and its human homolog XPA, also have affinity for damaged DNA (Guzder et al., 1993; Jones and Wood, 1993), elegant studies in human cells have shown that only binding of XPC/HR23B is necessary for efficient lesion detection *in vitro* (Sugasawa et al., 1998) and *in vivo* (Volker et al., 2001). The XPC/HR23B complex is only required for GG-NER (Venema et al., 1990b), whereas in yeast, the Rad4/Rad23 complex is required for both GG-NER and TC-NER (Gietz and Prakash, 1988;

Verhage et al., 1994), which represents an important difference between the yeast and the human NER reaction. The Rad4 and XPC subunits are responsible for recognising damaged DNA (Hoogstraten et al., 2008; Min and Pavletich, 2007). Importantly, binding of these proteins to DNA induces significant DNA bending, which is much more energetically favorable if helix distorting lesions are present, thus explaining the increased affinity for damaged DNA and the high versatility of the NER pathway.

In human cells, the HR23A and B proteins have both been shown to be involved in NER, to form a stable complex with XPC, and to increase the efficiency in the NER reaction *in vitro* only in the presence of XPC. This stimulatory activity is dependent on XPC-binding (Masutani et al., 1997; Sugasawa et al., 1996; Sugasawa et al., 1997). More recently it was shown that the stimulation of the NER reaction by HR23B can be explained by the stabilization of the XPC protein (Araki et al., 2001).

Yeast Rad23 has also been proposed to be required for stabilisation of Rad4 (Lommel et al., 2002), but a later study suggested that the reduced Rad4 levels in *rad23Δ* cells result from a decrease in *RAD4* transcription (Gillette et al., 2006). Rad23 clearly has an important function in NER, as *RAD23* deletion renders cells sensitive to UV irradiation and leads to severely impaired damage removal (Verhage et al., 1996b). It possesses an N-terminal ubiquitin-like (Ubl) domain (Watkins et al., 1993), important for its function in NER by recruiting subunits of the proteasome (Elsasser et al., 2002), which has non-proteolytic functions in the NER process (Gillette et al., 2001; Russell et al., 1999) (reviewed in (Reed and Gillette, 2007)).

Even though XPC/HR23B were initially isolated as a heterodimeric complex, further biochemical analysis revealed the presence of another member, Centrin2 (CEN2) (Araki et al., 2001). This protein interacts directly with XPC, and like HR23B, is also involved in promoting XPC stability (Araki et al., 2001). A similar factor was later also found in yeast and called Rad33 (den Dulk et al., 2006). Further work has shown that Rad33 shows homology to Centrin 2, that it can bind directly to Rad4, and that this binding is necessary to protect Rad4 from polyubiquitylation (den Dulk et al., 2008).

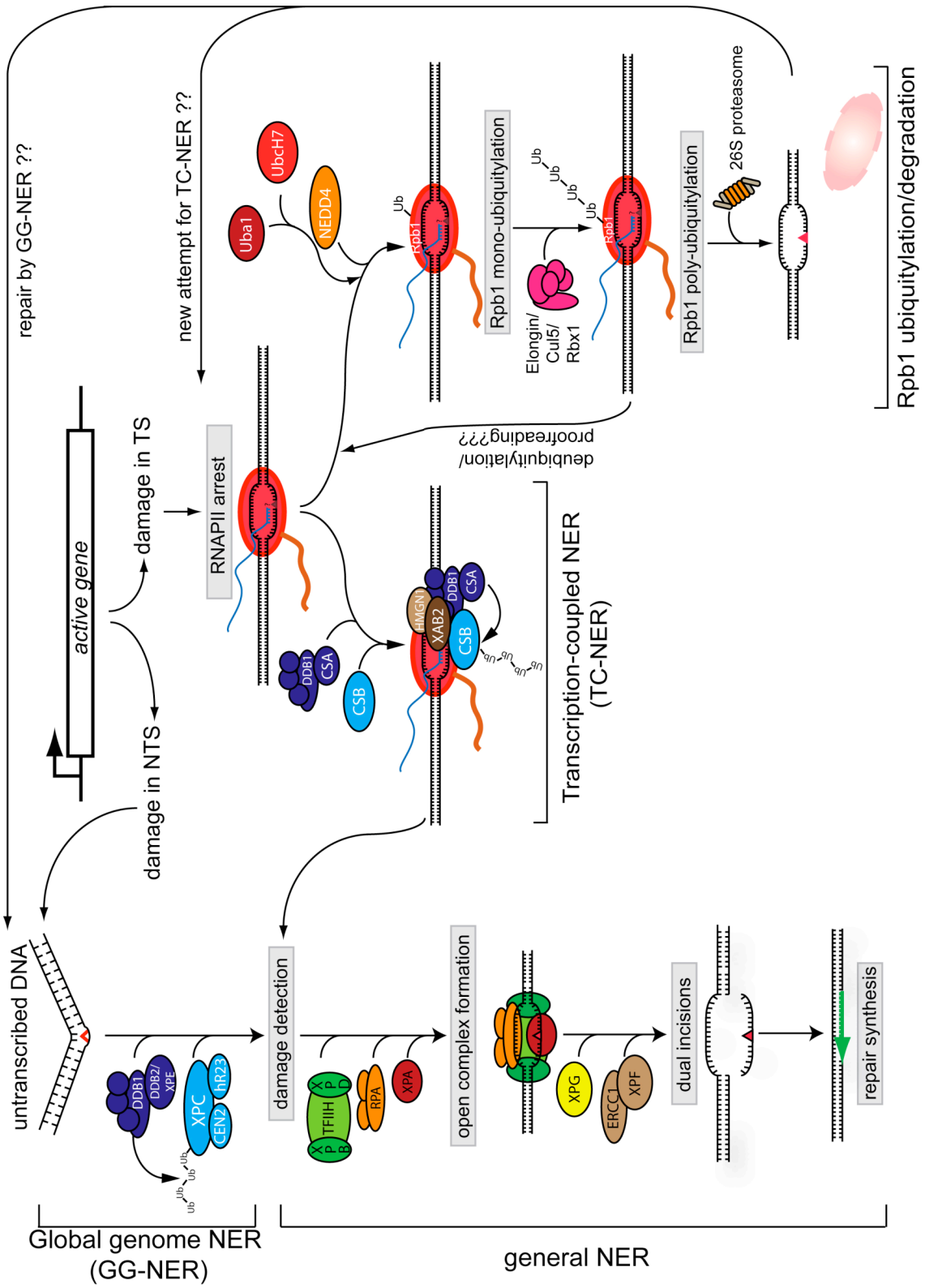

Figure 1-1 Simplified overview of the two NER subpathways and Rpb1 ubiquitylation/degradation in human cells

see text for details

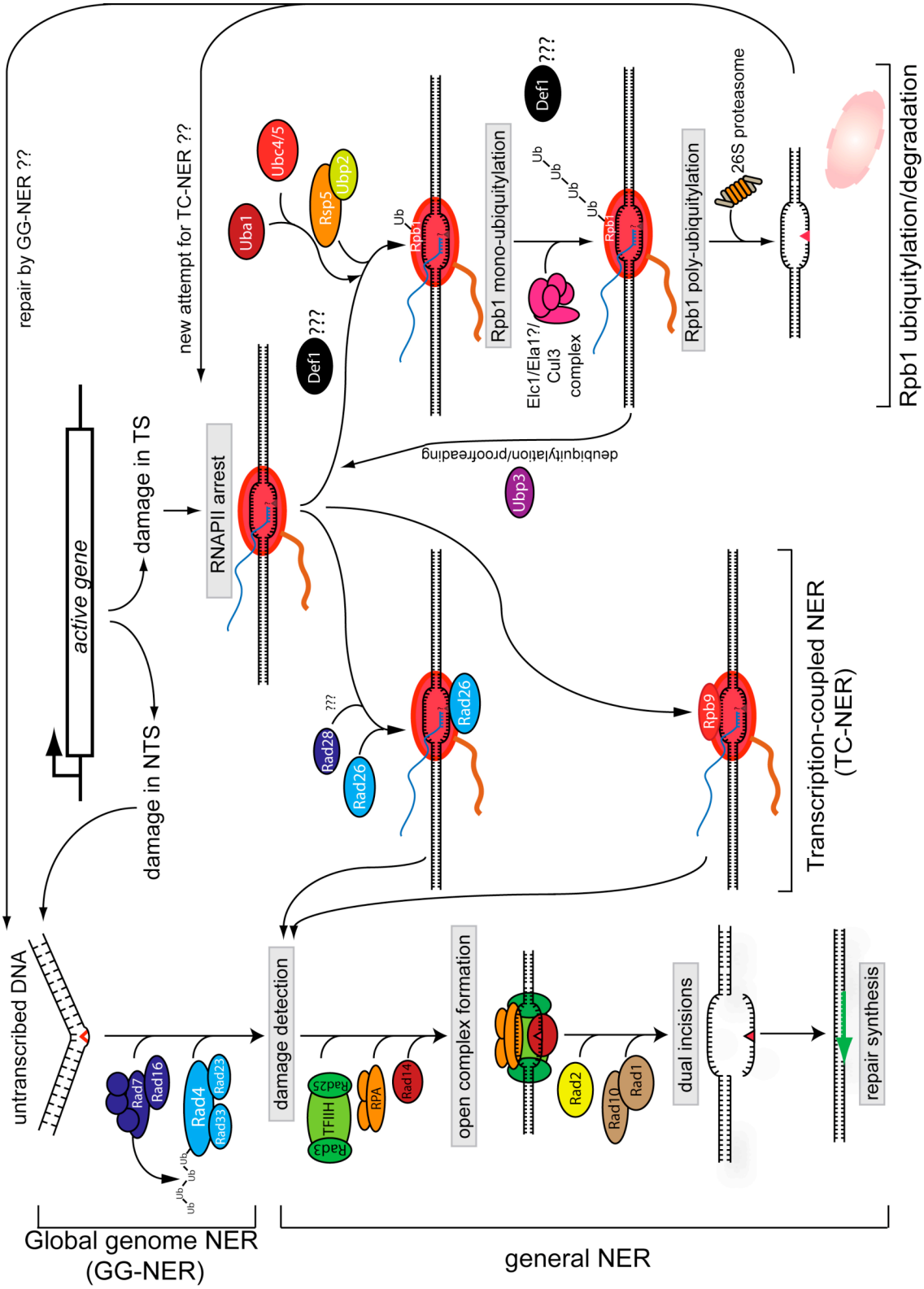

Figure 1-2 Simplified overview of the two NER subpathways and Rpb1 ubiquitylation/degradation in budding yeast cells

see text for details

1.2.2.1.2 The Rad7/Rad16 complex in yeast

The Rad7/Rad16 complex is solely involved in GG-NER in yeast, i. e. in the repair of untranscribed DNA, including the NTS of active genes (Bang et al., 1992; Terleth et al., 1990; Verhage et al., 1994). Consequently, deletion of the corresponding genes, either alone or in combination, results in UV sensitivity, which is less pronounced than in completely NER-deficient yeast mutants, such as *rad14Δ* (yeast XPA) (Verhage et al., 1996a). Rad7 and Rad16 form a complex with 1:1 stoichiometry, which can bind UV-damaged DNA in an ATP-dependent manner (Guzder et al., 1997). Interestingly, no clear homologues in humans have yet been identified for these factors. An additional member of the Rad7/Rad16 complex has later been found to be Abf1 (Autonomously replicating sequence (ARS) binding factor 1), which is encoded by an essential gene and has important roles during DNA replication (Diffley and Stillman, 1989). This factor has been shown to be required for NER, as depletion of Abf1 renders cells incapable of performing NER and sensitive to killing by UV light (Reed et al., 1999).

Rad16 is a member of the SWI2/SNF2 family of helicases (Bang et al., 1992), and because of its ability to bind DNA has been proposed to be involved in recognition of DNA damage during GG-NER, especially in the context of chromatin. Evidence for this comes from recent work showing that the repair defect in *rad16Δ* and *rad7Δ* strains can be suppressed by deletion of a histone deacetylase (Teng et al., 2008).

Using a reconstituted *in vitro* system for NER of damage in purified plasmid DNA, which allows to detect the incisions carried out by the NER reaction, it was shown that the Rad7/Rad16 complex is not required for NER *per se* (Guzder et al., 1995), but that it increases the efficiency of the reaction (Guzder et al., 1997). Based on these findings it was proposed that these factors assist in the recognition of the damage (Guzder et al., 1998b). However, a different *in vitro* system using yeast extracts, which measures repair synthesis rates, showed that Rad16 are Rad7 are required for the reaction (Wang et al., 1996). An explanation for these apparently contradicting results was obtained using an *in vitro* system that allows dissection of the sequential steps of dual incision, excision of the damaged DNA and repair synthesis. This work showed that Rad7 and Rad16 are not required for the incision step, but instead for excision of the oligomer and repair synthesis, showing that the Rad7/Rad16 complex affects post-incision events during NER (Reed et al., 1998). Later work showed that this can be explained by the fact that the Rad16 subunit of the complex creates superhelicity in DNA, and that this activity is necessary for excision of the damaged oligonucleotide (Yu et al., 2004).

The Rad7 and Rad16 proteins also have a different function in NER, acting in an E3 ubiquitin ligase complex together with Elc1 and Cul3. This complex targets the Rad4 protein for polyubiquitylation and subsequent degradation by the 26S proteasome after UV irradiation, but importantly, only ubiquitylation, but not degradation of Rad4 is required for efficient NER (Gillette et al., 2006). Taken together, the Rad16/Rad7 complex has important functions at various steps during the NER reaction. A similar ubiquitin ligase complex was recently shown to be involved in ubiquitylation of Rpb1, the largest RNA Polymerase II subunit (Ribar et al., 2006, 2007) Harreman et al, in preparation) (see Section 1.3.4), but the Rad7 and Rad16 proteins are not required for this (Ribar et al., 2006, 2007).

1.2.2.1.3 The damaged DNA binding complex (DDB) in humans

The Damaged DNA Binding proteins 1 and 2 (Ddb1 and 2), like the XPC/hRad23B complex, are involved exclusively in the GG-NER pathway in higher eukaryotes (Keeney et al., 1993). These proteins are unique to higher eukaryotes, and it is tempting to speculate that they may possibly have evolved as a replacement of the yeast-specific Rad16/Rad7 complex. The Ddb2 protein is responsible for the damaged DNA-binding activity of the complex (Li et al., 2006). The Ddb1 subunit also forms complexes with various other proteins, and therefore has a much broader spectrum of functions (Wittschieben and Wood, 2003). Mutations in the *DDB2* gene can be found in patients belonging to the XPE complementation group (Keeney et al., 1993; Keeney et al., 1994). The exact function of DDB/XPE has for a long time remained unknown, because reconstitution of NER *in vitro* does not require addition of this factor (Aboussekhra et al., 1995; Mu et al., 1995). The DDB complex has been shown to bind to damaged DNA with a preference for 6-4PPs over CPDs (Chu and Chang, 1988; Reardon et al., 1993).

More information about the involvement of DDB in NER was obtained when Groisman and colleagues identified a ubiquitin ligase complex containing both Ddb1 and Ddb2 as well as Cul4A, Roc1, and all the subunits of the COP9 signalosome (CSN), a negative regulator of E3 ligases. Microinjection of this complex into cells from XPE patients rescued the NER defect of these cell lines (Groisman et al., 2003). Furthermore, the complex was recruited to chromatin after UV irradiation of cells and CSN components disappeared from the complex, thereby activating the ubiquitin ligase activity (Groisman et al., 2003). A relevant substrate for the DDB-containing ubiquitin ligase was found later, when it was shown that it is involved in poly-ubiquitylation of XPC (Sugasawa et al., 2005). Importantly, this modification seems to be reversible and not to lead to proteasomal degradation, but instead alters the DNA binding properties of the protein.

Other targets of the Ddb1/2 containing ubiquitin ligase complex were found to be histones H3 and H4 (Wang et al., 2006). Upon UV-irradiation of cells, these modifications seem to lead to histone release from nucleosomes, and an increase in the efficiency of repair factor recruitment to the site of the lesion (Wang et al., 2006).

1.2.2.2 Open-complex formation

Upon lesion recognition, opening of the DNA double helix is a crucial step in the NER reaction in order to achieve efficient lesion excision, and it is achieved by the helicase acitivity of the multi-subunit TFIIH complex. The 'core-TFIIH' complex contains the 5' to 3' DNA helicase Rad3 and the 3' to 5' DNA helicase Rad25 in yeast, and their homologues XPD and XPB in higher eukaryotes (Guzder et al., 1994a; Guzder et al., 1994b; Sung et al., 1993a; Sung et al., 1987a; Sung et al., 1987b).

Surprisingly, the initial isolation of *rad3Δ* mutants revealed that it is an essential gene (Higgins et al., 1983; Naumovski and Friedberg, 1983), even though other central NER factors are not. The same was later found to be true for *rad25Δ* mutants (Park et al., 1992). The answer to this puzzle came a decade later, when the TFIIH-complex was shown to have dual roles in the cell, an essential function in gene transcription and a non-essential function in NER (Feaver et al., 1993; Schaeffer et al., 1993).

The core-TFIIH complex interacts with another complex, referred to as TFIIK or Cdk-activating kinase (CAK), to form the 'holo-TFIIH' complex. The CAK subcomplex is not required for NER (Sung et al., 1996; Svejstrup et al., 1995). Instead it is released from the complex on chromatin after UV irradiation, and this release is dependent on the XPA repair factor (Coin et al., 2008). After UV irradiation, transcription is temporarily inhibited, and the dissociation of CAK from TFIIH can potentially explain this. Importantly, after completion of DNA repair, the CAK subcomplex reappears with the core TFIIH, and this is accompanied by the restoration of the ability of TFIIH to function in transcription initiation (Coin et al., 2008).

After opening of the damaged DNA, the yeast Rad14 protein or its human homologue XPA binds the DNA lesion, which is thought be an important step in verification of the damage (Bankmann et al., 1992; Guzder et al., 1993; Jones and Wood, 1993; Tanaka et al., 1990). The undamaged strand is protected in the open complex by binding of the essential heterotrimeric RPA complex (Wold, 1997), and this binding is important for the NER reaction (Guzder et al., 1995; He et al., 1995; Mu et al., 1995).

1.2.2.3 Dual incisions and repair synthesis

Formation of an open complex leads to the binding of two endonucleases, which are responsible for the endonucleolytic cleavage reactions necessary for removal of the damaged strand. These endonucleases are Rad2 (Habraken et al., 1993) and the Rad1/Rad10 complex (Sung et al., 1993b; Tomkinson et al., 1993) in budding yeast, and their human homologues XPG (O'Donovan et al., 1994) and XPF/ERCC1 (Park et al., 1995). Rad1/Rad10 (XPF/ERCC1) (Matsunaga et al., 1995) is responsible for the 5' incision, while Rad2 (XPG) performs the 3' incision (O'Donovan et al., 1994). These incisions are placed asymmetrically around the lesion, with the 5' incision 15-24 nucleotides and the 3' incision 2-8 nucleotides away from the DNA lesion (Moggs et al., 1996). Rad2 and Rad1/Rad10 contribute more to the NER reaction than merely their endonucleolytic activites. In the absence of either factor, no nicking of DNA can be observed *in vitro* (Guzder et al., 1995), indicating that these proteins also serve a structural role necessary for the proper assembly of the NER complex at the site of a DNA lesion. This may be important to ensure that incision only occurs when both endonucleases are in place so that unscheduled DNA nicking is avoided.

The result of the incisions is the removal of a stretch of DNA containing the lesion. The length of this ssDNA fragment is typically 24-27 bases in yeast (Guzder et al., 1995), or 27-29 bases in humans (Huang et al., 1992). The resulting gap is filled by DNA Polymerase delta or epsilon (Budd and Campbell, 1995) bound to PCNA, and the remaining nick is sealed by DNA ligase I.

1.3 The interplay between DNA damage and transcription

1.3.1 The regulation of transcription elongation

Eukaryotic transcription of protein coding genes by RNA Polymerase II (RNAPII) is a complex process and can be viewed as a series of sequential and highly regulated steps, namely preinitiation complex assembly at the promoter, open complex formation and initiation, promoter clearance, transcription elongation, transcription termination, and RNAPII recycling (Svejstrup, 2004). During initiation, general transcription factors assemble at the promoter of a gene in a stepwise manner, culminating in the recruitment of RNAPII (Lee and Young, 2000). Additional factors, such as histone modifying enzymes and chromatin remodellers, are required to achieve efficient assembly in the context of chromatin (Lee and Young, 2000).

Most work on the regulation of transcription has focussed on these early events occurring at the promoter, and the subsequent step of transcriptional elongation has for a long time been thought of as the simple addition of nucleotides. It has, however, become increasingly clear that RNAPII frequently pauses or becomes blocked at this stage, requiring support from a large number of elongation factors (reviewed in (Arndt and Kane, 2003)). Transcriptional pausing occurs when RNAPII stops the addition of nucleotides to the growing RNA for some time, before resuming transcription on its own. Several factors, such as ELL (Shilatifard et al., 1996), Elongin (Bradsher et al., 1993a; Bradsher et al., 1993b), and CSB (Selby and Sancar, 1997a), among others, have been shown to suppress pausing and to stimulate the catalytic activity of RNAPII.

After undergoing transcriptional arrest, RNAPII cannot resume transcription efficiently without help from other factors (Arndt and Kane, 2003). When RNAPII stops, it can slide backwards on the DNA, which leads to misalignment of the 3' end of the growing RNA chain with the active site of the polymerase. The most important factor required to help RNAPII in such a case is TFIIS, which binds to arrested RNAPII complexes and stimulates an endonucleolytic activity of the polymerase itself, leading to truncation of the transcript and realignment of the end of the RNA with the active site of the enzyme (reviewed in (Wind and Reines, 2000)).

Other elongation factors are required to help RNAPII transcribe DNA in the context of chromatin, such as Elongator (Otero et al., 1999), FACT (Orphanides et al., 1998) and PAF (Krogan et al., 2003a; Krogan et al., 2003b). An especially serious impediment to the progression of RNAPII, which is most important for the work described here and will be discussed in more details below, is the presence of DNA lesions in the template.

1.3.2 Transcription in the presence of DNA damage

DNA lesions not only lead to mutations but also have the ability to interfere with essential processes on DNA, such as replication and transcription. In the case of damage-blocked DNA replication, specialised error-prone DNA polymerases can be employed to bypass the damage quickly, alleviating the cytotoxic effect of a blocked replication fork, and allowing the repair machinery to deal with the lesion later. Defects in this pathway can be found in XP-V patients, the only XP complementation group which has no defect in NER (Kannouche and Stary, 2003). Instead, XPV encodes a DNA damage-bypass polymerase (Cordonnier et al., 1999; Masutani et al., 1999a; Masutani et al., 1999b).

In the case of transcription, many DNA lesions are a complete block for transcribing RNA Polymerase II (RNAPII) and cannot be bypassed (Tornaletti, 2009). Such lesions include mainly bulky DNA adducts, such as UV-induced CPDs and 6-4PPs (Donahue et al., 1994; Selby et al., 1997), lesions induced by cisplatin (Damsma et al., 2007; Tornaletti et al., 2003), and aminofluorene/acetylaminofluorene (Donahue et al., 1996). Upon encountering such barriers, RNAPII is stopped and cannot transcribe across the lesion. Because of the physical impediment imposed by those lesions, general elongation factors such as TFIIS cannot help RNAPII to bypass the block (Donahue et al., 1994).

Recent work by several groups tried to investigate the effects of non-bulky DNA adducts, such as the oxidative lesions 8-oxoguanine (8-oxoG) and thymine glycol (Tg), on RNAPII elongation. Even though such lesions are able to obstruct RNAPII progression, general elongation factors, such as Elongin, CSB, and TFIIS can assist in order to bypass the obstacle at the expense of base misincorporation opposite the lesion, leading to transcriptional mutagenesis (Charlet-Berguerand et al., 2006; Kuraoka et al., 2007).

Whatever the lesion is which leads to RNAPII stopping, it has severe consequences for a cell with damaged DNA, as the blocked RNAPII complex represents a barrier for all the other polymerases behind it, leading to a potent block to gene transcription. The elongation complex is extremely stable, so RNAPII does not fall off the DNA when it encounters an obstacle. In theory, therefore, even a single DNA lesion in an essential gene can lead to cell death if it is not repaired. In higher eukaryotes additional problems arise from a block to transcription, as prolonged stalling of RNAPII has been shown to be a signal for the p53-mediated induction of apoptosis (Ljungman and Zhang, 1996). It is therefore not surprising that mechanisms for the efficient alleviation of damage-stalled transcription complexes have evolved (reviewed in (Svejstrup, 2003)), namely fast removal of the lesion by transcription-coupled DNA repair, or alternatively, removal of the stalled RNAPII complex by ubiquitylation and degradation of Rpb1, the largest RNAPII subunit. These mechanisms will be discussed below.

1.3.3 Transcription-coupled Nucleotide Excision Repair (TC-NER)

In 1985, Hanawalt and colleagues first showed that in Chinese Hamster Ovary (CHO) cells pyrimidine dimers are removed much faster from a transcribed gene than from an untranscribed region downstream of it (Bohr et al., 1985). In the following year the same was shown to be also true in human cells (Mellon et al., 1986). In theory this could be explained by increased accessibility of transcribed DNA, but further examination of repair rates in the 2 individual strands of a transcribed gene showed that fast removal of lesions was only observed in the

transcribed strand (TS), whereas the non-transcribed strand (NTS) was repaired with kinetics similar to those observed for untranscribed DNA (Mellon et al., 1987). This phenomenon, termed 'transcription-coupled repair' (TCR; TC-NER), was later also observed in yeast (Terleth et al., 1989) and even in *E.coli* (Mellon and Hanawalt, 1989), highlighting the general importance of the fast removal of transcription blocking DNA lesions. Further work on this repair pathway showed that the arrest of an RNAPII complex at a lesion in the transcribed strand serves as the signal for fast repair, meaning that the elongating RNAPII complex elicits efficient repair when stopped by DNA lesions (reviewed in (Svejstrup, 2002)). Specialised proteins, termed 'Transcription-Repair Coupling Factors' (TRCFs), are required to link the stalled RNAPII to the NER machinery, and the coupling factors from *E.coli, S.cerevisiae* and higher eukaryotes will be discussed below.

1.3.3.1 TC-NER in E.coli *and the role of the Mfd protein*

After the initial observation that preferential repair of the transcribed strand of the lac-operon in *E.coli* is only detectable when transcription is induced (Mellon and Hanawalt, 1989), Sancar and colleagues tried to reconstitute this phenomenon with highly purified factors *in vitro* (Selby and Sancar, 1990). They found that, as expected, a CPD in the TS, but not the NTS, of a gene represented a strong block to the progression of RNA Polymerase (RNAP), but that repair of these lesions by the uvrABC system was actually inhibited by transcription, most likely caused by steric hindrance of the stable elongation complex stalled at the dimer. They concluded that their highly defined *in vitro* system lacked the transcription-repair coupling factor (TRCF), whose functions should be on one hand to recruit the repair proteins to the lesion in the TS, and on the other hand to overcome the inhibitory effect of the stalled RNAP complex on repair. Preferential repair was shown to be possible in crude extracts, and a factor was partially purified which conferred strand selectivity to the highly defined *in vitro* system (Selby and Sancar, 1991). This TRCF was shown to be the Mfd protein (Selby et al., 1991), a factor encoded by a gene which, when mutated, abolished a phenomenon called 'Mutation frequency decline', i.e. the loss of ultraviolet-light-induced mutations when an irradiated E. coli culture is incubated in conditions that inhibit protein synthesis (Witkin, 1966).

The functional domains of the 130 kDa Mfd protein were determined by Selby and Sancar (Selby and Sancar, 1993, 1995a, b). It contains a region with helicase-like motifs, which enable Mfd to act as a DNA translocase, but not as a helicase, and a TRG motif (Translocation in RecG), which is necessary for the translocation activity (Chambers et al., 2003; Mahdi et al., 2003). Furthermore it has a UvrB-like domain, which allows it to recruit repair protein UvrA, and a domain responsible for the interaction with RNAP (Roberts and Park, 2004).

The exact mechanistic details of Mfd function were nicely shown *in vitro* in a completely defined system by Sancar and colleagues. Mfd-mediated repair of damage in the transcribed strand involves release of RNAP from the damage, and recruitment of the Uvr (NER) proteins so that the lesion can be removed (Selby and Sancar, 1993).

Mfd-dependent removal of elongation complexes is, however, not restricted to RNAP stalled at a DNA lesion in the transcribed strand. Using immobilized elongation complexes, Roberts and coworkers were able to show that if RNAP is stalled, either by a lesion in the template strand or by depletion of NTPs, it backtracks on the DNA, i.e. it slides backwards which moves the end of the RNA out of the active site of the enzyme (Park et al., 2002). The Mfd protein binds the DNA upstream of the complex and uses its translocase acitivity to push the polymerase forward, realigning the active site with the RNA. If continued transcription elongation is possible (no physical obstruction and presence of NTPs), RNAP can now continue transcription, and if not (DNA lesion or lack of NTPs), Mfd dissociates RNAP and its RNA, thereby allowing repair to take place (Park et al., 2002).

1.3.3.2 TC-NER in humans

1.3.3.2.1 Cockayne's syndrome – cellular phenoypes

Cockayne's syndrome (Cockayne, 1936; Nance and Berry, 1992) is a rare autosomal recessive disorder characterized by growth retardation, skeletal and retinal abnormalities, progressive neural degeneration and severe photosensitivity, but no increased predisposition to cancer (reviewed in (de Boer and Hoeijmakers, 2000)). Because of the severe developmental defects, most patients die very early in life, with an average life expectancy of 10-12 years. Patients can be divided into several complementation groups. About 90% of the patients belong to Cockayne's syndrome complementation groups A and B. Furthermore, certain mutations in XPB and XPD (TFIIH), and XPG give rise to a combined XP/CS phenotype (de Boer and Hoeijmakers, 2000).

Because of the photosensitivity of CS patients, it was initially proposed that CS cells have defects in the NER pathway, and that this defect is the underlying cause for the phenotypes of the affected individuals. Indeed, it was shown that despite normal overall NER proficiency (Mayne et al., 1982), active genes are repaired less efficiently in CS fibroblasts (Mullenders et al., 1988; Venema et al., 1990a). This decrease was later shown to be caused by an inability to

preferentially repair the transcribed strand of active genes (van Hoffen et al., 1993), indicating that the mutated genes in CS patients encode the human transcription-repair coupling factors. However, several lines of evidence have been obtained since then, which indicate that the lack of transcription-coupled repair is not the reason for the observed sensitivity to DNA damaging agents, and certainly not the underlying cause for the severe clinical phenotypes displayed by Cockayne's syndrome patients (see below).

Besides being sensitive to DNA damaging agents, another striking phenotype of CS cells is their inability to recover transcription after DNA damage (Mayne and Lehmann, 1982). In cells from healthy individuals, transcription is temporarily inhibited after induction of DNA lesions, but recovers after a few hours. In CS cells, such a recovery does not occur. It could be speculated that this is caused by the persistance of transcription-blocking lesions because of a defect in TC-NER, or *vice versa,* that the lack of transcription after DNA damage is the reason for the absence of transcription-dependent processes, such as TC-NER. Studies examining the effects of the DNA damaging agent N-acetoxy-2-acetylaminofluorene (NA-AAF) were able to shed some light into the relationship between transcriptional recovery and TC-NER. NA-AAF induces DNA lesions which are repaired at the same rate, and - most importantly - without strand bias, in normal and CS cells, yet CS cells can not recover transcription after treatment with this drug, and display a much higher sensitivity towards it (van Oosterwijk et al., 1998; van Oosterwijk et al., 1996). This indicates that the lack of fast damage-removal from the transcribed strand is not the reason for the lack of transcriptional recovery, and that the lack of TC-NER is not the reason for the damage-sensitivity of CS cells.

Further evidence for this comes from work analyzing the transcriptional acitivity in extracts. Extract from irradiated CS cells cannot carry out *in vitro* transcription, even if the template is undamaged (Rockx et al., 2000), indicating again that the main defect in CS cells might be a defect in transcription rather than repair, especially after DNA damage, and that Cockayne's syndrome is a transcription rather than a repair syndrome. Indeed, it was found that CSB cells display reduced rates of RNAPII transcription even in the absence of damage (Balajee et al., 1997). Other mechanisms potentially explaining the transcription defects after DNA damage in CS cells (reviewed in (Svejstrup, 2002)) include differences in RNAPII phosphorylation (Rockx et al., 2000), sequestration of the basal transcription initiation factor TFIID (Vichi et al., 1997), and defects in switching the TFIIH complex from a repair mode to a transcription mode (You et al., 1998).

1.3.3.2.2 CSA and CSB – the main factors mutated in CS patients

The genes mutated in patients from the two Cockayne's syndrome complementation groups were identified based on their ability to rescue the defects in cell lines of the respective patients.

The *CSB/ERCC6* gene encodes a member of a subfamily of putative translocases of the Swi2/Snf2 family (Troelstra et al., 1992) with a molecular weight of 168 kDa, which can interact with RNA Polymerase II (van Gool et al., 1997). Because of its similarity to Swi2/Snf2 family members it was speculated that it might act as a chromatin remodelling factor, and indeed, an ATP-dependent chromatin remodelling activity was demonstrated for this protein (Citterio et al., 2000). Based on the presence of translocase domains it was speculated that its functions are similar to the functions of the *E.coli* Mfd protein (Selby and Sancar, 1993, 1995a, b). As expected, CSB is a DNA-dependent ATPase, but lacks detectable helicase activity, but, unlike Mfd, it is unable to disrupt a ternary complex of stalled RNA Polymerase II *in vitro* (Selby and Sancar, 1997b). However, it enhances elongation by RNA Polymerase II and has been shown to enable RNAPII to add an extra nucleotide when stalled at a transcription-blocking DNA lesion, reminiscent of the 'pushing' activity of Mfd/TRCF described above, and indicative of a 'remodelling activity' of the interface between RNAPII and DNA (Selby and Sancar, 1997a).

The *CSA/ERCC8* gene encodes a 44 kDa protein containing several WD40-repeats, known to be capable of forming β-sheets and to mediate protein-protein interactions, and has been reported to bind to both CSB and a subunit of TFIIH (Henning et al., 1995). After UV irradiation as well as other damages that are subject to TC-NER, the CSA protein was shown to translocate to the nuclear matrix, where it co-localizes with hyperphosphorylated RNA Polymerase II (Kamiuchi et al., 2002). This translocation is dependent on TFIIH (Saijo et al., 2007) and on the presence of CSB, but not the GG-NER factor XPC, nor the central NER factor XPA (Kamiuchi et al., 2002), indicating that it represents an early event in TC-NER. The first insights into the function of CSA were obtained when the protein was shown to be a component of a ubiquitin-ligase complex together with DDB1, Cul4A, Rbx1 and all the subunits of the COP9 signalosome, and this complex can bind to RNA Polymerase II (Groisman et al., 2003). The complex was shown to have ubiquitin ligase activity, which was inhibited shortly after UV irradiation by the COP9 signalosome and came back at later timepoints after UV treatment (Groisman et al., 2003). A few years later, CSB was shown to be ubiquitylated and degraded in a manner dependent on the CSA protein and the proteasome, establishing the first clear functional link between the two main players involved in Cockayne's syndrome (Groisman et al., 2006). Degradation of CSB

was observed at a late stage of the repair process and shown to be necessary for efficient recovery of transcription after completion of TC-NER. This finding was in apparent agreement with previously published results showing that inhibition of the proteasome led to defects in transcription recovery but not TC-NER (McKay et al., 2001).

CSA and CSB are not only involved in Cockayne's syndrome, but also in a distinct disorder, called 'UV-sensitive syndrome' ($UV^{S}S$), first described by Yamaizumi and coworkers in 1994 (Itoh et al., 1994) (reviewed in (Spivak, 2005)). Cells from these patients are highly sensitive to UV irradiation, but do not have detectable changes in unscheduled DNA synthesis (UDS), which indicates normal GG-NER. However, further investigations showed that $UV^{S}S$ cells had a clear defect in recovery of RNA synthesis after DNA damage (Itoh et al., 1994), as well as TC-NER (Spivak et al., 2002). Even though initial cell fusion studies indicated that $UV^{S}S$ was not caused by any known factors responsible for XP or CS (Itoh et al., 1995; Itoh et al., 1994), later work led to the finding that at least one patient (UVs1KO) had a non-sense mutation in the *CSB* gene, resulting in a STOP-codon at position 77 of the protein (Horibata et al., 2004). Surprisingly, despite mutation of CSB, this patient only displayed sensitivity to sunlight, but lacked all the other, more severe abnormalities seen in CS patients. Analysis of CSB protein levels in $UV^{S}S$ and CSB patients showed that the severly truncated CSB protein involved in $UV^{S}S$ is not expressed, whereas a longer, but still truncated, mutant protein could be found in a patient with CS phenotypes (Horibata et al., 2004). The authors therefore speculated that complete absence of the CSB proteins leads to the mild $UV^{S}S$, whereas the presence of a truncated protein might negatively affect one or several cellular processes, causing the more severe CS phenotypes. It should be noted, however, that several severe cases of CSB have been identified since then, which are caused by a complete lack of the protein (Hashimoto et al., 2008; Laugel et al., 2008). Despite these contradictory results, it is obvious that depending on the mutation in CSB, the clinical outcomes are variable.

A mutation in CSA has only recently been shown to lead to $UV^{S}S$ (Nardo et al., 2009). The analyzed patient expressed a form of CSA with a single amino-acid substitution in the last WD-repeat, and, like the other $UV^{S}S$-patients, showed a lack of transcription recovery after UV irradiation, but no developmental abnormalities. These phenotypes could be corrected by expression of the wild-type CSA gene (Nardo et al., 2009).

1.3.3.2.3 Speculations about the molecular defect underlying the severe phenotypes of CS patients

As mentioned earlier, the severe sensitivity to sunlight and other types of damaging agents displayed by CS patients might be explained by the lack of transcriptional recovery after DNA damage. However, the exact reasons why these patients show the severe developmental and neurological symptoms is still a subject of speculation. They can certainly not be explained by the lack of fast removal of transcription blocking DNA lesions, as these also persist in completely NER-deficient patients, such as those belonging to the XPA complementation group, yet XP patients do not display these severe symptoms. Furthermore, $UV^{S}S$-patients are also deficient in transcriptional recovery and TC-NER, yet they develop normally and are only sensitive to sunlight (Itoh et al., 1994; Nardo et al., 2009; Spivak, 2005; Spivak et al., 2002). Several alternative possibilities have been envisaged (reviewed in (Nouspikel, 2008)).

The fact that several studies have linked CS proteins, especially CSB, to transcription by RNA Polymerase II (Balajee et al., 1997; Dianov et al., 1997; Selby and Sancar, 1997a; van Gool et al., 1997) has led to the model that CS is a transcription syndrome rather than a repair syndrome. This would also explain why certain mutations in XPB and XPD, subunits of the general transcription factor TFIIH (which is involved in both transcription and NER), give rise to a combined XP/CS phenotype. The involvement of XPG was harder to explain in this respect, until it was shown recently that XPG is involved in stabilising TFIIH (Ito et al., 2007). Importantly, wild type XPG was found to form a stable complex with TFIIH and CSB (Iyer et al., 1996). In cells from patients with combined XPG/CS symptoms, this association was not observed, and the CAK subcomplex as well as the XPD subunit were dissociated from TFIIH (Ito et al., 2007). Further evidence for an involvement of XPG in transcription comes from its yeast counterpart Rad2. This factor is required for efficient transcription by RNA Polymerase II (Lee et al., 2002a), similar to the requirement for Rad26, the yeast CSB homolog (Lee et al., 2001), and deletion of these genes individually led to a decline in transcription and defects in growth. Interestingly, these defects were much more pronounced in the *rad2 rad26* double mutant (Lee et al., 2002a).

A model, which is linked to the idea of transcription defects, implicates the factors underlying CS phenotypes in the switching between repair and transcription modes. TFIIH is involved in both processes, and after completion of repair it should be necessary to make this complex available for transcription again. As mentioned earlier, the CAK complex is lost from the TFIIH core complex after DNA damage, but comes back after successful DNA repair, allowing transcription to resume (Coin et al., 2008). It could be envisaged that CSB mediates this switching from the repair to the transcription mode. The involvement of XPG in the association of CAK with the core TFIIH nicely fits into this model (Ito et al., 2007). It could also explain the involvement of CSA, which is needed to remove CSB, and possibly other components of the

DNA repair machinery, once the lesion is removed (Groisman et al., 2006), in order to allow efficient transcriptional recovery.

Recent *in vivo* results by the Egly laboratory indicate that CSB is required for transcription of certain genes after DNA damage, even if these genes themselves are not damaged (Proietti-De-Santis et al., 2006). Chromatin-immunoprecipitation experiments showed that in cells from CSB patients, RNAPII as well as general transcription factors are quickly lost after UV irradiation from the promoters of the constitutively expressed DHFR and GAPDH genes, but not from the damage-inducible and p53-responsive MDM2 and GADD45 genes. Moreover, phosphorylated forms of Rpb1 (phosphorylated either on Serine 5 or Serine 2 of the C-terminal repeat domain) rapidly disappear in CSB cells, but not in wild type cells (Proietti-De-Santis et al., 2006). These results show that cells from CS patients may have a defect in transcription of certain genes, especially after DNA damage induction. Genome-wide expression analysis, comparing wild type cells and cells from a CSB patient, have been carried out, and the results indicate that the expression of a large number of genes are affected by the CSB protein, both positively and negatively (Newman et al., 2006). Interestingly, there is a considerable overlap between genes deregulated by loss of CSB and those affected by disruption of chromatin structure, for example by treatment of cells with histone deacetylase (HDAC) inhibitors. Many of the affected genes are involved in inflammation, and the authors speculated that the severe phenotypes in CS patients may be caused by misexpression of growth-suppressive, inflammatory, and pro-apoptotic pathways (Newman et al., 2006). If this is correct, CSA patients as well as cells from patients with combined XP/CS should display the same defects. Evidence for this has, however, not yet been reported.

In addition to the involvement of CSB, TFIIH and XPG in transcription by RNAPII, work from the Grummt laboratory has shown that these factors are also linked to synthesis of ribosomal RNA (rRNA) by RNA Polymerase I (RNAPI) (Bradsher et al., 2002; Iben et al., 2002). All of these proteins can be copurified in a complex with RNAPI, and CSB is found in the nucleolus (Bradsher et al., 2002). Most importantly, CSB stimulates transcription from rDNA both *in vitro* and *in vivo* (Bradsher et al., 2002). CSA was not involved in this process. One study has also linked CSB in transcription of RNA Polymerase III transcribed genes, affecting the elongation of transcription of highly structured RNAs (Yu et al., 2000).

Another hypothesis, which might be suitable to explain the neurological defects of CS-patients, is the involvement of the factors underlying Cockayne's syndrome in the removal of oxidative DNA damage. Because of the high metabolic activity of the brain, neuronal cells consume more oxygen than other cells, leading to byproducts such as reactive oxygen species (ROS) and consequently an increased incidence of oxidative lesions (Tsutakawa and Cooper, 2000). Even

though the main publication implicating XPG, TFIIH and CSB in the transcription-coupled repair of 8-oxoguanine lesions (Le Page et al., 2000) has been retracted, several other studies have since then implicated CSB in this process, carried out in both rodents (Khobta et al., 2009; Osterod et al., 2002; Sunesen et al., 2002; Trapp et al., 2007) and in human cell lines (Spivak and Hanawalt, 2006; Tuo et al., 2001). Convincing evidence supporting this model in human cells comes from studies comparing the effects of oxidative stress on cells from CS and UV^SS patients (Spivak and Hanawalt, 2006). Importantly, CSA and CSB cells display an increased sensitivity towards hydrogen peroxide compared to wild type cells, whereas UV^SS cells do not. Furthermore, even though host cell reactivation (HCR) experiments using a UV-damaged reporter gene showed that both CS and UV^SS cells display a similar defect, only CS cells, but not UV^SS cells, were deficient in HCR of reporter genes containing the oxidative lesions thymine glycol (Tg) or 8-oxoguanine (8-oxoG) (Spivak and Hanawalt, 2006). This study provided the first evidence for a difference between CS and UV^SS at the cellular level. More recently, analysis of the first UV^SS patient with a mutation in the CSA protein led to a similar result. Cells from this individual were no more sensitive to oxidative stress than wild-type cells, whereas cells from CSA patients were more sensitive (Nardo et al., 2009). Strikingly, expression of the mutated CSA protein found in the UV^SS patient in cells of the CSA patient was able to rescue sensitivity to oxidative damage, but not the sensitivity to UV damage, clearly showing that the functions of the CSA protein mediating survival after UV and oxidative damage can be separated by a single point-mutation (Nardo et al., 2009).

More evidence for an involvement of CSB in BER comes from studies on poly(ADP-ribose) polymerase I (PARP-1), a factor which plays important roles in BER. PARP-1 binds to several BER components, including XRCC1, DNA polymerase β, and DNA ligase III (Caldecott et al., 1996; Masson et al., 1998), and stimulates the general BER process (Dantzer et al., 2000; Durkacz et al., 1980). Interestingly, the PARP-1 dependent stimulation of repair depends on the presence of CSB (Flohr et al., 2003). Furthermore, CSB binds both *in vitro* and *in vivo* to PARP-1 (Thorslund et al., 2005). Upon oxidative stress, the CSB/PARP-1 complex relocates to the nucleus, and CSB gets modified by PARP-1, which negatively affects its ATPase activity (Thorslund et al., 2005). Importantly, cells lacking functional CSB were more sensitive to PARP-1 inhibition than wild type cells, indicating that CSB is required for an alternative pathway to the one mediated by PARP-1, and the authors speculated that this might be the transcription-coupled removal of oxidative lesions (Thorslund et al., 2005).

1.3.3.3 TC-NER in Saccharomyces cerevisiae

Based on sequence similarity, the budding yeast homologues of CSB and CSA were cloned and named *RAD26* and *RAD28*, respectively (Bhatia et al., 1996; van Gool et al., 1994). Whereas the *RAD26* gene was indeed shown to be involved in TC-NER in yeast cells (van Gool et al., 1994), mutant strains lacking *RAD28* were found to be TC-NER proficient, despite some genetic evidence that *RAD26* and *RAD28* act in the same pathway (Bhatia et al., 1996). No function has since then been reported for the Rad28 protein.

RAD26 encodes a protein of around 128 kDa which, like its bacterial and human counterparts, acts as a DNA-dependent ATPase, but despite the presence of helicase motifs lacks detectable helicase activity (Guzder et al., 1996). Evidence for additional functions of the Rad26 protein, besides activation of TC-NER, has been obtained. Similar to CSB, Rad26 has been shown to be required for efficient transcription elongation by RNA Polymerase II (Lee et al., 2001). Furthermore, it has been speculated that Rad26 functions independently of DNA repair in promoting transcription through damaged bases after treatment with Methyl-methane sulfonate (MMS) (Lee et al., 2002b). Most of the work on this factor has, however, been focused on its function in TC-NER.

Surprisingly, even though *rad26Δ* mutants were proposed to be completely deficient for TC-NER, they were not more sensitive to UV irradiation than wild type cells (van Gool et al., 1994). The reason for this is that yeast cells can remove DNA damage also in the transcribed strand rather efficiently by GG-NER, via the *RAD7* and *RAD16* gene products. Indeed, cells simultaneously lacking one of these GG-NER genes and *RAD26* are much more UV-sensitive that cells lacking only the GG-NER gene (Verhage et al., 1996a). In theory, if the Rad26 protein is required for all TC-NER and the Rad7/Rad16 complex is indispensible for GG-NER, then the *rad7Δ rad26Δ* and *rad16Δ rad26Δ* double mutants should display the same sensitivity as the completely NER deficient *rad14Δ* mutant. Unexpectedly, this was not the case, as the *rad14Δ* mutant was still more sensitive than the *rad7Δ rad16Δ rad26Δ* triple mutant (Verhage et al., 1996a). This puzzle was solved in 2002, when it was shown that budding yeast possesses a second TC-NER pathway, which is dependent on the Rpb9 protein (Li and Smerdon, 2002), a non-essential RNA Polymerase II subunit (Woychik et al., 1991). Thus, *rpb9Δ rad16Δ rad26Δ* cells are as sensitive to UV-irradiation as *rad14Δ* cells (Li and Smerdon, 2002).

1.3.3.4 Speculations about the mechanism of TC-NER in eukaroytic cells

Even though the fact that TC-NER is operative in rodents, humans and yeasts has been known for decades (Bohr et al., 1985; Mellon et al., 1986; Mellon et al., 1987; Terleth et al., 1989), and the factors responsible for the coupling between transcription and repair have been cloned and purified (Groisman et al., 2003; Henning et al., 1995; Selby and Sancar, 1997b; Troelstra et al., 1992), the exact mechanism of TC-NER in eukaryotic cells still remains a mystery. The fact that both CSB and Rad26 display some sequence and functional similarity with the *E.coli* Mfd protein makes it tempting to speculate that the mechanism of Mfd action has been conserved during evolution. Unfortunately, however, no *in vitro* system reconstituted with highly purified proteins, such as the one in *E.coli* (Selby and Sancar, 1993) has been established for eukaryotic TC-NER, and some characteristics of the coupling factors, such as disruption of a damage-stalled ternary complex, have already been shown to be different between the prokaryotic and eukaryotic proteins (Selby and Sancar, 1997b).

One fact that is definitely conserved between bacterial and eukaryotic TC-NER is that the arrest of a transcribing RNA Polymerase complex at the site of a DNA lesion serves as the initiating signal for this pathway. It has been convincingly shown that if transcription is inhibited, either by using the drug alpha-amanitin in mammalian cells (Christians and Hanawalt, 1992) or by using the temperature-sensitive *rpb1-1* mutant in yeast (Sweder and Hanawalt, 1992), TC-NER can no longer be observed.

The subsequent steps in the pathway are poorly understood, but several lines of evidence suggest that the eukaryotic coupling factors Rad26 and CSB, similar to Mfd, bind to damage-stalled RNA Polymerase II complexes and link it to components of the NER machinery, most importantly the TFIIH complex. In a reconstituted *in vitro* transcription system using tailed templates, Tantin and colleagues could show that CSB, but not CSA, is able to bind to a ternary elongation complex (Tantin et al., 1997), and that this complex is able to recruit another complex containing TFIIH subunits (Tantin, 1998). Further evidence for a bridging function between stalled RNAPII and TFIIH was obtained using high-resolution NER studies in budding yeast. The TFIIH complex only dissociates from RNAPII 30-40 bases downstream of the transcription initiation site. Interestingly, TC-NER in this region of the *URA3* gene is independent of the Rad26 protein (Tijsterman et al., 1997), suggesting that Rad26 is only required for TC-NER during the elongation phase, after dissociation of TFIIH. Another interesting finding of the same group was that repair of lesions in the NTS of *URA3*, but not in the TS, is influenced by the presence of nucleosomes, with CPDs in internucleosomal regions being repaired more efficiently than those located at the nucleosomal cores (Tijsterman et al., 1999). Surprisingly, lesions in internucleosomal regions are repaired less efficiently in the TS

than in the NTS in *rad26Δ* mutants, indicating that the stalled RNAPII complex is a physical impediment to DNA repair, and that Rad26 is required to somehow remove it, or at least move it out of the way (Tijsterman and Brouwer, 1999), a situation somewhat reminiscent of that in *E.coli* (Selby and Sancar, 1990).

Results from a reconstituted *in vitro* system using human cell extracts implicates not only CSB, but also XPG, in recognition of stalled RNA Polymerase II (Sarker et al., 2005), and provides an explanation for the involvement of a non-catalytic activity of XPG in TC-NER (Nouspikel et al., 1997). Interestingly, even though CSB was able to bind to transcription-sized DNA bubbles by itself, binding and ATPase activity was enhanced by XPG, and subsequent ATP-dependent remodelling by TFIIH was necessary for XPG-incision of the DNA (Sarker et al., 2005). A different *in vitro* system by Lainé and Egly used an RNAPII elongation complex stalled at a cisplatin lesion as a bait to identify factors in cellular extracts, which can bind to it (Laine and Egly, 2006). They identified the sequential recruitment of TFIIH, RPA, XPA, XPG and finally XPF. Surprisingly, CSB was not required for the recruitment of repair factors, but it was needed for incision (Laine and Egly, 2006). In contrast to this finding, work using *in vivo* crosslinking, followed by chromatin immunoprecipitation (ChIP) and Western blot, showed that after UV irradiation, hyperphosphorylated RNAPII seems to be bound to CSB at DNA damage, and this binding is required for the recruitment of the CSA-containing ubiquitin ligase complex (Fousteri et al., 2006). According to this study, CSB is also required to recruit all the NER factors. Binding of other factors, like XAB2 and HMGN1 required both CSB and CSA (Fousteri et al., 2006).

Reports by other groups, carried out mainly in budding yeast, are not as easy to reconcile with the model that the coupling factors recruit repair factors to stalled RNAPII complexes. Sweder and colleagues reported that the requirement for the Rad26 protein in TC-NER is dependent on the carbon-source used to grow the cells, with a TC-NER defect being obvious in the *rad26Δ* mutant only when it was grown in glucose, but not when it was grown on galactose (Bucheli et al., 2001). Furthermore, the TCR defect caused by deletion of *RAD26* was shown to be suppressed by additional deletion of *SPT4*, a factor involved in the regulation of transcription elongation (Jansen et al., 2000). The Spt4 protein is involved in regulating the transition between initiation and elongation (Wada et al., 2000; Yamaguchi et al., 1999), and one possible explanation for the observed lack of Rad26 requirement for TCR in the *spt4Δ* background is that TFIIH no longer dissociates from RNAPII during elongation. This would make sense in light of the finding that Rad26 is not required for TCR in the region where TFIIH is still bound to the transcription machinery (Tijsterman et al., 1997). Surprisingly, however, TFIIH localisation across the examined genes was not altered by loss of either *SPT4* or *RAD26*. (Jansen et al., 2002). Instead, DNA damage led to a loss of RNA Polymerase II phosphorylated

at serine 5 from promoters, and this was more pronounced in *rad26Δ* cells and less pronounced in *spt4Δ* cells. Most importantly, this increased loss in *rad26Δ* cells was suppressed by additional deletion of *SPT4*. Taken together, this work provided some evidence for the idea that the requirement of Rad26 in TC-NER is indirect, via the regulation of transcription after DNA damage (Jansen et al., 2002).

In conclusion, the exact mechanism of transcription-repair coupling in eukaryotic cells remains elusive, and more work will be necessary to gain further insight into this process and the roles of Rad26, CSB and CSA.

1.3.4 DNA damage-induced Rpb1 ubiquitylation and degradation

Regulated protein ubiquitylation, the covalent attachment of a small (<10 kDa) protein called ubiquitin to a lysine residue in the target protein, plays an essential role in virtually all cellular processes in eukaryotes, including DNA repair, transcription, replication, cell cycle progression, and signal transduction. The process involves an enzymatic cascade consisting of ubiquitin activating enzymes (E1), ubiquitin conjugating enzymes (E2), and ubiquitin ligases (E3) (reviewed in (Pickart and Eddins, 2004)). Target proteins can be modified either by mono-ubiquitylation or poly-ubiquitylation, and in the latter case different lysine residues in ubiquitin can be used for the formation of poly-ubiquitin chains, most importantly lysine 48 (K48) and lysine 63 (K63) (Pickart, 2001). In the case of K48-linked chains, modification is in most cases followed by degradation of the target by the 26S proteasome, while chains linked through other residues have mainly proteolysis-independent roles (Pickart, 2001).

1.3.4.1 Identification of Rpb1 as a substrate for ubiquitylation

An interesting target for ubiquitylation in both yeast and human cells is Rpb1, the largest subunit of the RNAPII complex (Bregman et al., 1996; Huibregtse et al., 1997) (see Figures 1.1 and 1.2). In both systems, this poly-ubiquitylation was shown to occur after DNA damage and this leads to degradation of Rpb1 by the 26S proteasome (Beaudenon et al., 1999; Bregman et al., 1996; Ratner et al., 1998). Later work indicated that this modification is not only seen after DNA damage, but also in other situations which result in problems with transcription elongation, such as treatment with the drug 6-azauracil (6-AU; restricts nucleotide availability), and the absence of the transcription elongation factor TFIIS (Somesh et al., 2005). The first factor shown to be involved in this reaction was the HECT-domain E3 ubiquitin ligase Rsp5 in budding yeast (Huibregtse et al., 1997), and later its human homologue, Nedd4 (Anindya et al.,

2007). The remaining enzymes required for the entire process in yeast were identified as Uba1 (E1) and Ubc4/5 (E2), when the entire reaction was reconstituted *in vitro* with highly purified factors (Somesh et al., 2005). The initial studies of Rpb1 ubiquitylation suggested that Rpb1 in the elongating form of RNAPII is targeted, because the modified form of the protein was phosphorylated on its CTD (Ratner et al., 1998). Indeed, the use of free RNAPII or RNAPII in a ternary complex showed that Rpb1 in a ternary complex was a much better substrate for the *in vitro* ubiquitylation reaction (Somesh et al., 2005).

The reconstitution of the ubiquitylation reaction *in vitro* with yeast proteins led to the identification of 2 distinct ubiquitylation sites on Rpb1, namely lysine 330 (K330) and lysine 695 (K695) (Somesh et al., 2007), and mutation of these residues leads to sensitivity to the drug 6-azauracil (6-AU; increases RNAPII stalling by restricting nucleotide availability), indicative of defects in transcription elongation. Surprisingly, the chains formed by Rsp5 *in vitro* were recently shown to be K63-linked, which is usually not linked to proteasomal degradation of proteins. Furthermore, experiments on the genetic requirements of Rpb1 degradation showed that another E3 ligase complex, containing Elc1, Cul3 and Ela1 is also required for this process (Ribar et al., 2006, 2007). A solution for the apparent paradox of an involvement of 2 distinct ubiquitin ligases in the ubiquitylation of a substrate comes from recent experiments in both yeast and human cells, showing that polyubiquitylation of Rpb1 is carried out in 2 sequential steps, mono-ubiquitylation by Rsp5/NEDD4, and the subsequent formation of a poly-ubiquitin chain by the Elongin/Cullin-complex based on this (Harreman et al, in preparation).

1.3.4.2 Def1, a factor controlling Rpb1 ubiquitylation in budding yeast

The Def1 protein was initially identified as a binding partner of Rad26 on chromatin in budding yeast, and was shown to be required specifically for Rpb1 degradation in response to UV irradiation (Woudstra et al., 2002). Identification of a factor responsible for RNAPII degradation in a complex with a factor involved in TC-NER was interesting in light of the finding that, at least in prokaryotes, RNAP has to be displaced from the damage in order for TC-NER to occur (Selby and Sancar, 1990). It was, however, shown that Def1 is only required for Rpb1 degradation and not for TC-NER, confirming earlier results using strains lacking the responsible E3 for Rpb1 ubiquityation, Rsp5 (Lommel et al., 2000). *Vice versa,* Rad26 was exclusively required for TC-NER and not for Rpb1 degradation, and it even had an inhibitory effect on this process. Interestingly, the Def1 protein was only required for Rpb1 degradation in the presence of Rad26, indicating that it is required after DNA damage to overcome the inhibitory effect of Rad26 (Woudstra et al., 2002). Surprisingly, genetic experiments showed that *DEF1* deletion does not lead to significant sensitivity to UV irradiation, but it dramatically

increases the sensitivity of completely NER deficient strains, such as *rad14Δ* (Woudstra et al., 2002). This finding led to the conclusion that ubiquitylation and degradation of RNAPII is a 'last resort' mechanism to remove irreversibly arrested RNAPII complexes that cannot be restarted by repair of the lesion responsible for the arrest.

Follow-up work on the exact function of the Def1 protein in the ubiquitylation reaction employed an *in vitro* system using cell-free exacts. Such extracts from wild type cells supported poly-ubiquitylation of Rpb1, whereas extract from *def1Δ* cells did not, but this defect could be rescued by adding back the purified Def1 protein (Reid and Svejstrup, 2004), showing that the effect of Def1 on the reaction is direct. Further strong evidence for a direct involvement was obtained using a reconstituted system with highly purified factors. Here, Def1 specifically enhanced modification of Rpb1 in a ternary elongation complex (Somesh et al., 2005). The exact mechanism of how this regulation is achieved mechanistically is, however, still not understood.

Besides regulating Rpb1 ubiquitylation and degradation, the Def1 protein is involved in other cellular processes, such as maintenance of telomeres (Chen et al., 2005). A similar factor controlling damage-induced Rpb1 polyubiquitylation in human cells has not yet been identified.

1.3.4.3 Reversal of Rpb1 ubiquitylation by Ubp3

In some cases, polyubiquitylation of Rpb1 will be sufficient to restart transcription, possibly by the recruitment of the 19S subunit of the proteasome, which has been shown to have proteolysis-independent roles in transcription elongation (Ferdous et al., 2001). In such a situation, it would be counterproductive to degrade the ubiquitylated protein, and a proofreading mechanism should exist to prevent such unnecessary degradation. Indeed, the ubiquitin-specific protease Ubp3 in budding yeast has been shown to deubiquitylate Rpb1 both *in vivo* and *in vitro* (Kvint et al., 2008). Consistent with a role in transcription elongation, deletion of *UBP3* leads to 6-AU sensitivity and increases the sensitivity of other elongation mutants, such as a *dst1Δ* strain lacking TFIIS. Furthermore, *ubp3Δ* cells display a higher level of Rpb1 ubiquitylation both in the absence and presence of damage, and they degrade Rpb1 faster after UV-treatment. Importantly, in strains with defects in NER, deletion of *UBP3* leads to a decrease in UV-sensitivity, providing further evidence that Rpb1 degradation is a 'last resort' mechanism and that efficient removal of RNAPII is important in situations in which the block to transcription can not be relieved by repair of the lesion (Kvint et al., 2008).

1.4 The DNA damage checkpoint

As already mentioned, faithful transmission of the genetic material between generations is essential for cell survival, and DNA repair mechanisms exist to ensure that DNA lesions are efficiently removed in order to preserve genomic integrity and prevent the formation of cancer (Hoeijmakers, 2001). Besides DNA repair pathways, eukaryotic cells have evolved another mechanism to safeguard their genome in the presence of DNA damage. A complex signal transduction cascade, termed the DNA damage checkpoint (DDC), is activated after genotoxic stress. Many of its components are protein kinases, and DDC activation leads to the phosphorylation of a vast number of cellular proteins which function in many cellular pathways (Albuquerque et al., 2008; Matsuoka et al., 2007; Smolka et al., 2007). Phosphorylation of these components by the DDC leads to desired cellular outcomes, most importantly delay of cell cycle progression, activation of DNA repair, activation of a damage-specific transcriptional program, stabilization of stalled replication forks, and in multicellular organisms the induction of apoptosis (reviewed in(Longhese et al., 1998; Rouse and Jackson, 2002a; Sancar et al., 2004)).

The key players of the DDC can be classified according to their function in the signal transduction pathway. Damage sensors are involved in the initial recognition of the DNA lesions, and effector proteins are responsible for achieving the desired outcome of checkpoint activation. In between these two classes of proteins are a number of signal transducers responsible for the relay of the signal from the sensors to the effectors (Longhese et al., 1998; Zhou and Elledge, 2000).

Of central importance for the DDC in budding yeast is the Mec1 kinase, whose activation is necessary for all checkpoint responses (Longhese et al., 1998). An important substrate for this kinase is the Rad9 adapter protein (Gilbert et al., 2001), phosphorylation of which is required to mediate its interaction with the downstream effector kinases Chk1 and Rad53. Phosphorylation of Chk1 and Rad53 by Mec1 leads to effector kinase activation (Sanchez et al., 1999; Sun et al., 1996). After replication stress, the adapter protein Mrc1 is thought to fulfill the function of Rad9 (Alcasabas et al., 2001). Once activation of Rad53 and Chk1 is achieved, these kinases mediate the downstream events in damage signalling by phosphorylating effector proteins (reviewed in (Lowndes and Murguia, 2000)). Another kinase, called Dun1, acts downstrem of Rad53 in the cascade (Zhou and Elledge, 1993).

A large number of connections exist between the DDC and the cell cycle, replication, transcription, and repair machineries of the cell. In this section I will give a brief introduction of the main players of the checkpoint in the yeast *S. cerevisiae*, as well as disease-related

homologues in humans, with a particular emphasis on the kinase components. The regulation of cell cycle progression will not be mentioned here, as this is not the focus of this work; instead, the main focus will be on the interplay between the DDC and DNA repair. A simplified overview of the DNA damage checkpoint in budding yeast can be found in Figure 1.3.

1.4.1 The main components of the DNA damage signalling pathway

1.4.1.1 The activation of the PI3K-like kinases

A family of serine/threonine protein kinases, which show strong similarity to the lipid kinase phosphatidyl-inositol-3-kinase (PI3K), plays an important role in the DDC in all eukaryotes. Members of this family include Mec1 and Tel1 in budding yeast and their homologues ATM, ATR and DNA-PK in humans (reviewed in (Elledge, 1996)).

Mec1 is required for all kinds of DNA damage responses (reviewed in (Longhese et al., 1998)). Deletion of *TEL1* results in telomere shortening (Smogorzewska and de Lange, 2004), but does not show obvious checkpoint signalling defects, or in increased sensitivity towards DNA damaging agents (Morrow et al., 1995). Despite the lack of severe checkpoint defects in the *tel1Δ* strain, deletion of *TEL1* in the background of a *mec1* mutant results in increased sensitivity to DNA damage, and increased expression of *TEL1* can alleviate the damage sensitivity of a *mec1* mutant (Morrow et al., 1995). These findings indicate that the Tel1 kinase has functions in the DNA damage response, but that its contribution is usually masked by Mec1.

In contrast to the situation in budding yeast, both ATM (the Tel1 homologue) and ATR (the Mec1 homologue) have important functions in the checkpoint response in mammalian cells, and are thought to be activated by different kinds of DNA damage. Whereas ATM is specifically involved in the response to unprocessed double-strand breaks (Jazayeri et al., 2006; Longhese et al., 2006), ATR appears to be activated by processed DSB ends, replicative stress, and intermediates of DNA repair pathways (Jazayeri et al., 2006; Longhese et al., 2003; Longhese et al., 2006).

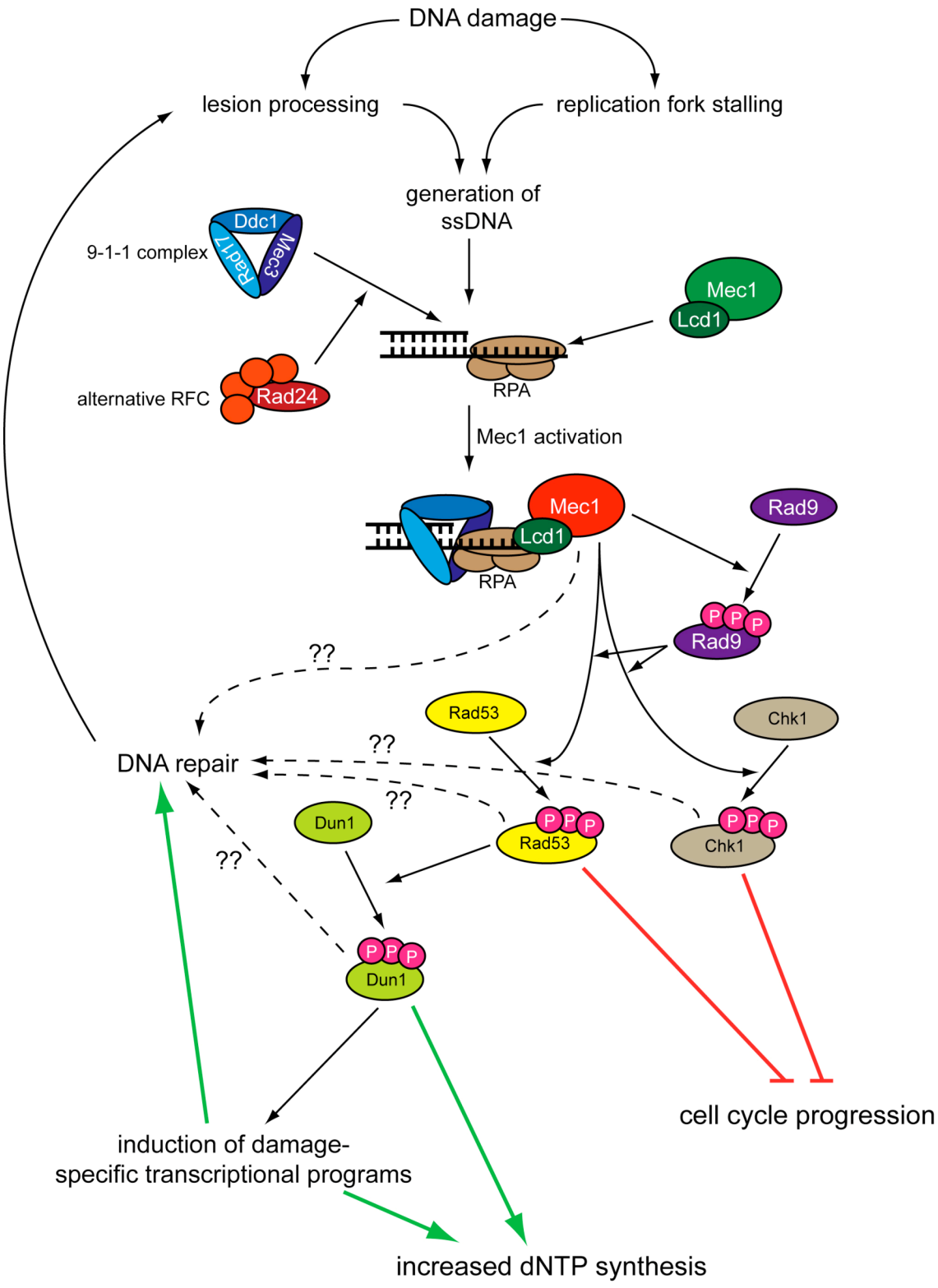

Figure 1-3 Simplified overview of the DNA damage checkpoint in budding yeast

see text for details

Both Mec1 and Tel1 are recruited to the sites of DNA lesions, but they are not thought to be able to directly recognize the damage. The Mec1 kinase exists in a heterodimeric complex with its binding partner Lcd1/Ddc2/Pie1, the yeast homolog of the human ATRIP protein (Cortez et al., 2001; Rouse and Jackson, 2000, 2002b; Wakayama et al., 2001). Lcd1 and ATRIP are required for the recruitment of Mec1 and ATR, respectively, to RPA-coated ssDNA, a structure commonly found after replicative stress or as a DNA repair intermediate (Rouse and Jackson, 2002b; Zou and Elledge, 2003). Neither Mec1 nor Lcd1 seem to have functions outside of the complex in the *sml1Δ* background, as the phenotype of the double mutant is not more dramatic than the phenotype of the single mutants (Rouse and Jackson, 2000).

Activation of PIKK family members also depends on other DNA damage sensors, such as the PCNA-like Ddc1-Mec3-Rad17 complex (the budding yeast homologs of the Rad9-Hus1-Rad1 complex, better known as the 9-1-1 complex) and the Rad24-Rfc2-5 alternative replication factor C (RFC) complex, which is responsible for 9-1-1 loading (Kondo et al., 2001; Melo et al., 2001). The 9-1-1 complex stimulates the kinase activity of Mec1 (Majka et al., 2006). Importantly, colocalization of the 9-1-1 checkpoint clamp and Mec1-Lcd1-RPA has been shown to be sufficient for the activation of the DNA damage checkpoint, even in the absence of DNA damage (Bonilla et al., 2008).

Both yeast Mec1/Lcd1 and human ATR/ATRIP have an important role during normal cell growth even in the absence of exogenous DNA damage. This is exemplified by the fact that both factors are encoded by essential genes (Brown and Baltimore, 2000; Desany et al., 1998; Paciotti et al., 2000; Wakayama et al., 2001). The same is true for budding yeast Rad53, one of the downstream effector kinases of Mec1 (see below). The important function of these factors during the normal cell cycle is the regulation of DNA replication. Cells lacking *MEC1* or *RAD53* display slower fork progression and difficulty in completely replicating their DNA (Raveendranathan et al., 2006; Tercero and Diffley, 2001), and *MEC1* prevents fork stalling and fragmentation of chromosomes at so-called 'replication slow zones' (RSZs) (Cha and Kleckner, 2002). Importantly, the lethality of both *MEC1* and *RAD53* deletion can be suppressed either by deletion of *SML1*, the gene encoding the inhibitor of the large subunit of the ribonucleotide reductase (RNR) (Zhao et al., 1998), or by overexpression of RNR subunits (Desany et al., 1998). This indicates that the essential funtion of these proteins during S-phase is to increase the availability of dNTPs and prevent prolonged fork stalling at defined locations.

1.4.1.2 The Rad9 adapter protein

Historically, the *RAD9* gene was the first checkpoint-component to be identified more than 20 years ago (Weinert and Hartwell, 1988). It is required for the damage checkpoint during all cell cycle phases and its loss leads to an increase in genomic instability (Weinert and Hartwell, 1988, 1990). Rad9 is an important regulator in the activation of the effector kinases Chk1 and Rad53 downstream of Mec1 (Sanchez et al., 1999). This function has been well-characterized in the case of Rad53 activation, but the exact role of Rad9 in activation of Chk1 remains enigmatic.

After DNA damage, Rad9 is phosphorylated in a Mec1-dependent manner (Vialard et al., 1998), and this phosphorylation allows Rad9 dimerization via its C-terminal BRCT-repeats (Soulier and Lowndes, 1999). Modified Rad9 can also be recognized by the Rad53 kinase through interactions between the Rad53 FHA domains and phosphorylated residues in Rad9 (Schwartz et al., 2002; Sun et al., 1998). The activation of the Rad53 kinase requires two different kinds of phosphorylation events, namely direct phosphorylation by the Mec1 kinase and Rad53 autophosphorylation (Gilbert et al., 2001; Sweeney et al., 2005), and both events seem to be mediated by Rad9. On one hand, Rad53 is recruited to the sites of DNA damage by Rad9, thereby allowing phosphorylation of Rad53 by Mec1 (Lisby et al., 2004; Sweeney et al., 2005). On the other hand, binding of Rad53 to Rad9 leads to a local increase in Rad53 concentration, which is a pre-requisite for Rad53 autophosphorylation (Gilbert et al., 2001; Sweeney et al., 2005).

After phosphorylation, Rad53 is released from Rad9, most likely because the modified protein has a lower affinity for the adaptor, and can then mediate the phosphorylation of its substrates (Gilbert et al., 2001). Besides its function in activation of downstream effector kinases, the Rad9 protein is involved in the DNA damage-specific induction of some repair and recombination genes (Aboussekhra et al., 1996) and may serve as an alternative DNA damage sensor in a pathway distinct from that mediated by Rad24-RFC and 9-1-1 complexes (de la Torre-Ruiz et al., 1998; Lydall and Weinert, 1995).

1.4.1.3 The effector kinases Rad53, Chk1 and Dun1

As outlined above, an important function of Mec1 after DNA damage is the activation of the downstream kinases Rad53 and Chk1 (Sanchez et al., 1999; Sun et al., 1996). Rad53 activates another kinase, Dun1, which is an important mediator of some of the downstream events of checkpoint signalling (Bashkirov et al., 2003; Zhou and Elledge, 1993). Together, these effector

kinases mediate the various functions of the DDC, including the phosphorylation of cell cycle regulators, the inhibition of late origin firing, the stabilisation of stalled replication forks, upregulation of dNTP pools, and establishment of DNA damage-induced transcriptional programs (reviewed in (Lowndes and Murguia, 2000; Rouse and Jackson, 2002a)).

Activation of Rad53 is an important, intermediary step in the DNA damage response in yeast (reviewed in (Branzei and Foiani, 2006)). Interestingly, as is the case for *MEC1*, *RAD53* is an essential gene and the lethality of *RAD53* deletion can also be suppressed by prior deletion of *SML1* (Desany et al., 1998; Zhao et al., 1998). Because of its robust hyperphosphorylation after checkpoint activation, modified Rad53 is widely used as an experimental marker for checkpoint activation. In addition to the decrease in its electrophoretic mobility after genomic insults, activated Rad53 has an autokinase activity, which can be measured in order to examine checkpoint activation (Pellicioli et al., 1999).

The Dun1 kinase, originally identified as a mutant deficient in the transcriptional induction of genes after DNA damage (Zhou and Elledge, 1993), is recruited to activated Rad53 through binding by the Dun1 FHA domain (Bashkirov et al., 2003), and then activated by Rad53 dependent phosphorylation of the Dun1 activation loop (Chen et al., 2007). Cells lacking this kinase are sensitive to DNA damage, highlighting its importance for the appropriate response to DNA damage (Zhou and Elledge, 1993). An extensively characterized Dun1 substrate is the ribonucleotide reductase (RNR) inhibitor Sml1. After Dun1-dependent phosphorylation of Sml1, it is targeted for degradation (Zhao and Rothstein, 2002). At the same time, Dun1 leads to the activation of a transcriptional program, involving upregulation of the RNR subunits (see below), and so this kinase controls both the abundance and activity of this enzyme. It is therefore surprising, that even though *MEC1* or *RAD53* deletion is lethal unless *SML1* is deleted or RNR subunits are overepressed (Desany et al., 1998; Zhao et al., 1998), deletion of *DUN1* is not. This suggests that deletion of *MEC1* or *RAD53*, but not *DUN1*, leads to defects requiring increased dNTP synthesis.

1.4.2 Human pathologies associated with defects in DNA damage signalling

1.4.2.1 Ataxia telangiectasia (AT), AT-like-disorder (A-T-LD) and Nijmegen breakage syndrome (NBS)

As already mentioned earlier, the ATM kinase (the human homologue of the yeast Tel1 kinase), responds primarily to unprocessed DSBs (Jazayeri et al., 2006; Longhese et al., 2006).

Mutations in ATM result in defects in G1-S, intra-S and G2-M checkpoints in response to DSB induction, and are associated with the human syndrome Ataxia telangiectasia (AT) (Savitsky et al., 1995; Shiloh, 2003). A characteristic feature of cells from these patients is the failure to stop replication after treatment with ionizing radiation ('radioresistant DNA synthesis'; RDS), and this is commonly used as a diagnostic marker for AT (reviewed in (Lavin, 2008)). The clinical phenotypes of AT patients include progressive neurological symptoms such as ataxia and occulomotor apraxia, as well as immunoglobin deficiencies and predisposition to lymphoma.

The MRN (Mre11/Rad50/Nbs1) complex plays important roles during DSB repair and initiation of ATM signalling, and it is required to recruit the ATM kinase to the site of a DSB (Lee and Paull, 2004). Mutations in the Nbs1 and Mre11 components of this complex lead to the disorders 'Nijmegen breakage syndrome' (NBS) and 'A-T-like disorder' (A-T-LD), respectively (Digweed and Sperling, 2004; Stewart et al., 1999). In agreement with a role of these proteins in DSB repair together with ATM, NBS and AT-L-D patients have a similar DSB repair defect to the one observed in AT patients. NBS patients display additional developmental abnormalities, such as growth retardation and microcephaly (Digweed and Sperling, 2004), which might be explained by partially deficient ATR signalling (see below).

1.4.2.2 Seckel syndrome

Seckel syndrome (SS) is a rare autosomal recessive disorder characterized by severe growth retardation, marked microcephaly, mental retardation, skeletal abnormalities, and characteristic facial features, including a receding forehead and chin, and a protruding nose. Because of the 'bird-like' faces of these patients, the disease was initally given the name 'bird-headed dwarfism' (Harper et al., 1967). Seckel syndrome is a genetically heterogenous disease, and at least 4 indiviual loci have been linked to it (Borglum et al., 2001; Faivre et al., 2002; Goodship et al., 2000; Kilinc et al., 2003), but only 2 genetic defects, in ATR and Pericentrin, have been identified.

The first causative mutation for Seckel syndrome was shown to be in the gene encoding the central checkpoint kinase ATR (leading to ATR-SS) (O'Driscoll et al., 2003). It is important to point out that knock-out of the gene encoding ATR, but not ATM, in mice results in chromosome fragmentation and early embryonic lethality, highlighting the central role of this kinase in the maintenance of genomic stability (Brown and Baltimore, 2000). This situation is reminiscent of the one in budding yeast, where deletion of *MEC1,* but not *TEL1*, results in lethality. In ATR-SS, a point mutation in the ATR gene leads to aberrant mRNA splicing and dramatic reduction, but not a complete loss, of the ATR protein (O'Driscoll et al., 2003). Cells

from ATR-SS patients display increased chromosomal instability in response to replicative stress (Casper et al., 2004), as well as clear defects in ATR-dependent checkpoint signalling, including impaired G2/M checkpoint, increased formation of HU-induced micronuclei, and impaired phosphorylation of ATR substrates (Alderton et al., 2004). Surprisingly, another striking phenotype was the presence of more than 2 centrosomes after nocodazole treatment in a subset of mitotic cells (Alderton et al., 2004). As proper centrosome function is important for normal development of the brain (Lu et al., 2000), this finding was interesting in light of the profound microcephaly found in SS patients.

The second factor found to be mutated in a different group of Seckel syndrome is Pericentrin (PCNT), a protein which plays a structural role in centrosomes, again linking Seckel syndrome to centrosomal function (Griffith et al., 2008). Interestingly, cells from PCNT-SS patients displayed similar defects in the ATR-dependent signalling pathway as the one observed the ATR-SS patients (Alderton et al., 2004), and several lines of evidence suggest that Pericentrin has a signalling role downstream of ATR in the pathway (Griffith et al., 2008).

As mentioned above, a special feature in patients suffering from NBS, which is not shared by AT and A-T-LD patients, is the presence of developmental abnormalities, most importantly growth retardation and microcephaly (Digweed and Sperling, 2004). Nbs1 has been shown to be required not only for signalling through ATM, but also through ATR (Stiff et al., 2005), providing yet another link between ATR-dependent phosphorylation events and the developmental defects in both SS and NBS.

1.4.3 Relationship between DNA repair and the DNA damage checkpoint

As already mentioned, activation of the DNA damage checkpoint cascade leads to a variety of cellular outcomes, including cell cycle delay, stabilization of stalled replication forks, activation of DNA repair pathways, and induction of apoptosis. As this work focusses on the interplay between DNA repair and checkpoint signalling, the following section will focus on this relationship.

1.4.3.1 Activation of the checkpoint by DNA repair intermediates

The signal required for the activation of the DNA damage checkpoint cascade is thought to be Rpa-coated ssDNA, which is efficiently produced when replication forks encounter replication

blocking lesions, thereby leading to uncoupling between the replicative helicase and the DNA polymerase (Rouse and Jackson, 2002a; Zou and Elledge, 2003). Several findings in both yeast and human cells revealed that in non-cycling cells, activation of the DNA damage checkpoint in G1 and G2 in response to UV irradiation requires NER-dependent processing of the lesions and generation of an intermediate structure containing Rpa-coated ssDNA (Bomgarden et al., 2006; Giannattasio et al., 2004; Marini et al., 2006). In yeast, both GG-NER and TC-NER are able to activate the checkpoint (Giannattasio et al., 2004), while in human cells only GG-NER can do so (Marini et al., 2006). It is currently not known whether the short stretches of ssDNA, occuring after processing of a lesion by NER, are sufficient for activating the checkpoint, or if additional processing is required to produce longer stretches, for example by the action of exonucleases. In this respect it is important to note that in budding yeast, Exo1 is involved in the activation of the G2 checkpoint after UV irradiation (Nakada et al., 2004).

Surprisingly, work in human cells has shown that ATR can bind directly to UV-damaged DNA without the need for RPA-coated ssDNA (Unsal-Kacmaz et al., 2002), and that ATR, RPA and the 9-1-1 complex can be found at sites of UV-lesions in the absence of replication and repair (Jiang and Sancar, 2006), showing that at least in some situations, checkpoint factors can directly detect lesions without the formation of repair intermediates.

1.4.3.2 Activation of damage-dependent transcription by the DDC

1.4.3.2.1 The SOS-response in E.coli

After exposure to DNA damage, stress responses result in specific alterations of gene expression patterns in both prokaryotic and eukaryotic cells. The prototype of such a transcriptional response is the SOS-system in *E.coli*, which leads to a coordinated induction of about 48 genes (Courcelle et al., 2001). These genes include factors involved in recombination, nucleotide excision repair, translesion synthesis, and inhibition of cell division. The prokaryotic SOS-response relies mainly on the function of 2 proteins, the RecA ssDNA-binding protein and the LexA transcriptional repressor (Little and Mount, 1982; Radman, 1975). Briefly, ssDNA is generated after damage which is bound by RecA, leading to the formation of RecA nucleoprotein filaments. LexA is a transcriptional repressor for SOS-responsive genes, and binding by the RecA nucleoprotein filament induces an autocatalytic cleavage of LexA, relieving the inhibition of target genes. One of these target genes is *lexA* itself, and the increased production of LexA, together with the decrease in ssDNA following repair, leads to a shut-down of the SOS-response.

1.4.3.2.2 Activation of damage-specific transcriptional programs in eukaryotes

The knowledge of damage-specific transcriptional regulation of genes in *E.coli* has led to a large number of studies in *S.cerevisiae,* aimed at the identification of a similar response in eukaryotes. High-throughput technologies, most importantly DNA microarrays, made it possible to study changes in transcriptional profiles after many different types of DNA damage, and have shown that the expression of more than 5 % of the entire yeast genome is affected by DNA damage, both positively and negatively (Gasch et al., 2001; Gasch et al., 2000; Jelinsky et al., 2000; Jelinsky and Samson, 1999). In contrast to the SOS-resonse in prokaryotes, only a small subset of the induced genes are involved in DNA repair.

The involvement of the DNA damage checkpoint in this transcriptional response became apparent when microarray experiments were performed, comparing damage-specific gene expression changes in various checkpoint mutants of *S. cerevisiae* (Gasch et al., 2001). For a large number of genes, such changes were dependent on the Mec1 kinase, and most of those were also influenced by the absence of Dun1, showing that the Mec1-Rad53-Dun1 pathway is mainly important for the transcriptional response to DNA damage. The mechanism of damage-specific transcriptional upregulation of genes have been most extensively studied for the *RNR* genes. Expression of all 4 *RNR* genes (*RNR1-4*) is induced by DNA damaging agents (Elledge and Davis, 1987, 1989, 1990; Huang and Elledge, 1997). In the absence of damage, transcription is repressed by binding of the Crt1 protein to the gene promoters, which in turn recuits the Tup1 and Ssn6 repressors. Activation of the checkpoint leads to active Dun1 kinase, which alleviates this repression by phosphorylation of Crt1 (Huang et al., 1998).

The Rad9 protein has also been implicated in the transcriptional regulation of genes after DNA damage, and target genes involved in NER were shown to be *RAD7, RAD16, RAD23,* and *RAD2* (Aboussekhra et al., 1996). The damage-inducible expression of these genes was also shown by other studies (Bang et al., 1995; Jones et al., 1990; Madura and Prakash, 1986; Siede et al., 1989). This damage-induced upregulation of transcription has been shown to be important for NER efficiency, mainly for efficient removal of lesions from the NTS of active genes (Al-Moghrabi et al., 2003, 2009). Taken together, it is obvious that the damage-induced *de novo* synthesis of repair factors is one way by which the DNA damage checkpoint can increase the repair capacity of cells after DNA damage.

A role for damage-specific transcriptional upregulation of NER factors in mammalian cells has been attributed to the p53 tumor suppressor (reviewed in (Adimoolam and Ford, 2003)).

Importantly, the presence of this factor is specifically required for GG-NER of UV induced DNA lesions (Ford et al., 1998; Ford and Hanawalt, 1995, 1997). This selective requirement of p53 for GG-NER might be explained by the p53-dependent transcriptional upregulation of the GG-NER damage recognition factors *XPC*, *p48* (*DDB2*) and *GADD45* (Adimoolam and Ford, 2002; Smith and Seo, 2002; Tan and Chu, 2002). Indeed, overexpression of *DDB2* enhances GG-NER in a p53-deficient background (Fitch et al., 2003).

1.4.3.3 Direct phosphorylation of repair factors by checkpoint kinases

Given that many factors in the DNA damage checkpoint cascade are protein kinases, it is conceivable that the activities of DNA repair factors are influenced by post-translational modifications. Indeed, several large-scale studies aimed at the identification of novel substrates for checkpoint factors, such as Mec1 and Rad53 in yeast and ATM/ATR in humans, have found a large number of phosphorylation targets, and many of them are involved in repair pathways (Albuquerque et al., 2008; Matsuoka et al., 2007; Smolka et al., 2007). For most of them, a physiological significance of the modification remains to be determined. For a few, phosphorylation has already been shown to have an influence on their activity. In budding yeast, the efficiencies of homologous recombination and NHEJ are altered by checkpoint-dependent phosphorylation of Rad55 (Herzberg et al., 2006) and Nej1 (Ahnesorg and Jackson, 2007), respectively. In mammalian BER, Chk2-dependent phosphorylation of the scaffold protein XRCC1 stimulates repair efficiency by increasing its interaction with DNA glycosylases (Chou et al., 2008).

A couple of lines of evidence, mainly from human cells, also suggest an involvement of checkpoint-dependent protein phosphorylation in NER efficiency. The central NER protein XPA was identified as a target for the ATR kinase, and this phosphorylation is required for efficient survival after UV irradiation (Wu et al., 2006b). Furthermore, ATR is required for nuclear import of XPA, although this is phosphorylation-independent, but instead relies on the physical association between ATR and XPA (Shell et al., 2009; Wu et al., 2006a). Using a novel flow-cytometry based assay for the evaluation of NER efficiency, it was shown that inhibition of ATR led to a total inhibition of UV lesion removal during S-phase in primary lung fibroblasts, highlighting the important role of damage signalling in this repair pathway (Auclair et al., 2008). A similar role for Mec1 in budding yeast has not yet been shown.

2 Materials and Methods

2.1 Buffers, Media and Solutions

Standard growth media were obtained from the media production services unit of Cancer Research UK. Deionised water was used for all media, and solid media additionally contained 1.6 % agar. Prior to addition of sugar, amino acids and drugs, the media was autoclaved for 15 minutes.

2.1.1 Yeast media

2.1.1.1 YPD

1 % w/v yeast extract (DIFCO)
1 % w/v peptone (DIFCO)
2 % w/v glucose
Supplemented with adenine to a concentration of 40 µg/ml

2.1.1.2 Selective yeast drop-out media

6.7 mg/ml Yeast nitrogen base without amino acids (DIFCO)
2 % w/v of sugar (glucose, galactose or raffinose)
1.4 mg/ml Yeast Synthetic Drop-Out Medium Supplement (Sigma)
40 µg/ml adenine
40 µg/ml uracil
80 µg/ml leucine
40 µg/ml tryptophane
40 µg/ml histidine

All components were dissolved in water to obtain medium. The particular amino-acids being selected for were not added to the growth medium. In order to pour selective plates, the water was replaced with 1.6 % agar.

2.1.2 Bacterial media

2.1.2.1 LB (rich medium)

1 % w/v bacto tryptone (DIFCO)

0.5 % w/v yeast extract (DIFCO)

1 % w/v NaCl

pH adjusted to 7

2.1.2.2 SOC medium

2 % w/v bacto-tryptone (DIFCO)

0.5 % w/v yeast extract (DIFCO)

10 mM NaCl

2.5 mM KCl

10 mM $MgCl_2$

10 mM $MgSO_4$

20 mM glucose

pH adjusted to 7

2.1.2.3 NZY medium

10 mg/ml yeast extract

5 mg/ml NaCl

2 mg/ml Glucose

16 mg/ml NZ-Amine A (Sigma)

pH adjusted to 7

2.1.3 General solutions

2.1.3.1 PBS (Phosphate Buffered Saline)

0.13 M NaCl

7 mM Na_2HPO_4

2 mM NaH_2PO_4

pH adjusted to 7.5

2.1.3.2 TE (Tris-EDTA)

1 mM Tris-Cl pH 7.5
0.1 mM EDTA pH 8.0

A 10 x stock solution was routinely used to prepare 1 x TE.

2.1.3.3 TBE (Tris-Borate-EDTA)

89 mM Tris
89 mM boric acid
2 mM EDTA

A 10 x stock buffer was routinely used to prepare 1 x TBE.

2.1.3.4 TE/LiOAc

1 x TE pH 7.5
0.1 M lithium acetate

2.1.3.5 PEG/TE/LiOAc

same composition as TE/LiOAc, but instead of water 50 % PEG (3350) was used to prepare the solution

2.1.3.6 10 x DNA loading buffer for agarose electrophoresis

20 mM EDTA pH 8.0
50 % glycerol
0.05 % bromophenol blue

2.1.3.7 5 x SDS-PAGE loading buffer

225 mM Tris-Cl pH 6.8
50 % glycerol
5 % SDS
0.05 % bromophenol blue
250 mM DTT

2.1.3.8 Formamide loading buffer for denaturing PAGE

95 % deionized formamide

20 mM EDTA pH 8.0

0.05 % Xylene cyanol FF

0.05 % bromophenol blue

2.1.3.9 100 x Protease inhibitor cocktail

28.4 µg/ml leupeptin

137 µg/ml pepstatin A

17 µg/ml PMSF

33 µg/ml benzamidine

all components were dissolved one by one in 100 % ethanol and the mix was stored at -20°C

2.1.3.10 Yeast lysis buffer

20 % glycerol

150 mM Tris-Acetate pH 7.5

3 mM EDTA

50 mM potassium acetate

0.1 % Triton X-100

2 mM N-Ethylmaleimide (NEM, Sigma)

20 µM lactacystin (Cayman Chemical Company)

1 x Protease inhibitor cocktail

2.1.3.11 TEV elution buffer

10 mM Tris-Cl pH 8.0

150 mM NaCl

2 mM beta-mercaptoethanol

2.1.4 Buffers for the Nucleotide Excision Repair assay

2.1.4.1 Sorbitol stock solution

0.9 M Sorbitol

100 mM Tris-Cl pH 8.0

100 mM EDTA pH 8.0

28 mM beta-mercaptoethanol and 1 mg/ml zymolyase 20 T were freshly added before use

2.1.4.2 2 x Lysis Buffer

4 M Urea

200 mM NaCl

100 mM Tris-Cl pH 8.0

10 mM CDTA (Sigma)

0.5 % w/v N-Lauroyl Sarcosine

This buffer was mixed 1:1 (v/v) with PBS to obtain 1 x Lysis buffer

2.1.4.3 Binding and Wash Buffer (BW Buffer)

1 M NaCl

5 mM Tris-Cl pH 8.0

0.5 mM EDTA pH 8.0

2.1.5 Buffers for Chromatin Immunoprecipitation (ChIP)

2.1.5.1 FA Lysis Buffer

50 mM Hepes-KOH pH 7.5

140 mM NaCl

1 mM EDTA

1 % Triton X-100

0.1 % sodium deoxycholate

1 x Protease Inhibitor Cocktail

2.1.5.2 FA 500

50 mM Hepes-KOH pH 7.5
500 mM NaCl
1 mM EDTA
1 % Triton X-100
0.1 % sodium deoxycholate

2.1.5.3 LiCl wash solution

10 mM Tris-HCl pH 8.0
250 mM LiCl
0.5 % NP-40
0.5 % sodium deoxycholate
1 mM EDTA

2.1.5.4 TES

10 mM Tris-HCl pH 8.0
1 mM EDTA
100 mM NaCl

2.1.5.5 ChIP elution buffer

100 mM Tris pH 7.8
10 mM EDTA
1 % SDS
400 mM NaCl

2.2 Bacterial techniques

2.2.1 Transformation of competent *E. coli* cells

TOP 10 competent *E.coli* cells were purchased from Invitrogen. 10 ng of pure plasmid DNA or 5 µl of a ligation mix were added to 50 µl aliquots of cells and the mixture was incubated on ice for 30 minutes. After a 42°C heat shock for 30 seconds, the cells were briefly incubated on ice for 2 minutes before 200 µl of SOC media was added. This cell suspension was then incubated

at 37°C for 1 hour, shaking at 200 rpm. After this incubation, 20 µl and 200 µl aliquots were plated on LB plates containing 100 µg/ml ampicillin and the plates were incubated at 37°C over night.

2.2.2 Plasmid mini-prep and maxi-prep

Mini- and Maxi-preps of plasmids were performed using the Plasmid Mini-Prep and Plasmid Maxi-Prep kits from Qiagen according to the instructions of the manufacturer. Standard culture volumes were 2 ml and 400 ml for mini-preps and maxi-preps, respectively. The purified plasmid DNA was analysed by restriction digest and agarose gel electrophoresis to confirm the identity of the obtained plasmid.

2.2.3 Preparation of extracts from Micrococcus luteus (ML extract)

An endonuclease activity specific for CPDs has been found in extracts of *Micrococcus luteus*. Crude extracts from this bacterial strain were prepared as described here and later used for the strand-specific nucleotide excision repair assay (Section 2.4.12).

3 grams of lyophilized *M. luteus* cells (Sigma) were dissolved in 100 ml of 10 mM Tris pH 8.0 and collected by centrifugation at 5000 rpm for 10 minutes. After removal of the supernatant, the pellet was resuspended in 150 ml of 0.2 M sucrose, 0.01 M Tris pH 8.0. 20 mg of Lysozyme (Sigma) were added and the cell suspension was mixed by shaking. The mixture was incubated at 30°C for 30 minutes and then put on ice. 125 ml of ice-cold water were added and mixed well by shaking.

The resulting lysate was transferred to a 500 ml beaker at 4°C. 30 ml of a 10 % streptomycin sulfate solution (Sigma) were added slowly over a 30 minute period, while the solution was constantly mixed with a magnetic stirrer. After addition of the enitre 30 ml, mixing was continued for another 30 minutes at 4°C. This streptomycin sulfate step ensures efficient precipitation and removal of high molecular weight DNA. The mixture was filtered using glass wool in a 100 ml syringe and then centrifuged at 8000 rpm for 60 minutes. The supernatant was carefully collected and the pellet was discarded. 195 g of ammonium sulfate (Sigma) were slowly added to the 300 ml of supernatant to precipitate proteins. After centrifugation at 8000 rpm for 10 minutes, the supernatant was removed and the protein pellet was resuspended in 50 ml of 10 mM Tris pH 7.5, 1 mM beta-mercaptoethanol, 10 % ethyleneglycol. This extract was then stored in 0.5 ml aliquots at -20°C for routine use, or at -80°C for long-term storage.

2.3 DNA techniques

2.3.1 Restriction digests and ligation reactions

All restriction enzymes were purchased from New England Biolabs and used according to the manufacturer's instructions. Ligation reactions were performed using T4 DNA ligase (Sigma), used as recommended by the manufacturer. Whole ligation reactions were used for transformation into *E. coli*.

2.3.2 DNA sequencing

Sequencing reactions were performed using the BigDye Terminator v3.1 Cycle Sequencing Kit (Applied Biosystems) according to the manufacturer's instructions. After generation of the products in a PCR machine, the excess dye was removed using the Dye-Ex kit (QIAGEN) according to the instructions of the manufacturer. The products were then analysed by the Cancer Research UK Sequencing Service.

2.3.3 Polymerase Chain Reaction (PCR)

All PCRs were performed using the KOD Hot Start DNA Polymerase Kit (Novagen).
A standard reaction of 50 µl contained:

5 µl of 10 x KOD Buffer
5 µl of dNTPs (2 mM each)
4 µl of 25 mM $MgSO_4$
3 µl of each primer (5 µM)
2 µl of DMSO
1 µl of KOD Hot Start DNA Polymerase
10 ng of template DNA

PCR grade water was used to reach the final reaction volume.

For tagging/deletion PCR amplification a standard temperature program was used:

1.	94°C	2 min
2.	94°C	30 sec
3.	57°C	30 sec
4.	72°C	2 min

(steps 2-4 were repeated 29 times)

5.	72°C	10 min
6.	4°C	forever

For analysis of successful gene deletion in yeast, another program was routinely used. After quick isolation of genomic yeast DNA from an overnight culture (Section 2.4.8), 1 µl of the obtained solution was used as a template in the reaction mix described above. Three primers were used in the mix, a forward primer 300 bp upstream of the start site, a reverse primer 300 bp downstream of the start site and a reverse primer which binds on the 5' end of the inserted deletion cassette. This primer combination allows to distinguish between the wildtype and the mutant yeast strains.

The annealing temperature in the PCR program was lowered to 53°C and the time for elongation reduced to 30 seconds, due to the shorter lengths of the products.

2.3.4 Purification of PCR products

For the use of PCR products in yeast transformations or DNA ligations, the products were purified using the PCR purification kit from Qiagen according to the instructions of the manufacturer. The products were routinely recovered from the column using 50 µl of TE.

2.3.5 Site-directed mutagenesis of plasmid DNA

All mutagenesis reactions were carried out using the QuikChange Multi Site-directed mutagenesis kit (Stratagene) according to the instructions of the manufacturer. The products were transformed into the supplied XL-10 Gold Ultracompetent Cells as recommended. Plasmids were recovered from the bacteria by mini-prep and the presence of the desired mutation was confirmed by DNA sequencing.

2.3.6 Agarose Gel Electrophoresis of DNA

For the separation and analysis of DNA fragments, horizontal agarose gels were routinely used. The percentage of agarose in the gel varied from 0.8 % to 2 %, depending on the size of the DNA fragments to be analysed. The agarose was dissolved in 1 x TBE and boiled. After cooling of the solution to around 50°C, SafeView Nucleic Acid Stain (NBS Biologicals) was added in order to visualize the DNA in the gel. 7 µl of the stain were routinely added to 100 ml of agarose. Samples were loaded into the wells of the gel using 10 x DNA loading buffer (Section 2.1.3.6). Gels were run at 5 V/cm. Hyperladder I or Hyperladder IV (Bioline) were used to determine the size of large and small DNA fragments, respectively.

2.3.7 Purification of DNA from agarose gels

The required band was excised from the gel, and the DNA was purified from the gel slice using the Gel Extraction Kit from Qiagen according to the manufacturer's instructions.

2.4 Yeast techniques

2.4.1 Yeast strains used in this study

All of the Saccharomyces cerevisiae strains used were congenic with strain W303 (*leu2-3,112 his3-11,15 ade2-1 ura3-1 trp1-1 can1-1*) and were grown and manipulated using standard techniques. A detailed list of the strains used in this study can be found in Table 2.1.

Table 2-1 Yeast strains used in this study

Name	Genotype	Reference
W303 1A	*MATa leu2-3,112 his3-11,15 ade2-1 ura3-1 trp1-1 can1-100*	
W303 1B	*MATα leu2-3,112 his3-11,15 ade2-1 ura3-1 trp1-1 can1-100*	
MGSC102	*MATα leu2-3,112 his3-11,15 ade2-1 ura3-1 trp1-1 can1-100 rad26Δ::HIS3*	Van Gool et al, 1994
MGSC126	*MATα leu2-3,112 his3-11,15 ade2-1 ura3-1 trp1-1 can1-100 rad16Δ::LEU2*	Verhage et al, 1994
MGSC107	*MATα leu2-3,112 his3-11,15 ade2-1 ura3-1 trp1-1 can1-100 rad16Δ::LEU2 rad26Δ::HIS3*	Verhage et al, 1994

JSY1105	*MATα leu2-3,112 his3-11,15 ade2-1 ura3-1 trp1-1 can1-100 URA3::MHRAD26*	This study
JSY1106	*MATα leu2-3,112 his3-11,15 ade2-1 ura3-1 trp1-1 can1-100 URA3::MHRAD26 rad16Δ::LEU2*	This study
JSY1121	*MATα leu2-3,112 his3-11,15 ade2-1 ura3-1 trp1-1 can1-100 rpb9Δ::TRP1*	This study
JSY1107	*MATα leu2-3,112 his3-11,15 ade2-1 ura3-1 trp1-1 can1-100 rad16Δ::LEU2 rpb9::TRP1*	This study
JSY1108	*MATα leu2-3,112 his3-11,15 ade2-1 ura3-1 trp1-1 can1-100 rad16Δ::LEU2 rpb9::TRP1 rad26::HIS3*	This study
JSY1109	*MATα leu2-3,112 his3-11,15 ade2-1 ura3-1 trp1-1 can1-100 URA3::MHRAD26 mec1Δ::HIS3 sml1Δ::TRP1*	This study
JSY1110	*MATα leu2-3,112 his3-11,15 ade2-1 ura3-1 trp1-1 can1-100 URA3::MHRAD26 chk1Δ::HIS3*	This study
JSY1111	*MATα leu2-3,112 his3-11,15 ade2-1 ura3-1 trp1-1 can1-100 URA3::MHRAD26 rad53Δ::HIS3 sml1Δ::TRP1*	This study
JSY1117	*MATα leu2-3,112 his3-11,15 ade2-1 ura3-1 trp1-1 can1-100 URA3::MHRAD26 tel1Δ::TRP*	This study
JSY1118	*MATα leu2-3,112 his3-11,15 ade2-1 ura3-1 trp1-1 can1-100 URA3::MHRAD26 dun1Δ::HIS*	This study
JSY1112	*MATa leu2-3,112 his3-11,15 ade2-1 ura3-1 trp1-1 can1-100 mec1Δ::HIS3 sml1Δ::TRP1*	This study
JSY1113	*MATa leu2-3,112 his3-11,15 ade2-1 ura3-1 trp1-1 can1-100 chk1Δ::HIS3*	This study
JSY1114	*MATa leu2-3,112 his3-11,15 ade2-1 ura3-1 trp1-1 can1-100 rad53Δ::HIS3 sml1Δ::TRP1*	This study
JSY1119	*MATα leu2-3,112 his3-11,15 ade2-1 ura3-1 trp1-1 can1-100 tel1Δ::TRP*	This study
JSY1120	*MATα leu2-3,112 his3-11,15 ade2-1 ura3-1 trp1-1 can1-100 dun1Δ::HIS*	This study
JSY1115	*MATa leu2-3,112 his3-11,15 ade2-1 ura3-1 trp1-1 can1-100 mec1Δ::HIS3 sml1Δ::TRP1 rad26Δ::KanMx*	This study
MGSC139	*MATα leu2-3,112 his3-11,15 ade2-1 ura3-1 trp1-1 can1-100 rad14Δ::LEU2*	Verhage et al, 1996
JSY569	*MATα leu2-3,112 his3-11,15 ade2-1 ura3-1 trp1-1 can1-100 def1Δ::URA3*	Woudstra et al, 2002
JSY626	*MATα leu2-3,112 his3-11,15 ade2-1 ura3-1 trp1-1 can1-100 def1Δ::URA3 rad14Δ::LEU2*	Woudstra et al, 2002

2.4.2 Growth conditions, drug treatments and cell cycle synchronisations

For all the experiments described in this work the yeast cells were grown at 30°C. Logarithmically growing cells were used for analysis, unless otherwise indicated. Cell densities

were measured using a Z2 Coulter Particle Count and Size Analyzer (Beckman-Coulter) according to the instructions of the manufacturer.

Antibiotics and drugs used in this study can be found in Table 2.2. Drugs were added to cells in liquid medium at the indicated final concentrations. In order to arrest cells in mitosis, 5 µg/ml Nocodazole (Sigma, 2 mg/ml stock in DMSO) were added to the culture for 2 hours (Jacobs et al, 1988). At this time point, at least 90 % of the cells were arrested, based on microscopical analysis of the number of large budded cells.

Arrest in the G1 phase of the cell cycle was achieved by adding 10 µg/ml alpha-factor mating pheromone (Duntze et al, 1973). This peptide with the sequence THTLQLKPGQPMY was obtained from the peptide synthesis laboratory at Cancer Research UK at a concentration of 5 mg/ml. Release of G1-synchronised cells into S-phase was achieved by harvesting arrested cells by centrifugation and resuspending them in fresh medium lacking alpha-factor after one wash in medium.

To arrest cells in S-phase, 0.2 M hydroxyurea (HU, Sigma) was added to an unsynchronised yeast culture for 2 hours. Efficient S-phase arrest was confirmed by microscopical analysis of the number of cells with small buds.

Table 2-2 Antibiotics and drugs used in this study

Drug	Organism	final concentration
Ampicillin	*E.coli*	100 µg/ml
Kanamycin	*E.coli*	50 µg/ml
5-FOA[a]	*S. cerevisiae*	1 mg/ml
G418 (geneticin)	*S. cerevisiae*	200 µg/ml
HU[b]	*S. cerevisiae*	0.2 M
MMS[c]	*S. cerevisiae*	0.05 %
4NQO[d]	*S. cerevisiae*	5 µg/ml
Bleomycin	*S. cerevisiae*	5 µg/ml
Nocodazole	*S. cerevisiae*	5 µg/ml

[a]5-fluoro-orotic acid

[b]hydroxyurea

[c]methyl-methane sulfonate

[d]4-nitroquinoline 1-oxide

2.4.3 Lithium-Acetate transformation of yeast cells

2 ml yeast cultures were grown in the appropriate growth medium over night at 30°C. In the morning, the cells were diluted in fresh medium to a cell density of 3 x 10^6 cells/ml and further grown at 30°C until the culture reached a cell density of 1 x 10^7 cells/ml. The cells were harvested by centrifugation at 3000 rpm for 5 minutes, the supernatant was discarded and the pellet was resuspended in 1 ml of water and transferred to a 1.5 ml Eppendorf tube. After centrifugation at 14000 rpm for 20 seconds the pellet was washed in 1 ml of TE/LiOAc solution (Section 2.1.3.4) and centrifuged again. Finally, the pellet was resuspended in an appropriate volume of Te/LiOAc solution to obtain a cell density of 10^9 cells/ml.

For the transformation of PCR products, in order to construct deletion strains as well as to tag yeast proteins by homologous recombination, a 100 µl aliquot of this yeast suspension was mixed with 20 µl of purified PCR product, 70 µl of 2 mg/ml salmon sperm DNA (boiled for 5 minutes and chilled on ice before use), and 600 µl of PEG/TE/LiOAc solution (Section 2.1.3.5). For transformation of plasmids, 50 µl of the yeast suspension was mixed with 100 ng of plasmid DNA, 35 µl of 2 mg/ml salmon sperm DNA and 300 µl of PEG/TE/LiOAc solution.

The mixture was briefly vortexted and then incubated at 30°C in an Eppendorf shaker (1000 rpm) for 1 hour. 70 µl or 35 µl of DMSO, for PCR products or plasmids, respectively, were added and the suspension was heat shocked in a 42°C water bath for 15 minutes. Finally, the cells were collected by centrifugation, washed briefly in 1 ml of water and then plated on the appropriate selective plates.

In the case of selection for *TRP*$^+$, *URA*$^+$, *HIS*$^+$ and *LEU*$^+$ cells, the pellet was directly plated onto selective plates. For *KanMx*$^+$ selection, as well as selection against *URA*$^+$ cells on 5-FOA, the pellet was first plated on YPD and incubated over night, before being replica-plated on appropriate plates containing the drug after about 16 hours.

2.4.4 Galactose-induced overexpression of proteins in yeast cells

For overexpression of proteins in yeast, the pYC2/CT vector (Invitrogen) was routinely used. It is a centromeric plasmid carrying a *URA3* marker, and your gene of interest can be cloned between a *GAL1* promoter and a *CYC1* terminator. The final constructs were transformed into

the appropriate yeast strain, and the resulting plasmid-containing cells were grown for 24 hours in 2 ml of SC-URA in the presence of raffinose as the only sugar. After this incubation the culture usually reached a cell density of 10^8 cells/ml. 500 µl of this culture were routinely used to inoculate a 150 ml culture, again in medium lacking uracil and containing raffinose. After incubation at 30°C for 12-16 hours, the cell density of the culture reached 5 x 10^6 cells/ml. Galactose was always added to the cells at this density to a final concentration of 2 % (w/v). Addition of glucose to a separate raffinose-culture served as a control for repression of the gene. Incubation in the presence of galactose/glucose was carried out for 2 hours before the cells were harvested. Protein extracts were then prepared for analysis by SDS-PAGE and/or immunoprecipitation and purification of the overexpressed protein.

2.4.5 Preparation of yeast extracts using glass beads

Yeast cells from a liquid culture were harvested by centrifugation at 3000 rpm for 5 minutes. The cell pellet was resuspended in 1 ml of PBS and transferred to a 1.5 ml tube (screw cap). The cells were harvested again by centrifugation in a table-top centrifuge (full speed, 20 seconds) and washed in 1 ml ice-cold lysis buffer (Section 2.1.3.10). After another round of centrifugation the pellet was resuspended in 700 µl of lysis buffer.

500 µl of 0.5 mm Zirconia/Silica Beads (BioSpec Products, Inc.) were added to the cell suspension and the cells were disrupted using a FastPrep-24 Tissue and Cell Homogenizer (MP Biomedicals). 6 rounds of shaking (30 seconds each) were carried out, separated by 2 minutes during which the tubes were incubated on ice in order to prevent sample heating.

After disruption of the cells, a small hole was made at the bottom of the 1.5 ml tube using a hypodermic needle and the tube was placed into a 2 ml Eppendorf tube. Centrifugation of these tubes at 5000 rpm for 2 minutes at 4°C ensured that the protein extract, as well as the chromatin and cell debris, were collected in the 2 ml tube while the beads remained in the 1.5 ml tube.

The cell debris and chromatin formed a pellet at the bottom of the tube after this centrifugation step. In order to solubilize proteins from the chromatin pellet, 2 mM $MgCl_2$ and 250 Units of benzonase (Novagen) were added to the extract. The pellet was then resuspended by pipetting and the tubes were rotated at 4°C for 1 hour. After this incubation the tubes were spun at 14000 rpm at 4°C for 15 minutes and the supernatant was transferred to a fresh tube.

2.4.6 Preparation of quick protein extracts from yeast

Rapid isolation of proteins from yeast cells was performed as described earlier (Kushnirov, 2000). About 10^7 yeast cells were harvested by centrifugation and the pellet was resuspended in 100 µl of water. 100 µl of 0.2 M NaOH were added and the tubes were briefly vortexed to ensure proper resuspension of the cells. After an incubation time of 5 minutes at room temperature the cells were pelleted, the supernatant was discarded and the pellet was resuspended in 50 µl of 1 x SDS loading buffer. This suspension was then boiled for 5 minutes and pelleted again. 10 µl of this supernatant were routinely analysed by SDS-PAGE.

2.4.7 Isolation of high quality genomic DNA from yeast

High quality genomic DNA from yeast was purified using the MasterPure Yeast DNA Purification Kit (Epicentre Biotechnologies) according to the instructions of the manufacturer. The supplied RNAse in the kit was used to further purify the DNA as recommended in the manual, and the RNAse was afterwards removed by phenol/chloroform purification and precipitation of the DNA.

2.4.8 Rapid isolation of genomic DNA from yeast

For analysis of successful gene deletion in yeast by PCR it is not necessary to obtain large quantities of high quality DNA. For this purpose, 0.5 ml cultures were set up from individual yeast colonies. After incubation at 30°C over night the cells reached densities of 1 – 2 x 10^8 cells/ml. 200 µl of these cultures were centrifuged at 14000 rpm for 2 minutes and the supernatant was discarded. The cell pellets were resuspended in 20 µl of 0.2 % SDS and boiled for 10 minutes. After a short centrifugation at 14000 rpm, the supernatant was transferred to a fresh tube. 1 µl of this solution was routinely used in PCR reactions to assess the success of a gene deletion approach.

2.4.9 Analysis of the UV sensitivity of yeast strains

The yeast strains to be analysed were grown overnight in 1 ml of the appropriate growth medium. In the morning, the cells were diluted to a cell density of 5 x 10^6 cells/ml and the incubation was continued in order to get the cells back into the logarithmic growth phase. As soon as the culture reached a cell density of 2 x 10^7 cells/ml, 4 10-fold serial dilutions were

prepared and 3 µl of these dilutions, as well as the undiluted culture, were spotted on appropriate yeast plates. After spotting of all the strains, one plate was transferred to the incubator without UV as a control for spotting equal numbers of cells. The other plates were irradiated with various doses of 254 nm UVC light using a UV Stratalinker 2400 (Stratagene) and then incubated at 30°C in the dark for growth.

2.4.10 Analysis of UV-induced degradation of Rpb1

The yeast strains to be analysed were grown overnight in the appropriate growth medium. On the next day, the cells were diluted in 150 ml of medium to obtain a cell density of 3 x 10^6 cells/ml. In order to get the cells back into log-phase, they were allowed to grow until they reached a cell density of 1 x 10^7 cells/ml.

50 µg/ml Cycloheximide (Sigma, 5 mg/ml stock in water) were added to the cultures for 1 hour in order to inhibit any new protein synthesis. After this incubation period, the cells were harvested by centrifugation (3000 rpm for 5 minutes), and resuspended in 150 ml of PBS. The supernatant was saved for the post-UV incubation period. After removing a 30 ml aliquot which served as a pre-UV control, the remaining cell suspension was UV-irradiated with a germicidal lamp at a dose of 400 J/m^2. After irradiation, the cells were harvested again by centrifugation and resuspended in 120 ml of the original growth medium containing cycloheximide. At various time points after the irradiation (every hour up to 4 hours post-UV), 30 ml aliquots were removed from the culture, the cells were harvested by centrifugation, washed once in PBS and then quickly frozen by dropping into liquid nitrogen.

After all the samples were collected, extracts were prepared as descibed (Section 2.4.5) and the protein concentrations of all extracts were determined using the Bradford assay. Equal amounts (10 µg) of extracts were loaded into the wells of a 4-12 % gradient gel (BioRad). SDS-PAGE was performed as described (Section 2.5.1), and the proteins were transferred to a Hybond-C Extra membrane (Section 2.5.2) for analysis by Western blot. Ponceau-S staining of the membrane was used to control if the loading was equal in all the lanes. The Rpb1 protein was detected with 8WG16 antibody.

2.4.11 Analysis of UV-induced ubiquitylation of Rpb1

Treatment of yeast cells with cycloheximide and UV was carried out as described for the analysis of UV-induced degradation of Rpb1 (Section 2.4.10) and extracts were prepared as

described (Section 2.4.5). After quantification of protein concentrations, 2 mg of total yeast extract were incubated with 50 µl of GST-Dsk2 beads (Anindya et al., 2007) to immunoprecipiate mono- and polyubiquitylated proteins. This incubation was carried out for 4 hours at 4°C on a rotating wheel. After binding, the beads were harvested by centrifugation (2000 rpm for 3 minutes), washed twice for 5 minutes each in ice-cold PBS and then once for 5 minutes in ice-cold PBS with 0.1 % Triton X-100. Finally, the beads were resuspended in 80 µl of 1 x SDS-PAGE loading buffer (Section 2.1.3.7) and boiled for 10 minutes. After a quick centrifugation step to collect the beads at the bottom of the tube, 15 µl of the supernatant were loaded on 4-12 % gradient gels and SDS-PAGE and Western blotting was carried out as described (Sections 2.5.1 and 2.5.2).

The membranes were stained with Ponceau S solution (Sigma) and the image was scanned. The stained GST-Dsk2 protein served as a control to comfirm that equal amounts of beads used in the immunoprecipitation step. Mono- and polyubiquitylated Rpb1 forms were detected using 4H8 antibody.

2.4.12 Strand-specific nucleotide excision repair (NER) assay

Analysis of strand specific nucleotide excision repair capacity in yeast cells was performed as described (Teng et al., 2005) with slight modifications. A schematic outline of the assay can be seen in Figure 2.1.

2.4.12.1 Irradiation and harvesting of samples

Yeast cells were grown in 500 ml of appropriate growth medium at 30°C until they reached a cell density of 4 x 10^7 cells/ml. The culture was harvested by centrifugation at 3000 rpm for 5 minutes and the supernatant was discarded. The pellet was resuspended in 1 l of ice-cold PBS, resulting in a cell-density of 2 x 10^7 cells/ml. An aliquot (one fifth or one sixth, depending on the total number of samples) was removed and kept on ice in the dark as an unirradiated (U) control. The remaining suspension was subjected to UVC-irradiation (254 nm) with 100 J/m^2 using a germicidal lamp. Directly after UV, another aliquot was removed and kept on ice in the dark. This sample was later used to determine the total amount of inflicted UV-damage (0). The rest of the suspension was harvested by centrifugation, the supernatant was discarded and the pellet was resuspended in fresh growth medium at a cell density of 4 x 10^7 cells/ml. At the desired time-points after UV irradiation, samples were removed, spun down at 3000 rpm for 5 min, and the pellet was resuspended in 50 ml of ice-cold PBS and kept in the dark.

After harvesting of all the time-points, the individual aliquots were again spun down, and the pellets were once again washed in 50 ml of ice-cold PBS. Finally, after another centrifugation step, the pellets were resuspended in 5 ml of Sorbitol solution (Section 2.1.4.1) containing 28 mM beta-mercaptoethanol and 5 mg of Zymolyase T-20 (MP Biomedicals) and the tubes were incubated at 4°C o/n in the dark to obtain spheroblasts.

2.4.12.2 Isolation of genomic DNA

Spheroblasts were spun down at 3000 rpm for 5 min and the pellet was carefully washed with 10 ml of Sorbitol solution (Section 2.1.4.1), and then finally dissolved in 5 ml of 1 x NER Lysis Buffer (Section 2.1.4.2) containing 200 µl of RNAse A stock solution (Sigma, 10 mg/ml in TE buffer). The solution was vortexed rigorously to lyse the spheroblasts and then incubated for 1 hour at 37°C with occasional shaking. 250 µl of Pronase stock stolution (Roche, 20 mg/ml in water) were added, and the tubes were incubated for another hour at 37°C after a brief vortexing step before another 1 hour incubation at 65°C.

After cooling down the samples to room temperature, an equal volume (5 ml) of phenol/chloroform/isoamylalcohol (PCI pH 8.0, Sigma) was added and the tubes were briefly vortexed to mix the phases. The resulting emulsion was transferred to 15 ml Corex-tubes and spun down for 10 min in an SS-34 rotor at 10000 rpm. The aqueous supernatant was transferred to a 15 ml Falcon-tube and another 5 ml of PCI were added. After vortexing, the tubes were spun at 4500 rpm for 10 minutes and the aqueous phase was again transferred to a fresh 15 ml Falcon-tube. 5 ml of chloroform were added, the emulsion was once again vortexed and spun at 4500 rpm for 10 min. The supernatant was transferred to a 50 ml Falcon-tube, and 10 ml of ice-cold 100 % ethanol were added to precipitate the genomic DNA. To obtain efficient precipitation, the samples were incubated at -20°C over night.

Genomic DNA was then harvested by centrifuation at 4500 rpm for 10 minutes at 4°C, the pellet was dissolved in 1 ml of TE buffer and transferred to a 2 ml Eppendorf tube. 1 ml of isopropanol was added, and after mixing the tubes were incubated at room temperature for 30 min to once again precipitate the DNA. The tubes were spun at 14000 rpm for 5 minutes at 4°C and the pellet was resuspended in 600 µl of TE-buffer, resulting in a DNA concentration of around 0.5 µg/µl for the culture volume stated above. 1 µl aliquots of the DNA samples were run in a 0.8 % agarose gel to make sure that the genomic DNA was intact and did not get degraded during the purification steps.

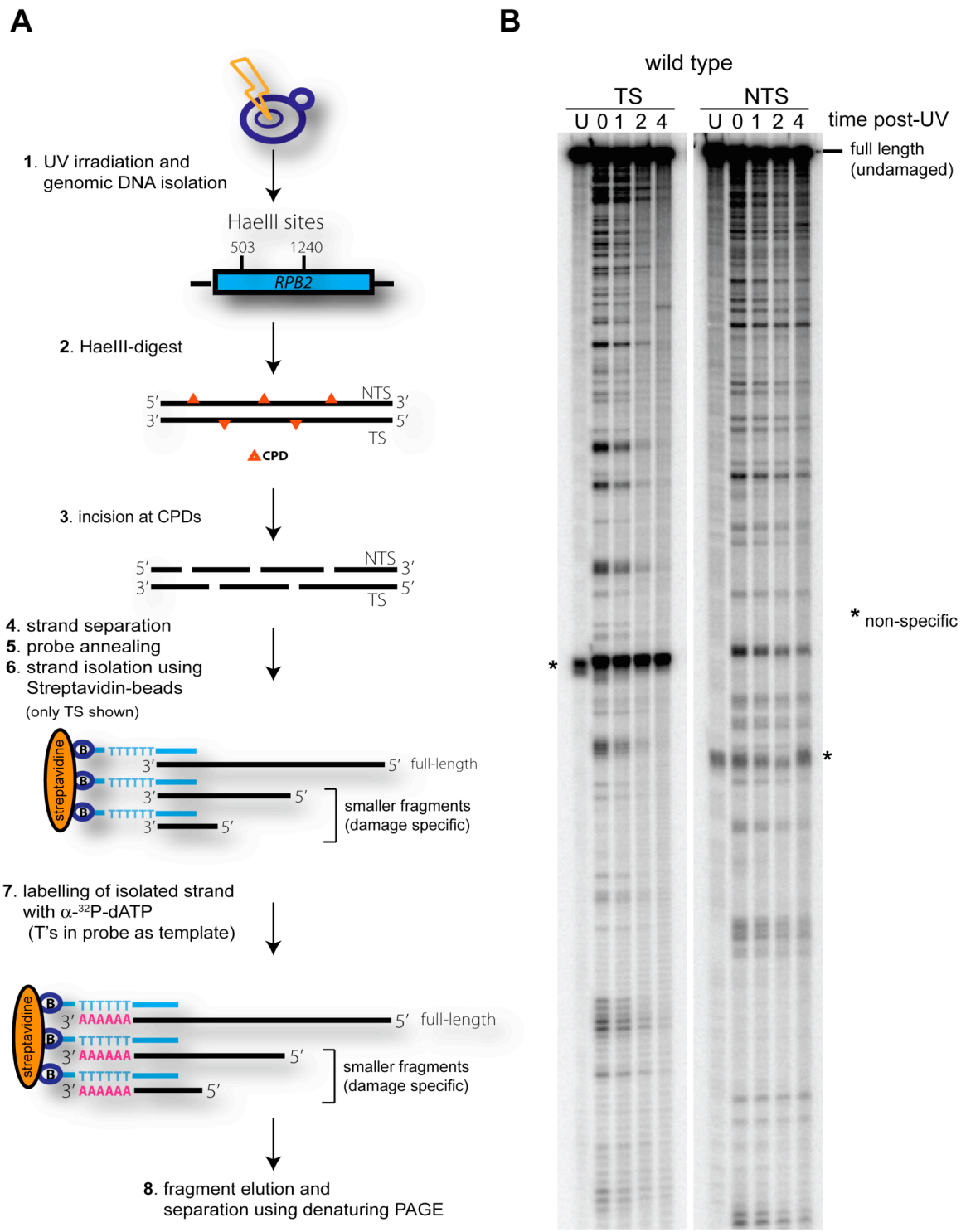

Figure 2-1 Analysis of strand-specific CPD repair at nucleotide resolution

(A) Schematic outline of the individual steps in the protocol (see text for details).
(B) Representative gel showing the result of such an experiment for the wild type strain (W303).

2.4.12.3 Preparation of genomic DNA for analysis

100 µl of genomic DNA (~ 50 µg) were digested with 60 units of HaeIII restriction enzyme (New England Biolabs) in 300 µl of 1 x restriction buffer (Buffer 2, New England Biolabs) for 2 hours at 37°C. A 5 µl aliquot was subjected to electrophoresis in a 1 % agarose gel to ensure that all the samples were completely digested and to check that similar amounts of DNA were present for all the time-points.

300 µl of PCI were added to the solution and mixed by vortexing. The two phases were separated using MaXtract Low Density tubes (QIAGEN) according to the manufacturer's instructions and the aqueous phase was transferred to a fresh 1.5 ml Eppendorf tube. 30 µl (1/10 volume) of 3 M sodium acetate pH 5.3 and 330 µl of isopropanol were added and the solution was incubated on dry ice for 15 minutes to precipitate DNA. The digested DNA was harvested by centrifugation in a table-top centrifuge at 14000 rpm for 5 min at 4°C, the supernatant was discarded and the pellet was dissolved in 100 µl of TE buffer. 10 µl of ML extract (Section 2.2.3) were added and the tubes were incubated at 37°C for 1 hour to induce incisions at CPDs. After this incubation the DNA was purified twice using MaXtract Low Density tubes, first with PCI and then with chloroform. The resulting aqueous phase (100 µl) was transferred to 0.5 ml PCR tubes (ANACHEM).

2.4.12.4 Isolation of RPB2 strands for labelling and analysis

25 µl of 5 M NaCl were added to the samples to obtain a final NaCl concentration of 1 M. 1 µl of biotinylated probe (2 mM stock), specific for either the TS or the NTS of the *RPB2* fragment, was added. The sequences of these probes were the following:

for isolation of the TS:
5' biotin-GATAGCTTTTTTCCGTTTACCGATTATGTTAAGATCAAAGAA 3'
for isolation of the NTS:
5' biotin-GATAGCTTTTTTCCAATAATGGACCTGCCAAATCTAATCT 3'

Regions of homology to the *RPB2* sequence are shown in red, and the 6 thymidines for labelling of the 3' end of the isolated DNA strand are shown in blue. The six nucleotides between the biotin and the thymidine stretch were included to ensure complete labelling by the DNA polymerase while the strand was still bound to streptavidin beads.

The resulting solution was incubated at 95°C for 5 min and then at 55°C for 15 minutes in a PCR machine. During this incubation, 10 µl of Dynabeads M-280 Streptavidine (Invitrogen, 6.7 x 10^8 beads/ml) per sample were washed once with water and twice with BW Buffer (Section 2.1.4.3). These washing steps were carried out using a Magnetic Particle Concentrator (MPC).

10 µl of the washed beads were added to each PCR tube, mixed by pipetting and incubated at room temperature for 15 minutes with occasional mixing. The tubes were then placed in the MPC and the supernatant was saved for isolation of the remaining DNA strand. The beads were resuspended in 50 µl of BW Buffer and the tubes were incubated at 58°C for 5 min in a PCR machine. After this high-stringency wash, the beads were washed two additional times with 50 µl of BW buffer at room temperature, before they were finally resuspended in 4.3 µl of water.

2.4.12.5 Radioactive labelling and analysis of the isolated DNA strands

Labelling of the DNA strands was performed using the Sequenase Version 2.0 DNA Sequencing Kit (USB). For each sample, 5.7 µl of a mix containing 2 µl of Sequenase Buffer, 2.4 µl of Sequenase Dilution Buffer, 0.7 µl of 100 mM DTT, 0.25 µl of water, 0.25 µl of alpha-^{32}P-dATP (Perkin Elmer, 6000 Ci/mmol) and 0.1 µl of Sequenase were added to the beads, and the suspension was mixed by pipetting. The labelling was allowed to proceed at room temperature for 15 minutes with occasional mixing. After this incubation, the tubes were placed in the MPC and the supernatant was discarded. The beads were washed three times with 50 µl of water before being resuspended in 5 µl of FA loading buffer (Section 2.1.3.8). Finally, the tubes were placed in a 100°C heat block for 1 minute to ensure complete release of the labelled DNA strands from the streptavidine beads.

6 % sequencing gels were used to separate the DNA fragments. These gels were prepared using SequaGel concentrate and diluent (National Diagnostics) according to the manufacturer's instructions. The gels were prerun at 65 Watts for 1 hour in order to heat the gel to 50°C. The tubes containing the samples were put in the MPC and the supernatants (5 µl) were loaded into individual wells of the gel. Electrophoresis was carried out at 65 Watts for 2.5 hours. The gel apparatus was disassembled, and the gel was dried at 80°C for 1 hour. For analysis of the fragments, the dried gel was placed in a Storage Phosphor Screen Cassette (Molecular Dynamics) for two days. An image of the gel was then obtained using a Typhoon Phosphor-Imager.

2.4.12.6 Calculation of damage half-lifes (T50%)

For each lane of the gel, the intensities of the prominent top band (full length, undamaged DNA strand) and the entire lower part of the lane (damage-specific bands, non-specific bands and background) were determined using the Image-Quant 5.0 Software. The intensity of the lower part of the U-lane was then subtracted from the intensities of the lower parts of all other lanes to subtract the background and non-specific bands, which are not due to inflicted damages. The resulting values ('damages') were then added to the intensities of the top band to obtain a value for the total signal per lane.

The total signal for the 0 lane (no repair incubation) was set to 1 and a correction factor for all the other lanes was determined, allowing to correct for loading differences between the lanes. The intensities of the damages in all the lanes were corrected using this factor. The damages in the 0 lane were then set to 1 and all the damages of the later time points were put in relation to the 0 time point. The values were plotted in a graph using the Microsoft Excel software (x axis = time, y axis = ratio of remaining damages), and the point on the x axis for which y=0.5 was determined. This value was the halflife of the damages (T50%).

2.4.13 Chromatin Immunoprecipitation (ChIP)

2.4.13.1 Cell growth and UV irradiation

Yeast strains were grown in appropriate medium over night at 30°C and diluted in the morning to achieve a cell density of 2.5 x 10^6 cells / ml. The cells were then allowed to divide twice in order to get back into the logarithmic growth phase, and were harvested when the cell density reached 1 x 10^7 cells / ml. After harvesting of the cells by centrifugation, the supernatant was discarded and the pellet was resuspended in the original culture volume of PBS. UV irradiation at the indicated dose was carried out using a germicidal lamp. A control of 10 ml was taken out before UV treatment. After UV irradiation, the cells were again collected by centrifugation, the supernatant was discarded, and the pellets were dissolved in the same volume of fresh medium. Incubation of the cultures was then continued.

2.4.13.2 Crosslinking, preparation of extracts and DNA shearing

At various time points after the UV irradiation step, 10 ml samples (corresponding to 1 x 10^8 cells) were removed and fixed with 1 % formaldehyde for 15 minutes. Crosslinking was stopped by adding 1/10 volume of 2 M glycine for 5 minutes. The cells were then harvested by centrifugation, washed twice with PBS and finally resuspended in 1 ml of FA Lysis Buffer. Extracts were prepared as described in section 2.4.5, with the difference that after spinning the extract and cellular debris from the bead-containing tube into the 2 ml tube, the chromatin-containing pellet was resuspended in the supernatant and transferred to a 15 ml Falcon-tube. 500 µl of fresh FA Lysis Buffer were added and the samples were sonicated using a BIORUPTOR (Diagenode). Ice was added to the water bath in order to keep the samples cold during the process. Sonication was carried out in 30 second intervals with 30 second breaks for a total time of 15 minutes. After this, the samples were transferred to fresh 1.5 ml tubes and spun at full speed twice for 10 minutes. After each centrifugation the pellet was discarded and the supernatant transferred to a fresh tube. The so obtained extracts containing solubilized chromatin were used for immunoprecipitation of the target protein.

2.4.13.3 Immunoprecipitation

150 µl of the extracts were diluted to 300 µl with fresh FA Lysis Buffer. 1 µg of antibody was added, and binding of the antibody to the target was performed over night at 4°C on a rotating wheel. After the binding, the extracts were centifuged at 14000 rpm for 10 minutes to remove precipitations. The supernatant was transferred to Spin-X Centrifuge Tube Filters (Costar) and 35 µl of a 1:1 slurry of Protein A beads (Pierce) in FA Lysis Buffer containing 1 mg/ml of BSA were added. Using the Spin-X Centrifuge tube filters ensured proper removal of all the liquids without losing any beads in the subsequent washing steps. Binding of the antibody/antigen complex to the Protein A beads was carried out at 4°C for 2 hours with constant shaking. The beads were then harvested by centrifugation and washed consecutively with FA Lysis Buffer, FA-500, LiCl wash solution and TES (recipes can be found in section 2.1.5) for 10 minutes each at 4°C with constant shaking. After removal of the TES, the filters containing the beads were transferred to a fresh 1.5 ml tubes and the beads were resuspended in 150 µl of ChIP elution buffer (Section 2.1.5.5). Elution was carried out at 37°C in an Eppendorf shaker for 30 minutes with constant shaking. The liquid containing the eluted protein/DNA complexes was harvested by centrifugation. 150 µl of water and 20 µg of Proteinase K (Roche) were added and reversal of crosslinks was achieved by incubation at 65°C over night. 3 µl of the extract used for IP were mixed with 150 µl water, 150 µl of ChIP elution buffer and 20 µg of Proteinase K

(Sigma), and then incubated over night at 65°C. These samples served as input controls for the IPs.

2.4.13.4 Analysis of immunoprecipitated DNA by Real time PCR

After reversal of the crosslinks, the DNA in the samples was purified using the Qiagen PCR purification kit according to the instructions of the manufacturer. The DNA was eluted in 50 µl of water, and then quantified by Real time PCR using a BioRad iCycler and the MyIQ software. PCR reactions were set up using the iQ SYBR Green Supermix (BioRad) in 96 well plates. Standard reactions of 20 µl contained:

10 µl of iQ SYBR Green Supermix
1 µl of eluted DNA
8 µl of water and
0.5 µl of both primers (10 µM).

Ct-values were obtained for both the DNA from the IPs and the inputs. The analysis was performed in triplicates for each sample, and the average between these 3 values was calculated. The resulting value (x) was used in the following formula: 2^(30-x). The so-obtained value for the IP of each time point was divided by the value obtained for the input of the same time point, in order to correct for input differences. Correction with a value for the telomere was then carried out in order to correct for non-specific signals. An example of such an analysis can be found in the Appendix.

2.5 Protein analysis

2.5.1 SDS Polyacrylamide Gel Electrophoresis (SDS-PAGE)

Precast 4-12% Bis-Tris gradient gels (Biorad) were routinely used to separate proteins. The running buffer was XT MOPS buffer (Biorad) and electrophoresis were carried out in Criterion chambers (Biorad). The Precision Plus protein marker from Biorad was used to determine the size of the detected protein on Western Blots or gel stains. 4-12 % gradient gels were usually run at 150 V for 90 minutes.

For analysis of high-molecular weight proteins, as well as post-translational modifications of Rad26, 3-8 % gradient gels (Biorad) were used together with XT Tricine buffer (Biorad). These gels were routinely run in the cold room at 90 V for 12-16 hours. After this time, the 100 kDa marker reached the bottom of the gel.

2.5.2 Transfer of proteins to membranes (Western Blot)

After successful electrophoresis of the proteins by SDS-PAGE, the gels were briefly washed in water and then transferred to transfer buffer (25 mM Tris, 60 mM glycine, 20 % methanol). A piece of Hybond C-Extra membrane (Amersham Biosciences) was placed on top of the gel and the obtained 'sandwich' was placed between 2 stacks of Whatman 3MM papers pre-wetted in transfer buffer. This setup was placed in a Biorad Criterion Blotter and completely submerged in transfer buffer. The transfer was carried out at 4°C for 70 minutes at 400 mA. After the transfer, the membrane was briefly washed and then routinely stained using Ponceau-S solution (Sigma) to check the efficiency of transfer and, in some cases, equal loading between the lanes. The stain was removed by washing in PBS twice for 5 minutes each.

Table 2-3 Antibodies used in this study

1. Primary antibodies			
Epitope	Source	Supplier	Dilution
Myc (9E10)	Mouse	CRUK antibody production	1:10000
HA	Rabbit	Abcam (ab9110)	1:5000
Rpb1 (4H8)	Mouse	CRUK antibody production	1:10000
Rpb1 (8WG16)	Mouse	CRUK antibody production	1:1000
Actin	Mouse	Abcam (ab8224)	1:1000

2. Secondary antibodies			
Name	Source	Supplier	Dilution
ECL™ anti-mouse-HRP	Sheep	GE Healthcare	1:10000
ECL™ anti-rabbit-HRP	Donkey	GE Healthcare	1:10000

all antibodies were diluted in 5 % milk/PBS

2.5.3 Detection of proteins on membranes

After transfer of proteins to the membranes, blocking was carried out with 5 % milk in PBS for at least 30 minutes at room temperature in order to decrease non-specific binding of the antibody to the membrane. Various antibodies were used in this study to detect the proteins of interest. These antibodies can be found in Table 2.3 together with the dilution used. The membrane was washed 3 times for 10 minutes in PBS after each antibody incubation. After the last wash, the membranes were briefly dried and the chemiluminescent substrate was added. These substrates were SuperSignal West Pico Chemiluminescent substrate (for routine use) and SuperSignal West Dura Extended Duration Substrate (for weak signals). Both were purchased from Thermo Scientific and used according to the instructions of the manufacturer. The chemiluminescent signals were detected using SuperRX medical X-Ray Films (Fujifilm).

2.5.4 Staining of proteins in SDS-Gels using SYPRO Ruby stain

For staining of gels after SDS-PAGE the gels were washed twice for 5 minutes in water and then fixed twice for 30 minutes in fixing solution (50 % methanol, 7 % acetic acid). This leads to shrinking of the gel which might reduce the quality of the staining. To avoid this, the gel was incubated in water twice for 10 minutes in order to rehydrate it. Afterwards the SYPRO Ruby protein gel stain (Molecular probes) was added, and the gel was incubated in the stain over night in the dark. After this incubation the gel was transferred to a fresh container and washed twice for 30 minutes in destaining solution (10 % methanol, 7 % acetic acid). Then it was again put in water for 10 minutes for rehydration, before it was analysed using a Typhoon Phosphor-Imager.

2.5.5 Mass spectrometry analysis of Rad26

Polyacrylamide gel slices (1-2 mm) containing Rad26 were prepared for mass spectrometric analysis using the Janus liquid handling system (Perkin Elmer). Briefly, the excised protein gel piece was placed in a well of a 96-well microtitre plate and destained with 50% v/v acetonitrile and 50 mM ammonium bicarbonate, reduced with 10 mM DTT, and alkylated with 55 mM iodoacetamide. After alkylation, Rad26 was digested with 6 ng/µl trypsin (Promega) overnight at 37 °C. The resulting peptides were extracted in 1% v/v formic acid, 2% v/v acetonitrile. The digest was analysed by nano-scale capillary LC-MS/MS using a nanoAcquity UPLC (Waters) to

deliver a flow of approximately 300 nL/min. A C18 Symmetry 5 µm, 180 µm x 20 mm µ-Precolumn (Waters), trapped the peptides prior to separation on a C18 BEH130 1.7 µm, 75 µm x 100 mm analytical UPLC column (Waters). Peptides were eluted with a gradient of acetonitrile. The analytical column outlet was directly interfaced via a modified nano-flow electrospray ionisation source, with a 2-D linear ion trap mass spectrometer (LTQ XL/ETD, ThermoScientific), equipped with a chemical ionization source to enable the generation and injection of fluoranthene radical anions for the electron transfer dissociation (ETD) reaction (Coon et al, 2004). The ETD process uses ion/ion chemistry to provide sequence information not available through conventional methods such as CID. Peptide fragmentation using an ETD approach augments the current methodologies available for the characterization of post-translational modifications by more accurately identifying the specific amino acids that is modified. Data dependent analysis was carried out in either CID or ETD mode, where automatic MS/MS were acquired on multiply charged precursor ions in the m/z range 300–2000 m/z. As predominantly doubly protonated ions are generated by tryptic digestion, a supplemental activation energy was used to improve fragmentation in the ETD experiments (Swaney et al, 2007). All LC-MS/MS data were then searched against a protein database (UniProt 13.6) using the Mascot search engine programme (Matrix Science, UK), with oxidised methionine, carbamidomethyl cysteine and phospho serine, threonine and tyrosine included as variable modifications (Perkins et al, 2007).

2.5.6 Immunoprecipitation of proteins from yeast extracts

After successful preparation of yeast extracts, 20-30 µl of Protein A beads coated with the desired antibody were added. The beads were washed in lysis buffer (Section 2.1.3.10) prior to addition to the extract. Binding to the beads was carried out over night at 4°C on a rotating wheel. After binding, the beads were harvested by centrifugation at 3000 rpm for 2 minutes and the supernatant was removed. The beads were washed once in lysis buffer containing 50 mM KOAc, 3 times in lysis buffer containing 500 mM KOAc (15 minutes for each), and again quickly in lysis buffer containing 50 mM KOAc. The immunoprecipitated protein, together with its binding partners, was either recovered from the beads by boiling in 1 x SDS loading buffer and then analysed by SDS-PAGE, or eluted from the beads using TEV protease if applicable.

2.5.7 ATPase assay

ATPase reactions with Rad26 were carried out in a total volume of 20 µl. The reactions contained the following components:

10 µl 2 x ATPase buffer (40 mM Tris pH8, 8 mM $MgCl_2$, 2 mM DTT, 0.05 mg/ml BSA)
1 µl of pRS316 plasmid DNA (100 ng/µl) or water as a control
1 µl of a mix of hot and cold gamma-^{32}P-ATP (1:9 labelled ATP: 1µM cold ATP)
5 µl of purified protein (about 250 ng)
3 µl of water

The tubes were then incubated at 37°C in an Eppendorf shaker.

4 µl aliquots were removed after 0, 2, 5 and 15 minutes and transferred to tubes containing 20 µl of 0.1 M HCl. After mixing, these tubes were kept on dry ice to completely stop the reaction. After all samples were obtained, 200 µl of charcoal solution (7 % activated charcoal, 50 mM HCl, 5 mM H_3PO_4) were added, the samples were quickly vortexed and then incubated at room temperature for 15 minutes. Finally, the tubes were centrifuged at 14000 rpm for 5 minutes and 100 µl of the clear supernatant containing inorganic phosphate were transferred to vials suitable for the Scintillation counter. Cerenkov counting was carried out using a Tricarb 1500 Liquid Scintillation Analyzer (Packard).

Quantification of ATPase activity was done by setting the value obtained for the 0 time point to 1 and putting all the later time points in relation to the 0 time point. These values were then used to obtain a graph using the Microsoft Excel software. Error bars were obtained by determining the standard deviation between independent experiments.

3 Results I – NER/TCR analysis at site-specific UV lesions

3.1 Project aim

DNA repair pathways are coordinated by the sequential assembly of many proteins at the site of a DNA lesion. Knowledge about the exact timing of recruitment of particular proteins, as well as the genetic requirements for the localization of particular factors to the DNA damage site, are important for elucidating the repair mechanism. Work on double strand break (DSB) repair has benefitted greatly from a system which allows the induction of a DSB in a temporally and spatially controlled manner. This system makes use of the HO endonuclease, a sequence-specific nuclease, which is normally involved in mating type switching (reviewed in (Haber, 1998)). The HO cleavage site (HO_{CS}) can be introduced at any location in the genome, and because its position and surrounding sequence is known, chromatin immunoprecipitation (ChIP) experiments can be carried out. This allows a researcher to investigate if, and when, a particular factor localizes to the DSB after induction of endonuclease expression, and which proteins are required for this localization. This system is widely used in the field of double-strand break repair.

The situation is more complicated for UV-induced DNA lesions, because every pair of pyrimidines in the genome represents a potential site for the formation of a cyclobutane pyrimidine dimer (CPD), or a 6-4 pyrimidine pyrimidone photoproduct (6-4PP) (Setlow and Carrier, 1966). When examining the recruitment of an NER-factor to a particular region in the genome by ChIP, only a small proportion of the examined molecules will actually have a lesion there. One way to increase the chance of damage is to increase the UV intensity, but this will inevitably lead to more damages in all other parts of the genome. This is problematic, because factors with low abundance might be titrated away from the region of interest, and may therefore never be detected. An alternative way to achieve efficient induction of UV damage at a specific location is to use a sequence that is highly damage-prone, even at relatively low doses of irradiation.

This project was aimed at setting up a system which should enable me to examine the recruitment of NER factors to a UV damage-prone region by ChIP, by using a construct containing a long stretch of pyrimidines, a ‘damage-hotspot’. This stretch should be damaged much more efficiently by UV *in vivo*. By putting the ‘hotspot’ in the context of an inducible gene (see below), it should be possible to distinguish TC-NER from GG-NER, and to examine UV-dependent ubiquitylation of elongating RNAPII *in vivo*. Such a system would be highly

valuable, as it would allow us to investigate if a particular factor binds to RNAPII stalled at a UV lesion, indicating an involvement in one or more processes taking place at such an arrested transcription complex.

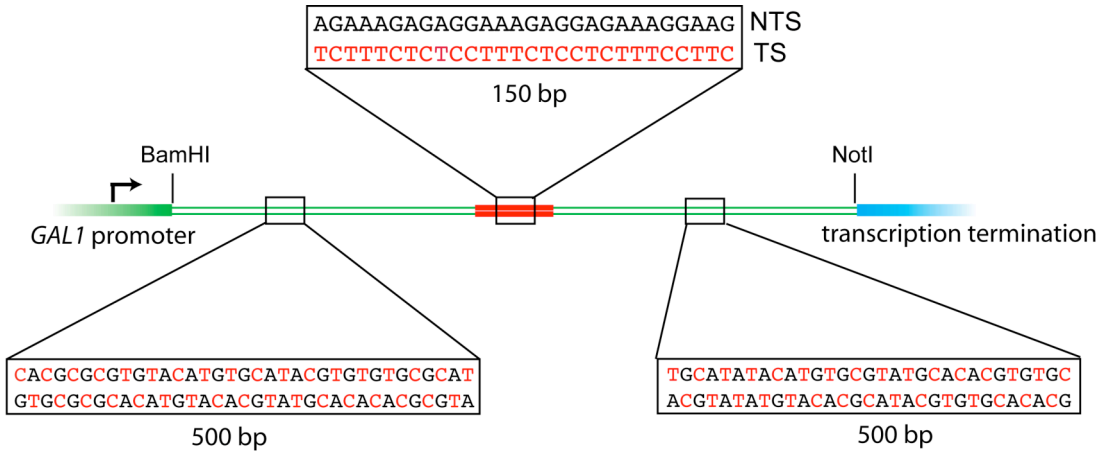

Figure 3-1 Schematic representation of the 'hotspot' gene

A 150 base long stretch of pyrimidinines is placed between two 500 bp long sequences without potential pyrimidine dimers. The entire sequence, which represents a continuous open-reading frame with the hotspot in the transcribed strand (TS), is transcribed under the control of the galactose-inducible *GAL1* promoter on the pYC2 plasmid (Invitrogen). Pyrimidines are shown in red, purines are shown in black. Blow-up boxes indicate examples of sequences in the various regions, not the entire sequence.

3.2 Design of the UV-hotspot construct

In order to achieve efficient damage by UV irradiation I decided to design a 150 bp 'hotspot' sequence (referred to simply as 'hotspot' from now on), by putting 150 pyrimidines next to each other (schematic drawing of the entire construct can be seen in Figure 3.1). This hotspot was flanked by unique primer binding sites for analysis by quantitative PCR after ChIP. On each side of the hotspot, 500 bp of DNA without potential UV damage sites (no adjacent pyrimidines in either strand) were placed. These stretches of DNA were meant to serve as control regions in the experiments, because repair factors should only be recruited to the hotspot and not to the flanking undamaged DNA. After designing the sequence of the entire construct, it was synthesized by a biotech-company (GeneArt).

I was particularly interested in designing a system which allows discrimination between TC-NER and GG-NER. Therefore I inserted the sequence behind a galactose-inducible promoter on the pYC2 vector (Invitrogen). The hotspot was inserted in such a way that the stretch of pyrimidines was located on the transcribed strand. After induction and UV irradiation, the lesions formed at the hotspot should lead to efficient RNAPII arrest, culminating in TC-NER and/or Rpb1 ubiquitylation.

It is important to point out that I avoided including any STOP-codons in this synthetic gene; therefore the construct represents a continuous open-reading-frame. One problem that arose from this is that the 500 bp damage-free flanking regions are highly repetitive, because only a limited number of codons are available, and can only be used in a limited number of combinations, in order to avoid having two adjacent pyrimidines in the TS or NTS of the gene. We now believe this underlies some of the inconsistencies in the results I obtained with the construct (see Discussion).

3.3 Analysis of the hotspot gene

3.3.1 The 'hotspot' sequence is efficiently damaged after UV irradiation

I first investigated if the stretch of 150 pyrimidines in the TS of the gene indeed represented a sequence which can be efficiently damaged by UV irradiation. In order to do so, the DNA construct containing it was irradiated in droplets of water on parafilm, using a UV Stratalinker (Stratagene). UV-induced lesions represent a strong block to the progression of Taq-Polymerase (Wellinger and Thoma, 1996), a fact which has been exploited for the mapping of lesions at nucleotide resolution on DNA (Thoma et al, 1993; Chandrasekhar and van Houten, 1994). After linearization of the plasmid with NotI (linearizing the plasmid downstream of the hotspot gene; see Fig. 3.1), irradiated and un-irradiated hotspot construct was used in primer extension reactions using a radioactively labelled primer. The same primer was also used on the un-irradiated sample in the presence of ddNTPs in order to create a sequencing ladder, which allows mapping of the lesions on the DNA at the nucleotide level. This primer extension reaction should yield a 625 base long DNA fragment from an undamaged DNA template. Lesions in the hotspot should lead to the appearance of shorter products (88-238 bases), which map to the pyrimidine stretch (see schematic drawing in Figure 3.2A). Analysis of the products on 6 % denaturing polyacrylamide gels indeed showed this pattern (Fig. 3.2B). The full-length fragment, and some unspecific bands, was seen when the reaction was performed with un-irradiated template. After irradiation of the DNA with increasing doses of UVC light, more and more short fragments were seen which mapped exactly to the long pyrimidine stretch (see sequencing ladder on the left in Figure 3.2B). Importantly, the fragments became increasingly shorter at higher doses of UV, indicative of the generation of more lesions at the beginning of the hotspot sequence. Importantly, no appearance of damage-specific bands was seen on the 500 bp sequence downstream of the hotspot (upper part of gel), which confirms that the pyrimidine dimer-free stretch of DNA indeed represents a sequence which cannot be damaged, even at high doses of UV.

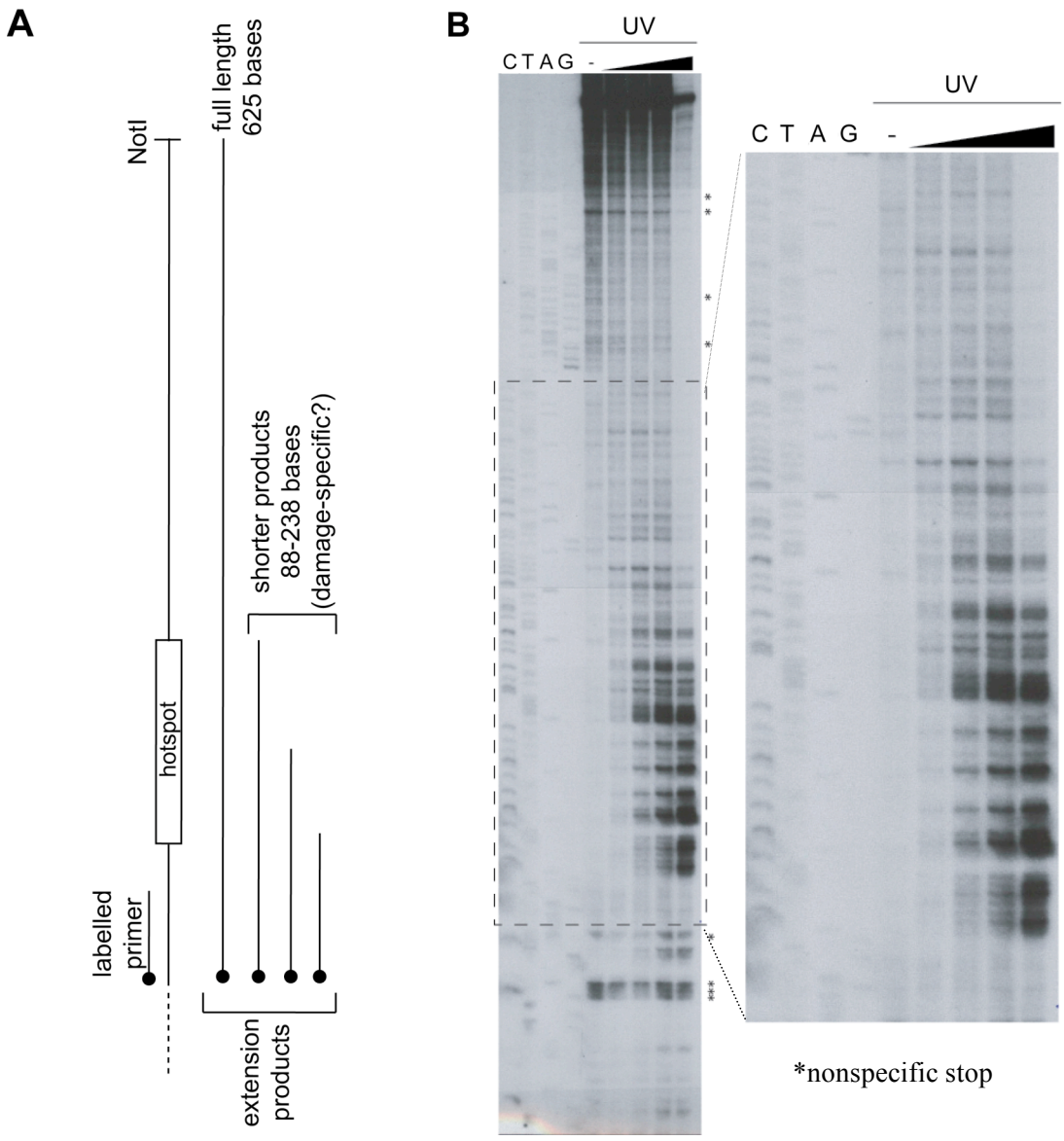

Figure 3-2 Mapping of UV-induced DNA lesions on the hotspot gene

(A) Outline of the experimental strategy to map lesions using primer extension
(B) Representative gel showing primer extension results (see text for details) , the increasing UV doses were 1, 2, 5 and 10 kJ/m^2

3.3.2 Analysis of RNAPII distribution across the hotspot gene

Having shown that the pyrimidine stretch in the hotspot gene is efficiently damaged by UV irradiation *in vitro*, I set out to determine its effect on RNAPII distribution before and after UV treatment *in vivo*. In order to do so, the plasmid containing the gene was transformed into the wild type W303 strain, and Rpb1 localization was examined by ChIP with 4H8 antibody, followed by Real time PCR analysis of the immunoprecipitated DNA. Three regions were chosen for this analysis, the *GAL1* promoter upstream of the gene ('start'), the pyrimidine

stretch in the middle of the gene ('hotspot'), and the termination sequence downstream of the gene ('end'). Unfortunately, because of the repetitive nature of the 500 bp damage-free regions flanking the hotspot, no useful primer pairs for Real time PCR analysis could be found there. Cells were grown in medium containing raffinose, and 2 % glucose or galactose was added at the desired cell density (5 x 10^6 cells/ml) to repress or activate transcription, respectively. A primer pair in the middle of the endogenous *GAL10* locus served as a control for efficient galactose-mediated transcriptional induction. Another primer pair in the *RPB2* open reading frame served as a control for a constitutively expressed gene. After 2 hours of induction, the cells were collected and UV-irradiated with 150 J/m^2 of UVC light, and aliquots were harvested either immediately after treatment, or after further incubation in medium for various lengths of time. An outline of the experimental strategy is shown in Figure 3.3.

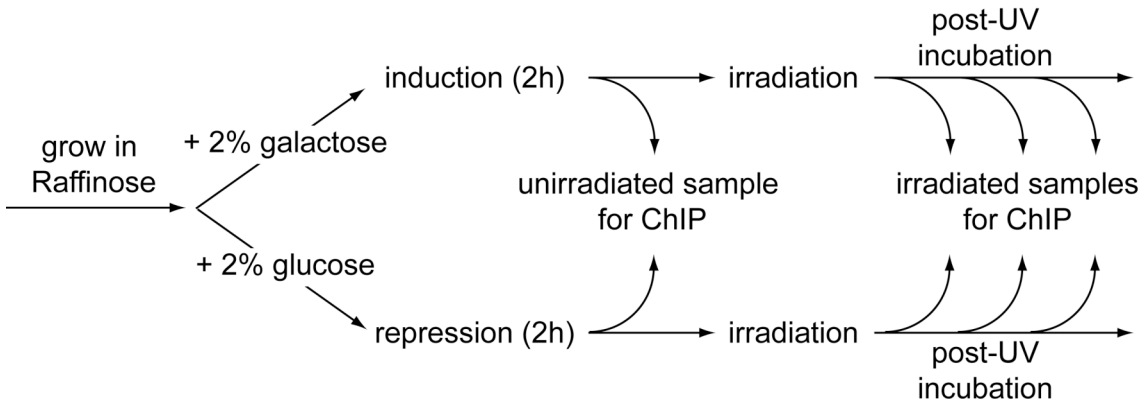

Figure 3-3 Experimental outline of Chromatin immunoprecipitation (ChIP)

Cells containing the hotspot construct were grown in raffinose-containing medium, and the gene was either induced (2 % galactose) or repressed (2 % glucose) for 2 hours. Samples were taken before and at one or more time points after irradiation with a dose of 150 J/m^2.

Results from these ChIP experiments are shown in Figure 3.4. One thing that immediately caught my attention was the difference in induction levels between the hotspot gene and the endogenous *GAL10* gene (Figure 3.4A). For the *GAL10* gene, these inductions (measured as the ratio between the ChIP-signals for RNAPII in galactose versus glucose) were consistently between 30 and 40-fold, as expected (Kristjuhan and Svejstrup, 2004). In sharp contrast to these values, induction levels of the hotspot gene varied between 1.5 and 6-fold and displayed a strong variation between independent experiments. In many cases, no detectable induction could be achieved. Nevertheless, I continued to look at RNAPII distribution across the hotspot gene before and after UV irradiation in the samples in which reasonably good induction could be detected (3-fold and above). I expected to detect more RNAPII complexes at the hotspot immediately after UV irradiation of cells grown in galactose, because the transient arrest of RNAPII at UV-induced DNA lesions should increase the likelihood of finding RNAPII there.

Surprisingly, this was not the case. Instead, the ChIP signal was quickly lost from all examined regions immediately after UV irradiation and reappeared thereafter. 90 minutes post-UV, the intensity of the RNAPII signal was back at the pre-UV level (Figure 3.4B). This indicates that transcription is transiently inhibited after UV irradiation, making it hard to show an increased localization of RNAPII at the hotspot after UV treatment.

As can be seen in Figure 3.4B, the decrease of the ChIP signal for RNAPII after UV irradiation was more pronounced at the 3'-end of the hotspot gene (termination sequence) compared to the start (promoter), or at the hotspot sequence itself. I therefore calculated the ratio between the ChIP signal at the beginning of the gene and that at the end of the gene. The ratio was significantly higher than 1 shortly after UV irradiation, indicating that not all the RNAPII complexes which start transcription reach the end of the gene, and that the presence of the pyrimidine stretch might indeed be an obstacle for polymerases after damage induction (Figure 3.4C). During the time course, this ratio returned to its initial value of 1, indicative of removal of the block. This result can be seen as an indication that upon UV irradiation the presence of the pyrimidine stretch indeed represents a problem for transcribing RNAPII complexes.

3.3.3 Analysis of repair factor recruitment to the hotspot

Even though, as explained above, a dramatic effect of the hotspot on RNAPII distribution was not obtained, I decided to carry on and try to detect the recruitment of NER factors to the pyrimidine stretch after UV irradiation. I chose the Rad14 protein, because this factor is indispensable for both NER subpathways (Prakash and Prakash, 2000). Rad14 was tagged on its C-terminus with 6 HA-tags, and the functionality of the tagged protein was confirmed by comparing the UV sensitivity of the tagged strain to the wild type as well as the *rad14Δ* deletion strains. The sensitivity of the strain expressing epitope-tagged Rad14 was indistinguishable from that of the wild type strain (W303), whereas *rad14Δ* was highly UV-sensitive (data not shown).

In order to determine if the tagged protein could be found at the hotspot after UV-treatment, the plasmid containing the hotspot gene was transformed into the tagged strain, and cells were grown up in medium containing raffinose. Transcription of the hotspot gene was again induced or repressed by adding 2% galactose or glucose, respectively. After 2 hours, cells were collected and irradiated, and then allowed to recover for another 2 hours in medium. This time point was chosen because the damage-halflife of lesions in the TS of active genes is reported to be between 1 and 2 hours, whereas it is more than 4 hours for the NTS. At the 2-hour time point it should be easy to distinguish between TC-NER and GG-NER. After chromatin

immunoprecipitation with HA antibody, real time PCR was carried out using the same primer pairs already used for analysis of RNAPII occupancy.

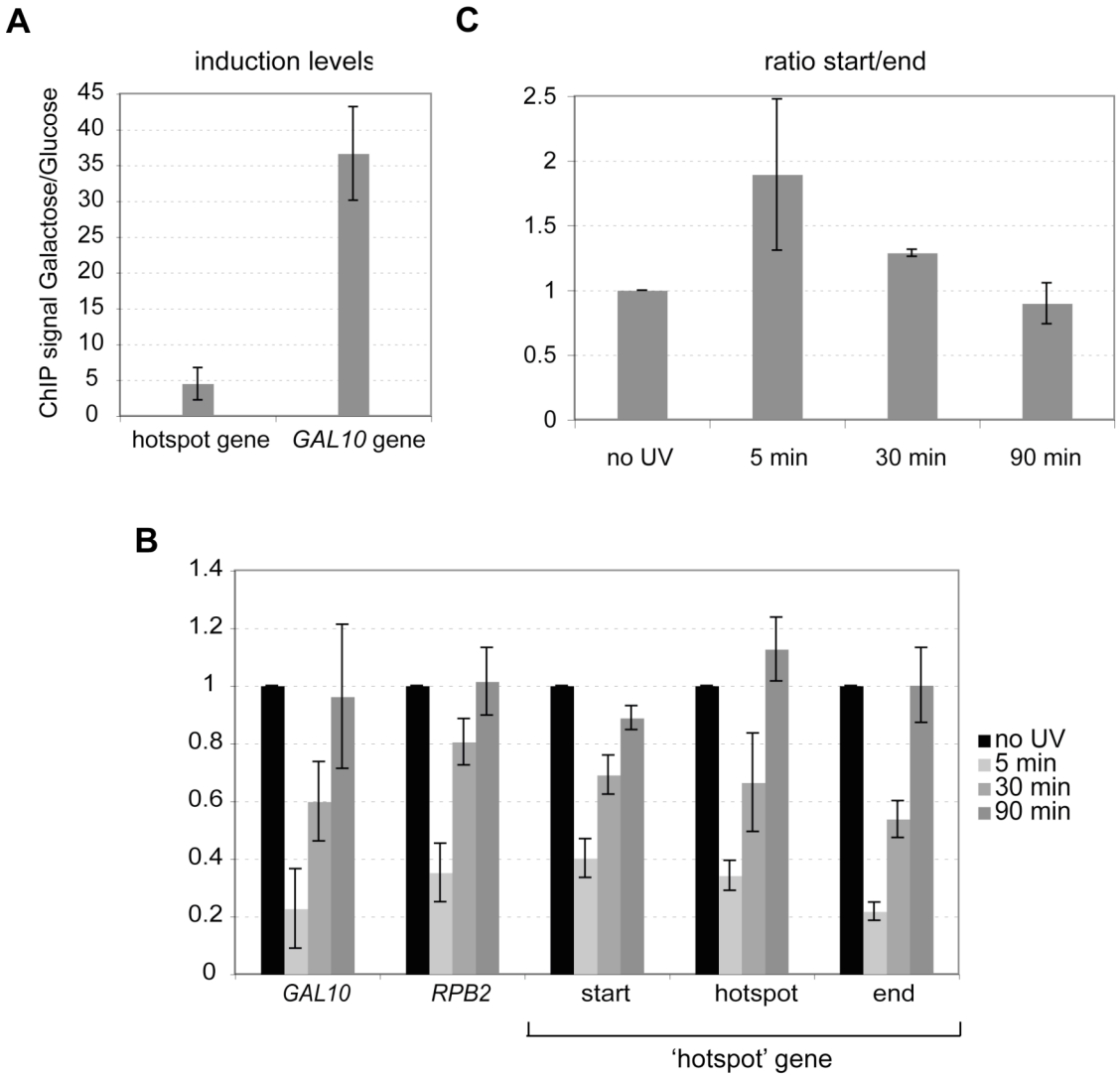

Figure 3-4 Analysis of RNAPII distribution at the hotspot gene

(A) Analysis of transcriptional induction. Rpb1 ChIP signals at the hotspot gene and the endogenous *GAL10* gene were obtained from cells grown in galactose (actived) and glucose (repressed). Ratios between galactose and glucose are shown. Error bars indicate the standard deviation between independent experiments.
(B) Analysis of the effect of UV irradiation of RNAPII distribution. Cells were treated as shown in Figure 3.3 and samples were collected before and after UV. Rpb1 ChIP signals were obtained for various regions of the hotspot genes as well as endogenous loci. Rpb1 signals were quickly lost from all examined regions after UV, but recovered during the time course. Error bars indicate the standard deviation between independent experiments.
(C) Alternative way to display the results for the hotspot gene shown in (B). For each post-UV time-point, the ratio of the Rpb1 ChIP signal at the start to the ChIP signal at the end of the gene were calculated. Error bars indicate the standard deviation between independent experiments.

The results of such ChIP experiments are shown in Figure 3.5. Strikingly, significant recruitment of Rad14 was restricted to the hotspot region, and was only seen when transcription of the gene was induced with galactose. A similar pattern was neither seen for the promoter (start) nor for the terminator sequences (end) of the same gene, and also not for the *GAL10* or *RPB2* genes. It is important to point out, however, that the extent of Rad14 recruitment varied significantly between independent experiments, and that there seemed to be a tight correlation between the level of transcriptional induction of the gene in galactose (which varied significantly), and the level of Rad14 recruitment to the hotspot. Figure 3.5 only shows the results from experiments, in which the level of induction was higher than 4 fold. However, in more than 50 % of the experiments, the induction was less, and no significant Rad14 recruitment was observed in these cases.

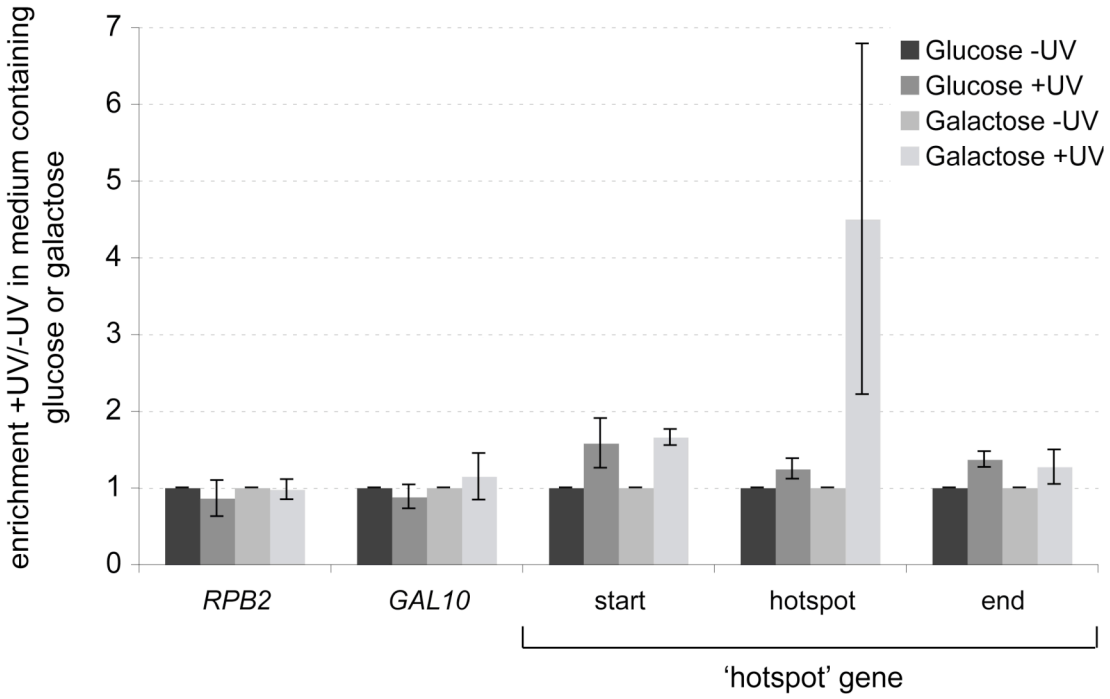

Figure 3-5 Analysis of UV-dependent Rad14 recruitment to DNA

Chromatin-immunoprecipitations for HA-tagged Rad14 to regions of the hotspot gene or endogenous genes were carried out before, and 2 hours after, UV treatment in glucose (repressed) or galactose (activated). Signals obtained for unirradiated samples are always set to 1, signals for the irradiated samples are set in relation to the unirradiated sample. Significant binding of Rad14 was only observed at the hotspot. Differences in transcriptional induction of the gene did however lead to significant variations in the obtained recruitment levels.

Because of these experimental inconsistencies, I tried very hard to solve the problem of inconsistency in transcriptional induction before looking more specifically at repair factor recruitment to the hotspot. Unfortunately, despite changing a number of experimental parameters (see Discussion), I was unable to get rid of these induction problems and therefore in the end did not carry on with the repair factor ChIPs, and other experiments that we hoped would have been possible with this experimental approach (see below).

4 Discussion I

4.1 Construction of a UV-damage-prone gene

For this project I have designed a plasmid-based construct containing a galactose-inducible gene, which has a highly damage-prone sequence (a stretch of pyrimidines; 'hotspot') inserted into surrounding 'non-damageable' DNA (free of adjacent pyrimidines). Indeed, mapping of *in vitro* inflicted UV lesions using primer extension (shown in Figure 3.2), clearly showed that the expectations were correct, and that the induced lesions were confined to the hotspot. Because the hotspot sequence is located on the transcribed strand, RNAPII should be efficiently arrested at this location after UV, making it possible to follow the recruitment of TC-NER factors (such as Rad26), general NER factors (such as TFIIH and Rad14), and possibly also Rpb1 ubiquitylation factors (such as Def1, Rsp5, Elc1), to this particular region by ChIP, either under inducing (galactose) or repressing conditions (glucose).

4.2 RNAPII does not accumulate at the hotspot after UV

One of my expectations was that RNAPII density would be dramatically increased at the hotspot after UV, when transcription was activated in galactose-containing medium. This was not the case; instead, RNAPII was rapidly lost after UV treatment from all the examined regions in the hotspot gene, as well as from the endogenous *GAL10* and *RPB2* genes. This situation is reminiscent of the one in human cells, where UV irradiation leads to a transient inhibition of transcriptional initiation, which is restored after several hours in wild type cells, but not in cells from CS patients (Mayne and Lehmann, 1982). In my experiments, transcription was restored after about 90 minutes in the wild type strain. Initial experiments in the *rad26Δ* strain led to the same result (data not shown), and so the transcriptional recovery (measured by Rpb1 ChIP) did not seem to be significantly influenced by Rad26-mediated removal of lesions from the transcribed strand, or other potential roles of the factor, such as in transcriptional initiation during DNA damage, as has been shown for CSB (Proietti-De-Santis et al., 2006). Even though the loss of RNAPII ChIP signals at the end of the hotspot gene after UV treatment was more pronounced than at the start (thereby increasing the start/end-ratio shown in Figure 3.4C) indicating that the hotspot sequence indeed represents a damage-induced barrier to RNAPII progression, these results rely on the comparison of different primer pairs, and cannot really be regarded as a definite proof of transcriptional impairment caused by the pyrimidine stretch. The

great variability in hotspot gene activation between experiments (even though the genomic *GAL10* induction was normal) was also a concern for the interpretation of these experiments. As the aim of this project was to design a system for the analysis of repair factor binding to UV damage sites in the presence or absence of active transcription, I instead carried on analysing the UV-dependent recruitment of an NER-factor to the hotspot.

4.3 Specific recruitment of an NER-factor to the damage-prone region

In order to investigate if NER proteins are preferentially recruited to the damage-prone pyrimidine stretch after UV depending on the transcriptional state of the gene, I analysed the binding of the general NER factor Rad14 to various regions of the hotspot construct, as well as to the *GAL10* and *RPB2* loci in the yeast genome. Two hours after UV treatment, at a time when TC-NER is taking place, but GG-NER is not yet activated efficiently (see Figures 5.1 and 5.2 in this thesis), Rad14 was only detected at the hotspot, and only after induction of the genes with galactose, indicating transcription-dependent recruitment of this repair factor. Unfortunately, significant differences in the levels of transcriptional induction of the hotspot gene led to great variations in the extent of Rad14 recruitment, and in many cases no recruitment could be observed. Because the first step in TC-NER is the transcriptional arrest of RNAPII at the site of the DNA lesion (Christians and Hanawalt, 1992; Sweder and Hanawalt, 1992), differences in transcription levels will inevitably lead to TC-NER differences, so it is clearly necessary to first find a solution for the observed variability of induction. Some changes to the construct I have already made, as well as some ideas for future alterations will be discussed below.

From the Rad14 ChIPs I carried out, it was clear that higher inductions led to more significant recruitment of the repair protein, making it tempting to speculate that achieving an induction level similar to the one observed for the *GAL10* gene will lead to even higher levels of Rad14 recruitment. Interestingly, no such Rad14 recruitment was ever observed at the constitutively expressed *RPB2* gene or at the galactose-inducible *GAL10* gene (Fig. 3.5), even though the levels of transcriptional induction of the latter locus were about 10-fold higher than that achieved for the hotspot construct (Figure 3.4A). Irradiation of cells will inevitably lead to the induction of photo-lesions in these regions, but my results clearly indicate that construction of a highly damage-prone sequence is required for efficient detection of NER-factors, at least of Rad14, on DNA after UV-irradiation. To my knowledge, this result is the first evidence of successful UV-dependent chromatin-immunoprecipitation of a protein involved in NER, showing that the ideas behind our experimental approach are valid. Finding a solution to the problems of transcriptional induction will hopefully make this system a valuable tool for the

analysis of events that take place at an elongating RNAPII complex irreversibly arrested *in vivo* at a UV-induced lesion, such as TC-NER and Rpb1 ubiquitylation.

4.4 Potential solutions for the problem of transcriptional induction

The hotspot gene was cloned between a *GAL1*-promoter and a *CYC1* transcriptional termination sequence. These elements were already present in the pYC2 vector (Invitrogen), a commercially available and tested vector, making it highly unlikely that these sequence elements are responsible for the observed variability in galactose-induced expression. I also used the same vector for galactose-driven overexpression of other genes, such as *RAD26* (see section 5.2.2.4), and never observed any induction problems.

Several possibilities can be envisaged to explain the lack of proper transcriptional induction of the synthetic gene containing the hotspot. First, the long stretch of pyrimidines in the transcribed strand of the gene might represent a barrier to the efficient progression of elongating RNAPII, even in the absence of UV-induced DNA damage. In order to investigate this, I reduced the length of the hotspot to 30 nucleotides (one fifth of its original length), or totally removed it from the construct. This, however, did not alleviate the lack of transcriptional induction, indicating that the pyrimidine stretch is not the main reason for the induction difficulties. A second possibility is that the sequences flanking the hotspot, i.e. the 500 bp stretches of 'damage-free' DNA, are the main cause for the observed problems. As mentioned earlier, these regions are highly repetitive, because of the limited number of codon combinations available for construction of a continuous open-reading-frame, without the formation of pyrimidine pairs in either strand. Because of the significant homology between these two regions, I cannot rule out recombination (perhaps transcription-associated) between these sequences, the formation of secondary DNA structures, or other events caused by repetitive DNA. In order to look more closely at this, I redesigned the gene and included potential pyrimidine dimers in the NTS. The TS of this new construct was, however, still kept dimer-free. This resulted in significant reduction of the repetitive nature of the 500 bp sequences. Unfortunately, it did not significantly improve transcriptional induction (data not shown). Taken together, my attempts to alleviate the transcription problems with the synthetic gene were not successful.

One further possibility to solve the problem in the future is to use naturally occuring sequences flanking the hotspot, in order to prevent the use of any synthetic DNA. It would be easy, for example, to insert the pyrimidine stretch into the endogenous *GAL10* locus, which was consistently induced at high levels in my experiments. My results showing that the presence and

the length of the hotspot sequence was apparently not the reason for the lack of induction makes it likely that the *GAL10* gene containing the hotspot will still be transcribed at a high rate. This construct will, of course, not rule out that damage occurs elsewhere in the gene, i.e. on both strands both in front of and behind the hotspot, but my preliminary Rad14 ChIP results (Fig. 3.5) indicate that detection of repair factor binding will be restricted to the pyrimidine stretch, presumably because the likelihood of damage there is so much higher.

4.5 Use of the hotspot sequence for analysis of GG-NER

Even though a solution for the induction problems will have to be found in order to establish a system which allows us to distinguish between transcripion-related and unrelated events at UV-damaged DNA *in vivo*, the analysis of RNAPII-independent events (i.e. GG-NER) should already be possible with the hotspot-construct in its present form. This will require the analysis of repair factor recruitment to the pyrimidine stretch during a longer time-course.

However, this was not the main purpose for making and characterizing the construct, so I did not pursue this line of research, but instead focused on alternative, more successful projects on regulation of NER and Rpb1 ubiquitylation by the DNA damage checkpoint (see next chapter).

5 Results II – Regulation of NER by the DNA damage checkpoint

5.1 Analysis of NER efficiency in checkpoint-deficient strains

The DNA damage checkpoint (DDC) orchestrates a plethora of cellular events in the presence of DNA lesions, including cell cycle arrest, stabilisation of stalled replication forks, induction of apoptosis and activation of DNA repair. Even though it is widely accepted that DNA repair is influenced by the checkpoint, to which extent the efficiency of specific DNA repair pathways is affected in response to mutations in checkpoint factors is largely unknown. In this study I investigated the role of the DDC in Nucleotide Excision Repair (NER) in the budding yeast, *S. cerevisiae*. To achieve this goal, I utilized a powerful method which allows analysis of strand-specific repair of UV-induced CPDs at nucleotide resolution (Teng et al., 2005).

5.1.1 Strains lacking the Mec1 kinase have NER defects

Strains lacking the central checkpoint kinase Mec1 are deficient in the activation of the DDC (Longhese et al., 1998). I constructed a strain lacking the *MEC1* and *SML1* genes (*SML1* deletion being necessary to suppress the lethality of deletion of *MEC1* (Zhao et al., 1998)), and analysed the repair of the transcribed strand (TS; transcription-coupled repair) and the non-transcribed strand (NTS: global genome repair) of the constitutively transcribed *RPB2* gene. Wild-type (W303) and TC-NER-deficient *rad26Δ* mutant strains (van Gool et al., 1994) served as controls.

A representative gel is shown in Figure 5.1. The signals for the individual lanes were quantified using a phosphor-imager, and the time required to remove 50 percent of the damaged nucleotides (t50%) in the TS and the NTS were calculated for individual strains (Fig. 5.2). As expected, the difference in repair kinetics between the preferentially repaired transcribed strand (TS) and the non-transcribed strand (NTS) was evident in the WT strain, while no clear strand specificity was observed in TC-NER-deficient *rad26Δ* cells. Interestingly, the cells lacking the checkpoint kinase Mec1 exhibited a dramatic impairment of NER, characterised by markedly slower repair of the TS, and virtually no detectable repair of the NTS at 4 hours post-UV irradiation. This indicates that a functional DNA damage checkpoint is required for both NER subpathways in yeast. Importantly, however, while repair of the NTS appears to be completely

DDC-dependent, repair of the TS in *mec1Δ sml1Δ* cells was still more rapid than in the TC-NER deficient *rad26Δ* strain. This indicates that TC-NER still occurs, but is severely compromised, in the absence of the Mec1 kinase.

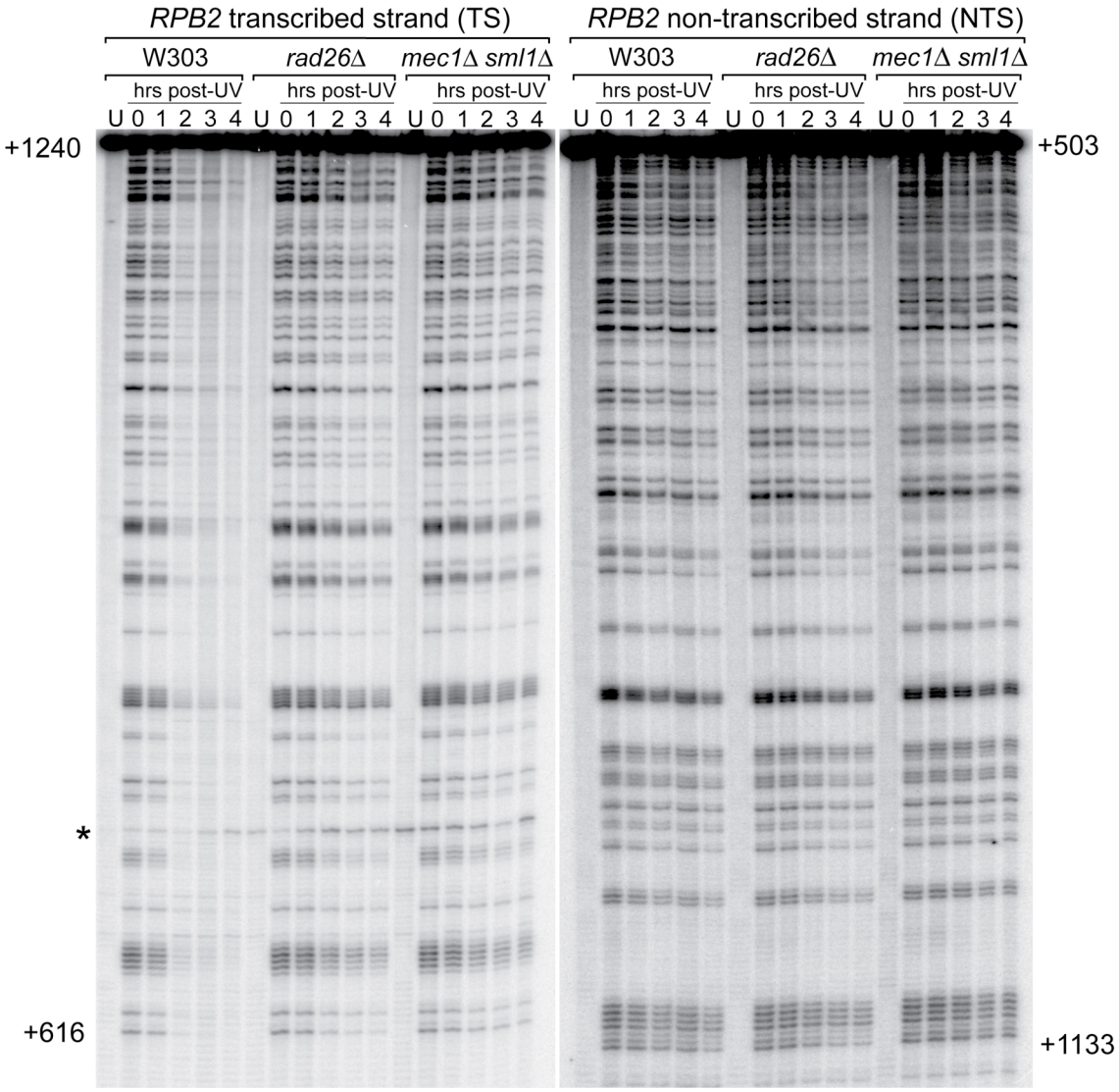

Figure 5-1 Normal NER requires the Mec1 kinase

Representative sequencing gel showing a comparison of NER kinetics in the TS and the NTS of *RPB2* in wild-type (W303), TC-NER-deficient (*rad26Δ)* and checkpoint deficient (*mec1Δ sml1Δ*) cells. Numbers on the left and on the right of the gel indicate the nucleotide position relative to the *RPB2* transcription start site on the TS and NTS, respectively. A non-specific band appearing also in the unirradiated control sample (U) is marked with an asterisk. The picture was supplied by Yumin Teng and Hefin Gill.

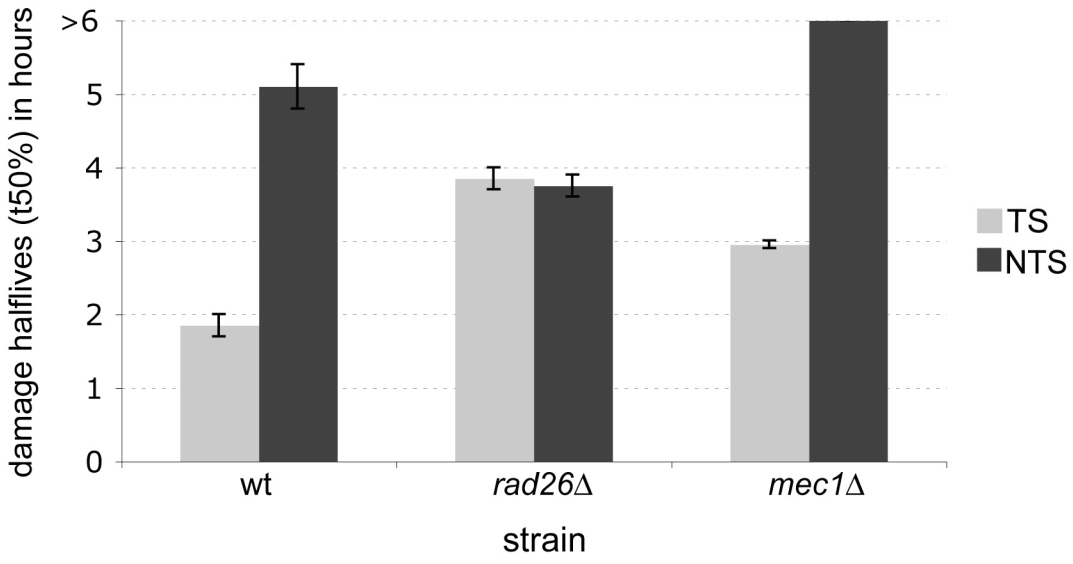

Figure 5-2 Quantification of the signals shown in Figure 5.1

Damages remaining at the post-UV time points were calculated and the time necessary for removal of 50 % of the damages (t50%) was determined for both the TS and the NTS in the different strains. Error bars show the standard error between independent experiments.

5.1.2 Strains lacking the Chk1, Rad53 and Dun1 kinases have normal NER

Mec1, in certain contexts, is the most upstream kinase in the DNA damage checkpoint pathway and activates several other kinases, the most important ones being Chk1, Rad53 and Dun1 (Sanchez et al., 1999; Zhou and Elledge, 1993). To determine whether Mec1 acts directly in NER or via one of these downstream effectors, NER rates were analysed in strains deleted for *CHK1*, *RAD53* and *DUN1*. As is the case for *mec1Δ* cells, prior deletion of *SML1* was required to suppress the lethality of *RAD53* deletion.

Interestingly, no significant alteration in the repair rates for the TS or the NTS were observed in the *chk1Δ* or *rad53Δ sml1Δ* strains, both of which displayed damage half lives comparable to the wild type strain (Figures 5.3). Similarly, deletion of *DUN1* had no observable effect on repair efficiency (Figures 5.4). These results suggest that the mechanism by which Mec1 regulates NER occurs independently of these factors, even though I can not rule out at this point that double or triple mutants could have an effect on NER.

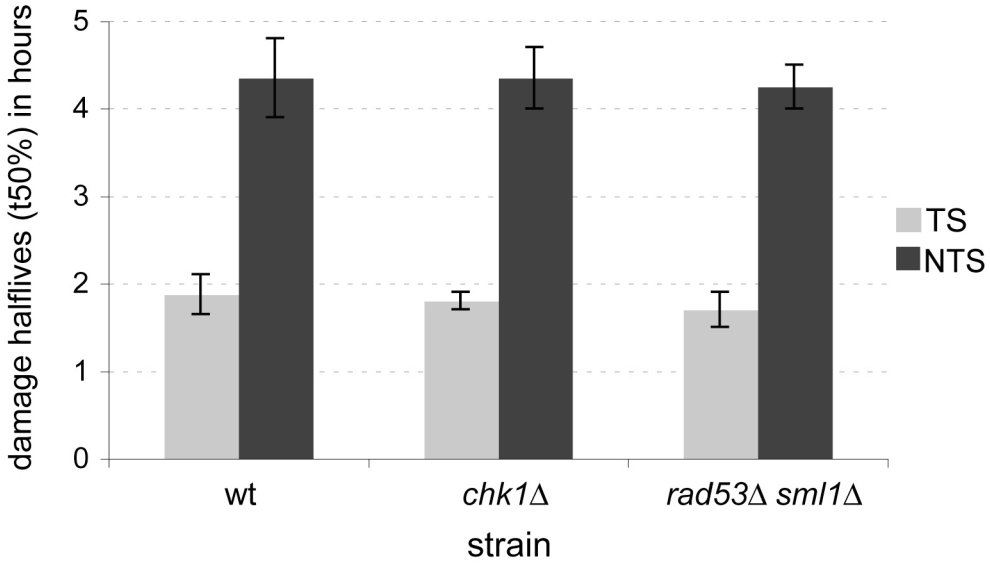

Figure 5-3 Efficient NER does not require the Chk1 and Rad53 kinases

The NER assay was carried out as described using the W303 (wt), *chk1Δ* and *rad53Δ sml1Δ* strains. Damages remaining at the post-UV time points were calculated and the time necessary for removal of 50 % of the damages (t50%) was determined for both the TS and the NTS in the different strains. Error bars show the standard error between independent experiments.

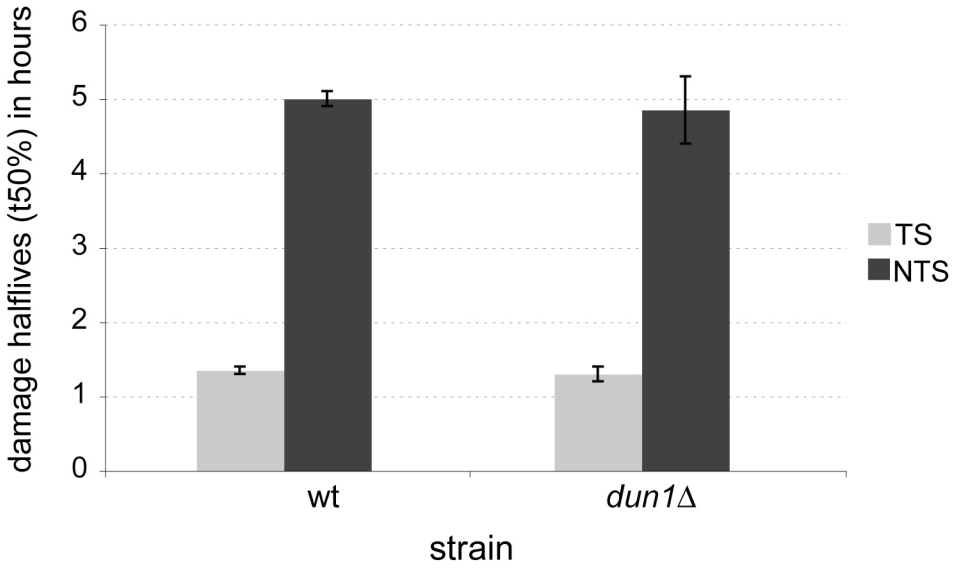

Figure 5-4 Efficient NER does not require the Dun1 kinase

The NER assay was carried out as described using the W303 (wt) and *dun1Δ* strains. Damages remaining at the post-UV time points were calculated and the time necessary for removal of 50 % of the damages (t50%) was determined for both the TS and the NTS in the different strains. Error bars show the standard error between independent experiments.

5.1.3 UV-induced *de novo* protein synthesis is required for efficient NTS repair

A well-known mechanism by which the DDC regulates DNA repair is via transcriptional induction of genes encoding factors involved in the repair of DNA lesions. These genes include NER factors, and it has already been shown that repair of the NTS of an active gene relies on the *de novo* synthesis of repair factors or of factors influencing the efficiency of repair (Al-Moghrabi et al., 2003, 2009), while the TS is repaired efficiently in the presence of the translation inhibitor cycloheximide, i.e. in the absence of damage-induced production of new protein, at least at the *URA3* and *GAL10* genes. I wanted to confirm this result using our method of CPD repair analysis and the *RPB2* gene. Cycloheximide was added 1 hour before UV irradiation at a concentration of 50 µg/ml. As expected, the absence of translation did not significantly affect repair of the TS (Figure 5.5). By contrast, repair of the NTS in the presence of cycloheximide was severely inhibited: CPD levels were essentially unchanged even 6 hours after UV irradiation. This defect was comparable to that observed in the absence of the Mec1 kinase. This suggests that the DDC may regulate repair of the NTS primarily by increasing the abundance of repair factors. Conversely, the role of the DDC in TC-NER appears not to involve upregulation of NER proteins. I therefore hypothesized that the DDC, and specifically the Mec1 kinase, regulates TC-NER mainly via direct post-translational modifications of target proteins.

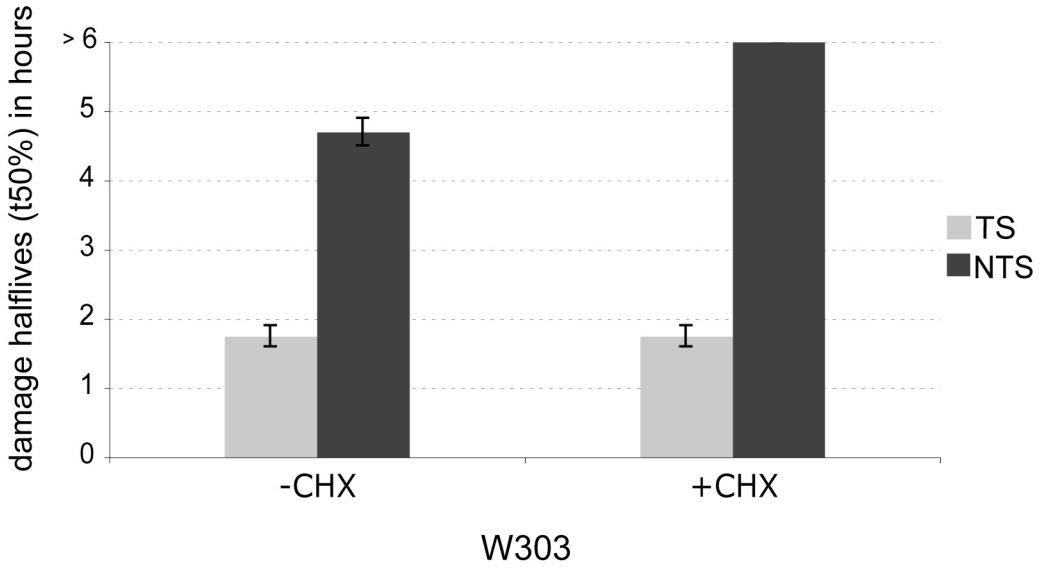

Figure 5-5 Efficient repair of the NTS, but not the TS, requires *de novo* protein synthesis

NER assays were carried out using the wild type strain (W303) in the absence (-CHX) or presence (+CHX) of the translation inhibitor cycloheximide. Damages remaining at the post-UV time points were calculated and the time necessary for removal of 50 % of the damages (t50%) was determined for both the TS and the NTS in the different strains. Error bars show the standard error between independent experiments.

5.2 Targets of the Mec1 kinase

5.2.1 Rad23 phosphorylation mutants do not display defects in NER

Having shown that Mec1 is likely to regulate TC-NER by one or more post-translational modification events, I set out to identify new Mec1 target proteins. Interestingly, the Rad23 protein has been identified as a target for Mec1 in proteome-wide screens in yeast (Albuquerque et al., 2008) and human cells (Matsuoka et al., 2007). Yeast Rad23, and its binding partner Rad4 are involved in both NER subpathways (Verhage et al., 1994; Verhage et al., 1996b). I speculated that phosphorylation of Rad23 by Mec1 might be required for its activation, a hypothesis that could explain the observed NER defects in *mec1Δ sml1Δ* cells. To investigate this possibility, I examined the NER efficiency of a *rad23Δ* deletion strain carrying vectors expressing wild type *RAD23 (RAD23^{wt})*, a mutant *RAD23* in which Serine 121, the residue targeted by Mec1 (Albuquerque et al., 2008), was mutated to alanine (*RAD23^{SA}*), or carrying the empty vector. As expected, repair of both the TS and the NTS was severely compromised in the *rad23Δ* deletion strain, with no detectable repair during the time course of 4 hours. Expression of wild type *RAD23* completely reversed this defect (Figures 5.6). Interestingly, expression of the *RAD23^{SA}* mutant also rescued the NER deficiency. This indicates that the NER defects of the *mec1Δ sml1Δ* mutant are not caused by a lack of Mec1-catalyzed Rad23 phosphorylation, at least at this residue.

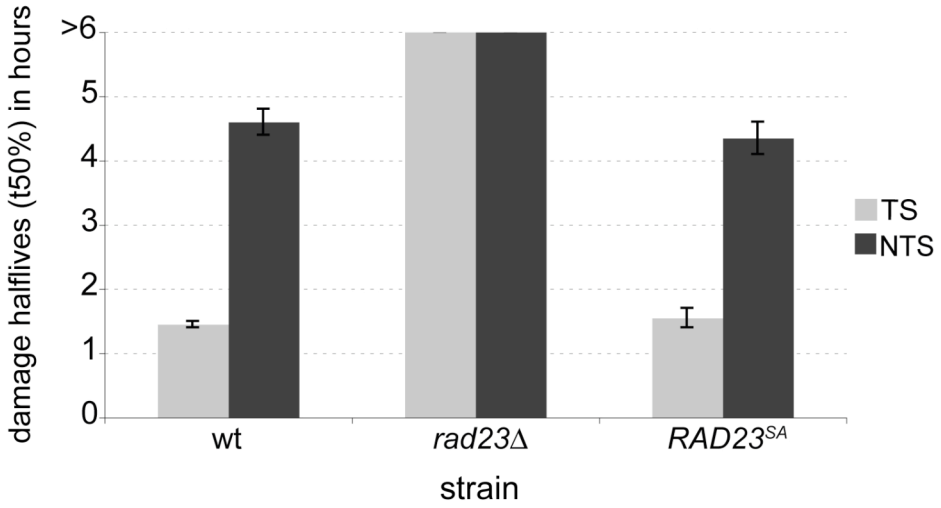

Figure 5-6 Checkpoint-dependent phosphorylation of Rad23 at S121 is not required for efficient NER

The NER assay was carried out using *rad23Δ* strains expressing either wild type Rad23 (wt), no Rad23 (*rad23Δ*), or a S121A mutant version of Rad23 (*RAD23^{SA}*). Damages remaining at the post-UV time points were calculated and the time necessary for removal of 50 % of the damages (t50%) was determined for both the TS and the NTS in the different strains. Error bars show the standard error between independent experiments.

To determine if checkpoint-dependent Rad23 Serine 121 phosphorylation plays a role in other functions of the protein that are involved in survival after UV irradiation, I tested the UV sensitivity of the *rad23Δ* strain, and strains expressing $RAD23^{wt}$, the S121A mutant of Rad23 ($RAD23^{SA}$), or a phosphorylation-mimic mutant, S121D ($RAD23^{SD}$). Futhermore, because I couldn't exclude the possibility that one or more potential Mec1-dependent phosphorylation sites were missed in the proteome-wide screen (Albuquerque et al., 2008), I also analysed Rad23 versions in which all the SQ-sites in the protein (S40, S73 and S121) were mutated to alanine ($RAD23^{3SA}$) or aspartic acid ($RAD23^{3SD}$). Figure 5.7 shows that, as expected, the *rad23Δ* deletion strain displayed strong sensitivity to treatment with UV light, in agreement with the observed defect in NER. Rescue of this strain with the wild type *RAD23* gene reduced this sensitivity to the level of the parental W303 strain. Surprisingly, all the mutant Rad23 versions behaved like the wild type protein in this assay, indicating that Rad23 functions required for survival after UV are not affected by inhibiting or mimicking phosphorylation at potential Mec1 (SQ) sites (Fig. 5.7).

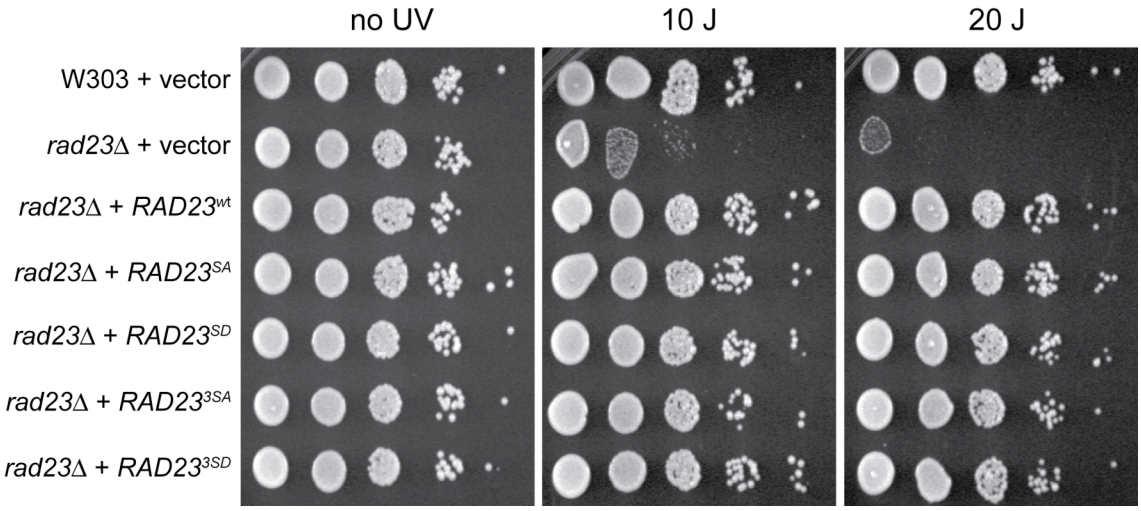

Figure 5-7 Mutation of potential checkpoint-phosphorylation sites in Rad23 does not affect survival after UV

The sensitivity of W303 was compared to *rad23Δ* mutants carrying either empty vector (vector) or vector expressing wildtype ($RAD23^{wt}$), serine 121 single point mutant versions of *RAD23* ($RAD23^{SA}$ and $RAD23^{SD}$, respectively) or serine 40/73/121 triple mutant versions of *RAD23* ($RAD23^{3A}$ and $RAD23^{3D}$, respectively). None of the point mutants displayed detectable differences in sensitivity to UV treatment compared to the wild type strain.

5.2.2 Analysis of checkpoint-dependent phosphorylation of Rad26

5.2.2.1 Construction of an N-terminally tagged Rad26 strain

One possible explanation for the TC-NER defects exhibited by *mec1Δ* cells is that the TC-NER-specific Rad26 protein is activated directly by Mec1-mediated phosphorylation. To identify potential post-translational modifications occurring on Rad26, I created a strain in which the genomic *RAD26* locus was tagged on its N-terminus with 9 Myc sequences, followed by 2 TEV cleavage sites and 8 histidines (*MHRAD26*). A schematic outline of the N-terminal tagging strategy is shown in Figure 5.8A. The tagged gene was still under control of its endogenous regulatory elements, avoiding artefacts due to a change in expression level. As expected, Rad26 tagging led to the appearance of an anti-Myc-reactive species with a molecular weight of around 140 kDa, which was absent in the parental W303 strain (Fig. 5.8B).

Since addition of a large tag could potentially render Rad26 non-functional, I also determined whether this protein can still initiate TC-NER. To investigate this, *MHRAD26* cells were crossed with a *rad16Δ* mutant and the resulting strains' UV sensitivity analysed. In agreement with previous studies (van Gool et al., 1994; Verhage et al., 1996a), the TC-NER-deficient *rad26Δ* strain strain did not show increased UV-sensitivity when compared to the wild type, whereas the GG-NER-deficient *rad16Δ* strain did (Fig. 5.8C). Additional deletion of *RAD26* in the *rad16Δ* background dramatically increased UV sensitivity. Importantly, the tagged *MHRAD26* gene did not cause increased UV sensitivity in the *rad16*Δ background, indicating that the tagged protein was functional.

5.2.2.2 Rad26 is phosphorylated in response to DNA damage

To investigate if Rad26 is phosphorylated after UV irradiation, I treated the *MHRAD26* strain with UV and analysed the electrophoretic mobility of the protein by SDS-PAGE and Western blotting. As shown in Figure 5.9A, a slower migrating form of the protein became visible after UV treatment, indicative of a post-translational modification. The modification became apparent just 10 minutes after UV treatment, peaked between 1 and 2 hours, and then started disappearing.

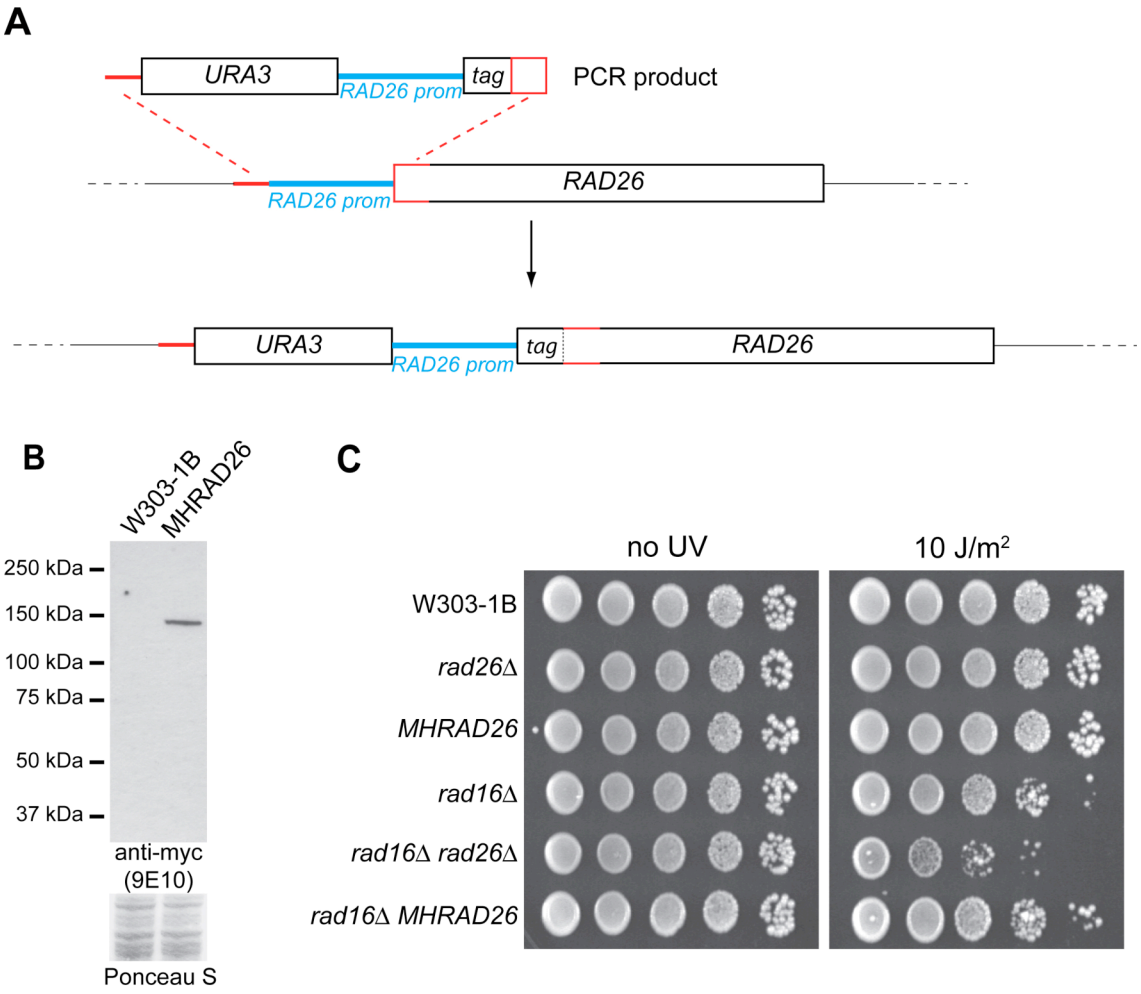

Figure 5-8 Construction and analysis of a strain with N-terminally tagged *RAD26*

(A) Schematic outline of the strategy used for creating an N-terminally tagged version of the gene which is still under control of the endogenous promoter. A 400 bp fragment of the *RAD26* promoter was cloned between a *URA3* marker and the sequence encoding the tag. A DNA fragment containing the region from the *URA3* gene until the tag was generated by PCR using primers designed to be able to replace the endogenous *RAD26* promoter and inserting the N-terminal tag in frame with the *RAD26* gene.
(B) Western Blot showing the appearance of a myc-reactive protein species in the tagged *MHRAD26* strain which is absent in the parental strain (W303). The presence of proteins in both lanes was confirmed by staining of the membrane with Ponceau S.
(C) Spotting assay showing the functionality of the N-terminally tagged Rad26 protein. *RAD26* deletion increases the UV-sensitivity of a GG-NER-deficient *rad16Δ* strain. In contrast, N-terminal tagging of *RAD26* does not show this increase in UV-sensitivity in the *rad16Δ* background, confirming that despite the addition of a large tag, the tagged Rad26 protein is still proficient for TC-NER.

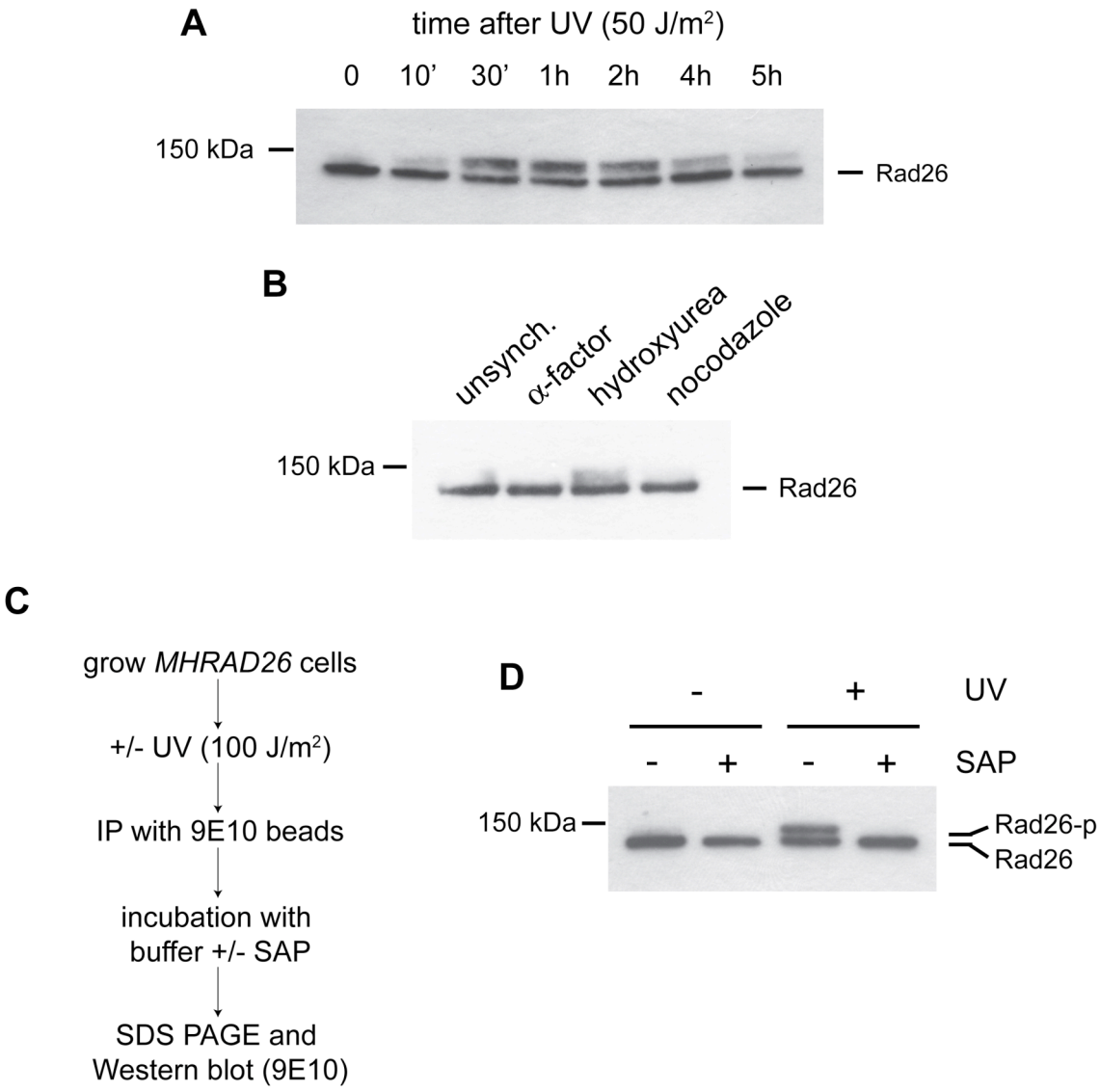

Figure 5-9 UV-induced phosphorylation of Rad26

(A) Western blot analysis of Rad26 from wildtype cells harvested either before (0) or at various time points after UV irradiation. The decrease in electrophoretic mobility after UV treatment indicates a post-translational modification. MHRad26 was detected with 9E10 antibodies.
(B) Western blot analysis of Rad26 from unsynchronized wild-type cells and cells which have been synchronised in G1 (alpha factor), S (hydroxyurea) or G2/M (nocodazole). MHRad26 was detected with 9E10 antibodies.
(C) Experimental outline of the procedure leading to the result shown in (D)
(D) Western blot analysis of Rad26 immunoprecipitated before and 2 hours after UV treatment and treated either with buffer alone or Shrimp alkaline phosphatase. MHRad26 was detected with 9E10 antibodies.

Longer exposures of the Western blots revealed that even in the absence of UV-damage a small amount of Rad26 is modified. Interestingly, this damage-independent modification appeared to be linked to the cell cycle, as it was absent in cells arrested in G1 and G2 (achieved by treatment with alpha-factor and nocodazole, respectively) and enriched in cells arrested in S-phase (by treatment with hydroxyurea) (Fig. 5.9B). Furthermore, I noted that no degradation of Rad26

was observed after UV irradiation, unlike observed previously for its human homologue CSB (Groisman et al., 2006). Because of the pronouced decrease in electrophoretic mobility of the protein, I first suspected Rad26 to be mono-ubiquitylated after DNA damage. However, analysis of the immunoprecipitated and modified protein with ubiquitin-specific antibodies did not give any signal, excluding an involvement of UV-specific Rad26 ubiquitylation (not shown). In order to determine if phosphorylation of Rad26 is responsible for the observed shift in electrophoretic mobility, I immunoprecipitated Rad26 before and after UV irradiation and treated the bead-bound material with Shrimp Alkaline Phosphatase (SAP) (experimental procedure outlined in Fig. 5.9C). The slower-migrating protein was again only clearly visible after UV-irradiation, and it was lost after incubation with phosphatase, indicating that it represents a phosphorylated form of Rad26 (Fig. 5.9D).

To determine whether Rad26 phosphorylation is a specific response to UV irradiation or if it occurs in response to other types of DNA damage, I treated cells with various chemical agents to induce different types of DNA lesions. All of these treatments caused Rad26 to be phosphorylated (Fig. 5.10A). Interestingly, other forms of cellular stress, including heat-shock and osmotic shock, did not result in modification of Rad26 (Fig. 5.10B).

Finally, because Rad26 is thought to be recruited to stalled RNA polymerase II complexes, and because UV-induced DNA lesions cause RNAPII stalling, I tested whether 6-azauracil (6AU, which causes frequent RNAPII stalling by restricting nucleotide availability) could also promote Rad26 phosphorylation. Treatment with this drug did not cause a detectable increase in the phosphorylated form of Rad26 (Fig. 5.10B). Thus, Rad26 phosphorylation appears to occur specifically in response to DNA damage.

5.2.2.3 Rad26 phosphorylation is dependent on the Mec1 checkpoint kinase

To determine whether the DDC is required for Rad26 phosphorylation, I tested whether this modification occurred in *mec1Δ sml1Δ* cells. Loss of the Mec1 checkpoint kinase completely abolished phosphorylation of Rad26 (Fig. 5.10C). To investigate whether this effect was specifically due to absence of the Mec1 kinase, or an indirect result of deletion of both *SML1* and *MEC1*, I reintroduced galactose-inducible forms of HA-tagged wildtype *MEC1 (MEC1^{wt})* or kinase-dead *MEC1 (MEC1^{kd})* into the *MHRAD26 mec1Δ sml1Δ* strain. Rad26 phosphorylation was recovered by growing cells expressing *MEC1*^{wt} in galactose, but not glucose, while the *MEC1*^{kd}-containing strain had no Rad26 phosphorylation in either carbon source, even though it expressed Mec1^{kd} at a level similar to that of the wild-type protein in

inducing conditions (Fig. 5.10D). These data indicate that the kinase activity of Mec1 is required for Rad26 phosphorylation.

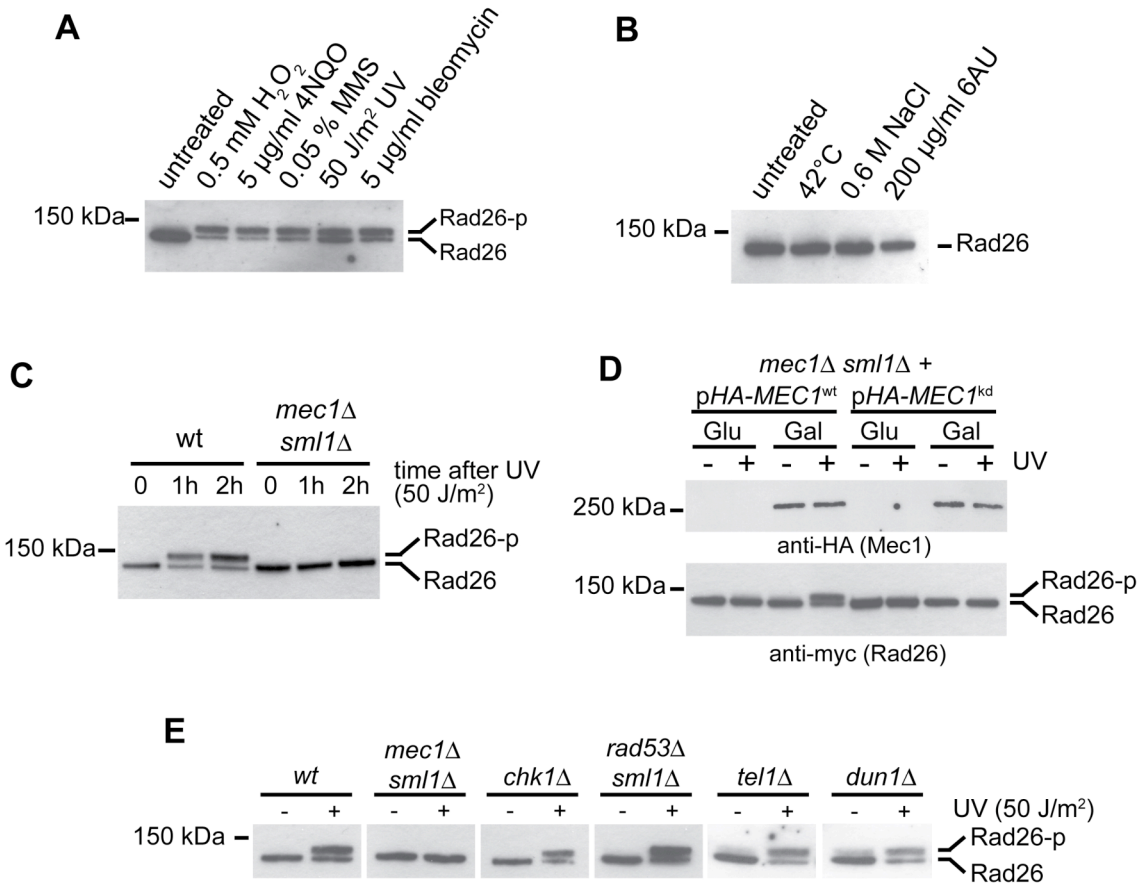

Figure 5-10 Involvement of the DNA damage checkpoint in Rad26 phosphorylation

(A) Western blot analysis of Rad26 after various kinds of DNA damage. MHRad26 was detected with 9E10 antibodies.
(B) Western blot analysis of Rad26 after infliction of cellular stress different from DNA damage. MHRad26 was detected with 9E10 antibodies.
(C) Western blot analysis of Rad26 phosphorylation in the absence of the Mec1 checkpoint kinase. MHRad26 was detected with 9E10 antibodies.
(D) Western blot analysis of Rad26 in *mec1sml1* cells expressing either galactose-inducible HA-tagged wildtype (wt) or kinase-dead (kd) Mec1. MHRad26 was detected with 9E10 antibodies.
(E) Western blot analysis of Rad26 in strains lacking various kinases of the DNA damage checkpoint cascade. MHRad26 was detected with 9E10 antibodies.

The absence of Mec1 leads to inactivation of downstream kinases, the most important of which are Chk1 and Rad53 (Longhese et al., 1998). To determine if phosphorylation of Rad26p was mediated by Chk1 or Rad53 (either directly or indirectly), I deleted their encoding genes and examined the phosphorylation state of Rad26 after UV-irradiation. Damage-induced

phosphorylation was evident in both of these strains, supporting the idea that Mec1 directly phosphorylates Rad26 without the involvement of downstream kinases (Fig. 5.10E). I also tested cells lacking Dun1, another kinase activated by Rad53 (Zhou and Elledge, 1993), and Tel1, the yeast homologue of ATM (Greenwell et al., 1995; Morrow et al., 1995). Dun1 acts downstream of Rad53, which itself had no role in Rad26 phosphorylation. Moreover, the complete absence of Rad26 phosphorylation in the *mec1Δ sml1Δ* strain suggests that there is no redundancy between Mec1 and Tel1 in this event as there are in certain others. Neither removal of Dun1 or Tel1 would therefore be expected to affect phosphorylation of Rad26. Indeed, both of these mutant strains exhibited normal Rad26 phosphorylation (Fig. 5.10E).

I tried to show biochemically using *in vitro* kinase assays that Rad26 is a direct target for the Mec1 kinase, but several attempts to get the *in vitro* kinase working with a positive control (PHAS-I), were not successful (data not shown), and direct biochemical evidence for such an event is still missing.

5.2.2.4 Identification of the Rad26 phosphorylation site

Mec1 phosphorylates serines and threonines that are immediately adjacent to a glutamine residue (SQ/TQ motifs). Rad26 possesses 1 TQ and 4 SQ consensus motifs (Fig. 5.11A). To identify the site of Rad26 phosphorylation, the *MHRAD26* locus was cloned into pRS316, and each of the residues predicted to be a Mec1 target site were individually mutated to alanine. The mutated plasmids were then re-introduced into *rad26Δ* cells, and the phosphorylation status of Rad26 was analyzed after induction of damage with 4NQO (4-nitroquinoline-1-oxide; a UV mimetic chemical compound which creates damages repaired by NER). As shown in Figure 5.11B, mutation of S27 in Rad26 led to the complete absence of a shifted Rad26 band, whereas all the other single point mutants behaved like the wild type protein.

This result suggested that S27 is the sole site of Mec1-catalyzed Rad26 phosphorylation. However, I could not rule out the possibility that another modification escaped detection by SDS-PAGE and Western blotting, for example because it did not lead to a noticeable change in Rad26 migration. Therefore, mass spectrometry (MS) was used as an alternative strategy to analyze post-translational modificiations of Rad26. Due to the low abundance of Rad26, I was unfortunately unable to purify enough modified protein from *MHRAD26* cells for MS analysis. To circumvent this problem, *MHRAD26* was placed under the control of a galactose-inducible promoter on a centromeric plasmid (pYC2 vector from Invitrogen; creating pYC2-*MHRAD26*) and this construct was then introduced into a *rad26Δ* deletion mutant. I first investigated whether the tagged Rad26 protein could be efficiently over-expressed from this vector. After

shifting cells from raffinose to galactose, the tagged form of Rad26 was rapidly and dramatically induced (Figure 5.11C).

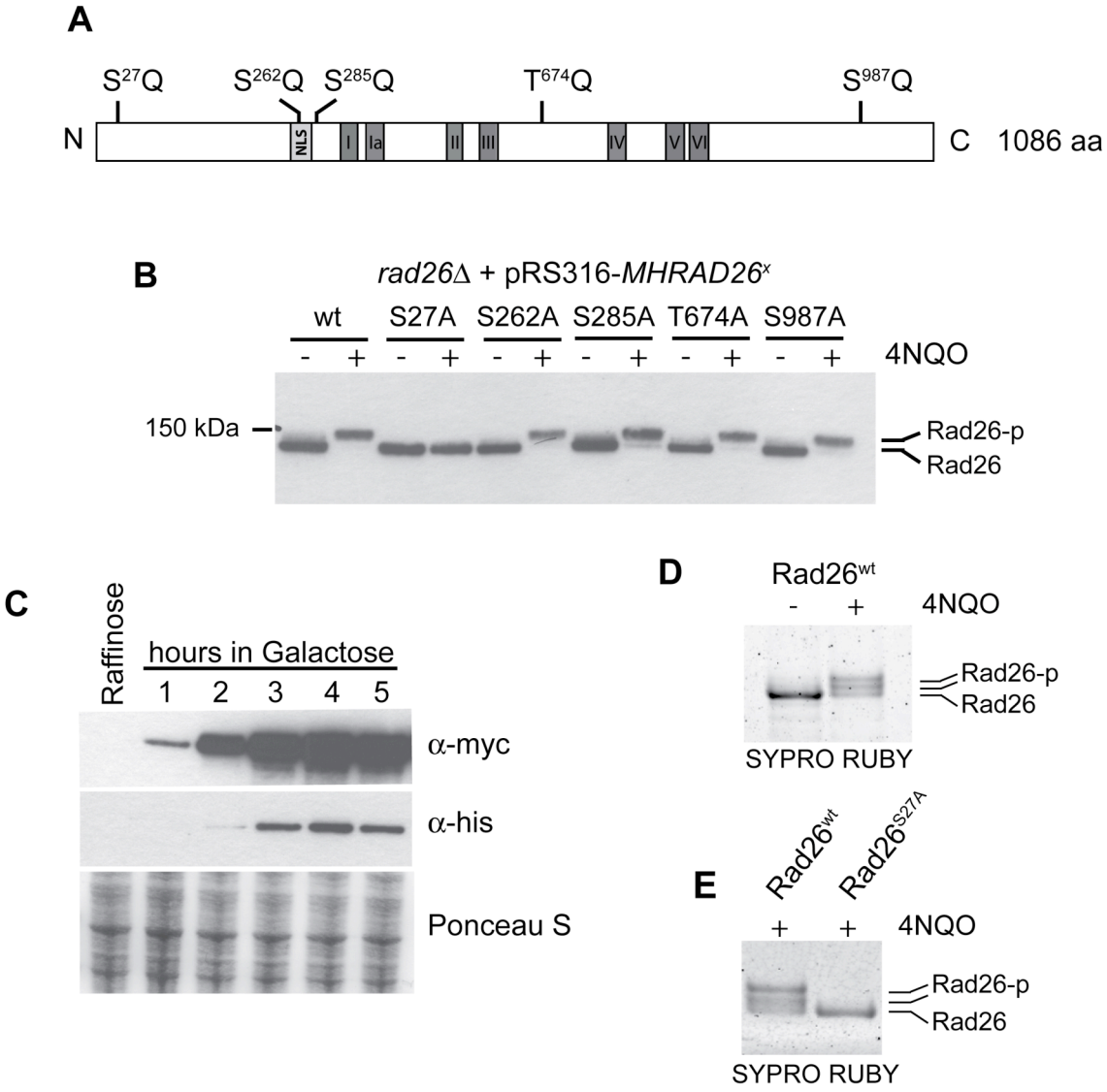

Figure 5-11 Identification of the Rad26 phosphorylation site

(A) Schematic representation of the Rad26 protein. Grey boxes indicate important protein domains. The NLS is shown in light grey, the seven conserved helicase domains are shown in dark grey. The 5 potential Mec1 target sites (SQ/TQ) are indicated above. MHRad26 was detected with 9E10 antibodies.
(B) Analysis of Rad26 SQ/TQ point mutants. The five SQ/TQ sites were mutated individually and the mutant genes were then expressed in a *rad26* mutant strain. The phosphorylation status of the proteins was determined after 4-NQO treatment.
(C) Galactose-induced overexpression of Rad26. The *MHRAD26* open reading frame was cloned behind a galactose-inducible promoter on the pYC2 plasmid (Invitrogen). Expression of the protein can be efficiently induced with 2 % galactose and detected by Western blotting with both anti-myc and anti-his antibodies. Similar loading was confirmed by staining of the membrane with Ponceau S.
(D) Purification of overexpressed Rad26 protein before and after damage with 4-NQO. Rad26 was immunoprecipitated from extracts and eluted from the beads with TEV protease. The eluate was analysed by SDS-PAGE on a 3-8 % gradient gel followed by SYPRO RUBY staining. More than one slower migrating form of Rad26 is visible.

(E) Purification of overexpressed wild-type and S27A Rad26 after damage with 4-NQO. No slower migrating form of Rad26 can be detected after DNA damage when the single point mutant version is expressed.

This over-expressed Rad26 was purified before and after 4-NQO treatment using Myc-affinity resin and eluted with TEV protease. Despite expressing Rad26 at non-physiological levels, the characteristic mobility shift was still visible after DNA damage. Interestingly, this analysis revealed two slower-migrating forms of the Rad26 protein (Fig. 5.11D), suggesting that more than one phosphate group was added to Rad26 after DNA damage. MS analysis verified this idea: both S27 and S30 were found to be phosphorylated in the sample. These sites of phosphorylation were identified following peptide fragmentation using both collision induced dissociation (CID) and electron transfer dissociation (ETD).

Interestingly, while this work was in progress, a proteome-wide study of checkpoint-dependent phosphorylation identified Mec1-dependent modification of S27 and S29 of Rad26 (Albuquerque et al., 2008). Surprisingly, neither S29 nor S30 exist in the context of a proper Mec1 consensus motif. Thus, I speculated that S27 is the primary Rad26 phosphorylation site, but that residues nearby might be targeted in a non-specific manner. In order to investigate this idea, I mutated S27 in the pYC2-*MHRAD26* plasmid (creating plasmid pYC2-*MHRAD26*^{S27A}) and purified both the wildtype and mutant protein after 4NQO treatment. Indeed, whereas the wildtype protein showed 2 distinct slower-migrating bands, no shift was observed with the S27A mutant (Figure 5.11E). The complete absence of Rad26 phosphorylation in this mutant was also confirmed by mass-spectrometry. These results demonstrate that mainly S27 (and sometimes also S29 and/or S30) of Rad26 are phosphorylated after DNA damage by the Mec1 kinase.

5.2.2.5 Analysis of an involvement of Rad26 phosphorylation in TC-NER

5.2.2.5.1 Rad26 phosphorylation does not lead to altered survival after UV irradiation

Given that I found that *MEC1* deletion affects TC-NER (see Figures 5.1 and 5.2) and that Rad26 is a direct target of Mec1 kinase, an obvious possibility was that this phosphorylation event plays a role in TC-NER. I first used genetics to investigate this possibility, taking advantage of the fact that the *rad16Δ rad26Δ* double mutant is much more UV-sensitive than either single mutant (Verhage et al., 1996a).

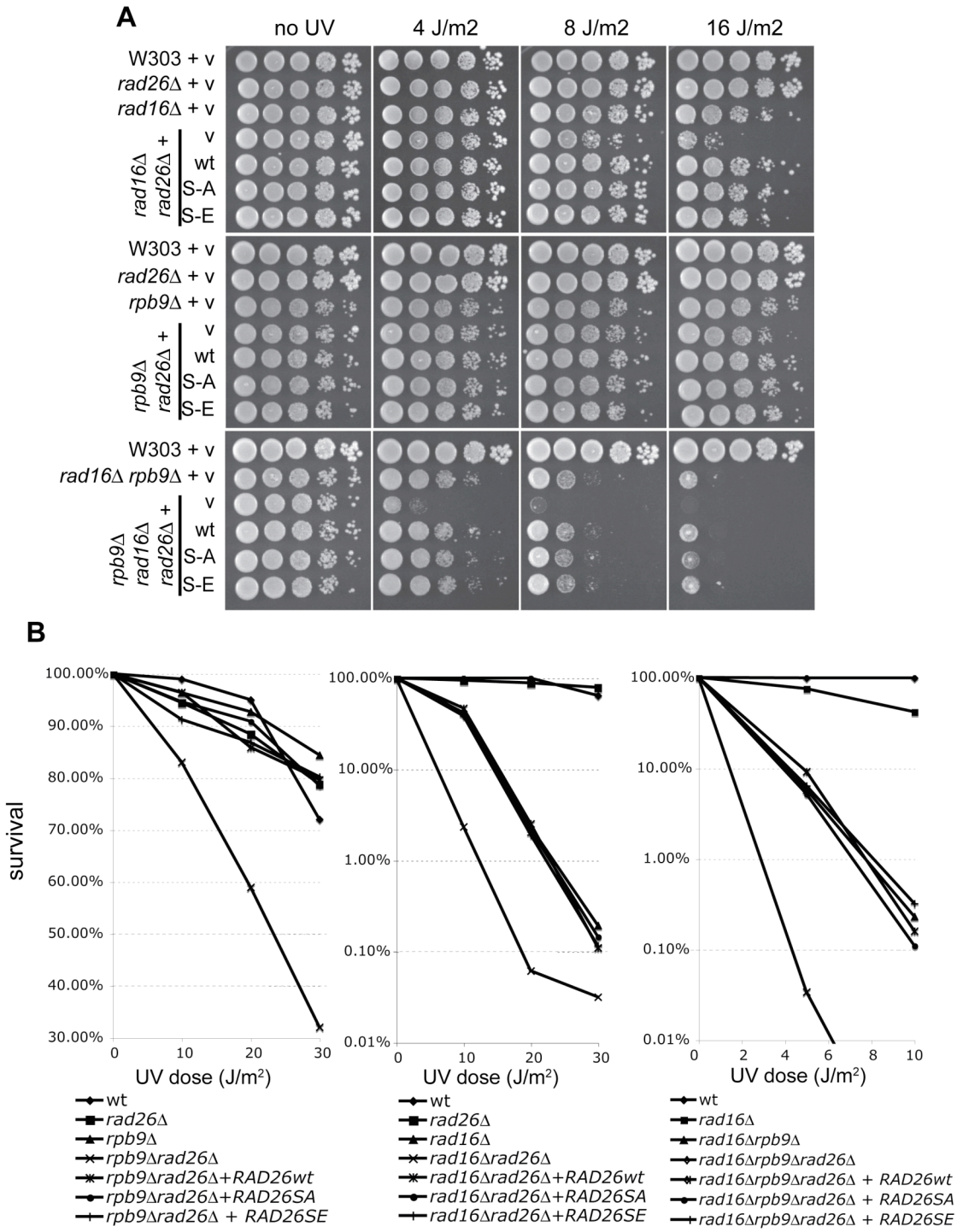

Figure 5-12 Analysis of survival after UV irradiation in various strain backgrounds expressing wild-type and mutant versions of Rad26

(A) Spotting assay showing no significant alteration in UV sensitivity when wild-type and point-mutant versions of Rad26 are expressed in the *rad16Δ* background (top panel), *rpb9Δ* background (middle panel) or *rad16Δ rpb9Δ* background (lower panel).

(B) Graphs showing survival rates after increasing doses of UV. No significant alteration in survival was detected in the *rpb9Δ* backgound (left), *rad16Δ* background (middle) or *rad16Δ rpb9Δ* background (right).

Point mutants in which S27 was mutated either to alanine (to prevent phosphorylation (*RAD26*^{SA})) or to glutamic acid (to mimic phosphorylation (*RAD26*^{SE})) were introduced into *rad16Δ rad26Δ* cells, and the UV sensitivity of these strains was tested by spotting assays. Like wild type Rad26, both mutated forms of Rad26 rescued the *rad16Δ rad26Δ* double mutant such that its UV-sensitivity was similar to that of the *rad16Δ* single mutant (Fig. 5.12A). In order to exclude the possibility that the effect of the point mutations in Rad26 is masked by the second TC-NER pathway in yeast, which is mediated by the Rpb9 protein (Li and Smerdon, 2002), I also carried out the same assay using a *rad26Δ rpb9Δ* double mutant and a *rad16Δ rad26Δ rpb9Δ* triple mutant. Again, the phosphorylation mutants acted like the wild type protein in these alternative strain backgrounds (Fig. 5.12A). As it is easy to miss slight differences in UV-sensitivity using this relatively crude assay, I also determined survival rates by plating defined numbers of cells and determining exact survival rates following UV treatment. This more sensitive assay confirmed that the phosphorylation mutants did not affect UV survival under these conditions (Figure 5.12B).

5.2.2.5.2 Rad26 phosphorylation increases the efficiency of TC-NER

The damage survival assays show that phosphorylation of Rad26 is not absolutely required for the function of the protein, but do not rule out the possibility that the modification affects the rate of TC-NER. To investigate this possibility, I analyzed these mutants using the strand-specific NER assay. Interestingly, the alanine mutant (which cannot be phosphorylated) exhibited a significant delay in TC-NER, while TC-NER in the glutamate mutant (which mimics persistent phosphorylation) appeared to be unaffected (see sequencing gel in Fig 5.13 and graphs in Fig. 5.14). Thus, whereas the half-life of damages in the transcribed strand was 1.7 hours in the wild type strain, it was 2.6 hours in the phosphorylation-site (SA) mutant (Fig. 5.14). As expected, repair of the NTS was not affected by either of the mutations (graph in Fig. 5.14, sequencing gel not shown). I conclude that damage-induced phosphorylation of Rad26 by Mec1 kinase increases the rate of TC-NER.

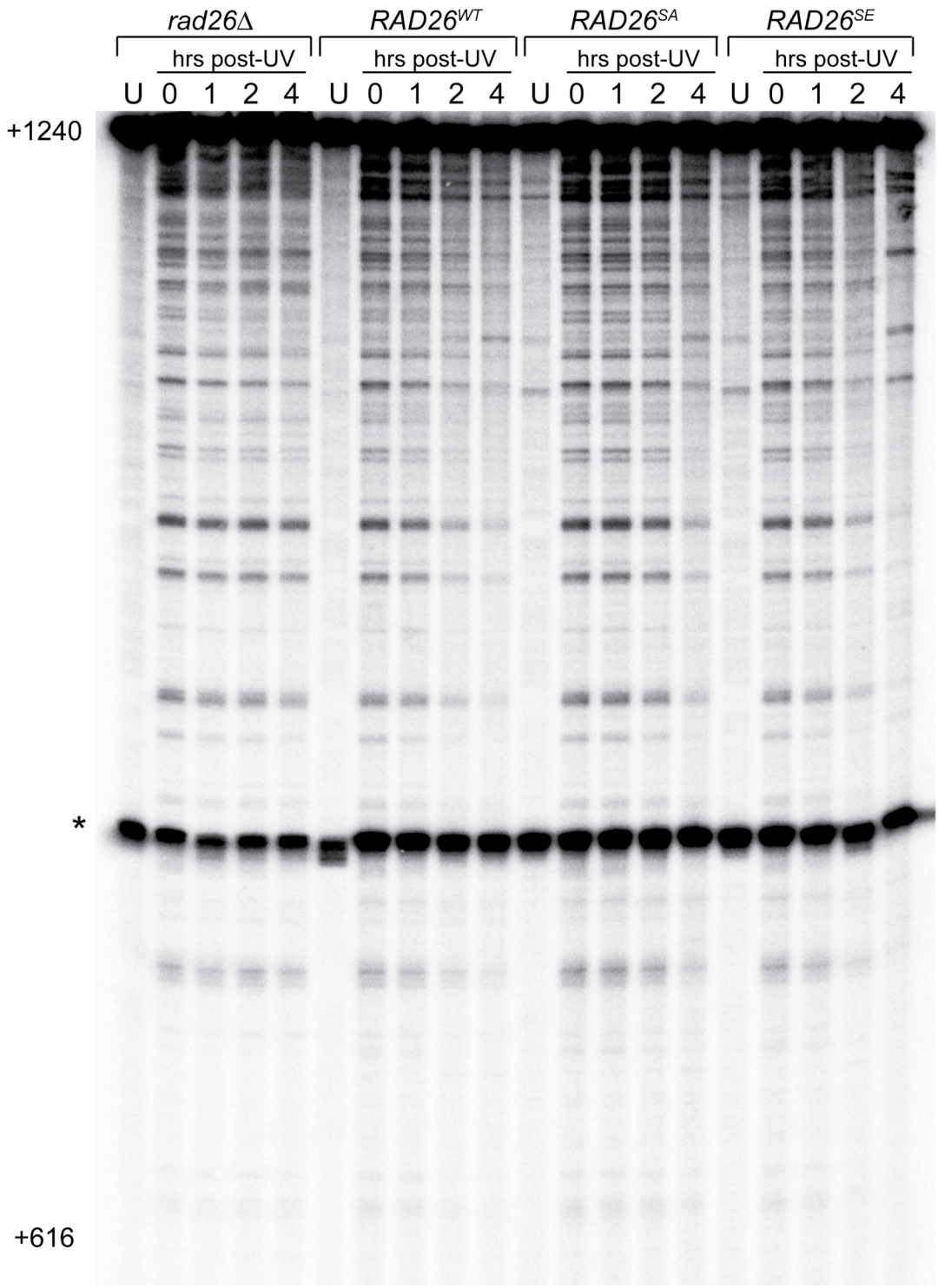

Figure 5-13 Rad26 phosphorylation is required for efficient TC-NER

Representative sequencing gel showing a comparison of NER kinetics in Rad26 mutants. Strand specific NER was analysed in the TS of *RPB2* in *rad26Δ* cells expressing either no *RAD26* (*rad26Δ*), wild-type *RAD26* ($RAD26^{WT}$), or mutant versions in which serine 27 is replaced by either alanine ($RAD26^{SA}$) or glutamate ($RAD26^{SE}$). Numbers on the left of the gel indicate the nucleotide position relative to the *RPB2* transcription start site on the TS. A non-specific band appearing also in the unirradiated control sample (U) is marked with an asterisk.

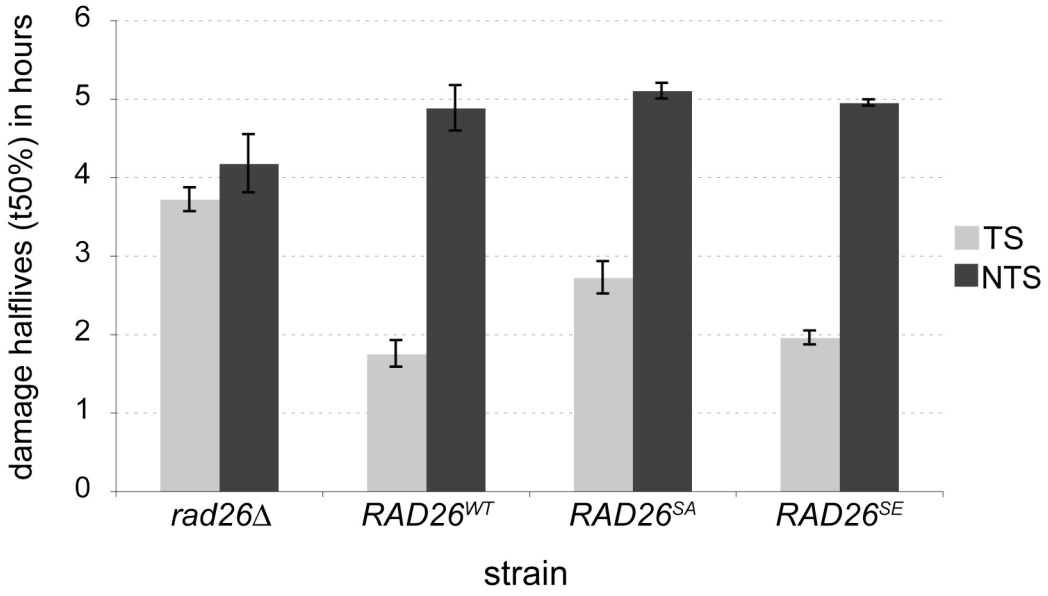

Figure 5-14 Quantification of the signals shown in Figure 5.14

Damages remaining at the post-UV time points were calculated, and the time necessary for removal of 50 % of the damages (t50%) was determined for both the TS and the NTS in the different strains. Error bars show the standard error between independent experiments.

5.2.2.6 Expression of a phosphomimic Rad26 mutant is not sufficient to overcome the TCR defects in a strain lacking the Mec1 kinase

Based on the findings that both the *mec1Δ sml1Δ* and the *RAD26*^{S27A} mutant, but not the *RAD26*^{SE} mutant, have defects in TC-NER, I speculated that the requirement for the Mec1 kinase in this process might be bypassed by expressing the *RAD26*^{SE} mutant in the *mec1Δ sml1Δ* strain. To investigate this possibility, I deleted the *RAD26* gene in the *mec1Δ sml1Δ* strain and transformed the resulting strain with either empty vector or plasmids expressing *RAD26*^{wt}, *RAD26*^{SA} or *RAD26*^{SE}, and then analysed NER kinetics in these cells.

As shown in Figures 5.15, TC-NER was completely absent when *RAD26* was deleted in the *mec1Δ sml1Δ* background, showing that, as expected, the remaining TC-NER in this background is entirely dependent on the presence of Rad26. Putting back the wild type version of *RAD26* completely restored TC-NER to the level previously observed for the *mec1Δ sml1Δ* mutant. The *RAD26*^{SA} mutant behaved exactly the same, confirming that mutating the phospho-acceptor residue to an alanine does not change the activity of the protein in a strain already deleted for kinase responsible for the phosphorylation event. Surprisingly, I did not observe increased TC-NER rates in the strain expressing the phosphomimic *RAD26*^{SE} mutant. This result indicates that the Mec1 kinase has additional phosphorylation targets which are involved in TC-

NER, and shows that the TC-NER defect in *mec1Δ sml1Δ* cells is not due to a lack of Rad26 phosphorylation by Mec1.

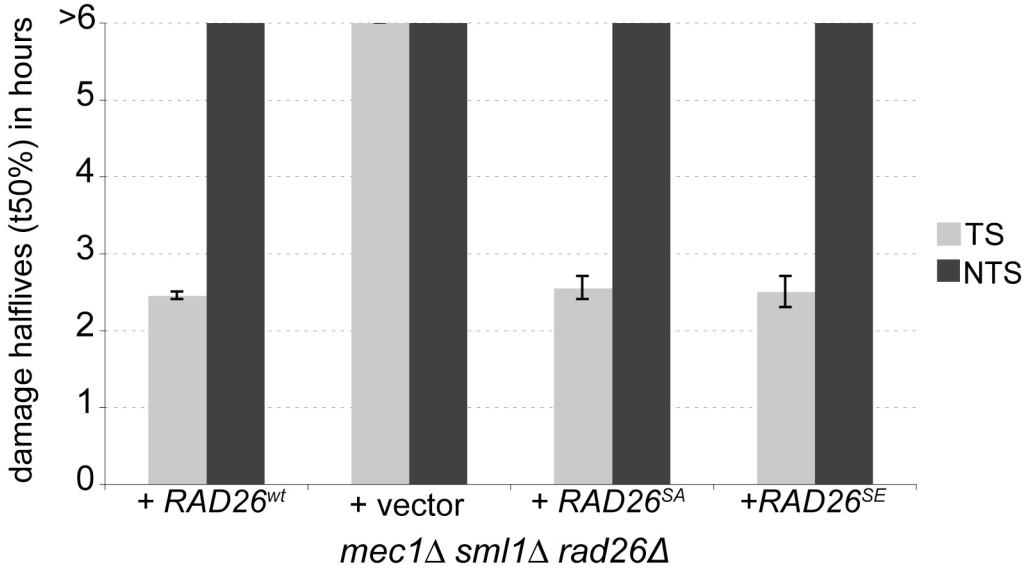

Figure 5-15 Analysis of NER *mec1Δ sml1Δ* cells expressing Rad26 mutants

NER kinetics were determined for the TS and NTS of *RPB2* in *mec1Δ sml1Δ rad26Δ* cells expressing either no *RAD26* (+ vector), wild-type *RAD26* (+ $RAD26^{wt}$), or mutant versions in which serine 27 is replaced by either alanine (+ $RAD26^{SA}$) or glutamate (+ $RAD26^{SE}$). Damages remaining at the post-UV time points were calculated and the time necessary for removal of 50 % of the damages (t50%) was determined for both the TS and the NTS in the different strains. Error bars show the standard error between independent experiments.

As expected, repair of the NTS was not influenced by *RAD26* deletion or by expressing the mutant versions of *RAD26* in the *mec1Δ sml1Δ* background, with little or no repair detected even at the latest time point in any of the strains (Fig. 5.15).

The complete absence of detectable NER on the analyzed *RPB2* fragment in the *mec1Δ sml1Δ rad26Δ* triple mutant might suggest that this strain should be considerably more UV sensitive than the *mec1Δ sml1Δ* double mutant, and I set out to investigate if this is really the case. Surprisingly, the two strains did not display significant differences in UV sensitivity when analysed by the spotting assay (Fig. 5.16), showing that the remaining repair of the TS in strains lacking only the Mec1 kinase does not result in increased survival after UV irradiation. This suggests that a considerable decrease in TC-NER does not necessarily correlate with a similar decrease in UV-sensitivity under normal conditions – even when GG-NER is also compromised - , and helps explain why the decrease in TC-NER observed in $RAD26^{SA}$ does not lead to decreased viability after UV-irradiation.

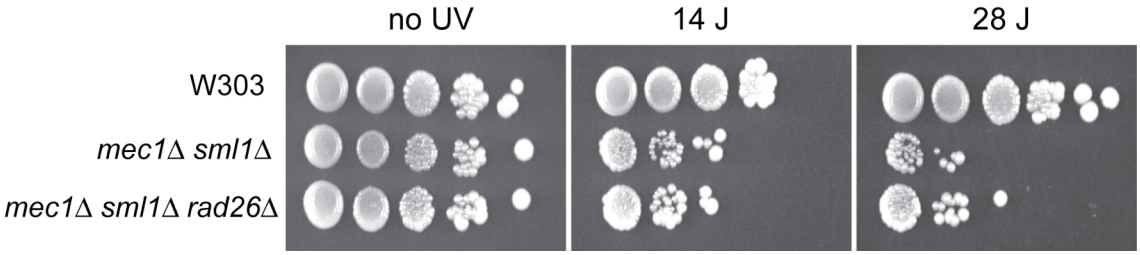

Figure 5-16 Analysis of the effect of *RAD26* deletion on the UV sensitivity of the checkpoint-deficient *mec1Δ sml1Δ* strain

Spotting assay comparing the UV sensitivity of wild-type (W303), *mec1Δ sml1Δ* and *mec1Δ sml1Δ rad26Δ* strains. Deletion of *RAD26* in the *mec1Δ sml1Δ* background does not lead to a significant increase in UV-sensitivity. If anything, there is a slight decrease, at least at the higher UV-dose.

5.2.2.7 Rad26 phosphorylation is not involved in ubiquitylation and degradation of RNA Polymerase II

Since Rad26 interacts with Def1 (Woudstra et al., 2002), the factor controlling UV-induced ubiquitylation and degradation of the RNAPII subunit Rpb1, I speculated that this process might be influenced by phosphorylation of Rad26. In theory, a decrease in TC-NER efficiency might be explained by faster degradation of Rpb1, because TC-NER and Rpb1-ubiquitylation are thought to act on the same substrate and might compete for it.

To determine if phosphorylation of Rad26 influences ubiquitylation and degradation of Rpb1, *rad26Δ* cells carrying either empty vector, $RAD26^{wt}$, $RAD26^{SA}$, or $RAD26^{SE}$ were treated with cycloheximide to abolish synthesis of new proteins, and irradiated with UV. Cells were then harvested at different time points (Figure 5.17A) and Rpb1 degradation was assessed by Western blotting using an 8WG16 antibody. To measure Rpb1 ubiquitylation, I utilised a method developed in our laboratory (Anindya et al., 2007), which relies on isolation of mono- and poly-ubiquitylated proteins using GST-Dsk2 beads, followed by Western blotting and detection of the protein of interest using specific antibodies.

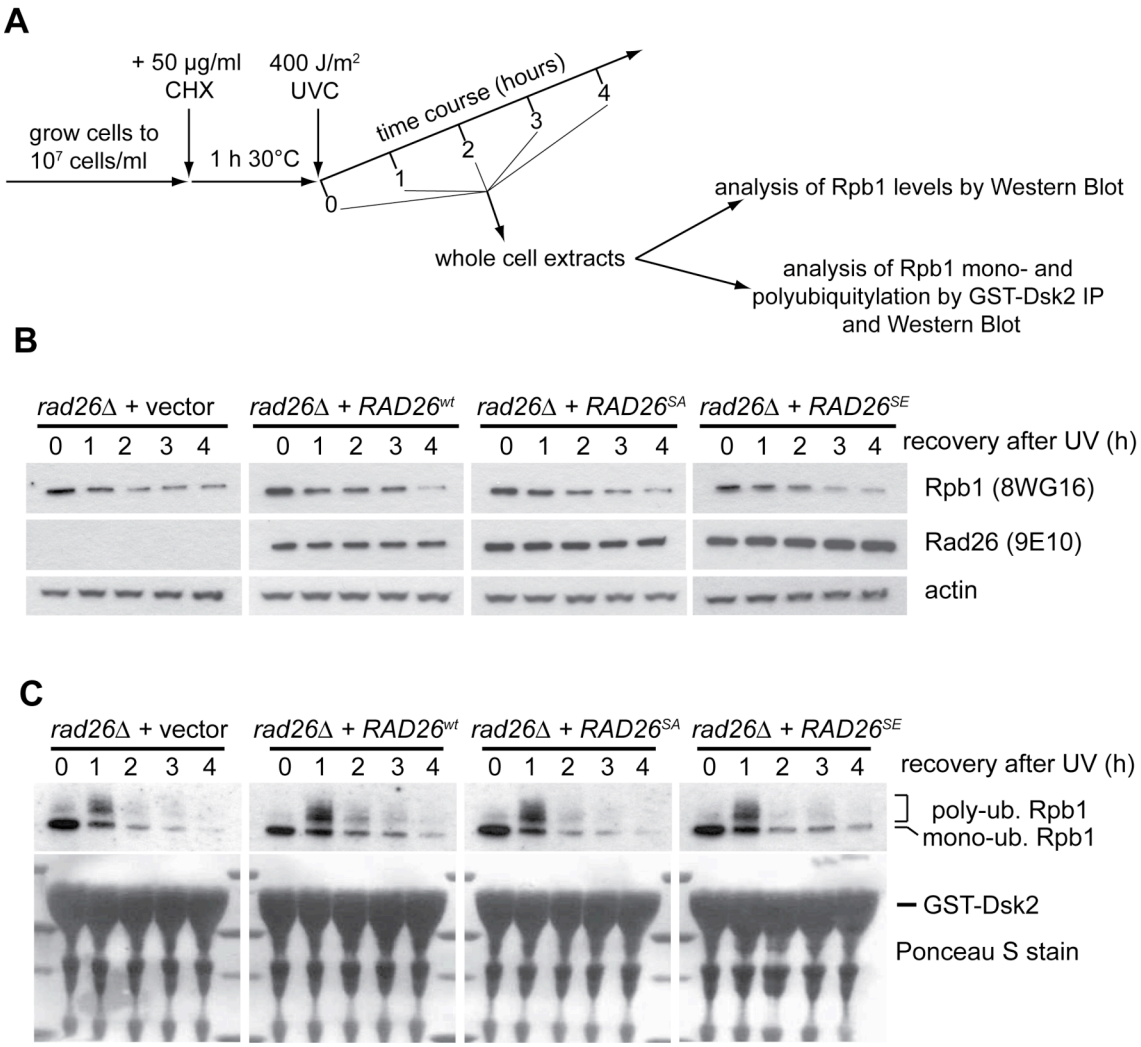

Figure 5-17 Rad26 phosphorylation does not seem to affect Rpb1 ubiquitylation/degradation

Analysis of Rpb1 ubiquitylation and degradation in *rad26Δ* cells expressing no *RAD26* (+vector), wild-type *RAD26* (+ $RAD26^{wt}$), or mutant versions in which serine 27 is replaced by either alanine (+ $RAD26^{SA}$) or glutamate (+ $RAD26^{SE}$).
(A) Experimental outline of the experiment.
(B) Western blot analysis of Rpb1 and Rad26 protein levels in extracts before and at the indicated times after UV-treatment. No significant difference in stability was observed for either of the two proteins. Equal loading was confirmed by detection of actin.
(C) Western blot analysis of Rpb1 after immunoprecipitation of mono- and polyubiquitylated proteins with GST-Dsk2. In agreement with the result shown in (B), no significant difference in Rpb1 ubiquitylation levels was observed. Ponceau S staining of the membrane was carried out to ensure that similar amounts of GST-Dsk2 beads were added to the individual IPs.

The result of the degradation experiment is shown in Figure 5.17B. Somewhat surprisingly, no dramatic difference between the *rad26Δ* strain carrying the empty vector and the one expressing $RAD26^{wt}$ was observed, although the *rad26*Δ strain did appear to degrade RNAPII slightly faster than the wild type, as previously reported (Woudstra et al., 2002). It should be pointed out, however, that the experimental setup here was different from the one used previously (Woudstra

et al., 2002). In the original report, no cycloheximide was used in order to abolish new protein synthesis, and Rpb1 degradation showed a markedly different pattern. Dramatic loss of the Rpb1 protein was already observed one hour after UV treatment, and then returned to pre-UV levels during the time course. In *rad26Δ* cells, loss of Rpb1 was more pronouced at early time points in the previous study, but it seemed to be specifically the re-appearance which was defective in this mutant. Interestingly, *rad26Δ* cells have been shown to have transcription problems after UV irradiation, most likely due to the persistance of transcription-blocking lesions in the TS of genes (Reagan and Friedberg, 1997), which will be especially pronounced for long genes, such as Rpb1. Despite trying several times to obtain the pattern shown by Woudstra *et al.*, I did not manage to see any pronounced decrease of Rpb1 levels even in the absence of cycloheximide. The reason for this is not clear at this point. More importantly, I can, however, say that under the conditions used in my experiments, cells expressing $RAD26^{SA}$ or $RAD26^{SE}$ degraded RNAPII like wild type, suggesting that the phosphorylation of Rad26 does not play a significant role in this process. Again it should be noted that in contrast to the situation in human cells, where CSB appears to be degraded in response to UV irradiation (Groisman et al., 2006), no such degradation was observed for Rad26, neither for the wild type nor for the mutant proteins, even though new protein synthesis was inhibited.

In agreement with the result of the degradation assay, no significant difference in mono- and poly-ubiquitylation of Rpb1 was observed using our technique (Fig. 5.17C). Ponceau S staining of the membrane after GST-Dsk2-IP, SDS-PAGE and Western blot confirmed that similar quantities of GST-Dsk2 were used in the IP step.

5.2.2.8 Rad26 phosphorylation does not affect DNA-dependent ATPase activity of the protein

The Rad26 protein is a DNA-dependent ATPase (Guzder et al., 1996) and this ATPase activity is required for its function in TC-NER. The observed TC-NER defect of the $RAD26^{SA}$ mutant might be explained if phosphorylation of Rad26 increases this activity to some extent. Having purified unphosphorylated as well as partially phosphorylated Rad26 (see Figure 5.11D), I set out to test the DNA-dependent ATPase activities of these proteins. As expected, and in agreement with previous publications (Guzder et al., 1996), in the absence of DNA the ATPase acitivity of the Rad26 protein could hardly be detected, but was greatly stimulated by its presence (Fig. 5.18). Importantly, partially phosphorylated Rad26 and its unmodified counterpart displayed the same level of ATPase activity in the presence of DNA, indicating that ATP hydrolysis by Rad26 is not significantly influenced by its phosphorylation.

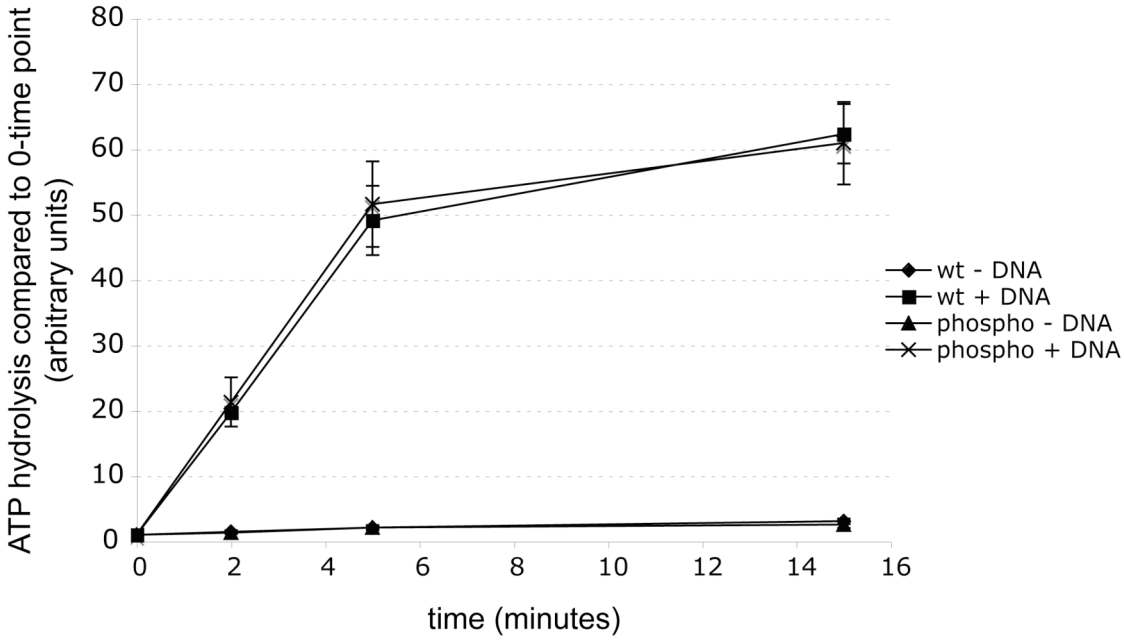

Figure 5-18 Rad26 phosphorylation does not affect the DNA-dependent ATPase activity of the protein

ATPase activity of purified unmodified Rad26 protein was determined in the absence (wt – DNA) and presence (wt + DNA) of plasmid DNA, and compared to that of the protein modified after 4-NQO treatment, again in the absence (phospho – DNA) and presence (phospho + DNA). Both versions of the proteins had no significant activity in the absence of the DNA cofactor, and were stimulated to the same extent by the addition of plasmid.

5.2.2.9 Analysis of gene expression changes in rad26Δ cells after UV-irradiation

The Rad26 and CSB proteins have general functions during transcription in yeast and human cells, respectively (Balajee et al., 1997; Lee et al., 2001; Selby and Sancar, 1997a). Furthermore, CSB has been shown to be required for transcription of certain genes after DNA damage (Proietti-De-Santis et al., 2006), and, even in the absence of damage, to also regulate a large number of genes whose expression is also affected by changes in chromatin structure (Newman et al., 2006). Based on this knowledge, I wanted to investigate if Rad26 is involved in the regulation of gene expression in a similar way in budding yeast, and if its phosphorylation plays a role in this regulation. As the modification of Rad26 occurs specifically after DNA damage, I isolated total RNA from wild type (W303) and *rad26Δ* cells before and 2 hours after UV irradiation, and sent the material for microarray analysis.

Table 5-1 Genes affected by *RAD26* deletion after UV

Genes with lower expression in the mutant compared to the wildtype

ORF	Name	Function
YBR291C	CTP1	Mitochondrial inner membrane citrate transporter
YNR050C	LYS9	Saccharopine dehydrogenase
YDL182W	LYS20	Homocitrate synthase isozyme,
YIL094C	LYS12	Homo-isocitrate dehydrogenase
YPL276W		NAD(+)-dependent formate dehydrogenase
YPL275W	FDH2	NAD(+)-dependent formate dehydrogenase
YOR388C	FDH1	NAD(+)-dependent formate dehydrogenase
YJL200C	ACO2	Putative mitochondrial aconitase isozyme
YJL089W	SIP4	C6 zinc cluster transcriptional activator
YBR147W		Putative protein of unknown function
YJL088W	ARG3	Ornithine carbamoyltransferase
YIR034C	LYS1	Saccharopine dehydrogenase
YLR377C	FBP1	Fructose-1,6-bisphosphatase
YJR154W		Putative protein of unknown function
YKL217W	JEN1	Lactate transporter,
YBR115C	LYS2	Alpha aminoadipate reductase
YBR054W	YRO2	Putative protein of unknown function
YGR125W		Putative protein of unknown function
YGR260W	TNA1	High affinity nicotinic acid plasma membrane permease
YGL184C	STR3	Cystathionine beta-lyase
YDR234W	LYS4	Homoaconitase
YMR107W	SPG4	Protein required for survival at high temperature
YJR155W	AAD10	Putative aryl-alcohol dehydrogenase
YNR066C		Putative membrane-localized protein of unknown function
YER024W	YAT2	Carnitine acetyltransferase
YER065C	ICL1	Isocitrate lyase
YPR124W	CTR1	High-affinity copper transporter of the plasma membrane
YCR005C	CIT2	Citrate synthase

Genes with higher expression in the mutant compared to the wildtype

ORF	Name	Function
YGL089C	MFa2	Mating pheromone alpha-factor
YKL071W		Putative protein of unknown function
YFL056C	AAD6	Putative aryl-alcohol dehydrogenase
YFL057C	AAD16	Putative aryl-alcohol dehydrogenase
YLR460C		Putative protein of unknown function
YCL027W	FUS1	Membrane protein localized to the shmoo tip
YEL021W	URA3	Orotidine-5'-phosphate (OMP) decarboxylase
YBR008C	FLR1	Plasma membrane multidrug transporter
YPL171C	OYE3	Widely conserved NADPH oxidoreductase
YJR004C	SAG1	Alpha-agglutinin of alpha-cells
YCL026C-A	FRM2	Protein of unknown function
YDL243C	AAD4	Putative aryl-alcohol dehydrogenase
YJL045W		Minor succinate dehydrogenase isozyme

This analysis led to the identification of several genes, whose expression after UV was either higher or lower in the *rad26Δ* mutant after UV relative to the parental W303 strain. A list of these ORFs can be found in table 5.1. Most of the identified genes were involved in biosynthetic pathways, for example genes involved in lysine, arginine and cystein synthesis, or genes with functions in the TCA (tricarboxylic acid) and glyoxylate cycles. Unfortunately, the changes in the UV-dependent expression of these ORFs could not explain any of the defects in *rad26Δ* cells, because none of the affected genes were linked to DNA repair in any known way. However, it can not be excluded that one or more of the identified genes affects DNA repair in a manner that still needs to be elucidated.

Nevertheless, I wanted to find out if Rad26 phosphorylation affected the observed changes in gene expression. In order to do so, I chose two of the affected genes, and compared the UV-dependent changes in mRNA level between *rad26Δ* cells carrying either empty vector, the vector expressing wildtype Rad26 ($RAD26^{WT}$), or the point mutants which had S27 mutated either to alanine ($RAD26^{SA}$) or glutamate ($RAD26^{SE}$). The *CTP1* gene showed a lower expression after UV in *rad26Δ* than in the wild type, whereas expression of the *AAD6* gene was higher.

Quantitative RT-PCR analysis confirmed the result from the microarray, but no difference was observed between the wild type and the mutated Rad26 proteins, indicating that Rad26-dependent regulation of gene expression after UV is not altered by the phosphorylation of the protein (Fig. 5.19). Although these experiments were only performed on a small subset of the affected genes, the results suggest that Rad26 phosphorylation is not required for the role played by Rad26 in damage-induced gene expression.

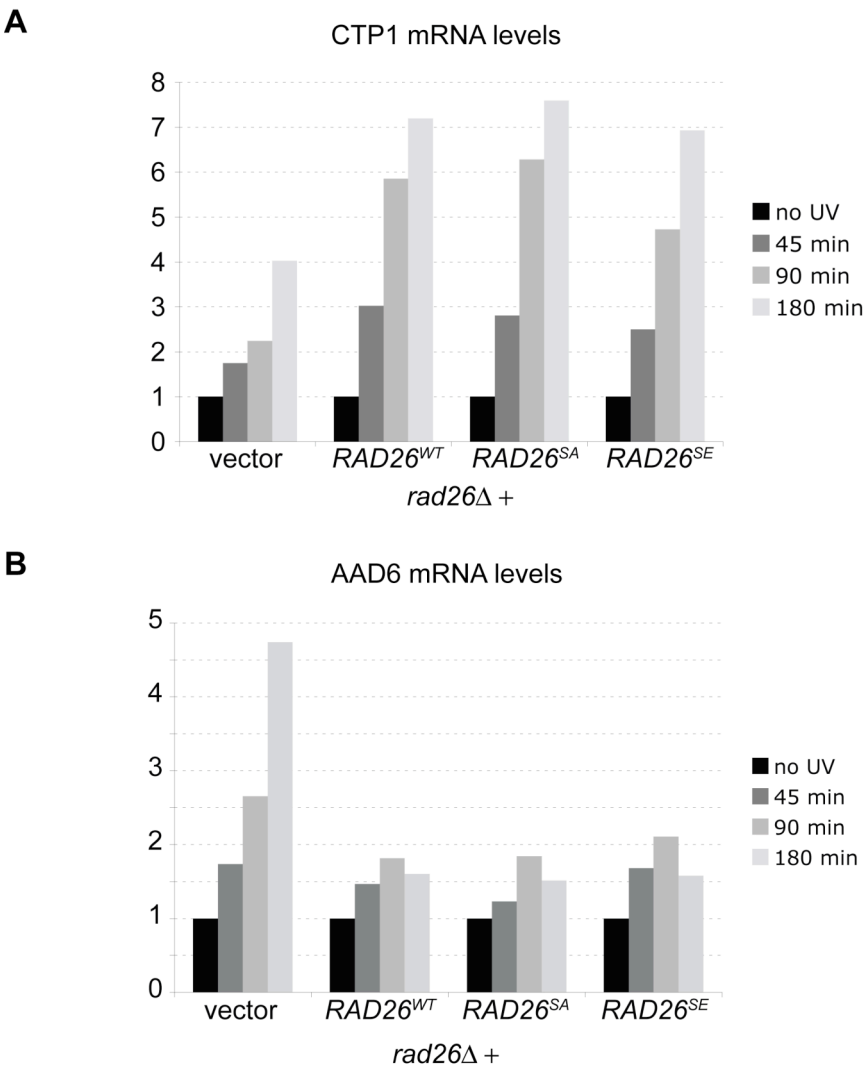

Figure 5-19 Rad26 phosphorylation does not affect gene expression changes after UV

Results from quantitative RT-PCRs, comparing the expression levels of two genes (**(A)** CTP1, **(B)** AAD6) known to be affected by *RAD26* deletion (see microarray data in Table 5.1). RNA was isolated before and at various time points after UV, and the UV-dependent changes in expression were compared between *rad26Δ* cells expressing either no Rad26 (vector), wild type Rad26 ($RAD26^{WT}$), or mutant versions of Rad26 in which S27 was mutated to either alanine ($RAD26^{SA}$) or glutamate ($RAD26^{SE}$). The presence of the phosphorylation site did not matter for the UV-dependent regulation of the two examined genes.

5.3 Analysis of an influence of the DNA damage checkpoint on ubiquitylation and degradation of Rpb1

Having created a number of yeast strains with deletions of various components of the DDC, I decided to determine not only the NER capacity of these cells, but also their ability to perform the alternative way of dealing with irreversibly stalled RNA polymerase II complexes, namely ubiquitylation and degradation of the Rpb1 subunit. As the DDC coordinates a large number of events after DNA damage, it was plausible that this is the case, and I could not find any evidence in the literature that this possibility had been investigated before.

5.3.1 Rpb1 ubiquitylation and degradation are influenced by the Mec1 and Rad53 kinases

In order to investigate if the DDC affects Rpb1 ubiquitylation and degradation, the checkpoint deficient *mec1Δ sml1Δ* strain, as well as the *chk1Δ* and *rad53Δ sml1Δ* mutants (lacking the two main downstream kinases) were chosen for analysis. Cell growth, cycloheximide treatment and UV-irradiation was performed as oulined in Figure 5.17A. The result of both the degradation experiment and the analysis of the ubiquitylation status of Rpb1 are shown in Figure 5.20.

In the wild-type W303 strain, degradation of Rpb1 becomes apparent around 2 hours after UV treatment and after 4 hours the protein level is dramatically decreased (Fig. 5.20A). In contrast to this, degradation is much less efficient in both the *mec1Δ sml1Δ* and the *rad53Δ sml1Δ* strain, indicating that the DDC indeed has an influence on the process. Deletion of *CHK1* did not seem to significantly affect Rpb1 degradation, showing that the Mec1-Rad53 branch of the DDC is mainly responsible for its regulation.

Rpb1 ubiquitylation levels were then examined by GST-Dsk2 pulldown, followed by Western blot analysis of Rpb1 using 4H8 antibodies. Different exposures of this Western blot are shown in the three top panels of Figure 5.20B. In agreement with the result of the degradation assay, the signals for both mono- and polyubiquitylated Rpb1 looked similar when the wild type (W303) was compared with the *chk1Δ* mutant strain. Mono-ubiquitylation, but little or no poly-ubiquitlyation, was observed before UV treatment, whereas poly-ubiquitylation was strong at the 1 hour time point after UV-irradiation, as expected. Signals started losing intensity at later time-points, in agreement with efficient degradation of Rpb1 in these strains (Fig. 5.20A).

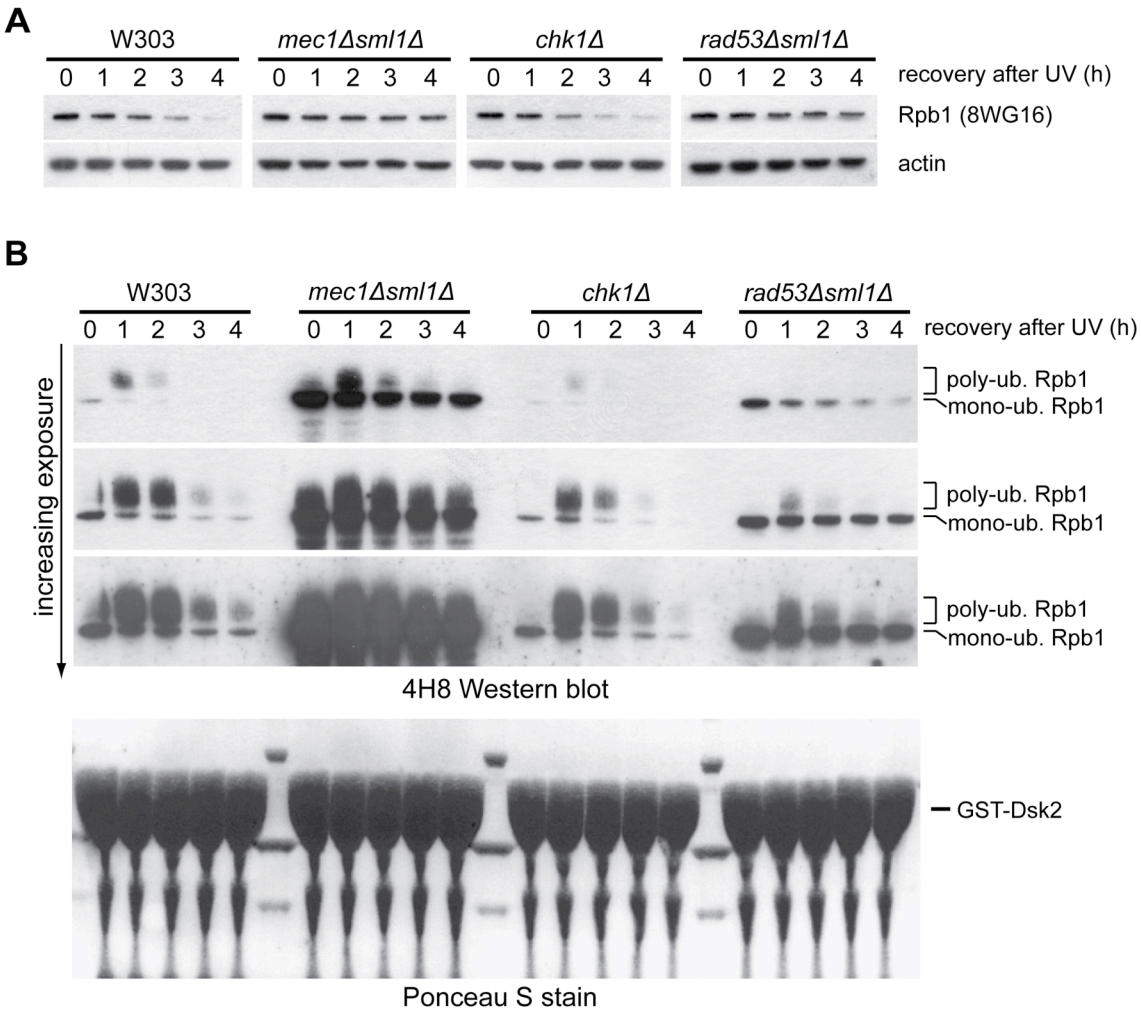

Figure 5-20 Analysis of the effect of checkpoint kinases on Rpb1 ubiquitylation/degradation

Analysis of Rpb1 ubiquitylation and degradation in wild-type (W303) and strains with deletions of various checkpoint kinases

(A) Western blot analysis of Rpb1 protein levels in extracts before and at the indicated times after UV-treatment. Degradation is severely impaired in cells lacking the Mec1 and Rad53 kinases, but not the Chk1 kinase. Equal loading was confirmed by detection of actin.

(B) Western blot analysis of Rpb1 after immunoprecipitation of mono- and polyubiquitylated proteins with GST-Dsk2. In agreement with the result shown in (A), significant differences in mono- and polyubiquitylation are observed between the wildtype and both the *mec1Δ sml1Δ* and *rad53Δ sml1Δ* strains, but not the *chk1Δ* strain.

The *mec1Δ sml1Δ* and *rad53Δ sml1Δ* strains showed a clear change in Rpb1 ubiquitylation. Interestingly, the patterns looked different in the two strains, suggesting that the Mec1 and Rad53 kinases have different effects on one or more steps controlling Rpb1 ubiquitylation/degradation. The most prominent change was the presence of a much stronger signal for mono-ubiquitylated Rpb1 in both strains, compared to wild type. This was more pronounced in the *mec1Δ sml1Δ* strain, but the *rad53Δ sml1Δ* strain also clearly had more of this modification than the wild type or *chk1Δ* strain. Despite the strong defect in Rpb1 degradation after UV damage in strains lacking either the Mec1 or Rad53 kinases, UV-induced

poly-ubiquitylation of Rpb1 could still be detected, even though the levels seemed to be different from the wild type strain. In the *rad53Δ sml1Δ* strain I detected slightly lower signals for poly-ubiquitylated Rpb1 (compare the signals at the 1 hour time point between W303 and *rad53Δ sml1Δ* in the middle panel of Figure 5.20B). Surprisingly, the *mec1Δ sml1Δ* strain seemed to have slightly increased Rpb1 poly-ubiquitylation levels after UV irradiation, despite having a defect in Rpb1 degradation, possibly suggesting a defect in proteasome function, or at least in post-ubiquitylation processes.

Taken together, these results show that the Mec1 and Rad53 kinases of the DDC somehow affect mono- and/or polyubiquitylation of Rpb1 and that they have a defect in UV-induced degradation of this protein.

5.3.2 DDC-dependent phosphorylation of Def1 is not involved in regulation of UV-induced Rpb1 degradation

Having shown that the DDC also controls ubiquitylation and degradation of Rpb1, I set out to determine the underlying mechanism. The possibility that the DDC induces synthesis of one or more factors involved in this process could be excluded, because the analysis of Rpb1 ubiquitylation and degradation was carried out in the presence of cycloheximide. I therefore focussed my attention on potential phosphorylation targets of the Mec1 and Rad53 kinases.

An obvious candidate was Def1, the factor required for normal Rpb1 ubiquitylation and degradation (Reid and Svejstrup, 2004; Woudstra et al., 2002). Interestingly, this protein was recently identified as a target of both the Mec1 and Rad53 kinases in proteome-wide screens (Albuquerque et al., 2008; Smolka et al., 2007), in apparent agreement with the RNAPII ubiquitylation defects observed in strains lacking these two kinases (shown in Fig. 5.19). These proteome-wide studies showed that Rad53 phosphorylates Def1 at serine 273 (Smolka et al., 2007), while Mec1 targets serine 497 (Albuquerque et al., 2008).

In order to investigate the possibility that these Def1 phosphorylation events are required for Rpb1 ubiquitylation and degradation, both of the sites were mutated to alanines on a plasmid carrying the *DEF1* locus, and the resulting mutated plasmids were transformed into a *def1Δ rad14Δ* strain. The functionality of the mutated Def1 protein was determined by spotting and UV treatment in this genetic background because Def1 controls a pathway which is thought to represent an alternative to DNA repair, namely the removal of irreversibly stalled RNA Polymerase II complexes (Woudstra et al., 2002).

Accordingly, the *rad14Δ def1Δ* double mutant is significantly more UV sensitive than the *rad14Δ* single mutant (Fig. 5.21). Expression of wild-type *DEF1* ($DEF1^{wt}$) reversed this sensitivity to the level of the *rad14Δ* single mutant. *DEF1* mutants that either had the phosphorylation sites mutated individually ($DEF1^{S273A}$ and $DEF1^{S497A}$) or in combination ($DEF1^{S273A/S497A}$), were equally efficient in rescuing the sensitivity of the *def1Δ rad14Δ* strain, suggesting that DDC-dependent phosphorylation of Def1, at least at the tested sites, is not required for the regulation of Rpb1 degradation.

This result shows that the DDC controls Rpb1 ubiquitylation and degradation at one or more steps, which are not linked to phosphorylation of Def1 at serine 273 or 497. Some possibilities will be presented in the next chapter.

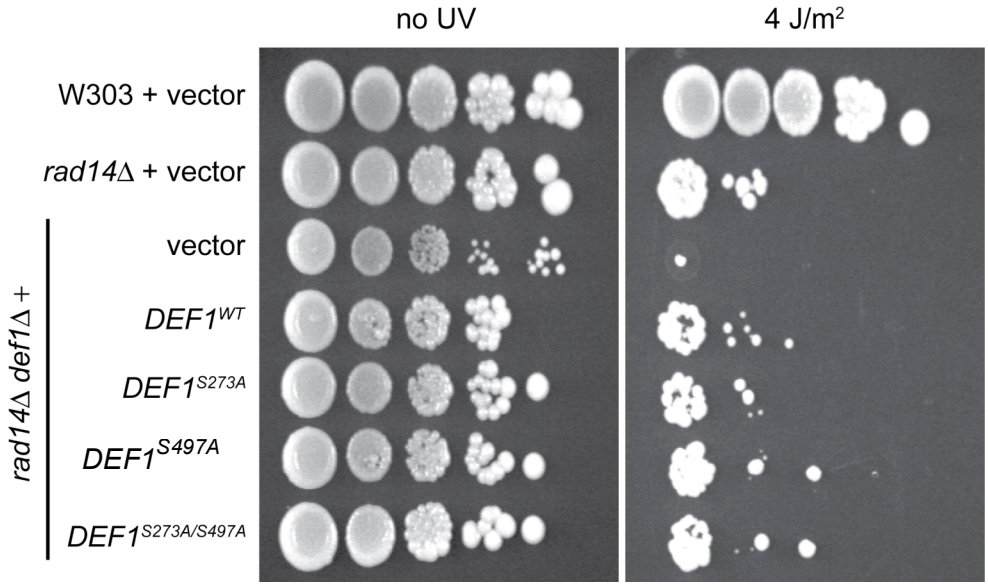

Figure 5-21 DDC dependent phosphorylation of Def1 at S273 and S497 is not involved in ubiquitylation/degradation of Rpb1

A *rad14Δ def1Δ* mutant was transformed either with empty vector, or vectors carrying wild type *DEF1* ($DEF1^{WT}$), single point mutants of *DEF1* ($DEF1^{S273A}$ and $DEF1^{S497A}$), or a double mutant ($DEF1^{S273A/S497A}$). The sensitivities of these strains were then compared to the wild type (W303) and *rad14Δ* strains to analyse an involvement of these phosphorylation sites in the ubiquitylation and degradation of Rpb1 after UV.

6 Discussion II

6.1 Regulation of NER by the DNA damage checkpoint

In this study I investigated possible links between the Nucleotide Excision Repair (NER) pathway and the DNA damage checkpoint (DDC), by examining the efficiency of CPD repair at both the TS and the NTS of the constitutively transcribed *RPB2* gene in various mutant yeast strains, lacking kinase components of the DDC. Interestingly, I found that repair on both strands is influenced by the absence of a functional DDC. This shows that both sub-pathways of NER are regulated by the checkpoint, and I have tried to find out how this regulation might be achieved. At this point I would like to mention that all the findings presented in this work about NER kinetics in the various mutant strains are restricted to the *RPB2* gene, and it would be interesting to find out if the observed requirement for individual checkpoint components also applies to others.

6.1.1 Regulation of NTS repair

6.1.1.1 de novo *protein synthesis is required for efficient NTS repair*

The non-transcribed strand (NTS) of active genes is repaired by the slow Global Genome Repair (GG-NER) pathway, because lesions in this strand do not block the progression of RNAPII complexes. In *S. cerevisiae* this pathway is dependent on the Rad7/Rad16 complex, as well as all the other central NER proteins (Verhage et al., 1994). The results presented in Figures 5.1 and 5.2 clearly show that in the absence of a functional DDC, achieved by deletion of the gene encoding the central Mec1 kinase, repair of the NTS is virtually undetectable during a time course of up to 6 hours. It is important to note at this point, that deletion of *MEC1* was carried out in an *sml1Δ* background, and I can not rule out that deletion of *SML1* itself has an effect on NER. One attractive possibility to make sure that the observed NER delays are really due to the absence of Mec1 would be to use temperature-sensitive or degron-versions of Mec1, which would allow to examine the effect of the absence of the Mec1 kinase in the wild type background.

In contrast to the result obtained for the *mec1Δ sml1Δ* mutant, strains with deletions of the genes encoding the Chk1, Rad53 and Dun1 kinases do not show any significant alteration in the CPD repair rate on the NTS. Previous reports showed a strong dependence of NTS repair, but not TS repair, on UV-induced *de novo* synthesis of repair proteins (Al-Moghrabi et al., 2003, 2009). These studies focussed on the *GAL10* and *URA3* genes. In order to also show this dependence of NTS repair on *de novo* protein synthesis for the *RPB2* gene, I analysed the efficiency of CPD removal from this locus in the absence or presence of the translational inhibitor cycloheximide. I found that repair of the NTS is strongly inhibited in the presence of this drug, while no significant defect could be detected on the TS.

All these results suggest that the DDC controls NTS repair by increasing the abundance of repair proteins. Indeed, the synthesis of various NER factors, including Rad2, Rad7, Rad16 and Rad23, has been shown to be induced by UV irradiation (Bang et al., 1995; Jones et al., 1990; Madura and Prakash, 1990; Siede et al., 1989). Surprisingly, however, it has been shown that most of the transcriptional changes after DNA damage are dependent on the Dun1 kinase (Gasch et al., 2001), which becomes phosphorylated, and thereby activated, by the Rad53 kinase after DNA damage (Chen et al., 2007; Zhou and Elledge, 1993). This would suggest that mutants with deletions of *DUN1* and *RAD53* should have a defect in GG-NER similar to the one observed after treatment with cycloheximide. This is clearly not the case, suggesting that the up-regulation of damage-inducible genes, necessary for efficient CPD repair on the NTS of *RPB2,* does not rely on these two kinases.

Damage-induced transcriptional upregulation of *RAD2, RAD7, RAD16* and *RAD23* has been shown to be controlled by the Rad9 protein (Aboussekhra et al., 1996). If the upregulation of these factors is required for efficient repair of the NTS, then the *rad9Δ* mutant should have the same NTS repair defects observed for the wildtype strain in the presence of cycloheximide. Even though I have not focussed on the role of the Rad9 protein in NER, previous studies by other groups have shown that repair on both the TS and the NTS is slower in the absence of this factor (Al-Moghrabi et al., 2009; Yu et al., 2001), yet not as slow as in the absence of protein synthesis (Al-Moghrabi et al., 2003). The most plausible explanation for this observed discrepancy is that the transcriptional induction of additional factors, which is dependent only on the Mec1 kinase but not the Rad9, Rad53, Chk1 and Dun1 proteins, is also important for efficient NTS repair. As this work focussed on the repair of the TS, I did not pursue this issue any further.

6.1.1.2 Phosphorylation of repair factors for efficient NTS repair?

Besides DDC-dependent activation of the transcriptional response to DNA damage, culminating in the upregulation of repair factors, it is also possible that post-translational modifications of repair factors by the Mec1 kinase contributes to efficient NTS repair. Interestingly, the Rad23 protein in *S. cerevisiae* as well as its human homolog hRad23A have recently been identified in proteome-wide screens for potential targets of the Mec1 and ATM/ATR kinases, respectively (Albuquerque et al., 2008; Matsuoka et al., 2007). In order to investigate if this modification plays a role in the NER process, I complemented a *rad23Δ* mutant strain with mutant versions of *RAD23,* in which the either only the identified Mec1 target residue, or all three potential Mec1 target residues (SQ-sites), were mutated. Surprisingly, I did not detect any defect in NER efficiency. Furthermore, the cells carrying the mutated versions of *RAD23* did not display any increase in UV-sensitivity than the parental wildtype strain, indicating that this modification does not contribute to efficient repair, at least not under these experimental conditions.

The Rad16 protein is required for NTS-repair, and this factor has also been identified as a phosphorylation target of Mec1 (Smolka et al., 2007). I mutated the Rad16 phosphorylation site, but again could not detect any significant difference in survival after UV between strains carrying the wildtype, or mutated, version of the *RAD16* gene (data not shown).

Even though I cannot rule out that phosphorylation of other repair proteins contributes to efficient repair of the NTS, I speculate that the main point at which the Mec1 dependent DDC influences NTS repair is at the level of UV-induced *de novo* protein synthesis.

6.1.2 Regulation of TC-NER

In Figures 5.1 and 5.2 I clearly showed that repair in the TS of *RPB2* is less efficient in a *mec1Δ sml1Δ* strain lacking a functional DDC. When compared to a *rad26Δ* strain, it is obvious that TC-NER is still possible, yet less efficient, in the absence of the Mec1 kinase. Again it should be noted that analysis of the effect of *MEC1* deletion was carried out in the *sml1Δ* background, and it can not be excluded at this point that *SML1* deletion on its own has some effect on NER. Importantly, cells lacking the *CHK1*, *RAD53* or *DUN1* genes have no detectable defect in TC-NER, indicating that the effect of the Mec1 kinase on the repair of the TS of *RPB2* is direct. Furthermore, in agreement with previous reports (Al-Moghrabi et al., 2003), UV induced *de novo* protein synthesis has no major effect on the efficient repair of this strand. This implies that the steady-state levels of NER factors are sufficient to ensure fast repair of transcription-blocking DNA lesions, and shows that the regulation of TC-NER efficiency occurs via post-translational modifications of one or more factors involved in this repair pathway.

6.2 Rad26, a Mec1 target involved in the regulation of DNA repair by the DDC

As the most obvious candidate target to explain the TC-NER defect in the *mec1Δ sml1Δ* strain is the TC-NER factor Rad26, I focussed my attention on this protein. In order to efficiently detect the weakly abundant Rad26 protein in extracts of *S. cerevisiae,* I created a strain carrying a tagged version of this gene. C-terminal tagging of Rad26 was not possible, as this leads to functional inactivation (Elies Woudstra, unpublished observation). I therefore created a strain with an N-terminal 9myc/2TEV/8His tag, using a strategy which ensures that the resulting gene is still under control of its endogenous regulatory elements, in order to avoid artefacts due to changes in expression levels. I was able to show genetically that the functionality of the tagged protein was not compromised by the presence of the tag.

6.2.1 Rad26 is phosphorylated after DNA damage by the Mec1 kinase

UV irradiation of cells leads to a post-translational modification of Rad26, which is clearly visible as the appearance of a form of the protein with reduced electrophoretic mobility (Fig. 5.9A), and I was able to show that Rad26 is phosphorylated. Treatment of the modified protein with a phosphatase (Fig. 5.9D) resulted in the complete loss of the electrophoretic mobility shift. Other sources of DNA damage (H_2O_2, MMS, bleomycine and 4-NQO), but not heat shock, osmotic shock or 6-AU-mediated induction of RNAPII stalling led to this modification, showing that Rad26 phosphorylation is a damage-specific response, and implicating a role of the DDC. Indeed, I was able to show that this event is strictly dependent on the Mec1 kinase (Fig. 5.10C). In contrast, the Tel1, Chk1, Rad53 and Dun1 components of the DDC are not required. This is in perfect agreement with my results for the NER kinetics, which show that only strains lacking the Mec1 kinase, but not Chk1, Rad53 or Dun1, have a clear defect in TC-NER.

Besides being efficiently induced by DNA damage, a low level of Rad26 phosphorylation can also be found in undamaged cells. Interestingly, this background level of modification seems to be restricted to the S-phase of the cell cycle, as it is undetectable in cells arrested in G1 or G2, but clearly visible in cells arrested in S-phase with the drug hydroxyurea (HU). This modification can also be detected after the release of G1-arrested cells into the cell cycle by the removal of the alpha-factor mating pheromone in the absence of HU (data not shown). The Mec1 kinase has an essential role in the control of DNA replication during an unperturbed S-phase. This cell-cycle dependent activation of Mec1 can be detected by the appearance of phosphorylated forms of the Rad53 kinase. I speculate that the presence of phosphorylated

Rad26 during S-phase is simply due to this transient activation of the responsible kinase, and that Rad26 phosphorylation has no role in S-phase. Interestingly, even though HU is a strong activator of Mec1, the phosphorylation level of Rad26 was low after HU treatment compared to the level after DNA damage. One possible explanation for this is that the kinase and the substrate are in close proximity only after DNA damage, thereby facilitating the phosphorylation of Rad26 by Mec1. Indeed, it has been shown by chromatin immunoprecipitation experiments that components of the DDC are recruited to sites of DNA lesions (Jiang and Sancar, 2006; Unsal-Kacmaz et al., 2002).

6.2.2 Serine 27 is the main phosphorylation site on Rad26

Serines or threonines followed by glutamines (SQ/TQ sites) are the main target sites for PIKKs such as Mec1, Tel1, ATM and ATR. Analysis of the Rad26 amio acid sequence revealed that 5 of these consensus sites can be found in this protein. These sites were mutated individually to alanines, and the phosphorylation status of these mutant versions after DNA damage was analysed by SDS-PAGE and Western blotting. This experiment revealed that only mutation of serine 27 abolished the shift in electrophoretic mobility. Interestingly, purification of overexpressed wildtype Rad26 before and after DNA damage, followed by SYPRO Ruby staining of the gel, showed the presence of more than one slower migrating form of the protein, and mass spectrometric analysis of the protein revealed that serine 30 is also modified. In contrast, Albuquerque et al showed that serines 27 and 29 are phosphorylated after damage (Albuquerque et al., 2008). I speculated that serine 27 is the main phosphorylation site (as it can be found in a consensus Mec1 target motif), and that nearby residues can be targeted non-specifically in addition to it. Indeed, mutation of serine 27 and purification of the overexpressed mutant protein after DNA damage revealed the absence of any slower migrating forms, and mass spec analysis indicated that no residual phosphorylations are detectable on this protein. One possibility, which cannot be excluded at this point, is that phosphorylation of serine 27 leads to modification of surrounding residues by a different kinase. In any case, the absence of phosphorylation in the S27A single mutant made me decide to use this version to carry out functional assays.

6.2.3 Rad26 phosphorylation is required for efficient TC-NER in the presence of a functional DDC

Strand-specific NER assays confirmed that the phosphorylation of Rad26 by the Mec1 kinase has a relevance *in vivo*. Cells carrying the S27A mutant of Rad26, but not the phosphorylation-

mimicking S27E mutant, had reproducible defects in TC-NER, detectable as an increase in the half-life of damages on the TS of *RPB2* by about 1 hour. Repair of the TS is still more efficient than in the TC-NER deficient *rad26Δ* strain, showing that TC-NER is compromised in the absence of the phosphorylation site, but that it is not completely dependent on this modification. This delay in TS repair is somewhat similar to the defect observed in the *mec1Δ sml1Δ* mutant. It should be noted that the most obvious difference between the wildtype and the S27A mutant strain is at early time points (1 hour time point in Figure 5.13), in agreement with a very early appearance of the modification after UV irradiation.

I also examined TC-NER efficiency in strains expressing various other Rad26 phosphorylation site mutants. These include a mutant in which all five (S/T)Q sites are mutated to alanines, and mutants in which serine 27 is mutated in combination with serine 29 and serine 30. I was unable to detect any significant differences between these mutants and the S27A single mutant. This is in agreement with the finding that no residual phosphorylations are detectable in this single mutant.

The finding that both deletion of the gene encoding the Mec1 kinase and mutation of the Mec1-dependent phosphorylation site on Rad26 lead to a similar effect on TC-NER, made me speculate that Rad26 might be the only relevant target for the Mec1 kinase to ensure efficient TC-NER. The full functionality of the S27E mutant (no delay in TC-NER compared to the wild type) led me to investigate if expression of this mutant in the *mec1Δ sml1Δ* strain can bypass the requirement for the DDC. This was not the case, as both wild type and S27E Rad26 showed the same rate of CPD removal from the TS of *RPB2* in the absence of a functional DDC. This clearly shows that the Mec1 dependent DDC has additional targets after DNA damage which lead to efficient TC-NER, and which are necessary for the phospho-mimic S27E mutant Rad26 to exert its effect.

This experiment also revealed that the remaining TS-repair in the *mec1Δ sml1Δ* mutant is entirely dependent on the Rad26 protein. The presence of functional Rad26 is important in this case because repair of the NTS is undetectable in the absence of the DDC. This situation is similar to the one in the *rad16Δ* background, where additional deletion of *RAD26* leads to a dramatic increase in UV sensitivity. It is therefore very surprising that the *mec1Δ sml1Δ rad26Δ* triple mutant is not more UV-sensitive than the *mec1Δ sml1Δ* double mutant (Fig. 5.16).

At this point I can only speculate why repair of the TS of active genes does not seem to be very important in this case. One possibility is that overall GG-NER is not, or only partially, defective in the absence of the Mec1 kinase. In this study I have only focussed on the NTS of active genes, and in agreement with previous studies I have shown that the main function of the DDC

is UV-induced *de novo* protein synthesis of repair factors (Al-Moghrabi et al., 2003, 2009). These studies have, however, also shown that protein synthesis is only required for repair of the NTS of active genes, but not for transcriptionally inactive DNA. This means that there might be two distinct GG-NER pathways, depending on the transcriptional state of the genomic locus. I can currently not say whether or not *MEC1* deletion affects the repair of untranscribed DNA, as this was not the focus of this work. If it is not affected, and untranscribed regions of the genome are still efficiently repaired in the absence of the Mec1 kinase, this might explain the fact that the *mec1Δ sml1Δ* mutant is significantly less UV-sensitive than the completely NER-deficient *rad14Δ* mutant.

Even if GG-NER of untranscribed DNA is still possible, it is still surprising that deletion of *RAD26* does not increase the UV-sensitivity of a *mec1Δ sml1Δ* mutant, given that apparently the lesions in the TS persist for a long time. One possibility which can be envisaged is that deletion of *RAD26* leads to other effects in the DDC-deficient cells, which compensate for the impairment of TC-NER. In light of my finding that the *mec1Δ sml1Δ* strain has a defect in ubiquitylation and degradation of Rpb1, which serves as the alternative way to TC-NER in order to deal with arrested RNAPII complexes, I can only speculate that after *RAD26* deletion this pathway is reactivated in these cells. In this respect it is important to note that indeed Rad26 has been suggested to have an inhibitory effect on RNAPII degradation (Woudstra et al., 2002).

6.2.4 Mutation of the Rad26 phosphorylation site does not affect survival or growth recovery after UV irradiation

Having established that UV-induced phosphorylation of Rad26 is required for efficient TC-NER, it was surprising that the UV sensitivity of strains carrying the Rad26 S27A mutant were not detectably more UV sensitive than the wild type. This can potentially be explained by the relatively small contribution of Rad26 phosphorylation to the efficiency of TC-NER. A delay in repair of about 1 hour might not be severe enough to render the cells more sensitive to UV irradiation.

I also speculated that I might be able detect a difference between the wildtype and the mutant Rad26 strain by looking at the rates of UV-induced mutagenesis, as this might be a more sensitive assay, but again I did not observe any significant change (data not shown).

In the original report which identified *RAD26* as the gene encoding the yeast homolog of CSB, the authors showed that despite not being UV-sensitive, the *rad26Δ* mutant has a slight delay in growth recovery after UV irradiation (van Gool et al., 1994). I wanted to investigate if mutation

of the phosphorylation site might lead to such growth defects, but failed to detect any delay even in the complete absence of the Rad26 protein (data not shown).

Because of my finding that Rad26 phosphorylation is induced by other types of DNA damage apart from UV-light, such as oxidative stress (induced by treatment with hydrogen peroxide; H_2O_2) and base alkylation (inflicted by treatment with methyl methane-sulfonate; MMS) (Fig. 5.10A), I could not rule out the possibility that mutation of the Rad26 phosphorylation site renders the cells more sensitive to these agents. Interestingly, it was previously found that *RAD26* deletion increases the MMS-sensitivity of *rad14Δ, mag1Δ,* and also *rad14Δ mag1Δ* cells, and it was speculated that Rad26 helps RNAPII transcribe through damaged bases (Lee et al., 2002b). I tested the Rad26 phosphorylation mutants in these backgrounds, but could not detect any significant differences in survival after MMS-treatment between the wild type and the mutant versions of the protein (data not shown). With respect to oxidative stress, it is important to point out that CS cells display increased sensitivity to H_2O_2 (Spivak and Hanawalt, 2006). I tested the sensitivity of *rad26Δ* cells towards this chemical, but this mutant was not more sensitive than the wild type strain (data not shown)

An interesting possibility is that an effect of mutation of the Rad26 phosphorylation site on cell viability after DNA damage can be seen in a genetic background different from the one I have examined. Recent advances in the genome-wide analysis of genetic interactions, such as the 'synthetic genetic array' (SGA) (Tong et al., 2001) and 'diploid-based synthetic lethality analysis on microarrays' (Pan et al., 2004), make it possible for researchers to quickly check genetic interactions between a 'gene of interest' and other genes in the yeast genome. In order to find out more about the function of the Rad26 phosphorylation in the future, an interesting possibility would be to perform such a genome-wide analysis of genetic interactions (Synthetic Genetic Array), specifically after DNA damage induction. This has, to our knowledge, not been done yet, but should lead to an increased understanding of the roles of Rad26 in DNA repair. This analysis can be done using the *rad26Δ* mutant to identify mutations in other genes which work in parallel or together with this protein in the DNA damage response. Once potential candidates have been identified, the plasmids expressing the wild type or phosphorylation site mutant Rad26 proteins can be transformed into these double mutants, in order to check if the phosphorylation mutant leads to increased/decreased rescue compared to wild type Rad26. We tried to set up a collaboration with a group experienced in SGAs, but this line of experimentation was still ongoing at the time of writing.

6.2.5 Speculation on the functional consequences of Rad26 phosphorylation

An important question, which arises from our finding that TC-NER efficiency is higher when Rad26 is phosphorylated, is the one about the mechanism by which this is achieved. Unfortunately, even the function of Rad26/CSB in eukaryotic TC-NER is not entirely understood, and no *in vitro* assays using purified components have been established for TC-NER which would enable me to directly compare the activities of unphosphorylated and phosphorylated Rad26 proteins. I did, however, look more closely at several possibilities.

Firstly, given that *RAD26* encodes a DNA-dependent ATPase (Guzder et al., 1996), I speculated that this biochemical activity, which is required for TC-NER, might be influenced by the modification of Rad26. If ATPase activity is increased by phosphorylation, this could explain the TC-NER defects observed for the S27A point mutant. However, I clearly show in Figure 5.18 that the DNA-dependent ATPase acitivities of unmodified and modified Rad26 proteins in the presence of DNA are indistinguishable. I would like to note that I have not been able to purify completely phosphorylated Rad26 after DNA damage, but instead always obtained a mixed population of Rad26 molecules (see Fig. 5.11D). Attempts to further enrich the modified protein were not successful. However, as more than half of the purified protein was phosphorylated in the preparation used for the ATPase assay, I assume that if the effect were significant, this would have been enough to detect a stimulation of ATPase activity compared to the unphosphorylated sample.

Secondly, because faster degradation of Rpb1 might lead to less efficient TC-NER due to accelerated removal of the substrate, I looked at ubiquitylation and degradation of this protein in the presence of Rad26 point mutants. Again I observed no significant difference between cells expressing the wild-type or the point-mutated versions of Rad26. In this experiment I also investigated whether or not Rad26 itself is destabilised after DNA damage and if phosphorylation might be involved in this process. This is an important question in light of the fact that CSB has been reported to be ubiquitylated and destabilised by a CSA-containing ubiquitin-ligase complex, and that this destabilisation provided the first functional connection between the main factors involved in Cockayne's syndrome in human cells (Groisman et al., 2006; Groisman et al., 2003). Interestingly, I did not detect any degradation of Rad26 after DNA damage up to 4 hours post-UV, despite the use of the translational inhibitor cycloheximide. This result shows a clear difference between the situation in yeast and humans, and rules out the possibility that the Rad28 protein, the yeast homolog of CSA (Bhatia et al., 1996), has a similar role as its human counterpart in destabilisation of Rad26, despite some genetic evidence that it acts in the same pathway (Bhatia et al., 1996).

Phosphorylation of Rad26 might also influence its binding partners after UV irradiation. A well known binding partner is the Def1 protein, the regulator of Rpb1 ubiquitylation and

degradation. However, I failed to detect any differences in binding of Def1 and wild type Rad26 in response to UV irradation, and consequently the UV-induced phosphorylation presumably had no effect on this interaction (data not shown). This is in apparent agreement with my finding that Rpb1 degradation is not affected by mutations of the Rad26 phosphorylation site. A second possibility is that phosphorylation of Rad26 increases its affinity for damage-stalled RNAPII, as this is thought to be the first step in the TC-NER mechanism. I was, however, never able to efficiently co-immunoprecipitate RNAPII with Rad26, neither wildtype nor mutant. This finding might be explained by the very transient nature of this interaction. Indeed, previous reports identified a physical interaction between Rad26 and RNAPII after damage only when the proteins were crosslinked with formaldehyde (Jansen et al., 2002). Importantly, this study used overexpressed Rad26 protein, and in my case the low endogenous expression level might make it even harder to detect potential binding partners. When I purified overexpressed Rad26 proteins from yeast cells (see Figure 5.11D), I also analysed weakly stained copurifying bands by mass spectrometry, but was unable to find interesting candidates to explain the observed influence of phosphorylation on TC-NER. I also failed to detect any RNAPII proteins in this preparation. An important drawback to this attempt to explain the TC-NER defect by differences in binding partners, is the fact that after mutation of the phosphorylation site, the protein is still functional for TC-NER and only the kinetics of the reaction are reduced. This means that every important binding partner will bind to both forms, maybe only with slightly different kinetics. It might therefore be difficult to convincingly link the TC-NER defect to such a slight difference in interactions.

The Rad26 protein is thought to bind to damage-stalled RNAPII complexes on chromatin after UV irradiation in order to start the TC-NER process. I therefore thought it would be possible to detect Rad26 on genes by chromatin immunoprecipitation (ChIP) after DNA damage, and speculated that the kinetics of chromatin recruitment might be comparable to the observed differences in TC-NER kinetics, i.e. that the phosphorylated form of Rad26 was recruited faster. Unfortunately, I was unable to detect Rad26 above background using this assay, despite looking at a number of genes with different expression levels. In a previous study, Jansen et al were able to ChIP Rad26 from genes, however, the authors have again used overexpressed Rad26 in their experiments (Jansen et al., 2002). In my case, the low endogenous levels of the Rad26 proteins probably prohibited detection of Rad26 by ChIP. I also tried to overexpress Rad26 from a galactose-inducible promoter, and to detect it after UV irradiation at the highly transcribed *GAL10* gene or the *RPB2* gene, but again failed to obtain levels above background. The reason for my lack of success with Rad26 ChIP is not known. In light of the finding that the observed TC-NER defect is not very dramatic, it is, however, questionable if overexpression of Rad26 is a good strategy for my purpose, as this increases the efficiency of TC-NER (Bucheli and Sweder, 2004) and might mask the effect of the phosphorylation.

As mentioned in the introduction, an alternative function of Rad26, different to the classical view of binding to damage-arrested RNAPII and recruiting NER factors, has been obtained by the Brouwer lab. The TC-NER defect caused by *RAD26* deletion can be suppressed by additional deletion of *SPT4* (Jansen et al., 2000), and this has been linked to regulation of transcription after UV (Jansen et al., 2002). Importantly, deletion of *RAD26* accelerated, whereas deletion of *SPT4* inhibited, loss of RNAPII phosphorylated at serine 5 on the CTD from promoters after UV. This result represents an interesting possibility for the involvement of the Rad26 phosphorylation. I carried out ChIP experiments using an antibody specific for this phosphorylated form of RNAPII, but unfortunately this antibody did not work in ChIP in my hands. Nevertheless, the possibility that the loss of this form of RNAPII from promoters after UV is more dramatic in *rad26Δ* cells expressing the Rad26 phosphorylation mutant, compared to those expressing the wild type protein, is an important possibility for future experiments.

Interestingly, a link between checkpoint components and Rad26 was previously found by Yu et al, when they showed that both Rad9, Rad24 and Rad26 are required for 'inducible NER', i. e. the faster removal of UV-induced lesions after pre-treatment of cells with a low dose of UV irradiation (Yu et al., 2001). I investigated this possibility, but was unable to reproduce this faster 'inducible' NER even in the wild type strain, which might be explained by technical difficulties. Further attempts to show an involvement of Rad26 phosphorylation in inducible NER might be another interesting possibility for future investigations.

6.3 Phosphorylation of CSB by ATM/ATR?

A crucial question about the relevance of my results from *S. cerevisiae* is whether this phosphorylation is conserved in human cells. The absence of human CSB clearly leads to much a more severe phenotype than the deletion of *RAD26* in yeast, giving rise to the severe neurodegenerative disease Cockayne's syndrome (see Section 1.3.3.2), so obviously the importance of this factor has increased during the evolution of higher eukaryotes. Interestingly, while this work was in progress, a screen for novel ATM/ATR substrates revealed that CSB is phosphorylated in an ATM/ATR-dependent manner (Matsuoka et al., 2007), and so this phosphorylation event might have functional consequences for its activities.

It will be very interesting to see whether or not mutation of the relevant phosphorylation site(s) on CSB leads to defects in its function. Because of the severe phenotypes resulting from loss of CSB, including a defect in transcription recovery after DNA damage (Mayne and Lehmann, 1982), general transcription defects in the absence of exogenous DNA damage (Balajee et al.,

1997; van Gool et al., 1997), a lack of the transcription-coupled removal of lesions which are substrates for NER (Troelstra et al., 1992), defects in the BER pathway (Spivak and Hanawalt, 2006; Tuo et al., 2001), and defects in transcription by RNA Polymerase I (Bradsher et al., 2002), it might be much easier to detect a contribution of this post-translational modification in one of these functions.

Interestingly, both Seckel syndrome patients (ATR defect) and Cockayne syndrome patients (CSB defect) have overlapping phenotypes, including growth defects, progressive neurological defects and skeletal abnormalities. The exact reason why CS patients display these abnormalities is not understood, but it is certainly not due to the persistence of NER lesions in the TS of active genes, as these lesions also persist in several classes of XP patients (XPA, XPD, XPB, XPF and XPG), yet these patients do not display severe developmental defects (de Boer and Hoejimakers, 2000). Furthermore, cells from $UV^{S}S$ patients lack these severe abnormalities, despite having a defect in TC-NER (Spivak et al., 2002). One possiblity is that CS cells display a defect in the transcription-coupled removal of oxidative lesions, which are substrates for the BER pathway (Hanawalt, 2000; Tsutakawa and Cooper, 2000). This might be of special importance in terminally differentiated cells of the nervous system for several reasons. Firstly, the brain consumes far more oxygen than any other organ, thereby creating a stressful environment by producing harmful metabolic by-products such as reactive oxygen species (ROS). These ROS will create oxidative lesions, which may lead to stalling of RNAPII complexes. In light of the finding that neurons have a high transcriptional activity this will inevitably lead to problems. Secondly, levels of several enzymes of the BER pathway are downregulated in the brain (Wilson and McNeill, 2007). This probably reduces the overall efficiency of this repair pathway, making the transcription-coupled removal of such lesions from the TS of active genes very important. Attenuated stalling of RNAPII is a strong signal for apoptosis (Ljungman and Zhang, 1996), which is detrimental in the brain where cells cannot be replaced.

Oxidative DNA damage will also lead to the activation of the DNA damage response, and it can be envisaged that CSB is phosphorylated by ATM/ATR in order to increase its protective activity in these cells.

6.4 Regulation of Rpb1 ubiquitylation and degradation by the DDC

The experiments on Rpb1 ubiquitylation and degradation in checkpoint mutants (Figure 5.20) clearly show that the DDC not only controls TC-NER, but also the alternative way to remove irreversibly arrested RNAPII complexes. This process is not only influenced by the central

Mec1 kinase, but also by the Rad53 kinase downstream of it. An involvement of transcriptional upregulation of genes required for RNAPII ubiquitylation, which might be absent in checkpoint-mutants, can be clearly excluded, as all RNAPII ubiquitylation and degradation experiments were carried out in the presence of the translational inhibitor cycloheximide, blocking UV-induced *de novo* protein synthesis. Therefore, the checkpoint is likely to influence this event by post-translational modification of target proteins. Even though Def1, which would be the most obvious target for regulating ubiquitylation of RNAPII (Reid and Svejstrup, 2004; Woudstra et al., 2002), was identified as a target of both of these kinases (Albuquerque et al., 2008; Smolka et al., 2007), mutation of the identified phosphorylation sites did not lead to any detectable defects in this particular function of this factor, examined by analysis of the UV-sensitivity in the *rad14Δ* background. I cannot, however, rule out the possibility that other Def1 functions, such as telomere maintenance (Chen et al., 2005), might be regulated by this phosphorylation event.

In light of the knowledge that Rpb1 polyubiquitylation is a two-step process involving first mono-ubiquitylation by Rsp5, and subsequently polyubiquitylation by an Elc1/Cul3 ubiquitin ligase complex (Harreman et al, in preparation), I speculate that the DDC exerts its influence at the second step. An indication for this is the finding that in cells deficient for the Mec1 and Rad53 kinases, the amount of mono-ubiquitylated Rpb1 is dramatically increased, presumably because the next step can not be carried out efficiently. Preliminary results from our lab also indicate that purification of the Elc1/Cul3 containing ubiquitin ligase from 4-NQO damaged cells increases its activity in Rpb1 polyubiquitylation *in vitro* when compared to a complex purified from undamaged cells (Michelle Harreman, unpublished observation). This makes us speculate that one or more components of this E3 ligase could be targeted for modification by checkpoint kinases, or that additional factors could be included in the complex after DNA damage, in a checkpoint-dependent manner. Preliminary results indicate that the latter possibility is less likely, as purification of the complex before and after DNA damage did not lead to significant differences in complex composition (Michelle Harreman, unpublished observation). Interestingly, The Cul3 subunit of the E3 ligase responsible for Rpb1 polyubiquitylation is neddylated, a modification which has been shown to increase the activity of ubiquitin ligases (reviewed in Merlet, 2009). Therefore, an attractive possibility is that after DNA damage the DDC ultimately leads to Cul3 neddylation, thereby affecting specifically the poly-ubiquitylation, but not mono-ubiquitylation, of Rpb1.

Again, I can only speculate that the findings presented here from *S.cerevisiae* might be conserved in higher eukaryotes, and that Rpb1 ubiquitylation and degradation could also be influenced by the checkpoint in human cells. This would be an interesting finding, as it could point out another cellular defect in patients with mutations of checkpoint components.

Prelimiary results from our lab show that in ATR-deficient Seckel syndrome cells, Rpb1 degradation is not significantly affected (Beate Friedrich, unpublished observation). I would like to point out, however, that Seckel syndrome cells still have low levels of ATR (O'Driscoll et al., 2003), since the complete absence of ATR is lethal (Brown and Baltimore, 2000), and that this residual activity might account for the observed proficient degradation of Rpb1. Future experiments should focus on RNAi of ATR, or alternatively on the specific inhibition of ATR using chemical compounds, and will hopefully shed light into the potential conservation of a link between RNAPII degradation and the DDC in humans.

7 References

Aboussekhra, A., Biggerstaff, M., Shivji, M.K., Vilpo, J.A., Moncollin, V., Podust, V.N., Protic, M., Hubscher, U., Egly, J.M., and Wood, R.D. (1995). Mammalian DNA nucleotide excision repair reconstituted with purified protein components. Cell *80*, 859-868.

Aboussekhra, A., Vialard, J.E., Morrison, D.E., de la Torre-Ruiz, M.A., Cernakova, L., Fabre, F., and Lowndes, N.F. (1996). A novel role for the budding yeast RAD9 checkpoint gene in DNA damage-dependent transcription. EMBO J *15*, 3912-3922.

Adimoolam, S., and Ford, J.M. (2002). p53 and DNA damage-inducible expression of the xeroderma pigmentosum group C gene. Proc Natl Acad Sci U S A *99*, 12985-12990.

Adimoolam, S., and Ford, J.M. (2003). p53 and regulation of DNA damage recognition during nucleotide excision repair. DNA Repair (Amst) *2*, 947-954.

Ahnesorg, P., and Jackson, S.P. (2007). The non-homologous end-joining protein Nej1p is a target of the DNA damage checkpoint. DNA Repair (Amst) *6*, 190-201.

Al-Moghrabi, N.M., Al-Sharif, I.S., and Aboussekhra, A. (2003). UV-induced de novo protein synthesis enhances nucleotide excision repair efficiency in a transcription-dependent manner in S. cerevisiae. DNA Repair (Amst) *2*, 1185-1197.

Al-Moghrabi, N.M., Al-Sharif, I.S., and Aboussekhra, A. (2009). The RAD9-dependent gene trans-activation is required for excision repair of active genes but not for repair of non-transcribed DNA. Mutat Res *663*, 60-68.

Albuquerque, C.P., Smolka, M.B., Payne, S.H., Bafna, V., Eng, J., and Zhou, H. (2008). A multidimensional chromatography technology for in-depth phosphoproteome analysis. Mol Cell Proteomics *7*, 1389-1396.

Alcasabas, A.A., Osborn, A.J., Bachant, J., Hu, F., Werler, P.J., Bousset, K., Furuya, K., Diffley, J.F., Carr, A.M., and Elledge, S.J. (2001). Mrc1 transduces signals of DNA replication stress to activate Rad53. Nat Cell Biol *3*, 958-965.

Alderton, G.K., Joenje, H., Varon, R., Borglum, A.D., Jeggo, P.A., and O'Driscoll, M. (2004). Seckel syndrome exhibits cellular features demonstrating defects in the ATR-signalling pathway. Hum Mol Genet *13*, 3127-3138.

Anindya, R., Aygun, O., and Svejstrup, J.Q. (2007). Damage-induced ubiquitylation of human RNA polymerase II by the ubiquitin ligase Nedd4, but not Cockayne syndrome proteins or BRCA1. Mol Cell *28*, 386-397.

Araki, M., Masutani, C., Takemura, M., Uchida, A., Sugasawa, K., Kondoh, J., Ohkuma, Y., and Hanaoka, F. (2001). Centrosome protein centrin 2/caltractin 1 is part of the xeroderma pigmentosum group C complex that initiates global genome nucleotide excision repair. J Biol Chem *276*, 18665-18672.

Arndt, K.M., and Kane, C.M. (2003). Running with RNA polymerase: eukaryotic transcript elongation. Trends Genet *19*, 543-550.

Auclair, Y., Rouget, R., Affar el, B., and Drobetsky, E.A. (2008). ATR kinase is required for global genomic nucleotide excision repair exclusively during S phase in human cells. Proc Natl Acad Sci U S A *105*, 17896-17901.

Balajee, A.S., May, A., Dianov, G.L., Friedberg, E.C., and Bohr, V.A. (1997). Reduced RNA polymerase II transcription in intact and permeabilized Cockayne syndrome group B cells. Proc Natl Acad Sci U S A *94*, 4306-4311.

Bang, D.D., Timmermans, V., Verhage, R., Zeeman, A.M., van de Putte, P., and Brouwer, J. (1995). Regulation of the Saccharomyces cerevisiae DNA repair gene RAD16. Nucleic Acids Res *23*, 1679-1685.

Bang, D.D., Verhage, R., Goosen, N., Brouwer, J., and van de Putte, P. (1992). Molecular cloning of RAD16, a gene involved in differential repair in Saccharomyces cerevisiae. Nucleic Acids Res *20*, 3925-3931.

Bankmann, M., Prakash, L., and Prakash, S. (1992). Yeast RAD14 and human xeroderma pigmentosum group A DNA-repair genes encode homologous proteins. Nature *355*, 555-558.

Bashkirov, V.I., Bashkirova, E.V., Haghnazari, E., and Heyer, W.D. (2003). Direct kinase-to-kinase signaling mediated by the FHA phosphoprotein recognition domain of the Dun1 DNA damage checkpoint kinase. Mol Cell Biol *23*, 1441-1452.

Beaudenon, S.L., Huacani, M.R., Wang, G., McDonnell, D.P., and Huibregtse, J.M. (1999). Rsp5 ubiquitin-protein ligase mediates DNA damage-induced degradation of the large subunit of RNA polymerase II in Saccharomyces cerevisiae. Mol Cell Biol *19*, 6972-6979.

Bhatia, P.K., Verhage, R.A., Brouwer, J., and Friedberg, E.C. (1996). Molecular cloning and characterization of Saccharomyces cerevisiae RAD28, the yeast homolog of the human Cockayne syndrome A (CSA) gene. J Bacteriol *178*, 5977-5988.

Bhattacharyya, N., and Banerjee, S. (2001). A novel role of XRCC1 in the functions of a DNA polymerase beta variant. Biochemistry *40*, 9005-9013.

Bohr, V.A., Smith, C.A., Okumoto, D.S., and Hanawalt, P.C. (1985). DNA repair in an active gene: removal of pyrimidine dimers from the DHFR gene of CHO cells is much more efficient than in the genome overall. Cell *40*, 359-369.

Boiteux, S., and Guillet, M. (2004). Abasic sites in DNA: repair and biological consequences in Saccharomyces cerevisiae. DNA Repair (Amst) *3*, 1-12.

Bomgarden, R.D., Lupardus, P.J., Soni, D.V., Yee, M.C., Ford, J.M., and Cimprich, K.A. (2006). Opposing effects of the UV lesion repair protein XPA and UV bypass polymerase eta on ATR checkpoint signaling. EMBO J *25*, 2605-2614.

Bonilla, C.Y., Melo, J.A., and Toczyski, D.P. (2008). Colocalization of sensors is sufficient to activate the DNA damage checkpoint in the absence of damage. Mol Cell *30*, 267-276.

Borglum, A.D., Balslev, T., Haagerup, A., Birkebaek, N., Binderup, H., Kruse, T.A., and Hertz, J.M. (2001). A new locus for Seckel syndrome on chromosome 18p11.31-q11.2. Eur J Hum Genet *9*, 753-757.

Boyce, R.P., and Howard-Flanders, P. (1964). Release of Ultraviolet Light-Induced Thymine Dimers from DNA in E. Coli K-12. Proc Natl Acad Sci U S A *51*, 293-300.

Bradsher, J., Auriol, J., Proietti de Santis, L., Iben, S., Vonesch, J.L., Grummt, I., and Egly, J.M. (2002). CSB is a component of RNA pol I transcription. Mol Cell *10*, 819-829.

Bradsher, J.N., Jackson, K.W., Conaway, R.C., and Conaway, J.W. (1993a). RNA polymerase II transcription factor SIII. I. Identification, purification, and properties. J Biol Chem *268*, 25587-25593.

Bradsher, J.N., Tan, S., McLaury, H.J., Conaway, J.W., and Conaway, R.C. (1993b). RNA polymerase II transcription factor SIII. II. Functional properties and role in RNA chain elongation. J Biol Chem *268*, 25594-25603.

Branzei, D., and Foiani, M. (2006). The Rad53 signal transduction pathway: Replication fork stabilization, DNA repair, and adaptation. Exp Cell Res *312*, 2654-2659.

Bregman, D.B., Halaban, R., van Gool, A.J., Henning, K.A., Friedberg, E.C., and Warren, S.L. (1996). UV-induced ubiquitination of RNA polymerase II: a novel modification deficient in Cockayne syndrome cells. In Proc Natl Acad Sci U S A, pp. 11586-11590.

Brown, E.J., and Baltimore, D. (2000). ATR disruption leads to chromosomal fragmentation and early embryonic lethality. Genes Dev *14*, 397-402.

Bucheli, M., Lommel, L., and Sweder, K. (2001). The defect in transcription-coupled repair displayed by a Saccharomyces cerevisiae rad26 mutant is dependent on carbon source and is not associated with a lack of transcription. Genetics *158*, 989-997.

Bucheli, M., and Sweder, K. (2004). In UV-irradiated Saccharomyces cerevisiae, overexpression of Swi2/Snf2 family member Rad26 increases transcription-coupled repair and repair of the non-transcribed strand. Mol Microbiol *52*, 1653-1663.

Budd, M.E., and Campbell, J.L. (1995). DNA polymerases required for repair of UV-induced damage in Saccharomyces cerevisiae. Mol Cell Biol *15*, 2173-2179.

Caldecott, K.W., Aoufouchi, S., Johnson, P., and Shall, S. (1996). XRCC1 polypeptide interacts with DNA polymerase beta and possibly poly (ADP-ribose) polymerase, and DNA ligase III is a novel molecular 'nick-sensor' in vitro. Nucleic Acids Res *24*, 4387-4394.

Caron, P.R., and Grossman, L. (1988). Involvement of a cryptic ATPase activity of UvrB and its proteolysis product, UvrB* in DNA repair. Nucleic Acids Res *16*, 10891-10902.

Caron, P.R., Kushner, S.R., and Grossman, L. (1985). Involvement of helicase II (uvrD gene product) and DNA polymerase I in excision mediated by the uvrABC protein complex. Proc Natl Acad Sci U S A *82*, 4925-4929.

Casper, A.M., Durkin, S.G., Arlt, M.F., and Glover, T.W. (2004). Chromosomal instability at common fragile sites in Seckel syndrome. Am J Hum Genet *75*, 654-660.

Cha, R.S., and Kleckner, N. (2002). ATR homolog Mec1 promotes fork progression, thus averting breaks in replication slow zones. Science *297*, 602-606.

Chambers, A.L., Smith, A.J., and Savery, N.J. (2003). A DNA translocation motif in the bacterial transcription--repair coupling factor, Mfd. Nucleic Acids Res *31*, 6409-6418.

Charlet-Berguerand, N., Feuerhahn, S., Kong, S.E., Ziserman, H., Conaway, J.W., Conaway, R., and Egly, J.M. (2006). RNA polymerase II bypass of oxidative DNA damage is regulated by transcription elongation factors. EMBO J *25*, 5481-5491.

Chen, S.H., Smolka, M.B., and Zhou, H. (2007). Mechanism of Dun1 activation by Rad53 phosphorylation in Saccharomyces cerevisiae. J Biol Chem *282*, 986-995.

Chen, Y.B., Yang, C.P., Li, R.X., Zeng, R., and Zhou, J.Q. (2005). Def1p is involved in telomere maintenance in budding yeast. J Biol Chem *280*, 24784-24791.

Chou, W.C., Wang, H.C., Wong, F.H., Ding, S.L., Wu, P.E., Shieh, S.Y., and Shen, C.Y. (2008). Chk2-dependent phosphorylation of XRCC1 in the DNA damage response promotes base excision repair. EMBO J *27*, 3140-3150.

Christians, F.C., and Hanawalt, P.C. (1992). Inhibition of transcription and strand-specific DNA repair by alpha-amanitin in Chinese hamster ovary cells. Mutat Res *274*, 93-101.

Chu, G., and Chang, E. (1988). Xeroderma pigmentosum group E cells lack a nuclear factor that binds to damaged DNA. Science *242*, 564-567.

Citterio, E., Van Den Boom, V., Schnitzler, G., Kanaar, R., Bonte, E., Kingston, R.E., Hoeijmakers, J.H., and Vermeulen, W. (2000). ATP-dependent chromatin remodeling by the Cockayne syndrome B DNA repair-transcription-coupling factor. Mol Cell Biol *20*, 7643-7653.

Cleaver, J.E. (1968). Defective repair replication of DNA in xeroderma pigmentosum. Nature *218*, 652-656.

Cockayne, E.A. (1936). The Inheritance of Opaque Nerve Fibres in the Retina (Papilla Leporina). Br J Ophthalmol *20*, 569-575.

Coin, F., Oksenych, V., Mocquet, V., Groh, S., Blattner, C., and Egly, J.M. (2008). Nucleotide excision repair driven by the dissociation of CAK from TFIIH. Mol Cell *31*, 9-20.

Cordonnier, A.M., Lehmann, A.R., and Fuchs, R.P. (1999). Impaired translesion synthesis in xeroderma pigmentosum variant extracts. Mol Cell Biol *19*, 2206-2211.

Cortez, D., Guntuku, S., Qin, J., and Elledge, S.J. (2001). ATR and ATRIP: partners in checkpoint signaling. Science *294*, 1713-1716.

Courcelle, J., Khodursky, A., Peter, B., Brown, P.O., and Hanawalt, P.C. (2001). Comparative gene expression profiles following UV exposure in wild-type and SOS-deficient Escherichia coli. Genetics *158*, 41-64.

Daley, J.M., Palmbos, P.L., Wu, D., and Wilson, T.E. (2005). Nonhomologous end joining in yeast. Annu Rev Genet *39*, 431-451.

Damsma, G.E., Alt, A., Brueckner, F., Carell, T., and Cramer, P. (2007). Mechanism of transcriptional stalling at cisplatin-damaged DNA. Nat Struct Mol Biol *14*, 1127-1133.

Dantzer, F., de La Rubia, G., Menissier-De Murcia, J., Hostomsky, Z., de Murcia, G., and Schreiber, V. (2000). Base excision repair is impaired in mammalian cells lacking Poly(ADP-ribose) polymerase-1. Biochemistry *39*, 7559-7569.

de Boer, J., and Hoeijmakers, J.H. (2000). Nucleotide excision repair and human syndromes. Carcinogenesis *21*, 453-460.

de la Torre-Ruiz, M.A., Green, C.M., and Lowndes, N.F. (1998). RAD9 and RAD24 define two additive, interacting branches of the DNA damage checkpoint pathway in budding yeast normally required for Rad53 modification and activation. EMBO J *17*, 2687-2698.

de Laat, W.L., Jaspers, N.G., and Hoeijmakers, J.H. (1999). Molecular mechanism of nucleotide excision repair. Genes Dev *13*, 768-785.

den Dulk, B., Sun, S.M., de Ruijter, M., Brandsma, J.A., and Brouwer, J. (2006). Rad33, a new factor involved in nucleotide excision repair in Saccharomyces cerevisiae. DNA Repair (Amst) *5*, 683-692.

den Dulk, B., van Eijk, P., de Ruijter, M., Brandsma, J.A., and Brouwer, J. (2008). The NER protein Rad33 shows functional homology to human Centrin2 and is involved in modification of Rad4. DNA Repair (Amst) *7*, 858-868.

Desany, B.A., Alcasabas, A.A., Bachant, J.B., and Elledge, S.J. (1998). Recovery from DNA replicational stress is the essential function of the S-phase checkpoint pathway. Genes Dev *12*, 2956-2970.

Dianov, G.L., Houle, J.F., Iyer, N., Bohr, V.A., and Friedberg, E.C. (1997). Reduced RNA polymerase II transcription in extracts of cockayne syndrome and xeroderma pigmentosum/Cockayne syndrome cells. Nucleic Acids Res *25*, 3636-3642.

Diffley, J.F., and Stillman, B. (1989). Similarity between the transcriptional silencer binding proteins ABF1 and RAP1. Science *246*, 1034-1038.

Digweed, M., and Sperling, K. (2004). Nijmegen breakage syndrome: clinical manifestation of defective response to DNA double-strand breaks. DNA Repair (Amst) *3*, 1207-1217.

Divine, K.K., Gilliland, F.D., Crowell, R.E., Stidley, C.A., Bocklage, T.J., Cook, D.L., and Belinsky, S.A. (2001). The XRCC1 399 glutamine allele is a risk factor for adenocarcinoma of the lung. Mutat Res *461*, 273-278.

Doetsch, P.W., and Cunningham, R.P. (1990). The enzymology of apurinic/apyrimidinic endonucleases. Mutat Res *236*, 173-201.

Donahue, B.A., Fuchs, R.P., Reines, D., and Hanawalt, P.C. (1996). Effects of aminofluorene and acetylaminofluorene DNA adducts on transcriptional elongation by RNA polymerase II. J Biol Chem *271*, 10588-10594.

Donahue, B.A., Yin, S., Taylor, J.S., Reines, D., and Hanawalt, P.C. (1994). Transcript cleavage by RNA polymerase II arrested by a cyclobutane pyrimidine dimer in the DNA template. Proc Natl Acad Sci U S A *91*, 8502-8506.

Doolittle, R.F., Johnson, M.S., Husain, I., Van Houten, B., Thomas, D.C., and Sancar, A. (1986). Domainal evolution of a prokaryotic DNA repair protein and its relationship to active-transport proteins. Nature *323*, 451-453.

Durkacz, B.W., Omidiji, O., Gray, D.A., and Shall, S. (1980). (ADP-ribose)n participates in DNA excision repair. Nature *283*, 593-596.

Elledge, S.J. (1996). Cell cycle checkpoints: preventing an identity crisis. Science *274*, 1664-1672.

Elledge, S.J., and Davis, R.W. (1987). Identification and isolation of the gene encoding the small subunit of ribonucleotide reductase from Saccharomyces cerevisiae: DNA damage-inducible gene required for mitotic viability. Mol Cell Biol *7*, 2783-2793.

Elledge, S.J., and Davis, R.W. (1989). Identification of the DNA damage-responsive element of RNR2 and evidence that four distinct cellular factors bind it. Mol Cell Biol *9*, 5373-5386.

Elledge, S.J., and Davis, R.W. (1990). Two genes differentially regulated in the cell cycle and by DNA-damaging agents encode alternative regulatory subunits of ribonucleotide reductase. Genes Dev *4*, 740-751.

Elsasser, S., Gali, R.R., Schwickart, M., Larsen, C.N., Leggett, D.S., Muller, B., Feng, M.T., Tubing, F., Dittmar, G.A., and Finley, D. (2002). Proteasome subunit Rpn1 binds ubiquitin-like protein domains. Nat Cell Biol *4*, 725-730.

Faivre, L., Le Merrer, M., Lyonnet, S., Plauchu, H., Dagoneau, N., Campos-Xavier, A.B., Attia-Sobol, J., Verloes, A., Munnich, A., and Cormier-Daire, V. (2002). Clinical and genetic heterogeneity of Seckel syndrome. Am J Med Genet *112*, 379-383.

Feaver, W.J., Svejstrup, J.Q., Bardwell, L., Bardwell, A.J., Buratowski, S., Gulyas, K.D., Donahue, T.F., Friedberg, E.C., and Kornberg, R.D. (1993). Dual roles of a multiprotein complex from S. cerevisiae in transcription and DNA repair. Cell *75*, 1379-1387.

Ferdous, A., Gonzalez, F., Sun, L., Kodadek, T., and Johnston, S.A. (2001). The 19S regulatory particle of the proteasome is required for efficient transcription elongation by RNA polymerase II. Mol Cell *7*, 981-991.

Fitch, M.E., Cross, I.V., Turner, S.J., Adimoolam, S., Lin, C.X., Williams, K.G., and Ford, J.M. (2003). The DDB2 nucleotide excision repair gene product p48 enhances global genomic repair in p53 deficient human fibroblasts. DNA Repair (Amst) *2*, 819-826.

Flohr, C., Burkle, A., Radicella, J.P., and Epe, B. (2003). Poly(ADP-ribosyl)ation accelerates DNA repair in a pathway dependent on Cockayne syndrome B protein. Nucleic Acids Res *31*, 5332-5337.

Ford, J.M., Baron, E.L., and Hanawalt, P.C. (1998). Human fibroblasts expressing the human papillomavirus E6 gene are deficient in global genomic nucleotide excision repair and sensitive to ultraviolet irradiation. Cancer Res *58*, 599-603.

Ford, J.M., and Hanawalt, P.C. (1995). Li-Fraumeni syndrome fibroblasts homozygous for p53 mutations are deficient in global DNA repair but exhibit normal transcription-coupled repair and enhanced UV resistance. Proc Natl Acad Sci U S A *92*, 8876-8880.

Ford, J.M., and Hanawalt, P.C. (1997). Expression of wild-type p53 is required for efficient global genomic nucleotide excision repair in UV-irradiated human fibroblasts. J Biol Chem *272*, 28073-28080.

Fousteri, M., Vermeulen, W., van Zeeland, A.A., and Mullenders, L.H. (2006). Cockayne syndrome A and B proteins differentially regulate recruitment of chromatin remodeling and repair factors to stalled RNA polymerase II in vivo. Mol Cell *23*, 471-482.

Frosina, G., Fortini, P., Rossi, O., Carrozzino, F., Raspaglio, G., Cox, L.S., Lane, D.P., Abbondandolo, A., and Dogliotti, E. (1996). Two pathways for base excision repair in mammalian cells. J Biol Chem *271*, 9573-9578.

Gasch, A.P., Huang, M., Metzner, S., Botstein, D., Elledge, S.J., and Brown, P.O. (2001). Genomic expression responses to DNA-damaging agents and the regulatory role of the yeast ATR homolog Mec1p. Mol Biol Cell *12*, 2987-3003.

Gasch, A.P., Spellman, P.T., Kao, C.M., Carmel-Harel, O., Eisen, M.B., Storz, G., Botstein, D., and Brown, P.O. (2000). Genomic expression programs in the response of yeast cells to environmental changes. Mol Biol Cell *11*, 4241-4257.

Giannattasio, M., Lazzaro, F., Longhese, M.P., Plevani, P., and Muzi-Falconi, M. (2004). Physical and functional interactions between nucleotide excision repair and DNA damage checkpoint. Embo J *23*, 429-438.

Gietz, R.D., and Prakash, S. (1988). Cloning and nucleotide sequence analysis of the Saccharomyces cerevisiae RAD4 gene required for excision repair of UV-damaged DNA. Gene *74*, 535-541.

Gilbert, C.S., Green, C.M., and Lowndes, N.F. (2001). Budding yeast Rad9 is an ATP-dependent Rad53 activating machine. Mol Cell *8*, 129-136.

Gillette, T.G., Huang, W., Russell, S.J., Reed, S.H., Johnston, S.A., and Friedberg, E.C. (2001). The 19S complex of the proteasome regulates nucleotide excision repair in yeast. Genes Dev *15*, 1528-1539.

Gillette, T.G., Yu, S., Zhou, Z., Waters, R., Johnston, S.A., and Reed, S.H. (2006). Distinct functions of the ubiquitin-proteasome pathway influence nucleotide excision repair. EMBO J *25*, 2529-2538.

Goodship, J., Gill, H., Carter, J., Jackson, A., Splitt, M., and Wright, M. (2000). Autozygosity mapping of a seckel syndrome locus to chromosome 3q22. 1-q24. Am J Hum Genet *67*, 498-503.

Greenwell, P.W., Kronmal, S.L., Porter, S.E., Gassenhuber, J., Obermaier, B., and Petes, T.D. (1995). TEL1, a gene involved in controlling telomere length in S. cerevisiae, is homologous to the human ataxia telangiectasia gene. Cell *82*, 823-829.

Griffith, E., Walker, S., Martin, C.A., Vagnarelli, P., Stiff, T., Vernay, B., Al Sanna, N., Saggar, A., Hamel, B., Earnshaw, W.C.*, et al.* (2008). Mutations in pericentrin cause Seckel syndrome with defective ATR-dependent DNA damage signaling. Nat Genet *40*, 232-236.

Groisman, R., Kuraoka, I., Chevallier, O., Gaye, N., Magnaldo, T., Tanaka, K., Kisselev, A.F., Harel-Bellan, A., and Nakatani, Y. (2006). CSA-dependent degradation of CSB by the ubiquitin-proteasome pathway establishes a link between complementation factors of the Cockayne syndrome. Genes Dev *20*, 1429-1434.

Groisman, R., Polanowska, J., Kuraoka, I., Sawada, J., Saijo, M., Drapkin, R., Kisselev, A.F., Tanaka, K., and Nakatani, Y. (2003). The ubiquitin ligase activity in the DDB2 and CSA complexes is differentially regulated by the COP9 signalosome in response to DNA damage. Cell *113*, 357-367.

Guzder, S.N., Habraken, Y., Sung, P., Prakash, L., and Prakash, S. (1995). Reconstitution of yeast nucleotide excision repair with purified Rad proteins, replication protein A, and transcription factor TFIIH. J Biol Chem *270*, 12973-12976.

Guzder, S.N., Habraken, Y., Sung, P., Prakash, L., and Prakash, S. (1996). RAD26, the yeast homolog of human Cockayne's syndrome group B gene, encodes a DNA-dependent ATPase. J Biol Chem *271*, 18314-18317.

Guzder, S.N., Qiu, H., Sommers, C.H., Sung, P., Prakash, L., and Prakash, S. (1994a). DNA repair gene RAD3 of S. cerevisiae is essential for transcription by RNA polymerase II. Nature *367*, 91-94.

Guzder, S.N., Sung, P., Bailly, V., Prakash, L., and Prakash, S. (1994b). RAD25 is a DNA helicase required for DNA repair and RNA polymerase II transcription. Nature *369*, 578-581.

Guzder, S.N., Sung, P., Prakash, L., and Prakash, S. (1993). Yeast DNA-repair gene RAD14 encodes a zinc metalloprotein with affinity for ultraviolet-damaged DNA. Proc Natl Acad Sci U S A *90*, 5433-5437.

Guzder, S.N., Sung, P., Prakash, L., and Prakash, S. (1997). Yeast Rad7-Rad16 complex, specific for the nucleotide excision repair of the nontranscribed DNA strand, is an ATP-dependent DNA damage sensor. J Biol Chem *272*, 21665-21668.

Guzder, S.N., Sung, P., Prakash, L., and Prakash, S. (1998a). Affinity of yeast nucleotide excision repair factor 2, consisting of the Rad4 and Rad23 proteins, for ultraviolet damaged DNA. J Biol Chem *273*, 31541-31546.

Guzder, S.N., Sung, P., Prakash, L., and Prakash, S. (1998b). The DNA-dependent ATPase activity of yeast nucleotide excision repair factor 4 and its role in DNA damage recognition. J Biol Chem *273*, 6292-6296.

Haber, J.E. (1998). Mating-type gene switching in Saccharomyces cerevisiae. Annu Rev Genet *32*, 561-599.

Habraken, Y., Sung, P., Prakash, L., and Prakash, S. (1993). Yeast excision repair gene RAD2 encodes a single-stranded DNA endonuclease. Nature *366*, 365-368.

Hanawalt, P.C. (2000). DNA repair. The bases for Cockayne syndrome. Nature *405*, 415-416.

Hanawalt, P.C., and Haynes, R.H. (1965). Repair Replication of DNA in Bacteria: Irrelevance of Chemical Nature of Base Defect. Biochem Biophys Res Commun *19*, 462-467.

Harper, R.G., Orti, E., and Baker, R.K. (1967). Bird-beaded dwarfs (Seckel's syndrome). A familial pattern of developmental, dental, skeletal, genital, and central nervous system anomalies. J Pediatr *70*, 799-804.

Hashimoto, S., Suga, T., Kudo, E., Ihn, H., Uchino, M., and Tateishi, S. (2008). Adult-onset neurological degeneration in a patient with Cockayne syndrome and a null mutation in the CSB gene. J Invest Dermatol *128*, 1597-1599.

He, Z., Henricksen, L.A., Wold, M.S., and Ingles, C.J. (1995). RPA involvement in the damage-recognition and incision steps of nucleotide excision repair. Nature *374*, 566-569.

Henning, K.A., Li, L., Iyer, N., McDaniel, L.D., Reagan, M.S., Legerski, R., Schultz, R.A., Stefanini, M., Lehmann, A.R., Mayne, L.V., and et al. (1995). The Cockayne syndrome group A gene encodes a WD repeat protein that interacts with CSB protein and a subunit of RNA polymerase II TFIIH. Cell *82*, 555-564.

Herzberg, K., Bashkirov, V.I., Rolfsmeier, M., Haghnazari, E., McDonald, W.H., Anderson, S., Bashkirova, E.V., Yates, J.R., 3rd, and Heyer, W.D. (2006). Phosphorylation of Rad55 on serines 2, 8, and 14 is required for efficient homologous recombination in the recovery of stalled replication forks. Mol Cell Biol *26*, 8396-8409.

Higgins, D.R., Prakash, S., Reynolds, P., Polakowska, R., Weber, S., and Prakash, L. (1983). Isolation and characterization of the RAD3 gene of Saccharomyces cerevisiae and inviability of rad3 deletion mutants. Proc Natl Acad Sci U S A *80*, 5680-5684.

Hoeijmakers, J.H. (2001). Genome maintenance mechanisms for preventing cancer. Nature *411*, 366-374.

Hoogstraten, D., Bergink, S., Ng, J.M., Verbiest, V.H., Luijsterburg, M.S., Geverts, B., Raams, A., Dinant, C., Hoeijmakers, J.H., Vermeulen, W., and Houtsmuller, A.B. (2008). Versatile DNA damage detection by the global genome nucleotide excision repair protein XPC. J Cell Sci *121*, 2850-2859.

Horibata, K., Iwamoto, Y., Kuraoka, I., Jaspers, N.G., Kurimasa, A., Oshimura, M., Ichihashi, M., and Tanaka, K. (2004). Complete absence of Cockayne syndrome group B gene product gives rise to UV-sensitive syndrome but not Cockayne syndrome. Proc Natl Acad Sci U S A *101*, 15410-15415.

Howard-Flanders, P., Boyce, R.P., and Theriot, L. (1966). Three loci in Escherichia coli K-12 that control the excision of pyrimidine dimers and certain other mutagen products from DNA. Genetics *53*, 1119-1136.

Huang, J.C., Svoboda, D.L., Reardon, J.T., and Sancar, A. (1992). Human nucleotide excision nuclease removes thymine dimers from DNA by incising the 22nd phosphodiester bond 5' and the 6th phosphodiester bond 3' to the photodimer. Proc Natl Acad Sci U S A *89*, 3664-3668.

Huang, M., and Elledge, S.J. (1997). Identification of RNR4, encoding a second essential small subunit of ribonucleotide reductase in Saccharomyces cerevisiae. Mol Cell Biol *17*, 6105-6113.

Huang, M., Zhou, Z., and Elledge, S.J. (1998). The DNA replication and damage checkpoint pathways induce transcription by inhibition of the Crt1 repressor. Cell *94*, 595-605.

Huibregtse, J.M., Yang, J.C., and Beaudenon, S.L. (1997). The large subunit of RNA polymerase II is a substrate of the Rsp5 ubiquitin-protein ligase. Proc Natl Acad Sci U S A *94*, 3656-3661.

Iben, S., Tschochner, H., Bier, M., Hoogstraten, D., Hozak, P., Egly, J.M., and Grummt, I. (2002). TFIIH plays an essential role in RNA polymerase I transcription. Cell *109*, 297-306.

Ip, S.C., Rass, U., Blanco, M.G., Flynn, H.R., Skehel, J.M., and West, S.C. (2008). Identification of Holliday junction resolvases from humans and yeast. Nature *456*, 357-361.

Ito, S., Kuraoka, I., Chymkowitch, P., Compe, E., Takedachi, A., Ishigami, C., Coin, F., Egly, J.M., and Tanaka, K. (2007). XPG stabilizes TFIIH, allowing transactivation of nuclear receptors: implications for Cockayne syndrome in XP-G/CS patients. Mol Cell *26*, 231-243.

Itoh, T., Fujiwara, Y., Ono, T., and Yamaizumi, M. (1995). UVs syndrome, a new general category of photosensitive disorder with defective DNA repair, is distinct from xeroderma pigmentosum variant and rodent complementation group I. Am J Hum Genet *56*, 1267-1276.

Itoh, T., Ono, T., and Yamaizumi, M. (1994). A new UV-sensitive syndrome not belonging to any complementation groups of xeroderma pigmentosum or Cockayne syndrome: siblings showing biochemical characteristics of Cockayne syndrome without typical clinical manifestations. Mutat Res *314*, 233-248.

Iyer, N., Reagan, M.S., Wu, K.J., Canagarajah, B., and Friedberg, E.C. (1996). Interactions involving the human RNA polymerase II transcription/nucleotide excision repair complex TFIIH, the nucleotide excision repair protein XPG, and Cockayne syndrome group B (CSB) protein. Biochemistry *35*, 2157-2167.

Jansen, L.E., Belo, A.I., Hulsker, R., and Brouwer, J. (2002). Transcription elongation factor Spt4 mediates loss of phosphorylated RNA polymerase II transcription in response to DNA damage. Nucleic Acids Res *30*, 3532-3539.

Jansen, L.E., den Dulk, H., Brouns, R.M., de Ruijter, M., Brandsma, J.A., and Brouwer, J. (2000). Spt4 modulates Rad26 requirement in transcription-coupled nucleotide excision repair. Embo J *19*, 6498-6507.

Jansen, L.E., Verhage, R.A., and Brouwer, J. (1998). Preferential binding of yeast Rad4.Rad23 complex to damaged DNA. J Biol Chem *273*, 33111-33114.

Jazayeri, A., Falck, J., Lukas, C., Bartek, J., Smith, G.C., Lukas, J., and Jackson, S.P. (2006). ATM- and cell cycle-dependent regulation of ATR in response to DNA double-strand breaks. Nat Cell Biol *8*, 37-45.

Jelinsky, S.A., Estep, P., Church, G.M., and Samson, L.D. (2000). Regulatory networks revealed by transcriptional profiling of damaged Saccharomyces cerevisiae cells: Rpn4 links base excision repair with proteasomes. Mol Cell Biol *20*, 8157-8167.

Jelinsky, S.A., and Samson, L.D. (1999). Global response of Saccharomyces cerevisiae to an alkylating agent. Proc Natl Acad Sci U S A *96*, 1486-1491.

Jiang, G., and Sancar, A. (2006). Recruitment of DNA damage checkpoint proteins to damage in transcribed and nontranscribed sequences. Mol Cell Biol *26*, 39-49.

Jones, C.J., and Wood, R.D. (1993). Preferential binding of the xeroderma pigmentosum group A complementing protein to damaged DNA. Biochemistry *32*, 12096-12104.

Jones, J.S., Prakash, L., and Prakash, S. (1990). Regulated expression of the Saccharomyces cerevisiae DNA repair gene RAD7 in response to DNA damage and during sporulation. Nucleic Acids Res *18*, 3281-3285.

Kamiuchi, S., Saijo, M., Citterio, E., de Jager, M., Hoeijmakers, J.H., and Tanaka, K. (2002). Translocation of Cockayne syndrome group A protein to the nuclear matrix: possible relevance to transcription-coupled DNA repair. Proc Natl Acad Sci U S A *99*, 201-206.

Kannouche, P., and Stary, A. (2003). Xeroderma pigmentosum variant and error-prone DNA polymerases. Biochimie *85*, 1123-1132.

Keeney, S., Chang, G.J., and Linn, S. (1993). Characterization of a human DNA damage binding protein implicated in xeroderma pigmentosum E. J Biol Chem *268*, 21293-21300.

Keeney, S., Eker, A.P., Brody, T., Vermeulen, W., Bootsma, D., Hoeijmakers, J.H., and Linn, S. (1994). Correction of the DNA repair defect in xeroderma pigmentosum group E by injection of a DNA damage-binding protein. Proc Natl Acad Sci U S A *91*, 4053-4056.

Khobta, A., Kitsera, N., Speckmann, B., and Epe, B. (2009). 8-Oxoguanine DNA glycosylase (Ogg1) causes a transcriptional inactivation of damaged DNA in the absence of functional Cockayne syndrome B (Csb) protein. DNA Repair (Amst) *8*, 309-317.

Kilinc, M.O., Ninis, V.N., Ugur, S.A., Tuysuz, B., Seven, M., Balci, S., Goodship, J., and Tolun, A. (2003). Is the novel SCKL3 at 14q23 the predominant Seckel locus? Eur J Hum Genet *11*, 851-857.

Kondo, T., Wakayama, T., Naiki, T., Matsumoto, K., and Sugimoto, K. (2001). Recruitment of Mec1 and Ddc1 checkpoint proteins to double-strand breaks through distinct mechanisms. Science *294*, 867-870.

Kristjuhan, A., and Svejstrup, J.Q. (2004). Evidence for distinct mechanisms facilitating transcript elongation through chromatin in vivo. Embo J *23*, 4243-4252.

Krogan, N.J., Dover, J., Wood, A., Schneider, J., Heidt, J., Boateng, M.A., Dean, K., Ryan, O.W., Golshani, A., Johnston, M.*, et al.* (2003a). The Paf1 complex is required for histone H3 methylation by COMPASS and Dot1p: linking transcriptional elongation to histone methylation. Mol Cell *11*, 721-729.

Krogan, N.J., Kim, M., Tong, A., Golshani, A., Cagney, G., Canadien, V., Richards, D.P., Beattie, B.K., Emili, A., Boone, C.*, et al.* (2003b). Methylation of histone H3 by Set2 in Saccharomyces cerevisiae is linked to transcriptional elongation by RNA polymerase II. Mol Cell Biol *23*, 4207-4218.

Krokan, H.E., Standal, R., and Slupphaug, G. (1997). DNA glycosylases in the base excision repair of DNA. Biochem J *325 (Pt 1)*, 1-16.

Kunkel, T.A., and Erie, D.A. (2005). DNA mismatch repair. Annu Rev Biochem *74*, 681-710.

Kuraoka, I., Suzuki, K., Ito, S., Hayashida, M., Kwei, J.S., Ikegami, T., Handa, H., Nakabeppu, Y., and Tanaka, K. (2007). RNA polymerase II bypasses 8-oxoguanine in the presence of transcription elongation factor TFIIS. DNA Repair (Amst) *6*, 841-851.

Kushnirov, V.V. (2000). Rapid and reliable protein extraction from yeast. Yeast *16*, 857-860.

Kvint, K., Uhler, J.P., Taschner, M.J., Sigurdsson, S., Erdjument-Bromage, H., Tempst, P., and Svejstrup, J.Q. (2008). Reversal of RNA polymerase II ubiquitylation by the ubiquitin protease Ubp3. Mol Cell *30*, 498-506.

Laine, J.P., and Egly, J.M. (2006). Initiation of DNA repair mediated by a stalled RNA polymerase IIO. Embo J *25*, 387-397.

Laugel, V., Dalloz, C., Stary, A., Cormier-Daire, V., Desguerre, I., Renouil, M., Fourmaintraux, A., Velez-Cruz, R., Egly, J.M., Sarasin, A., and Dollfus, H. (2008). Deletion of 5' sequences of the CSB gene provides insight into the pathophysiology of Cockayne syndrome. Eur J Hum Genet *16*, 320-327.

Lavin, M.F. (2008). Ataxia-telangiectasia: from a rare disorder to a paradigm for cell signalling and cancer. Nat Rev Mol Cell Biol *9*, 759-769.

Le Page, F., Kwoh, E.E., Avrutskaya, A., Gentil, A., Leadon, S.A., Sarasin, A., and Cooper, P.K. (2000). Transcription-coupled repair of 8-oxoguanine: requirement for XPG, TFIIH, and CSB and implications for Cockayne syndrome. Cell *101*, 159-171.

Lee, J.H., and Paull, T.T. (2004). Direct activation of the ATM protein kinase by the Mre11/Rad50/Nbs1 complex. Science *304*, 93-96.

Lee, S.K., Yu, S.L., Prakash, L., and Prakash, S. (2001). Requirement for yeast RAD26, a homolog of the human CSB gene, in elongation by RNA polymerase II. Mol Cell Biol *21*, 8651-8656.

Lee, S.K., Yu, S.L., Prakash, L., and Prakash, S. (2002a). Requirement of yeast RAD2, a homolog of human XPG gene, for efficient RNA polymerase II transcription. implications for Cockayne syndrome. Cell *109*, 823-834.

Lee, S.K., Yu, S.L., Prakash, L., and Prakash, S. (2002b). Yeast RAD26, a homolog of the human CSB gene, functions independently of nucleotide excision repair and base excision repair in promoting transcription through damaged bases. Mol Cell Biol *22*, 4383-4389.

Lee, T.I., and Young, R.A. (2000). Transcription of eukaryotic protein-coding genes. In Annu Rev Genet, pp. 77-137.

Li, G.M. (2008). Mechanisms and functions of DNA mismatch repair. Cell Res *18*, 85-98.

Li, J., Wang, Q.E., Zhu, Q., El-Mahdy, M.A., Wani, G., Praetorius-Ibba, M., and Wani, A.A. (2006). DNA damage binding protein component DDB1 participates in nucleotide excision repair through DDB2 DNA-binding and cullin 4A ubiquitin ligase activity. Cancer Res *66*, 8590-8597.

Li, S., and Smerdon, M.J. (2002). Rpb4 and Rpb9 mediate subpathways of transcription-coupled DNA repair in Saccharomyces cerevisiae. Embo J *21*, 5921-5929.

Lindahl, T. (1993). Instability and decay of the primary structure of DNA. Nature *362*, 709-715.

Lisby, M., Barlow, J.H., Burgess, R.C., and Rothstein, R. (2004). Choreography of the DNA damage response: spatiotemporal relationships among checkpoint and repair proteins. Cell *118*, 699-713.

Little, J.W., and Mount, D.W. (1982). The SOS regulatory system of Escherichia coli. Cell *29*, 11-22.

Ljungman, M., and Zhang, F. (1996). Blockage of RNA polymerase as a possible trigger for u.v. light-induced apoptosis. Oncogene *13*, 823-831.

Lommel, L., Bucheli, M.E., and Sweder, K.S. (2000). Transcription-coupled repair in yeast is independent from ubiquitylation of RNA pol II: implications for Cockayne's syndrome. Proc Natl Acad Sci U S A *97*, 9088-9092.

Lommel, L., Ortolan, T., Chen, L., Madura, K., and Sweder, K.S. (2002). Proteolysis of a nucleotide excision repair protein by the 26 S proteasome. Curr Genet *42*, 9-20.

Longhese, M.P., Clerici, M., and Lucchini, G. (2003). The S-phase checkpoint and its regulation in Saccharomyces cerevisiae. Mutat Res *532*, 41-58.

Longhese, M.P., Foiani, M., Muzi-Falconi, M., Lucchini, G., and Plevani, P. (1998). DNA damage checkpoint in budding yeast. EMBO J *17*, 5525-5528.

Longhese, M.P., Mantiero, D., and Clerici, M. (2006). The cellular response to chromosome breakage. Mol Microbiol *60*, 1099-1108.

Lowndes, N.F., and Murguia, J.R. (2000). Sensing and responding to DNA damage. Curr Opin Genet Dev *10*, 17-25.

Lu, B., Jan, L., and Jan, Y.N. (2000). Control of cell divisions in the nervous system: symmetry and asymmetry. Annu Rev Neurosci *23*, 531-556.

Lydall, D., and Weinert, T. (1995). Yeast checkpoint genes in DNA damage processing: implications for repair and arrest. Science *270*, 1488-1491.

Madura, K., and Prakash, S. (1986). Nucleotide sequence, transcript mapping, and regulation of the RAD2 gene of Saccharomyces cerevisiae. J Bacteriol *166*, 914-923.

Madura, K., and Prakash, S. (1990). Transcript levels of the Saccharomyes cerevisiae DNA repair gene RAD23 increase in response to UV light and in meiosis but remain constant in the mitotic cell cycle. Nucleic Acids Res *18*, 4737-4742.

Mahdi, A.A., Briggs, G.S., Sharples, G.J., Wen, Q., and Lloyd, R.G. (2003). A model for dsDNA translocation revealed by a structural motif common to RecG and Mfd proteins. EMBO J *22*, 724-734.

Majka, J., Niedziela-Majka, A., and Burgers, P.M. (2006). The checkpoint clamp activates Mec1 kinase during initiation of the DNA damage checkpoint. Mol Cell *24*, 891-901.

Marini, F., Nardo, T., Giannattasio, M., Minuzzo, M., Stefanini, M., Plevani, P., and Muzi Falconi, M. (2006). DNA nucleotide excision repair-dependent signaling to checkpoint activation. Proc Natl Acad Sci U S A *103*, 17325-17330.

Marston, A.L., and Amon, A. (2004). Meiosis: cell-cycle controls shuffle and deal. Nat Rev Mol Cell Biol *5*, 983-997.

Masson, M., Niedergang, C., Schreiber, V., Muller, S., Menissier-de Murcia, J., and de Murcia, G. (1998). XRCC1 is specifically associated with poly(ADP-ribose) polymerase and negatively regulates its activity following DNA damage. Mol Cell Biol *18*, 3563-3571.

Masutani, C., Araki, M., Sugasawa, K., van der Spek, P.J., Yamada, A., Uchida, A., Maekawa, T., Bootsma, D., Hoeijmakers, J.H., and Hanaoka, F. (1997). Identification and characterization of XPC-binding domain of hHR23B. Mol Cell Biol *17*, 6915-6923.

Masutani, C., Araki, M., Yamada, A., Kusumoto, R., Nogimori, T., Maekawa, T., Iwai, S., and Hanaoka, F. (1999a). Xeroderma pigmentosum variant (XP-V) correcting protein from HeLa cells has a thymine dimer bypass DNA polymerase activity. EMBO J *18*, 3491-3501.

Masutani, C., Kusumoto, R., Yamada, A., Dohmae, N., Yokoi, M., Yuasa, M., Araki, M., Iwai, S., Takio, K., and Hanaoka, F. (1999b). The XPV (xeroderma pigmentosum variant) gene encodes human DNA polymerase eta. Nature *399*, 700-704.

Matsunaga, T., Mu, D., Park, C.H., Reardon, J.T., and Sancar, A. (1995). Human DNA repair excision nuclease. Analysis of the roles of the subunits involved in dual incisions by using anti-XPG and anti-ERCC1 antibodies. J Biol Chem *270*, 20862-20869.

Matsuoka, S., Ballif, B.A., Smogorzewska, A., McDonald, E.R., 3rd, Hurov, K.E., Luo, J., Bakalarski, C.E., Zhao, Z., Solimini, N., Lerenthal, Y., *et al.* (2007). ATM and ATR substrate analysis reveals extensive protein networks responsive to DNA damage. Science *316*, 1160-1166.

Mayne, L.V., and Lehmann, A.R. (1982). Failure of RNA synthesis to recover after UV irradiation: an early defect in cells from individuals with Cockayne's syndrome and xeroderma pigmentosum. Cancer Res *42*, 1473-1478.

Mayne, L.V., Lehmann, A.R., and Waters, R. (1982). Excision repair in Cockayne syndrome. Mutat Res *106*, 179-189.

Mazur, S.J., and Grossman, L. (1991). Dimerization of Escherichia coli UvrA and its binding to undamaged and ultraviolet light damaged DNA. Biochemistry *30*, 4432-4443.

McKay, B.C., Chen, F., Clarke, S.T., Wiggin, H.E., Harley, L.M., and Ljungman, M. (2001). UV light-induced degradation of RNA polymerase II is dependent on the Cockayne's syndrome A and B proteins but not p53 or MLH1. Mutat Res *485*, 93-105.

Mellon, I., Bohr, V.A., Smith, C.A., and Hanawalt, P.C. (1986). Preferential DNA repair of an active gene in human cells. Proc Natl Acad Sci U S A *83*, 8878-8882.

Mellon, I., and Hanawalt, P.C. (1989). Induction of the Escherichia coli lactose operon selectively increases repair of its transcribed DNA strand. Nature *342*, 95-98.

Mellon, I., Spivak, G., and Hanawalt, P.C. (1987). Selective removal of transcription-blocking DNA damage from the transcribed strand of the mammalian DHFR gene. Cell *51*, 241-249.

Melo, J.A., Cohen, J., and Toczyski, D.P. (2001). Two checkpoint complexes are independently recruited to sites of DNA damage in vivo. Genes Dev *15*, 2809-2821.

Min, J.H., and Pavletich, N.P. (2007). Recognition of DNA damage by the Rad4 nucleotide excision repair protein. Nature *449*, 570-575.

Modrich, P., and Lahue, R. (1996). Mismatch repair in replication fidelity, genetic recombination, and cancer biology. Annu Rev Biochem *65*, 101-133.

Moggs, J.G., Yarema, K.J., Essigmann, J.M., and Wood, R.D. (1996). Analysis of incision sites produced by human cell extracts and purified proteins during nucleotide excision repair of a 1,3-intrastrand d(GpTpG)-cisplatin adduct. J Biol Chem *271*, 7177-7186.

Morrow, D.M., Tagle, D.A., Shiloh, Y., Collins, F.S., and Hieter, P. (1995). TEL1, an S. cerevisiae homolog of the human gene mutated in ataxia telangiectasia, is functionally related to the yeast checkpoint gene MEC1. Cell *82*, 831-840.

Mu, D., Park, C.H., Matsunaga, T., Hsu, D.S., Reardon, J.T., and Sancar, A. (1995). Reconstitution of human DNA repair excision nuclease in a highly defined system. J Biol Chem *270*, 2415-2418.

Mullenders, L.H., van Kesteren van Leeuwen, A.C., van Zeeland, A.A., and Natarajan, A.T. (1988). Nuclear matrix associated DNA is preferentially repaired in normal human

fibroblasts, exposed to a low dose of ultraviolet light but not in Cockayne's syndrome fibroblasts. Nucleic Acids Res *16*, 10607-10622.

Nakada, D., Hirano, Y., and Sugimoto, K. (2004). Requirement of the Mre11 complex and exonuclease 1 for activation of the Mec1 signaling pathway. Mol Cell Biol *24*, 10016-10025.

Nance, M.A., and Berry, S.A. (1992). Cockayne syndrome: review of 140 cases. Am J Med Genet *42*, 68-84.

Nardo, T., Oneda, R., Spivak, G., Vaz, B., Mortier, L., Thomas, P., Orioli, D., Laugel, V., Stary, A., Hanawalt, P.C.*, et al.* (2009). A UV-sensitive syndrome patient with a specific CSA mutation reveals separable roles for CSA in response to UV and oxidative DNA damage. Proc Natl Acad Sci U S A *106*, 6209-6214.

Naumovski, L., and Friedberg, E.C. (1983). A DNA repair gene required for the incision of damaged DNA is essential for viability in Saccharomyces cerevisiae. Proc Natl Acad Sci U S A *80*, 4818-4821.

Newman, J.C., Bailey, A.D., and Weiner, A.M. (2006). Cockayne syndrome group B protein (CSB) plays a general role in chromatin maintenance and remodeling. Proc Natl Acad Sci U S A *103*, 9613-9618.

Nouspikel, T. (2008). Nucleotide excision repair and neurological diseases. DNA Repair (Amst) *7*, 1155-1167.

Nouspikel, T., Lalle, P., Leadon, S.A., Cooper, P.K., and Clarkson, S.G. (1997). A common mutational pattern in Cockayne syndrome patients from xeroderma pigmentosum group G: implications for a second XPG function. Proc Natl Acad Sci U S A *94*, 3116-3121.

O'Donovan, A., Scherly, D., Clarkson, S.G., and Wood, R.D. (1994). Isolation of active recombinant XPG protein, a human DNA repair endonuclease. J Biol Chem *269*, 15965-15968.

O'Driscoll, M., Ruiz-Perez, V.L., Woods, C.G., Jeggo, P.A., and Goodship, J.A. (2003). A splicing mutation affecting expression of ataxia-telangiectasia and Rad3-related protein (ATR) results in Seckel syndrome. Nat Genet *33*, 497-501.

Oh, E.Y., Claassen, L., Thiagalingam, S., Mazur, S., and Grossman, L. (1989). ATPase activity of the UvrA and UvrAB protein complexes of the Escherichia coli UvrABC endonuclease. Nucleic Acids Res *17*, 4145-4159.

Orphanides, G., LeRoy, G., Chang, C.H., Luse, D.S., and Reinberg, D. (1998). FACT, a factor that facilitates transcript elongation through nucleosomes. Cell *92*, 105-116.

Osterod, M., Larsen, E., Le Page, F., Hengstler, J.G., Van Der Horst, G.T., Boiteux, S., Klungland, A., and Epe, B. (2002). A global DNA repair mechanism involving the Cockayne syndrome B (CSB) gene product can prevent the in vivo accumulation of endogenous oxidative DNA base damage. Oncogene *21*, 8232-8239.

Otero, G., Fellows, J., Li, Y., de Bizemont, T., Dirac, A.M., Gustafsson, C.M., Erdjument-Bromage, H., Tempst, P., and Svejstrup, J.Q. (1999). Elongator, a multisubunit component of a novel RNA polymerase II holoenzyme for transcriptional elongation. Mol Cell *3*, 109-118.

Paciotti, V., Clerici, M., Lucchini, G., and Longhese, M.P. (2000). The checkpoint protein Ddc2, functionally related to S. pombe Rad26, interacts with Mec1 and is regulated by Mec1-dependent phosphorylation in budding yeast. Genes Dev *14*, 2046-2059.

Pan, X., Yuan, D.S., Xiang, D., Wang, X., Sookhai-Mahadeo, S., Bader, J.S., Hieter, P., Spencer, F., and Boeke, J.D. (2004). A robust toolkit for functional profiling of the yeast genome. Mol Cell *16*, 487-496.

Paques, F., and Haber, J.E. (1999). Multiple pathways of recombination induced by double-strand breaks in Saccharomyces cerevisiae. Microbiol Mol Biol Rev *63*, 349-404.

Park, C.H., Bessho, T., Matsunaga, T., and Sancar, A. (1995). Purification and characterization of the XPF-ERCC1 complex of human DNA repair excision nuclease. J Biol Chem *270*, 22657-22660.

Park, E., Guzder, S.N., Koken, M.H., Jaspers-Dekker, I., Weeda, G., Hoeijmakers, J.H., Prakash, S., and Prakash, L. (1992). RAD25 (SSL2), the yeast homolog of the human xeroderma pigmentosum group B DNA repair gene, is essential for viability. Proc Natl Acad Sci U S A *89*, 11416-11420.

Park, J.S., Marr, M.T., and Roberts, J.W. (2002). E. coli Transcription repair coupling factor (Mfd protein) rescues arrested complexes by promoting forward translocation. Cell *109*, 757-767.

Pellicioli, A., Lucca, C., Liberi, G., Marini, F., Lopes, M., Plevani, P., Romano, A., Di Fiore, P.P., and Foiani, M. (1999). Activation of Rad53 kinase in response to DNA damage and its effect in modulating phosphorylation of the lagging strand DNA polymerase. EMBO J *18*, 6561-6572.

Peltomaki, P., and de la Chapelle, A. (1997). Mutations predisposing to hereditary nonpolyposis colorectal cancer. Adv Cancer Res *71*, 93-119.

Petit, C., and Sancar, A. (1999). Nucleotide excision repair: from E. coli to man. Biochimie *81*, 15-25.

Pickart, C.M. (2001). Mechanisms underlying ubiquitination. Annu Rev Biochem *70*, 503-533.

Pickart, C.M., and Eddins, M.J. (2004). Ubiquitin: structures, functions, mechanisms. Biochim Biophys Acta *1695*, 55-72.

Prakash, S., and Prakash, L. (2000). Nucleotide excision repair in yeast. Mutat Res *451*, 13-24.

Proietti-De-Santis, L., Drane, P., and Egly, J.M. (2006). Cockayne syndrome B protein regulates the transcriptional program after UV irradiation. Embo J *25*, 1915-1923.

Radman, M. (1975). SOS repair hypothesis: phenomenology of an inducible DNA repair which is accompanied by mutagenesis. Basic Life Sci *5A*, 355-367.

Ratner, J.N., Balasubramanian, B., Corden, J., Warren, S.L., and Bregman, D.B. (1998). Ultraviolet radiation-induced ubiquitination and proteasomal degradation of the large subunit of RNA polymerase II. Implications for transcription-coupled DNA repair. J Biol Chem *273*, 5184-5189.

Raveendranathan, M., Chattopadhyay, S., Bolon, Y.T., Haworth, J., Clarke, D.J., and Bielinsky, A.K. (2006). Genome-wide replication profiles of S-phase checkpoint mutants reveal fragile sites in yeast. EMBO J *25*, 3627-3639.

Reagan, M.S., and Friedberg, E.C. (1997). Recovery of RNA polymerase II synthesis following DNA damage in mutants of Saccharomyces cerevisiae defective in nucleotide excision repair. Nucleic Acids Res *25*, 4257-4263.

Reardon, J.T., Mu, D., and Sancar, A. (1996). Overproduction, purification, and characterization of the XPC subunit of the human DNA repair excision nuclease. J Biol Chem *271*, 19451-19456.

Reardon, J.T., Nichols, A.F., Keeney, S., Smith, C.A., Taylor, J.S., Linn, S., and Sancar, A. (1993). Comparative analysis of binding of human damaged DNA-binding protein (XPE) and Escherichia coli damage recognition protein (UvrA) to the major ultraviolet photoproducts: T[c,s]T, T[t,s]T, T[6-4]T, and T[Dewar]T. J Biol Chem *268*, 21301-21308.

Reed, S.H., Akiyama, M., Stillman, B., and Friedberg, E.C. (1999). Yeast autonomously replicating sequence binding factor is involved in nucleotide excision repair. Genes Dev *13*, 3052-3058.

Reed, S.H., and Gillette, T.G. (2007). Nucleotide excision repair and the ubiquitin proteasome pathway--do all roads lead to Rome? DNA Repair (Amst) *6*, 149-156.

Reed, S.H., You, Z., and Friedberg, E.C. (1998). The yeast RAD7 and RAD16 genes are required for postincision events during nucleotide excision repair. In vitro and in vivo studies with rad7 and rad16 mutants and purification of a Rad7/Rad16-containing protein complex. J Biol Chem *273*, 29481-29488.

Reid, J., and Svejstrup, J.Q. (2004). DNA damage-induced Def1-RNA polymerase II interaction and Def1 requirement for polymerase ubiquitylation in vitro. J Biol Chem *279*, 29875-29878.

Ribar, B., Prakash, L., and Prakash, S. (2006). Requirement of ELC1 for RNA polymerase II polyubiquitylation and degradation in response to DNA damage in Saccharomyces cerevisiae. Mol Cell Biol *26*, 3999-4005.

Ribar, B., Prakash, L., and Prakash, S. (2007). ELA1 and CUL3 are required along with ELC1 for RNA polymerase II polyubiquitylation and degradation in DNA-damaged yeast cells. Mol Cell Biol *27*, 3211-3216.

Roberts, J., and Park, J.S. (2004). Mfd, the bacterial transcription repair coupling factor: translocation, repair and termination. Curr Opin Microbiol *7*, 120-125.

Rockx, D.A., Mason, R., van Hoffen, A., Barton, M.C., Citterio, E., Bregman, D.B., van Zeeland, A.A., Vrieling, H., and Mullenders, L.H. (2000). UV-induced inhibition of transcription involves repression of transcription initiation and phosphorylation of RNA polymerase II. Proc Natl Acad Sci U S A *97*, 10503-10508.

Rouse, J., and Jackson, S.P. (2000). LCD1: an essential gene involved in checkpoint control and regulation of the MEC1 signalling pathway in Saccharomyces cerevisiae. EMBO J *19*, 5801-5812.

Rouse, J., and Jackson, S.P. (2002a). Interfaces between the detection, signaling, and repair of DNA damage. Science *297*, 547-551.

Rouse, J., and Jackson, S.P. (2002b). Lcd1p recruits Mec1p to DNA lesions in vitro and in vivo. Mol Cell *9*, 857-869.

Russell, S.J., Reed, S.H., Huang, W., Friedberg, E.C., and Johnston, S.A. (1999). The 19S regulatory complex of the proteasome functions independently of proteolysis in nucleotide excision repair. Mol Cell *3*, 687-695.

Saijo, M., Hirai, T., Ogawa, A., Kobayashi, A., Kamiuchi, S., and Tanaka, K. (2007). Functional TFIIH is required for UV-induced translocation of CSA to the nuclear matrix. Mol Cell Biol *27*, 2538-2547.

Sancar, A., Lindsey-Boltz, L.A., Unsal-Kacmaz, K., and Linn, S. (2004). Molecular mechanisms of mammalian DNA repair and the DNA damage checkpoints. Annu Rev Biochem *73*, 39-85.

Sanchez, Y., Bachant, J., Wang, H., Hu, F., Liu, D., Tetzlaff, M., and Elledge, S.J. (1999). Control of the DNA damage checkpoint by chk1 and rad53 protein kinases through distinct mechanisms. Science *286*, 1166-1171.

Sarker, A.H., Tsutakawa, S.E., Kostek, S., Ng, C., Shin, D.S., Peris, M., Campeau, E., Tainer, J.A., Nogales, E., and Cooper, P.K. (2005). Recognition of RNA Polymerase II and Transcription Bubbles by XPG, CSB, and TFIIH: Insights for Transcription-Coupled Repair and Cockayne Syndrome. Mol Cell *20*, 187-198.

Savitsky, K., Bar-Shira, A., Gilad, S., Rotman, G., Ziv, Y., Vanagaite, L., Tagle, D.A., Smith, S., Uziel, T., Sfez, S*., et al.* (1995). A single ataxia telangiectasia gene with a product similar to PI-3 kinase. Science *268*, 1749-1753.

Schaeffer, L., Roy, R., Humbert, S., Moncollin, V., Vermeulen, W., Hoeijmakers, J.H., Chambon, P., and Egly, J.M. (1993). DNA repair helicase: a component of BTF2 (TFIIH) basic transcription factor. Science *260*, 58-63.

Schwartz, M.F., Duong, J.K., Sun, Z., Morrow, J.S., Pradhan, D., and Stern, D.F. (2002). Rad9 phosphorylation sites couple Rad53 to the Saccharomyces cerevisiae DNA damage checkpoint. Mol Cell *9*, 1055-1065.

Selby, C.P., Drapkin, R., Reinberg, D., and Sancar, A. (1997). RNA polymerase II stalled at a thymine dimer: footprint and effect on excision repair. Nucleic Acids Res *25*, 787-793.

Selby, C.P., and Sancar, A. (1990). Transcription preferentially inhibits nucleotide excision repair of the template DNA strand in vitro. J Biol Chem *265*, 21330-21336.

Selby, C.P., and Sancar, A. (1991). Gene- and strand-specific repair in vitro: partial purification of a transcription-repair coupling factor. Proc Natl Acad Sci U S A *88*, 8232-8236.

Selby, C.P., and Sancar, A. (1993). Molecular mechanism of transcription-repair coupling. Science *260*, 53-58.

Selby, C.P., and Sancar, A. (1995a). Structure and function of transcription-repair coupling factor. I. Structural domains and binding properties. J Biol Chem *270*, 4882-4889.

Selby, C.P., and Sancar, A. (1995b). Structure and function of transcription-repair coupling factor. II. Catalytic properties. J Biol Chem *270*, 4890-4895.

Selby, C.P., and Sancar, A. (1997a). Cockayne syndrome group B protein enhances elongation by RNA polymerase II. Proc Natl Acad Sci U S A *94*, 11205-11209.

Selby, C.P., and Sancar, A. (1997b). Human transcription-repair coupling factor CSB/ERCC6 is a DNA-stimulated ATPase but is not a helicase and does not disrupt the ternary transcription complex of stalled RNA polymerase II. J Biol Chem *272*, 1885-1890.

Selby, C.P., Witkin, E.M., and Sancar, A. (1991). Escherichia coli mfd mutant deficient in "mutation frequency decline" lacks strand-specific repair: in vitro complementation with purified coupling factor. Proc Natl Acad Sci U S A *88*, 11574-11578.

Setlow, R.B., and Carrier, W.L. (1964). The Disappearance of Thymine Dimers from DNA: An Error-Correcting Mechanism. Proc Natl Acad Sci U S A *51*, 226-231.

Setlow, R.B., and Carrier, W.L. (1966). Pyrimidine dimers in ultraviolet-irradiated DNA's. J Mol Biol *17*, 237-254.

Shell, S.M., Li, Z., Shkriabai, N., Kvaratskhelia, M., Brosey, C., Serrano, M.A., Chazin, W.J., Musich, P.R., and Zou, Y. (2009). Checkpoint kinase ATR promotes nucleotide excision repair of UV-induced DNA damage via physical interaction with XPA. J Biol Chem.

Shilatifard, A., Lane, W.S., Jackson, K.W., Conaway, R.C., and Conaway, J.W. (1996). An RNA polymerase II elongation factor encoded by the human ELL gene. Science *271*, 1873-1876.

Shiloh, Y. (2003). ATM and related protein kinases: safeguarding genome integrity. Nat Rev Cancer *3*, 155-168.

Siede, W., Robinson, G.W., Kalainov, D., Malley, T., and Friedberg, E.C. (1989). Regulation of the RAD2 gene of Saccharomyces cerevisiae. Mol Microbiol *3*, 1697-1707.

Smith, M.L., and Seo, Y.R. (2002). p53 regulation of DNA excision repair pathways. Mutagenesis *17*, 149-156.

Smogorzewska, A., and de Lange, T. (2004). Regulation of telomerase by telomeric proteins. Annu Rev Biochem *73*, 177-208.

Smolka, M.B., Albuquerque, C.P., Chen, S.H., and Zhou, H. (2007). Proteome-wide identification of in vivo targets of DNA damage checkpoint kinases. Proc Natl Acad Sci U S A *104*, 10364-10369.

Somesh, B.P., Reid, J., Liu, W.F., Sogaard, T.M., Erdjument-Bromage, H., Tempst, P., and Svejstrup, J.Q. (2005). Multiple mechanisms confining RNA polymerase II ubiquitylation to polymerases undergoing transcriptional arrest. Cell *121*, 913-923.

Somesh, B.P., Sigurdsson, S., Saeki, H., Erdjument-Bromage, H., Tempst, P., and Svejstrup, J.Q. (2007). Communication between distant sites in RNA polymerase II through ubiquitylation factors and the polymerase CTD. Cell *129*, 57-68.

Soulas-Sprauel, P., Rivera-Munoz, P., Malivert, L., Le Guyader, G., Abramowski, V., Revy, P., and de Villartay, J.P. (2007). V(D)J and immunoglobulin class switch recombinations: a paradigm to study the regulation of DNA end-joining. Oncogene *26*, 7780-7791.

Soulier, J., and Lowndes, N.F. (1999). The BRCT domain of the S. cerevisiae checkpoint protein Rad9 mediates a Rad9-Rad9 interaction after DNA damage. Curr Biol *9*, 551-554.

Spivak, G. (2005). UV-sensitive syndrome. Mutat Res *577*, 162-169.

Spivak, G., and Hanawalt, P.C. (2006). Host cell reactivation of plasmids containing oxidative DNA lesions is defective in Cockayne syndrome but normal in UV-sensitive syndrome fibroblasts. DNA Repair (Amst) *5*, 13-22.

Spivak, G., Itoh, T., Matsunaga, T., Nikaido, O., Hanawalt, P., and Yamaizumi, M. (2002). Ultraviolet-sensitive syndrome cells are defective in transcription-coupled repair of cyclobutane pyrimidine dimers. DNA Repair (Amst) *1*, 629-643.

Stewart, G.S., Maser, R.S., Stankovic, T., Bressan, D.A., Kaplan, M.I., Jaspers, N.G., Raams, A., Byrd, P.J., Petrini, J.H., and Taylor, A.M. (1999). The DNA double-strand break repair gene hMRE11 is mutated in individuals with an ataxia-telangiectasia-like disorder. Cell *99*, 577-587.

Stiff, T., Reis, C., Alderton, G.K., Woodbine, L., O'Driscoll, M., and Jeggo, P.A. (2005). Nbs1 is required for ATR-dependent phosphorylation events. EMBO J *24*, 199-208.

Sugasawa, K., Masutani, C., Uchida, A., Maekawa, T., van der Spek, P.J., Bootsma, D., Hoeijmakers, J.H., and Hanaoka, F. (1996). HHR23B, a human Rad23 homolog, stimulates XPC protein in nucleotide excision repair in vitro. Mol Cell Biol *16*, 4852-4861.

Sugasawa, K., Ng, J.M., Masutani, C., Iwai, S., van der Spek, P.J., Eker, A.P., Hanaoka, F., Bootsma, D., and Hoeijmakers, J.H. (1998). Xeroderma pigmentosum group C protein complex is the initiator of global genome nucleotide excision repair. Mol Cell *2*, 223-232.

Sugasawa, K., Ng, J.M., Masutani, C., Maekawa, T., Uchida, A., van der Spek, P.J., Eker, A.P., Rademakers, S., Visser, C., Aboussekhra, A.*, et al.* (1997). Two human homologs of Rad23 are functionally interchangeable in complex formation and stimulation of XPC repair activity. Mol Cell Biol *17*, 6924-6931.

Sugasawa, K., Okuda, Y., Saijo, M., Nishi, R., Matsuda, N., Chu, G., Mori, T., Iwai, S., Tanaka, K., and Hanaoka, F. (2005). UV-induced ubiquitylation of XPC protein mediated by UV-DDB-ubiquitin ligase complex. Cell *121*, 387-400.

Sugawara, N., Wang, X., and Haber, J.E. (2003). In vivo roles of Rad52, Rad54, and Rad55 proteins in Rad51-mediated recombination. Mol Cell *12*, 209-219.

Sugo, N., Aratani, Y., Nagashima, Y., Kubota, Y., and Koyama, H. (2000). Neonatal lethality with abnormal neurogenesis in mice deficient in DNA polymerase beta. EMBO J *19*, 1397-1404.

Sun, Z., Fay, D.S., Marini, F., Foiani, M., and Stern, D.F. (1996). Spk1/Rad53 is regulated by Mec1-dependent protein phosphorylation in DNA replication and damage checkpoint pathways. Genes Dev *10*, 395-406.

Sun, Z., Hsiao, J., Fay, D.S., and Stern, D.F. (1998). Rad53 FHA domain associated with phosphorylated Rad9 in the DNA damage checkpoint. Science *281*, 272-274.

Sunesen, M., Stevnsner, T., Brosh Jr, R.M., Dianov, G.L., and Bohr, V.A. (2002). Global genome repair of 8-oxoG in hamster cells requires a functional CSB gene product. Oncogene *21*, 3571-3578.

Sung, P. (1997). Function of yeast Rad52 protein as a mediator between replication protein A and the Rad51 recombinase. J Biol Chem *272*, 28194-28197.

Sung, P., Bailly, V., Weber, C., Thompson, L.H., Prakash, L., and Prakash, S. (1993a). Human xeroderma pigmentosum group D gene encodes a DNA helicase. Nature *365*, 852-855.

Sung, P., Guzder, S.N., Prakash, L., and Prakash, S. (1996). Reconstitution of TFIIH and requirement of its DNA helicase subunits, Rad3 and Rad25, in the incision step of nucleotide excision repair. J Biol Chem *271*, 10821-10826.

Sung, P., Prakash, L., Matson, S.W., and Prakash, S. (1987a). RAD3 protein of Saccharomyces cerevisiae is a DNA helicase. Proc Natl Acad Sci U S A *84*, 8951-8955.

Sung, P., Prakash, L., Weber, S., and Prakash, S. (1987b). The RAD3 gene of Saccharomyces cerevisiae encodes a DNA-dependent ATPase. Proc Natl Acad Sci U S A *84*, 6045-6049.

Sung, P., Reynolds, P., Prakash, L., and Prakash, S. (1993b). Purification and characterization of the Saccharomyces cerevisiae RAD1/RAD10 endonuclease. J Biol Chem *268*, 26391-26399.

Svejstrup, J.Q. (2002). Mechanisms of transcription-coupled DNA repair. Nat Rev Mol Cell Biol *3*, 21-29.

Svejstrup, J.Q. (2003). Rescue of arrested RNA polymerase II complexes. In J Cell Sci, pp. 447-451.

Svejstrup, J.Q. (2004). The RNA polymerase II transcription cycle: cycling through chromatin. In Biochim Biophys Acta, pp. 64-73.

Svejstrup, J.Q., Wang, Z., Feaver, W.J., Wu, X., Bushnell, D.A., Donahue, T.F., Friedberg, E.C., and Kornberg, R.D. (1995). Different forms of TFIIH for transcription and DNA repair: holo-TFIIH and a nucleotide excision repairosome. In Cell, pp. 21-28.

Sweder, K.S., and Hanawalt, P.C. (1992). Preferential repair of cyclobutane pyrimidine dimers in the transcribed strand of a gene in yeast chromosomes and plasmids is dependent on transcription. Proc Natl Acad Sci U S A *89*, 10696-10700.

Sweeney, F.D., Yang, F., Chi, A., Shabanowitz, J., Hunt, D.F., and Durocher, D. (2005). Saccharomyces cerevisiae Rad9 acts as a Mec1 adaptor to allow Rad53 activation. Curr Biol *15*, 1364-1375.

Szostak, J.W., Orr-Weaver, T.L., Rothstein, R.J., and Stahl, F.W. (1983). The double-strand-break repair model for recombination. Cell *33*, 25-35.

Tan, T., and Chu, G. (2002). p53 Binds and activates the xeroderma pigmentosum DDB2 gene in humans but not mice. Mol Cell Biol *22*, 3247-3254.

Tanaka, K., Miura, N., Satokata, I., Miyamoto, I., Yoshida, M.C., Satoh, Y., Kondo, S., Yasui, A., Okayama, H., and Okada, Y. (1990). Analysis of a human DNA excision repair gene involved in group A xeroderma pigmentosum and containing a zinc-finger domain. Nature *348*, 73-76.

Tantin, D. (1998). RNA polymerase II elongation complexes containing the Cockayne syndrome group B protein interact with a molecular complex containing the transcription factor IIH components xeroderma pigmentosum B and p62. J Biol Chem *273*, 27794-27799.

Tantin, D., Kansal, A., and Carey, M. (1997). Recruitment of the putative transcription-repair coupling factor CSB/ERCC6 to RNA polymerase II elongation complexes. Mol Cell Biol *17*, 6803-6814.

Tebbs, R.S., Flannery, M.L., Meneses, J.J., Hartmann, A., Tucker, J.D., Thompson, L.H., Cleaver, J.E., and Pedersen, R.A. (1999). Requirement for the Xrcc1 DNA base excision repair gene during early mouse development. Dev Biol *208*, 513-529.

Teng, Y., Liu, H., Gill, H.W., Yu, Y., Waters, R., and Reed, S.H. (2008). Saccharomyces cerevisiae Rad16 mediates ultraviolet-dependent histone H3 acetylation required for efficient global genome nucleotide-excision repair. EMBO Rep *9*, 97-102.

Teng, Y., Yu, Y., Ferreiro, J.A., and Waters, R. (2005). Histone acetylation, chromatin remodelling, transcription and nucleotide excision repair in S. cerevisiae: studies with two model genes. DNA Repair (Amst) *4*, 870-883.

Tercero, J.A., and Diffley, J.F. (2001). Regulation of DNA replication fork progression through damaged DNA by the Mec1/Rad53 checkpoint. Nature *412*, 553-557.

Terleth, C., Schenk, P., Poot, R., Brouwer, J., and van de Putte, P. (1990). Differential repair of UV damage in rad mutants of Saccharomyces cerevisiae: a possible function of G2 arrest upon UV irradiation. Mol Cell Biol *10*, 4678-4684.

Terleth, C., van Sluis, C.A., and van de Putte, P. (1989). Differential repair of UV damage in Saccharomyces cerevisiae. Nucleic Acids Res *17*, 4433-4439.

Theis, K., Skorvaga, M., Machius, M., Nakagawa, N., Van Houten, B., and Kisker, C. (2000). The nucleotide excision repair protein UvrB, a helicase-like enzyme with a catch. Mutat Res *460*, 277-300.

Thorslund, T., von Kobbe, C., Harrigan, J.A., Indig, F.E., Christiansen, M., Stevnsner, T., and Bohr, V.A. (2005). Cooperation of the Cockayne syndrome group B protein and poly(ADP-ribose) polymerase 1 in the response to oxidative stress. Mol Cell Biol *25*, 7625-7636.

Tijsterman, M., and Brouwer, J. (1999). Rad26, the yeast homolog of the cockayne syndrome B gene product, counteracts inhibition of DNA repair due to RNA polymerase II transcription. J Biol Chem *274*, 1199-1202.

Tijsterman, M., de Pril, R., Tasseron-de Jong, J.G., and Brouwer, J. (1999). RNA polymerase II transcription suppresses nucleosomal modulation of UV-induced (6-4) photoproduct and cyclobutane pyrimidine dimer repair in yeast. Mol Cell Biol *19*, 934-940.

Tijsterman, M., Verhage, R.A., van de Putte, P., Tasseron-de Jong, J.G., and Brouwer, J. (1997). Transitions in the coupling of transcription and nucleotide excision repair within RNA polymerase II-transcribed genes of Saccharomyces cerevisiae. Proc Natl Acad Sci U S A *94*, 8027-8032.

Tomkinson, A.E., Bardwell, A.J., Bardwell, L., Tappe, N.J., and Friedberg, E.C. (1993). Yeast DNA repair and recombination proteins Rad1 and Rad10 constitute a single-stranded-DNA endonuclease. Nature *362*, 860-862.

Tong, A.H., Evangelista, M., Parsons, A.B., Xu, H., Bader, G.D., Page, N., Robinson, M., Raghibizadeh, S., Hogue, C.W., Bussey, H.*, et al.* (2001). Systematic genetic analysis with ordered arrays of yeast deletion mutants. Science *294*, 2364-2368.

Tornaletti, S. (2009). DNA repair in mammalian cells: Transcription-coupled DNA repair: directing your effort where it's most needed. Cell Mol Life Sci *66*, 1010-1020.

Tornaletti, S., Patrick, S.M., Turchi, J.J., and Hanawalt, P.C. (2003). Behavior of T7 RNA polymerase and mammalian RNA polymerase II at site-specific cisplatin adducts in the template DNA. J Biol Chem *278*, 35791-35797.

Trapp, C., Reite, K., Klungland, A., and Epe, B. (2007). Deficiency of the Cockayne syndrome B (CSB) gene aggravates the genomic instability caused by endogenous oxidative DNA base damage in mice. Oncogene *26*, 4044-4048.

Troelstra, C., van Gool, A., de Wit, J., Vermeulen, W., Bootsma, D., and Hoeijmakers, J.H. (1992). ERCC6, a member of a subfamily of putative helicases, is involved in Cockayne's syndrome and preferential repair of active genes. Cell *71*, 939-953.

Tsutakawa, S.E., and Cooper, P.K. (2000). Transcription-coupled repair of oxidative DNA damage in human cells: mechanisms and consequences. Cold Spring Harb Symp Quant Biol *65*, 201-215.

Tuo, J., Muftuoglu, M., Chen, C., Jaruga, P., Selzer, R.R., Brosh, R.M., Jr., Rodriguez, H., Dizdaroglu, M., and Bohr, V.A. (2001). The Cockayne Syndrome group B gene product is involved in general genome base excision repair of 8-hydroxyguanine in DNA. J Biol Chem *276*, 45772-45779.

Unsal-Kacmaz, K., Makhov, A.M., Griffith, J.D., and Sancar, A. (2002). Preferential binding of ATR protein to UV-damaged DNA. Proc Natl Acad Sci U S A *99*, 6673-6678.

van Gool, A.J., Citterio, E., Rademakers, S., van Os, R., Vermeulen, W., Constantinou, A., Egly, J.M., Bootsma, D., and Hoeijmakers, J.H. (1997). The Cockayne syndrome B protein, involved in transcription-coupled DNA repair, resides in an RNA polymerase II-containing complex. Embo J *16*, 5955-5965.

van Gool, A.J., Verhage, R., Swagemakers, S.M., van de Putte, P., Brouwer, J., Troelstra, C., Bootsma, D., and Hoeijmakers, J.H. (1994). RAD26, the functional S. cerevisiae homolog of the Cockayne syndrome B gene ERCC6. Embo J *13*, 5361-5369.

van Hoffen, A., Natarajan, A.T., Mayne, L.V., van Zeeland, A.A., Mullenders, L.H., and Venema, J. (1993). Deficient repair of the transcribed strand of active genes in Cockayne's syndrome cells. Nucleic Acids Res *21*, 5890-5895.

van Oosterwijk, M.F., Filon, R., de Groot, A.J., van Zeeland, A.A., and Mullenders, L.H. (1998). Lack of transcription-coupled repair of acetylaminofluorene DNA adducts in human fibroblasts contrasts their efficient inhibition of transcription. J Biol Chem *273*, 13599-13604.

van Oosterwijk, M.F., Versteeg, A., Filon, R., van Zeeland, A.A., and Mullenders, L.H. (1996). The sensitivity of Cockayne's syndrome cells to DNA-damaging agents is not due to defective transcription-coupled repair of active genes. Mol Cell Biol *16*, 4436-4444.

Venema, J., Mullenders, L.H., Natarajan, A.T., van Zeeland, A.A., and Mayne, L.V. (1990a). The genetic defect in Cockayne syndrome is associated with a defect in repair of UV-induced DNA damage in transcriptionally active DNA. Proc Natl Acad Sci U S A *87*, 4707-4711.

Venema, J., van Hoffen, A., Natarajan, A.T., van Zeeland, A.A., and Mullenders, L.H. (1990b). The residual repair capacity of xeroderma pigmentosum complementation group C fibroblasts is highly specific for transcriptionally active DNA. Nucleic Acids Res *18*, 443-448.

Verhage, R., Zeeman, A.M., de Groot, N., Gleig, F., Bang, D.D., van de Putte, P., and Brouwer, J. (1994). The RAD7 and RAD16 genes, which are essential for pyrimidine dimer removal from the silent mating type loci, are also required for repair of the nontranscribed strand of an active gene in Saccharomyces cerevisiae. Mol Cell Biol *14*, 6135-6142.

Verhage, R.A., van Gool, A.J., de Groot, N., Hoeijmakers, J.H., van de Putte, P., and Brouwer, J. (1996a). Double mutants of Saccharomyces cerevisiae with alterations in global genome and transcription-coupled repair. Mol Cell Biol *16*, 496-502.

Verhage, R.A., Zeeman, A.M., Lombaerts, M., van de Putte, P., and Brouwer, J. (1996b). Analysis of gene- and strand-specific repair in the moderately UV-sensitive Saccharomyces cerevisiae rad23 mutant. Mutat Res *362*, 155-165.

Verhoeven, E.E., van Kesteren, M., Moolenaar, G.F., Visse, R., and Goosen, N. (2000). Catalytic sites for 3' and 5' incision of Escherichia coli nucleotide excision repair are both located in UvrC. J Biol Chem *275*, 5120-5123.

Vialard, J.E., Gilbert, C.S., Green, C.M., and Lowndes, N.F. (1998). The budding yeast Rad9 checkpoint protein is subjected to Mec1/Tel1-dependent hyperphosphorylation and interacts with Rad53 after DNA damage. EMBO J *17*, 5679-5688.

Vichi, P., Coin, F., Renaud, J.P., Vermeulen, W., Hoeijmakers, J.H., Moras, D., and Egly, J.M. (1997). Cisplatin- and UV-damaged DNA lure the basal transcription factor TFIID/TBP. Embo J *16*, 7444-7456.

Volker, M., Mone, M.J., Karmakar, P., van Hoffen, A., Schul, W., Vermeulen, W., Hoeijmakers, J.H., van Driel, R., van Zeeland, A.A., and Mullenders, L.H. (2001). Sequential assembly of the nucleotide excision repair factors in vivo. Mol Cell *8*, 213-224.

Wada, T., Orphanides, G., Hasegawa, J., Kim, D.K., Shima, D., Yamaguchi, Y., Fukuda, A., Hisatake, K., Oh, S., Reinberg, D., and Handa, H. (2000). FACT relieves DSIF/NELF-mediated inhibition of transcriptional elongation and reveals functional differences between P-TEFb and TFIIH. Mol Cell *5*, 1067-1072.

Wakayama, T., Kondo, T., Ando, S., Matsumoto, K., and Sugimoto, K. (2001). Pie1, a protein interacting with Mec1, controls cell growth and checkpoint responses in Saccharomyces cerevisiae. Mol Cell Biol *21*, 755-764.

Wang, H., Zhai, L., Xu, J., Joo, H.Y., Jackson, S., Erdjument-Bromage, H., Tempst, P., Xiong, Y., and Zhang, Y. (2006). Histone H3 and H4 ubiquitylation by the CUL4-DDB-ROC1 ubiquitin ligase facilitates cellular response to DNA damage. Mol Cell *22*, 383-394.

Wang, J.C. (2002). Cellular roles of DNA topoisomerases: a molecular perspective. Nat Rev Mol Cell Biol *3*, 430-440.

Wang, X., and Haber, J.E. (2004). Role of Saccharomyces single-stranded DNA-binding protein RPA in the strand invasion step of double-strand break repair. PLoS Biol *2*, E21.

Wang, Z., Wu, X., and Friedberg, E.C. (1996). A yeast whole cell extract supports nucleotide excision repair and RNA polymerase II transcription in vitro. Mutat Res *364*, 33-41.

Watkins, J.F., Sung, P., Prakash, L., and Prakash, S. (1993). The Saccharomyces cerevisiae DNA repair gene RAD23 encodes a nuclear protein containing a ubiquitin-like domain required for biological function. Mol Cell Biol *13*, 7757-7765.

Weinert, T.A., and Hartwell, L.H. (1988). The RAD9 gene controls the cell cycle response to DNA damage in Saccharomyces cerevisiae. Science *241*, 317-322.

Weinert, T.A., and Hartwell, L.H. (1990). Characterization of RAD9 of Saccharomyces cerevisiae and evidence that its function acts posttranslationally in cell cycle arrest after DNA damage. Mol Cell Biol *10*, 6554-6564.

West, S.C. (2003). Molecular views of recombination proteins and their control. Nat Rev Mol Cell Biol *4*, 435-445.

Wilson, D.M., 3rd, and McNeill, D.R. (2007). Base excision repair and the central nervous system. Neuroscience *145*, 1187-1200.

Wind, M., and Reines, D. (2000). Transcription elongation factor SII. Bioessays *22*, 327-336.

Witkin, E.M. (1966). Radiation-induced mutations and their repair. Science *152*, 1345-1353.

Wittschieben, B.O., and Wood, R.D. (2003). DDB complexities. DNA Repair (Amst) *2*, 1065-1069.

Wold, M.S. (1997). Replication protein A: a heterotrimeric, single-stranded DNA-binding protein required for eukaryotic DNA metabolism. Annu Rev Biochem *66*, 61-92.

Wolner, B., van Komen, S., Sung, P., and Peterson, C.L. (2003). Recruitment of the recombinational repair machinery to a DNA double-strand break in yeast. Mol Cell *12*, 221-232.

Woudstra, E.C., Gilbert, C., Fellows, J., Jansen, L., Brouwer, J., Erdjument-Bromage, H., Tempst, P., and Svejstrup, J.Q. (2002). A Rad26-Def1 complex coordinates repair and RNA pol II proteolysis in response to DNA damage. Nature *415*, 929-933.

Woychik, N.A., Lane, W.S., and Young, R.A. (1991). Yeast RNA polymerase II subunit RPB9 is essential for growth at temperature extremes. J Biol Chem *266*, 19053-19055.

Wu, X., Shell, S.M., Liu, Y., and Zou, Y. (2006a). ATR-dependent checkpoint modulates XPA nuclear import in response to UV irradiation. Oncogene.

Wu, X., Shell, S.M., Yang, Z., and Zou, Y. (2006b). Phosphorylation of nucleotide excision repair factor xeroderma pigmentosum group A by ataxia telangiectasia mutated and Rad3-related-dependent checkpoint pathway promotes cell survival in response to UV irradiation. Cancer Res *66*, 2997-3005.

Yamaguchi, Y., Takagi, T., Wada, T., Yano, K., Furuya, A., Sugimoto, S., Hasegawa, J., and Handa, H. (1999). NELF, a multisubunit complex containing RD, cooperates with DSIF to repress RNA polymerase II elongation. Cell *97*, 41-51.

You, Z., Feaver, W.J., and Friedberg, E.C. (1998). Yeast RNA polymerase II transcription in vitro is inhibited in the presence of nucleotide excision repair: complementation of inhibition by Holo-TFIIH and requirement for RAD26. Mol Cell Biol *18*, 2668-2676.

Yu, A., Fan, H.Y., Liao, D., Bailey, A.D., and Weiner, A.M. (2000). Activation of p53 or loss of the Cockayne syndrome group B repair protein causes metaphase fragility of human U1, U2, and 5S genes. Mol Cell *5*, 801-810.

Yu, S., Owen-Hughes, T., Friedberg, E.C., Waters, R., and Reed, S.H. (2004). The yeast Rad7/Rad16/Abf1 complex generates superhelical torsion in DNA that is required for nucleotide excision repair. DNA Repair (Amst) *3*, 277-287.

Yu, S., Teng, Y., Lowndes, N.F., and Waters, R. (2001). RAD9, RAD24, RAD16 and RAD26 are required for the inducible nucleotide excision repair of UV-induced cyclobutane pyrimidine dimers from the transcribed and non-transcribed regions of the Saccharomyces cerevisiae MFA2 gene. Mutat Res *485*, 229-236.

Zhao, X., Muller, E.G., and Rothstein, R. (1998). A suppressor of two essential checkpoint genes identifies a novel protein that negatively affects dNTP pools. Mol Cell *2*, 329-340.

Zhao, X., and Rothstein, R. (2002). The Dun1 checkpoint kinase phosphorylates and regulates the ribonucleotide reductase inhibitor Sml1. Proc Natl Acad Sci U S A *99*, 3746-3751.

Zhou, B.B., and Elledge, S.J. (2000). The DNA damage response: putting checkpoints in perspective. Nature *408*, 433-439.

Zhou, Z., and Elledge, S.J. (1993). DUN1 encodes a protein kinase that controls the DNA damage response in yeast. Cell *75*, 1119-1127.

Zou, L., and Elledge, S.J. (2003). Sensing DNA damage through ATRIP recognition of RPA-ssDNA complexes. Science *300*, 1542-1548.

Zou, Y., and Van Houten, B. (1999). Strand opening by the UvrA(2)B complex allows dynamic recognition of DNA damage. EMBO J *18*, 4889-4901.

8. Appendix

8.1 Example of the analysis of Real-time PCR results from ChIPs

Ct-values were obtained from the Real-time PCR machine

samples:	Rad14 IP Glucose no UV	1
	Rad14 IP Glucose 2 h post UV	2
	Rad14 IP Galactose no UV	3
	Rad14 IP Galactose 2 h post UV	4
	input Glucose no UV	5
	input Glucose 2 h post UV	6
	input Galactose no UV	7
	input Galactose 2 h post UV	8

sample	primer pair	Ct	average	sample	primer pair	Ct	average
1	hotspot	23.62	23.690	5	hotspot	23.24	23.340
		23.72				23.49	
		23.73				23.29	
2	hotspot	23.07	23.027	6	hotspot	22.97	23.130
		22.98				23.28	
		23.03				23.14	
3	hotspot	24.9	25.247	7	hotspot	23.58	23.637
		25.37				23.62	
		25.47				23.71	
4	hotspot	23.77	24.083	8	hotspot	23.57	23.680
		24.1				23.75	
		24.38				23.72	
1	*GAL10*	30.26	30.047	5	*GAL10*	24.66	24.580
		29.85				24.44	
		30.03				24.64	
2	*GAL10*	29.88	29.833	6	*GAL10*	24.5	24.570
		29.69				24.65	
		29.93				24.56	
3	*GAL10*	29.1	28.993	7	*GAL10*	24.9	24.973
		28.86				24.77	
		29.02				25.25	
4	*GAL10*	29.66	29.643	8	*GAL10*	25.26	25.180
		29.11				25.07	
		30.16				25.21	
1	telomere	29.64	29.573	5	telomere	24.31	24.260
		29.28				24.1	
		29.8				24.37	
2	telomere	29.08	29.217	6	telomere	24.29	24.203
		29.21				24.01	
		29.36				24.31	
3	telomere	28.54	28.593	7	telomere	24.31	24.483
		28.41				24.51	
		28.83				24.63	
4	telomere	28.63	29.127	8	telomere	24.7	24.587
		28.99				24.59	
		29.76				24.47	

The average Ct-values were then summarised in a table:

Rad14					
		Glu - UV	Glu + UV	Gal - UV	Gal + UV
hotspot	IP	23.690	23.027	25.247	24.083
	input	23.340	23.130	23.637	23.680
GAL10	IP	30.047	29.833	28.993	29.643
	input	24.580	24.570	24.973	25.180
telomere	IP	29.573	29.217	28.593	29.127
	input	24.260	24.203	24.483	24.587

Then a new value was calculated for each sample using the following formula:

value = 2^(30-x) x ….. value for each sample in the table shown above

		Glu - UV	Glu + UV	Gal - UV	Gal + UV
hotspot	IP	79.3413	125.6558	26.9709	60.4080
	input	101.1253	116.9704	82.3293	79.8932
GAL10	IP	0.9682	1.1225	2.0093	1.2805
	input	42.8137	43.1115	32.5970	28.2465
telomere	IP	1.3441	1.7211	2.6512	1.8319
	input	53.4456	55.5867	45.7807	42.6163

In order to correct for differences in the input, the value for each IP was divided by the value for the respective input:

	Glu - UV	Glu + UV	Gal - UV	Gal + UV
hotspot	0.784584098	1.074252648	0.327598351	0.75610928
GAL10	0.022613582	0.026036271	0.061639544	0.045331781
telomere	0.02514938	0.030962519	0.057911754	0.042985682

In order to correct for non-specific signals, the values were divided by the value obtained for the telomere sequence from the same time point:

	Glu - UV	Glu + UV	Gal - UV	Gal + UV
hotspot	31.19695538	34.69525985	5.656854249	17.58979381
GAL10	0.899170536	0.840896415	1.064370182	1.05457863

Finally, the values were set in relation to a reference. In this example, the value for the '+UV' sample was set in relation to the '-UV' sample, both for Glucose and for Galactose:

	Glu - UV	Glu + UV	Gal - UV	Gal + UV
hotspot	1	1.112136086	1	3.109465621
GAL10	1	0.935191248	1	0.990800613

Such values were used for the display of the results in graphs.

8.2 Original data for Figure 3.4A (inductions)

	induction	average	Standard Deviation
hotspot	6.4	4.666666667	2.273030283
	8.2		
	4.7		
	3.4		
	2.1		
	3.2		
GAL10	32.4	36.23333333	6.084954122
	34.8		
	48.1		
	36.5		
	34.2		
	31.4		

8.3 Original data for Figure 3.4B (RNAPII density)

AVERAGES

	no UV	5 min	30 min	90 min
GAL10	1	0.227014229	0.59856849	0.96261085
RPB2	1	0.352054156	0.805467416	1.015051407
start	1	0.40189201	0.691366	0.88892577
hotspot	1	0.341949	0.6647873	1.12664307
end	1	0.21713486	0.5374842	1.002055632

STANDARD DEVIATIONS

	no UV	5 min	30 min	90 min
GAL10	0	0.137612556	0.137761244	0.24986106
RPB2	0	0.101029499	0.080715696	0.117438284
start	0	0.06717117	0.06804729	0.041920161
hotspot	0	0.052327033	0.171063131	0.110663385
end	0	0.031606146	0.064270632	0.129785435

8.4. Original data for Figure 3.5 (Rad14 recruitment)

	Glucose		Galactose	
	-UV	+UV	-UV	+UV
RPB2	1	0.696566663	1	1.070536016
	1	1.029302237	1	0.886791389
GAL10	1	0.771996743	1	1.358172444
	1	0.993092495	1	0.931955732
start	1	1.806670402	1	1.731073122
	1	1.3492992	1	1.5838423
hotspot	1	1.123759517	1	4.964562776
	1	1.208597056	1	7.490177979
	1	1.212793001	1	3.301984466
	1	1.4349293	1	2.24938443
end	1	1.43893358	1	1.113421618
	1	1.2944429	1	1.4293822

AVERAGES

	Glucose		Galactose	
	-UV	+UV	-UV	+UV
RPB2	1	0.86293445	1	0.978663703
GAL10	1	0.882544619	1	1.145064088
start	1	1.577984801	1	1.657457711
hotspot	1	1.245019719	1	4.501527413
end	1	1.36668824	1	1.271401909

STANDARD DEVIATIONS

RPB2	0	0.235279581	0	0.129927072
GAL10	0	0.156338306	0	0.301380727
start	0	0.323410278	0	0.104107913
hotspot	0	0.133085007	0	2.284548479
end	0	0.10217034	0	0.22341787

8.5. Data for the quantifications in Figure 5.2

first experiment – transcribed strand

	WT				
	0	1	2	3	4
top band	1001388.053	1627432.574	997727.198	885618.046	813959.963
total damage	630066.767	772347.73	157053.521	53833.495	44633.991
sum	1631454.82	2399780.304	1154780.719	939451.541	858593.954
ratio	1	1.470944996	0.707822678	0.575836689	0.526275042
adjusted damage	630066.767	525069.076	221882.5788	93487.43502	84811.14899
	0	1	2	3	4
damage (%)	100	83.33546594	35.21572481	14.83770291	13.46066059
repair (%)	0	16.66453406	64.78427519	85.16229709	86.53933941
			t50% 1.7		

	rad26				
	0	1	2	3	4
top band	930251.69	654265.951	745717.923	698077.504	684905.913
total damage	605916.859	465973.235	300522.791	208688.633	188738.726
sum	1536168.549	1120239.186	1046240.714	906766.137	873644.639
ratio	1	0.729242365	0.681071563	0.590277765	0.568716655
adjusted damage	605916.859	638982.6719	441249.9472	353543.1039	331867.7663
	0	1	2	3	4
damage (%)	100	105.4571535	72.82351376	58.34845138	54.77117221
repair (%)	0	-5.457153477	27.17648624	41.65154862	45.22882779
			t50% 4.0		

	mec1				
	0	1	2	3	4
top band	1124924.852	1531041.256	1165542.983	1429369.387	998624.132
total damage	817366.844	632444.449	399777.446	361813.451	215339.682
sum	1942291.696	2163485.705	1565320.429	1791182.838	1213963.814
ratio	1	1.113883002	0.805914185	0.922200739	0.62501622
adjusted damage	817366.844	567783.5535	496054.6092	392336.9778	344534.5498
	0	1	2	3	4
damage remaining (%)	100	69.46496027	60.68934809	48.00010922	42.15176482
repair (%)	0	30.53503973	39.31065191	51.99989078	57.84823518
			t50% 3.0		

second experiment – transcribed strand

	WT				
	0	1	2	3	4
top band	281064.637	268446.926	274526.338	393213.259	329901.274
total damage	210196.384	135853.492	43449.984	30325.552	18695.135
sum	491261.021	404300.418	317976.322	423538.811	348596.409
ratio	1	0.822984932	0.647265524	0.862146177	0.709595091
adjusted damage	210196.384	165074.094	67128.53136	35174.48992	26346.20114
damage (%)	100	78.53327008	31.93610189	16.734108	12.53408866
repair (%)	0	21.46672992	68.06389811	83.265892	87.46591134
			t50%= 1.8		
	0	1	2	3	4
top band	293255.579	311091.82	274032.593	267507.498	295224.652
total damage	198124.07	170532.052	109801.684	80044.623	67977.287
sum	491379.649	481623.872	383834.277	347552.121	363201.939
ratio	1.000241477	0.980382834	0.781324511	0.707469362	0.739325783
adjusted damage	198076.2392	173944.3471	140532.7523	113142.1759	91944.97009
damage (%)	100	87.81686678	70.94881894	57.12051903	46.41898011
repair (%)	0	12.18313322	29.05118106	42.87948097	53.58101989
			t50%=3.8		
	0	1	2	3	4
top band	264113.694	267996.195	278155.939	272040.821	240036.634
total damage	193166.05	141049.258	86529.976	68064.597	50850.006
sum	457279.744	409045.453	364685.915	340105.418	290886.64
ratio	0.930828469	0.83264382	0.742346531	0.692311019	0.59212237
adjusted damage	207520.5652	169399.2733	116562.7808	98315.05659	85877.52901
damage remaining (%)	100	81.63011369	56.16926719	47.37605474	41.38265955
repair (%)	0	18.36988631	43.83073281	52.62394526	58.61734045
			t50% 2.9		

summary TS

	average t50%	STDEV	STD-Error
wt	1.8	0.141421356	0.100298834
rad26	3.9	0.141421356	0.100298834
mec1	2.95	0.070710678	0.050149417

first experiment – non-transcribed strand

	WT				
	0	1	2	3	4
top band	650116.866	1073939.161	730777.335	489818.719	771437.962
total damage	375548.648	574451.425	338672.902	189644.293	185262.511
sum	1025665.514	1648390.586	1069450.237	679463.012	956700.473
ratio	1	1.607142449	1.042689086	0.66246062	0.93276069
adjusted damage	375548.648	357436.533	324807.1804	286272.5532	198617.4084
damage remaining (%)	100	95.17715878	86.48870983	76.22782154	52.88726493
repair (%)	0	4.822841221	13.51129017	23.77217846	47.11273507
			t50% = 4.8		

	rad26				
	0	1	2	3	4
top band	855661.338	826154.502	616409.418	850555.049	880239.629
total damage	440059.724	422576.028	231175.977	229747.088	147315.284
sum	1295721.062	1248730.53	847585.395	1080302.137	1027554.913
ratio	1.263297873	1.217483198	0.826376029	1.053269436	1.00184212
adjusted damage	348342.013	347089.8233	279746.7119	218127.5562	147044.4105
damage remaining (%)	100	99.64052865	80.30805973	62.61879075	42.21265454
repair (%)	0	0.359471346	19.69194027	37.38120925	57.78734546
			t50% = 3.7		

	mec1				
	0	1	2	3	4
top band	962550.814	1014754.542	1051627.703	1271249.7	676688.404
total damage	551525.385	628017.793	551922.565	530319.477	332970.097
sum	1514076.199	1642772.335	1603550.268	1801569.177	1009658.501
ratio	1.476189048	1.601664785	1.563424183	1.756488009	0.984393535
adjusted damage	373614.3319	392103.141	353021.6374	301920.3514	338248.9677
damage remaining (%)	100	104.9486349	94.48824826	80.81069853	90.53425922
repair (%)	0	-4.948634869	5.511751739	19.18930147	9.465740781
			t50%=more than 6 hours		

second experiment – non-transcribed strand

	WT				
	0	1	2	3	4
top band	1420621.061	1113659.404	924010.245	1336602.163	1323936.455
total damage	804561.212	641212.88	457670.5	557023.413	340901.656
sum	2225182.273	1754872.284	1381680.745	1893625.576	1664838.111
ratio	1	0.788642039	0.620929243	0.85099796	0.748180556
adjusted damage	804561.212	813059.4726	737073.5151	654553.1704	455640.8919
damage remaining (%)	100	101.0562603	91.61186298	81.35529784	56.63222202
repair (%)	0	-1.056260297	8.388137022	18.64470216	43.36777798
			t50% = 5.3		

	rad26				
	0	1	2	3	4
top band	1571086.701	1715304.93	1528921.921	1790145.039	1801049.19
total damage	707187.503	661082.273	413508.166	331612.114	263825.784
sum	2278274.204	2376387.203	1942430.087	2121757.153	2064874.974
ratio	1.023859587	1.067951705	0.872930775	0.953520608	0.927957677
adjusted damage	690707.5068	619018.8842	473700.9825	347776.5571	284307.9921
damage remaining (%)	100	89.6209869	68.58199424	50.35077129	41.1618506
repair (%)	0	10.3790131	31.41800576	49.64922871	58.8381494
			t50% = 3.9		

	mec1				
	0	1	2	3	4
top band	1115033.796	1587842.171	1452173.426	1086754.966	952422.93
total damage	691886.175	701979.177	620437.33	472786.193	435533.421
sum	1806919.971	2289821.348	2072610.756	1559541.159	1387956.351
ratio	0.812032341	1.02904889	0.931434149	0.70085996	0.623749509
adjusted damage	852042.634	682163.0963	666109.7093	674580.1158	698250.5228
damage remaining (%)	100	80.06208481	78.17797875	79.17210816	81.95018593
repair (%)	0	19.93791519	21.82202125	20.82789184	18.04981407
			t50%=more than 6 hours		

summary NTS

	average t50%	STDEV	STD-Error
wt	5.05	0.353553391	0.250747086
rad26	3.8	0.141421356	0.100298834
mec1	more than 6	0	0

8.6 Data for the quantifications in Figure 5.3

first experiment – transcribed strand

	wt				
	U	0	1	2	4
total	197780956.5	211578376.3	214171417.5	196690459.2	171518282.7
ratio	0.934788138	1	1.0122557	0.929634033	0.810660738
damage	71543123.2	129799795.1	121315608.3	96603857.44	79558735.3
ratio	76534051.15	129799795.1	119846801.8	103916007.9	98140605
corrected		53265743.98	43312750.67	27381956.71	21606553.84
		1	0.813144574	0.514063161	0.405636948
			t 50% = 2.1 h		

	chk1				
	U	0	1	2	4
total	275533726.7	285215777.2	273807961.2	233300238.5	182550719.2
ratio	0.966053594	1	0.960002858	0.817978026	0.640044253
damage	148801873.6	193589824.4	175991185.6	131070280.9	94752039.15
ratio	154030661	193589824.4	183323606	160236921.7	148039824.9
corrected		44787950.79	34521732.39	11435048.09	-762048.757
		1	0.77078169	0.255315278	-0.017014593
			t50% = 1.9 h		

	rad53				
	U	0	1	2	4
total	257738974.5	317784509.6	266201534.3	221940517.1	220514815.3
ratio	0.811049522	1	0.83767939	0.69839942	0.693913041
damage	143214274	224553737.1	184106940.8	142705718.8	143224705.8
ratio	176578951.3	224553737.1	219782106.3	204332527.7	206401519.3
corrected		47974785.82	36803154.96	21353576.4	23422567.97
		1	0.767135368	0.445099984	0.488226629
			t50% = 1.9 h		

second experiment – transcribed strand

	wt				
	U	0	1	2	4
total	15225860.81	14179200.85	15244344.31	13839327.27	11493361.12
ratio	1.073816569	1	1.075120133	0.976030131	0.810578906
damage	5768791.53	8560741.47	8382602.73	5962289	4900463.4
nonsp	1256271.42	782290.41	1011318.69	821204.59	747772.31
	4512520.11	7778451.06	7371284.04	5141084.41	4152691.09
corr	4202319.316	7778451.06	6856242.21	5267341.903	5123117.634
backgr		3576131.744	2653922.895	1065022.587	920798.3188
			1	0.74212112	0.297814136	0.257484451
				t50% = 1.65 h		

	chk1				
	U	0	1	2	4
total	17405507.92	15710803.82	16068222.54	14804502.03	9543281.57
ratio	1.107868707	1	1.022749868	0.942313468	0.607434329
damage	5901923.07	9024069.21	8292413.11	6469004.47	3844003.12
nonsp	1057768.93	350535.48	638716.58	968545.89	213801.9
	4844154.14	8673533.73	7653696.53	5500458.58	3630201.22
corr	4372498.391	8673533.73	7483449.049	5837185.573	5976285.911
backgr		4301035.339	3110950.658	1464687.183	1603787.521
			1	0.723302743	0.340542931	0.37288406
				t50%= 1.7 h		

	rad53				
total	U	0	1	2	4
ratio	19895959.43	22054282.02	16369977.23	13953920.55	14666754.04
	0.902135894	1	0.742258452	0.632707995	0.665029767
damage					
nonsp	9181780.39	14932291.22	9454815	6848793	7984534
	2237339.5	1419127.59	991306.82	879443.54	1411854.14
corr	6944440.89	13513163.63	8463508.18	5969349.46	6572679.86
backgr	7697776.948	13513163.63	11402373.6	9434604.131	9883286.708
		5815386.682	3704596.657	1736827.183	2185509.76
			1	0.63703359	0.298660653	0.375815037
				t50% = 1.5 h		

first experiment – non-transcribed strand

	wt				
	u	0	1	2	4
top	173141412.4	188954519.8	167818361.8	141281562.5	117030865.3
	0.916312627	1	0.888141559	0.747701419	0.619359968
damage	44135115.84	92926253.5	79910156.52	59457835	46784517
corrected	48166002	92926253.5	89974571.85	79520826.78	75536875.84
backgr		44760251.5	41808569.85	31354824.78	27370873.83
		1	0.93405574	0.700506001	0.611499554
			t50% = 4.8 h		
	chk1				
	U	0	1	2	4
top	175279628.3	212979766.2	218480066.6	174536789.8	120671043.9
	0.822987232	1	1.02582546	0.819499396	0.566584545
damage	60295225.24	115515962.2	120553533	89813924.86	54657087.2
corrected	73263864.71	115515962.2	117518562.1	109596084.2	96467663.44
backgr		42252097.45	44254697.34	36332219.52	23203798.73
		1	1.047396461	0.859891502	0.549175074
			t50%= 4.7 h		
	rad53				
	U	0	1	2	4
top	175248198.9	256206911.3	148568184.6	107907857.1	106436986.7
	0.684010427	1	0.579875788	0.421174653	0.415433706
damage	59643390.58	158634362.3	85457936	58645134	53457841
corrected	87196610.16	158634362.3	147372830.1	139241840.7	128679594.9
backgr		71437752.17	60176219.96	52045230.55	41482984.7
		1	0.842358811	0.728539588	0.58068715
			t50% = 4.5 h		

second experiment – non-transcribed strand

	wt				
	u	0	1	2	4
total	21145731.25	19391508.65	20492418.92	17337044.69	11517124.38
ratio	1.090463441	1	1.056772801	0.894053423	0.593926166
damage	7776655.29	11951486.54	11673375.33	9465846.68	5636813.48
ratio	7131513.994	11951486.54	11046248.84	10587562.71	9490764.687
corrected		4819972.546	3914734.844	3456048.711	2359250.692
		1	0.812190278	0.717026638	0.489473886
			t50% = 3.9 h		

	chk1				
	U	0	1	2	4
total	24447569.24	15421898.5	22675180.7	19150554.73	12632396.3
ratio	1.585250301	1	1.47032356	1.241776733	0.8191207
damage	8810999.37	8203435.9	11549764	9145675	5678942
ratio	5558112.409	8203435.9	7855253.304	7364991.435	6932973.367
corrected		2645323.491	2297140.895	1806879.026	1374860.958
		1	0.868378065	0.683046528	0.519732639
			t50% = 4 h		

	rad53				
	U	0	1	2	4
total	24426052.89	27472742.71	15759173.95	12705587.13	11016577.73
ratio	0.889101359	1	0.573629438	0.462479748	0.401000288
damage	10524330.3	17012726.16	9145648	7145678	5814579
ratio	11837042.19	17012726.16	15943477.44	15450791.15	14500186.61
corrected		5175683.973	4106435.258	3613748.963	2663144.418
		1	0.793409196	0.698216696	0.514549272
			t50% = 4 h		

summary TS and NTS

TS			
	wt	chk1	rad53
exp 1	2.1	1.9	1.9
exp 2	1.65	1.7	1.5
AVERAGE	1.875	1.8	1.7
STD-Dev	0.318198052	0.141421356	0.282842712
STD-Error	0.225672377	0.100298834	0.200597668

NTS			
	wt	chk1	rad53
exp 1	4.8	4.7	4.5
exp 2	3.9	4	4
AVERAGE	4.35	4.35	4.25
STD-Dev	0.636396103	0.494974747	0.353553391
STD-Error	0.451344754	0.35104592	0.250747086

8.7 Summary of the data shown in Figure 5.4

TS			NTS	
	wt	dun1	wt	dun1
1	1.3	1.2	4.9	4.4
2	1.4	1.4	5.1	5.3
AVERAGE	1.35	1.3	5	4.85
STD DEV	0.070710678	0.141421356	0.141421356	0.636396103
STD Error	0.050149417	0.100298834	0.100298834	0.451344754

8.8 Summary of the data shown in Figure 5.5

TS			NTS	
	- CHX	+ CHX	- CHX	+ CHX
1	1.9	1.7	4.9	6
2	1.6	1.8	4.5	6
AVERAGE	1.75	1.75	4.7	6
STD DEV	0.212132034	0.070710678	0.282842712	0
STD error	0.150448251	0.050149417	0.200597668	0

8.9 Summary of the data shown in Figure 5.6

TS				NTS		
	wt	delta	SA	wt	delta	SA
1	1.5	6	1.7	4.4	6	4.1
2	1.4	6	1.4	4.8	6	4.6
AVERAGE	1.45	6	1.55	4.6	6	4.35
STD dev	0.070710678	0	0.212132034	0.282842712	0	0.353553391
STD error	0.050149417	0	0.150448251	0.200597668	0	0.250747086

8.10 Summary of the data shown in Figure 5.14

RPB2 transcribed strand t50 %

v	wt	SA	SE
3.25	1.9		2.1
4	1	2.4	1.8
3.9	1.9	2.66	1.96
	1.3	3.1	
	1.9		
	1.95		
	2.3		
MEAN 3.716666667	1.75	2.72	1.953333333
STDEV 0.407226391	0.442530602	0.35383612	0.15011107
STERR 0.154252421	0.167625228	0.204529549	0.086769405

RPB2 non-transcribed strand

v	wt	SA	SE
4.6	5.6	5.2	5
5	5.2	5	
3.6	5.2		4.9
3.5	4.2		
	4.2		
MEAN 4.175	4.88	5.1	4.95
STDEV 0.741057803	0.641872261	0.141421356	0.070710678
STERR 0.370528901	0.287835095	0.101015254	0.040873224

8.11 Summary of the data shown in Figure 5.15

TS

mec1	*mec1rad26*	*mec1rad26 + RAD26wt*	*mec1rad26 + RAD26SE*
2.5	6	2.7	2.7
2.4	6	2.4	2.3
2.45	6	2.55	2.5
0.070710678	0	0.212132034	0.282842712
0.050149417	0	0.150448251	0.200597668

only the results from the TS are shown here, the t50% values for the NTS were always more than 6 hours.